universität
wien

DIPLOMARBEIT

Titel der Diplomarbeit

„Characterization of budding yeast centromere proteins“

Verfasser

Michael Maier

angestrebter akademischer Grad

Magister der Naturwissenschaften (Mag.rer.nat.)

Wien, 2013

Studienkennzahl lt. Studienblatt:	A 490
Studienrichtung lt. Studienblatt:	Diplomstudium Molekulare Biologie
Betreuer:	Dr. Stefan Westermann

Contents

1.Abstract ... 4

2.Introduction ... 6

2.1 Preface ... 6

2.2 Cell cycle and mitosis in budding yeast ... 7

2.3 The cell cycle control system ... 9

2.4 The spindle assembly checkpoint ... 12

  2.4.1 The SAC blocks anaphase by inhibiting Cdc20-APC/C ... 12

  2.4.2 Activating the SAC ... 13

2.5 The mitotic spindle ... 15

  2.5.1 Microtubule dynamics and regulation by MT associated proteins ... 15

  2.5.2 Spindle assembly and kinetochore attachment in yeast and animals ... 18

  2.5.3 Poleward flux, kFibers and anaphase A ... 21

  2.5.4 Chromosome oscillation during animal prometaphase and metaphase ... 23

2.6 The kinetochore ... 24

  2.6.1 The KMN network ... 25

  2.6.2 Outer kinetochore and corona components ... 27

  2.6.3 The Dam1 and Ska complexes ... 28

  2.6.4 The constitutive chromatin associated network (CCAN) ... 28

  2.6.5 The CCAN as a recruitment platform for outer kinetochore assembly ... 32

  2.6.6 Recruitment and tension/attachment sensitivity of kintochore-bound kinases ... 33

  2.6.7 Regulation of kMT dynamics, attachment and error correction ... 35

  2.6.8 Involvement of the structural kinetochore in SAC activation. ... 42

2.7 Centromere inheritance in animals and budding yeast ... 45

3. Results ... 49

  3.1 In vivo characterization of the budding yeast CCAN ... 49

  3.2 Identification of Wip1 as the budding yeast CENP-W homologue. ... 57

  3.3 Cloning of ScCCAN subcomplexes for bacterial expression ... 59

  3.4 Determining expression conditions ... 61

3.5 Establishment of a purification protocol suitable for isolation of recombinant S iScCENP-Q/U/P/O, ScCENP-Q/U, ScCENP-P/O and ScCENP-L/N 64

3.6 Interactions of the ScCENP-Q/U/P/O complex. 72

3.7 Phosphorylation-site analysis of the budding yeast CCAN. 76

4. Discussion 81

4.1 Conservation of CENP-T/W and CENP-S/X complexes in budding yeast 81

4.2 Conservation of the CENP-Q/U/P/O/R complex and the CENP-L/M/N group in iiiiiiiyeast 82

4.3 Interactions of the ScCENP-Q/U/P/O^{COMA} complex with ScMIS12C, iiiiiimicrotubules and DNA 83

4.4 Regulation of and by the budding yeast CCAN 85

4.5 Model and future directions 86

5. Materials and methods 92

5.1 Strain and plasmid construction 92

5.2 Biochemistry 97

5.3 Mass spectrometry 101

5.4 Live cell fluorescence microscopy 102

6. References 103

7. Supplementary Information 148

7.1 Oligo sequences 148

7.2 Strains and Plasmids 150

7.3 Mass spectrometry data 152

8.Appendix: Published results 200

8.1 Molecular architecture and connectivity of the budding yeast Mtw1 kinetochore complex 200

8.2 CENP-T proteins are conserved centromere receptors of the Ndc80 complex 216

9. Curriculum vitae 228

10.Acknowledgements 229

1.Abstract

The kinetochore is a conserved eukorytic organelle, pivotal during the cell cycle. In order to partition chromosomes equally during division, it provides a microtubule attachment platform that facilitates correct sister chromatid sorting and segregation. It is a complex structure, which in vertebrate cells is assembled during the course of the cell cycle from more than a hundred proteins onto a specialized chromosomal locus, the centromere. Many of these protein components are well conserved between yeast and man, most prominently those of the core microtubule attachment platform, the KMN network. Some of the centromere proximal proteins of the vertebrate CCAN have established homologues in the budding yeast Ctf19 complex but overall conservation appears weaker between these two protein networks. This could be due to different mechanisms yeast and vertebrate cells use to define the centromere locus. However, our bioinformatic analysis indicated hitherto unknown yeast CCAN homologues, including known Ctf19 complex proteins, budding yeast centromeric proteins and proteins that had not yet been identified as centromeric constituents in yeast. Here I aim to substantiate our theory, that the CCAN is a protein network conserved between yeast and man, through biochemical and proteomic analysis of recombinant and native proteins. Furthermore I investigate potential cell cycle dependent regulation of budding yeast CCAN proteins by CDK1. I found a number of functionally conserved relations within the budding yeast CCAN, supporting conservation of this protein network. I also identified a number of CDK1 phosphorylation sites within the budding yeast CCAN, the most striking being a cluster of CDK1 sites at the amino-terminus of ScCENP-U.

Das Kinetochor ist eine konservierte eurkaryotische Organelle welches eine Schlüsselrolle im Zellzyklus spielt. Um die Chromosomen während der Zellteilung gleich aufzuteilen fungiert es als Mikrotubuli-Bindungsplattform, die das korrekte Sortieren und Segregieren der Schwesterchromatiden ermöglicht. Es ist ein komplexes Gefüge das, beispielsweise in Wirbeltier-Zellen, im Laufe des Zellzyklus aus über einhundert verschiedenen Proteinen an einem speziellen chromosomalen Locus, dem Zentromer, zusammengefügt wird. Viele dieser Protein-Bausteine sind wohl konserviert zwischen Pilzen und Menschen. Die zentrale Mikrotubuli-Bindungsplattform, das KMN Netzwerk, ist vermutlich das bemerkenswerteste Beispiel. Einige der Zentromernahen Proteine des Wirbeltier-CCAN's besitzen bekannte homologe im Ctf19-Komplex der Bäckerhefe, allerdings scheint die Konservierung zwischen diesen beiden Proteinnetzwerken insgesamt geringer. Ein Grund hierfür mögen die unterschiedlichem Mechanismen sein mit denen Hefezellen und Wirbeltierzellen den Locus ihres Zentromeres definieren. Unsere Bioinformatische Analyse jedoch wies auf bis dato unbekannte CCAN homologe in Hefe hin, einschließlich bekannter Ctf19-Komplex Proteine, Proteine des Hefe-Zentromeres und Hefeproteine die noch nicht als Zentromerproteine identifiziert wurden. Hier untermauere ich unsere Theorie, das das CCAN ein zwischen Hefe und Mensch konserviertes Proteinnetzwerk ist, durch biochemische und proteomische Analyse von rekombinanten und nativen Proteinen. Weiterhin untersuche ich eine mögliche Zellzyklus-abhängige Regulation des Hefe-CCAN's durch CDK1. Ich fand einige funktionell konservierte Zusammenhänge innerhalb des Hefe-CCAN's was eine Konservierung dieses Proteinnetzwerkes bestätigt. Weiterhin identifizierte ich einige von CDK1 phosphorylierte Stellen innerhalb des Hefe-CCAN's, wovon eine Ansammlung dieser am Amino-Terminus von ScCENP-U das hervorstechendste Merkmal ist.

2.Introduction

2.1 Preface

Walther Flemming, writing the first textbook on nuclear division, carefully noted that nuclear division is likely important for cell division as nuclear division can occur without cell division but the reverse is never observed[1]. Almost 150 years later, the importance of nuclear division in either mitosis or meiosis can hardly be overstated. As the genome contains the information to make a new organism, be it through cell division in unicellular organisms or fusion of two gametes into a zygote that will ultimately develop into a human, it is paramount that each cell or gamete receives the full information of an entire genome and no part of it in excess. Errors during mitosis may lead to death of the individual in the case of a single celled organism or cancer in humans[2]. Meiotic errors in turn are a leading cause for pregnancy loss and developmental defects[3].

Faithful segregation of the complete duplicated genome into both daughter cells is a formidable problem for a eukaryotic cell as their genome comes encoded on a number of chromosomes, which it cannot discern or count[4-8]. To overcome this, it employs an ingenious strategy: after replicating its chromosomes, the resulting two identical copies, the sister chromatids, remain cohesed[9]. Cohesed chromosomes are subsequently attached to microtubules (MTs) of the mitotic spindle. The spindle is a bipolar structure and each pole defines a location within one of the future daughter cells, as cytokinesis will take place on a plane between both poles. Of the two sister chromatids, each one only attaches to one of the two opposite poles yielding a bioriented chromosome. This effectively sorts sister chromatids and targets one of them to each daughter cell. Once sorting is complete, cohesion between the two sisters is resolved and complementary chromatids move to opposite poles.

This work concerns itself with the budding yeast kinetochore. Kinetochores (KTs) are pivotal during mitosis as they integrate many of the functions required for faithful chromosome segregation. They not only provide a load bearing attachment point for spindle microtubules but also regulate the dynamics of the attached MTs. Importantly, they harbor an error correction mechanism to resolve erroneous attachments, the occurrence of which is increased by miniscule perturbations, such as small drops in temperature. When sister chromatids separate, the cell loses its ability to tell them apart. To ensure that anaphase only initiates once sorting is complete, kinetochores generate a checkpoint signal until all chromosomes are bioriented [10]. Additionally, KTs are able to nucleate MTs and drive spindle assembly in absence of dominant microtubule organizing centers (MTOCs) such as centrosomes. Lastly, components of the kinetochore participate in an epigenetic mechanism that directs inheritance of the centromere locus.

Budding yeast affords the opportunity to study mitosis and specifically the kinetochore in a simplified system. Although its mitosis is morphologically very different from animal mitosis, many of the key components and mechanisms are conserved. Recently this list has been extended as bioinformatic analysis suggests extensive conservation of centromeric or inner kinetochore proteins between yeast and vertebrates. The constitutively centromere associated network (CCAN) of vertebrates appears to correspond to the budding yeast Ctf19 complex and the Sim4 complex of fission yeast[11]. Here I aimed to firstly investigate interactions between Ctf19 complex proteins and other kinetochore proteins, DNA and microtubules to refine existing models of kinetochore assembly. Secondly I sought to support the notion that the CCAN is conserved between humans and budding yeast experimentally, by finding conserved interactions within the CCAN and between CCAN and other kinetochore proteins.

2.2 Cell cycle and mitosis in budding yeast

Mitosis in budding yeast differs from the animal system in a few important points. The mitotic spindle is assembled intra-nuclear. The poles are defined by spindle pole bodies (SPB), budding yeast centrosome equivalents, situated inside the nuclear envelope (NE). During mitosis, SPBs bracket a spindle that spans the nucleus while projecting astral MTs towards the cell cortex[12-14]. The spindle is assembled before DNA replication is complete and the site of cytokinesis is not defined by astral microtubules or the midzone, but is predefined to be where the bud extrudes from the mother cell. The spindle aligns along the mother bud axis and cytokinesis takes place at the bud neck, the bridge connecting mother and bud after chromosomes have segregated[15-18].

Generally, the cell cycle is divided into S and M phase, the time when DNA replicates and the time when mitosis and cytokinesis occur, respectively. Gap phases, G1 following M phase and G2 following S phase, separate S and M phase. Budding yeast does not have a clearly defined G2 phase and S and M partially overlap[19, 20]. In G1 the future bud site is specified by placement of cortical landmark proteins and a precursor of the SPB assembles next to the mother SPB on a projection along the cytoplasmic face of the NE termed a half bridge[14, 21-24]. Further, chromosomal origins are licensed for replication by assembly of a Pre-replicative complex (PreRC) during G1[25-27]. Once the decision to duplicate is made, cells become insensitive to mating pheromones and are committed to mitosis, unable to undergo the alternative meiotic pathway until the current cell cycle has completed[28, 29]. Commitment happens when a point in time termed START is traversed and S phase is initiated. This triggers three independent processes, SPB separation and spindle assembly, budding, which entails polarization of the actin cytoskeleton towards the bud site and polarized secretion, and DNA replication through conversion of PreRCs into pre-initiation complexes (PreICs) and then into replisomes by loading of DNA polymerase[14, 20, 21, 23, 26, 30-33]. Following the previous division, the old SPB faces away from the bud scar and needs to reorient towards the bud site, in haploid cells placed next to the previous bud site [34, 35]. Astral MTs emanating from the old SPB and the half bridge interact with cortical myosin through the MT +end binding protein ScEB1 and the APC (Adenomatous polyposis coli) related protein Kar9. This allows the transport of astral MTs and thereby pulls the SPB towards the bud site along the same actin cables used for polarized secretion which supplies the bud site with membrane and cell wall material[31, 36-40]. During this time the spindle is asymmetric, only one of the two SPBs accumulates Kar9 and is targeted towards the bud[41-44].

Budding yeast enters M phase before S phase is completed, the spindle assembles and swiftly contacts kinetochores that have assembled on the early replicating centromeres[45]. Many of the hallmarks of the 5 mitotic phases are absent in budding yeast. During prophase chromosomes do condense but not to the same extent as in other systems, they do not become visible under light or electron microscopy[12, 13, 46]. Furthermore in animals the transition into prometaphase is marked by nuclear envelope breakdown (NEBD), followed by the individual biorientation of all chromosomes. NEBD never happens in budding yeast as the nucleus remains intact throughout mitosis[47]. During prometaphase bioriented chromosomes do not congress to form a defined metaphase plate, which marks the onset of metaphase in animal cells[48, 49]. Once DNA replication is complete and all chromosomes have bioriented, anaphase A is initiated, drawing chromosomes to the pole along shortening MTs, followed by anaphase B as the spindle expands into the bud[43, 48]. The latter is aided by cortical Dynein pulling astral MTs of both SPBs into either mother or bud[35, 50]. Once anaphase has completed, during telophase, the spindle is fully disassembled and the nucleus pinches off, followed by cytokinesis at the bud neck.

Some peculiarities of budding yeast prometaphase need to be mentioned. In addition to not displaying the same extent of chromosome condensation, centromeres in budding yeast separate as soon as they have become bioriented in an event termed transient separation[51, 52]. In animals and budding yeast the Cohesin complex mediates sister chromatid cohesion. Cohesin is a ring-shaped complex that is loaded during replication and is thought to entrap both sisters topologically[53-57]. Animal Cohesin is removed by two pathways prior to anaphase, the prophase pathway in which polo like kinase (Plk1) removes Cohesin along chromosome arms but spares two points of cohesion flanking the centromere. This last point of contact is severed at anaphase onset as seperase becomes active and permits chromatid separation. The pool of Cohesin at the centromere is specifically protected from Plk1 by Shugoshin (Sgo), which recruits Protein phosphatase 2A (PP2A) to counteract phosphorylation by Plk1 [58-64]. Budding yeast removes all Cohesin by Separase cleavage in anaphase of mitosis and requires Shugoshin for cohesion only in meiosis[65, 66]. Furthermore in budding yeast Cohesin is loaded preferentially at the centromere and this requires a number of kinetochore proteins. As kinetochores undergo transient separation, a region of at least 18kb centered on the centromere seperates while cohesion is retained at arms[51, 52, 66-68].

2.3 The cell cycle control system

It is readily apparent that the events of the cell cycle need to proceed in an ordered and unidirectional fashion if they are to generate two viable daughter cells. Attempting chromosome segregation before DNA replication has initiated or completed will lead to aneuploidy or DNA damage. This illustrates two important points of the cell cycle control machinery. Firstly it drives unidirectional progression through a strictly defined series of events, some of which occur in parallel. Secondly it is gated at specific points during this series to allow all required parallel events to complete. In budding yeast for example budding, DNA replication and spindle assembly are independent parallel events. Each is monitored by a checkpoint that retards anaphase until the event has completed, ensuring that anaphase initiates only when all have completed[69-72].

The cell cycle control system drives a cell forward through the cell cycle and the kinase CDK1 is central to its function[33, 73-77]. CDK1 phosphorylation triggers many of the sequential events, yet its levels remain constant through the cell cycle[78, 79]. CDK1 is activated by binding to one of the 9 sequentially expressed cyclins[80-84]. The earliest cyclin, Cln3, appears during early G1 while Cln1 and Cln2 peak during late G1 before entry into S which roughly coincides with the appearance of the first two B cyclins Clb5 and Clb6. Subsequently, Clb3 and Clb4 appear, followed by Clb1 and Clb2 which peak shortly before anaphase onset[15, 79, 83, 85-92]. Sequential association with cyclins is one possibility to explain control of a temporally ordered set of events by a kinase that does not change in abundance during the cell cycle. It would require cyclins to confer substrate specificity or specific localization. This has been demonstrated as Cln3 is primarily nuclear, Cln2 is also found in the cytoplasm, Clb4 localizes to the new SPB and Clb2 also localizes to the bud neck at late mitosis[44, 93, 94]. Furthermore, a limited number of CDK1 substrates are preferentially targeted by the early Clb5-CDK1 rather than the late Clb2-CDK1, including Ase1 and Fin1 which have a role in stabilizing the central spindle during anaphase B elongation but are detrimental to viability when a loss of CDK1 phosphorylation allows them to bind the spindle before anaphase onset. Here suppression by Clb5-CDK1, activation by Cdc14 and subsequent destruction by the APC allows the restriction of their activity to a narrow window during anaphase B [95-99]. A targeting subdomain of Clb5, the hydrophobic patch (HP), is one factor for substrate specificity. Clb5-HP interacts with RXL motifs to target CDK1 phosphorylation[100]. An alternative explanation for cell cycle regulation is that it is the rise in CDK1 activity that drives progression through the cell cycle, triggering the appropriate events once the required kinase activity threshold has been reached by accumulation of cyclins[101]. In line with this, Clb2 is a much more potent activator for CDK1 than Clb5 [95]. Furthermore, only few CDK1 substrates are specifically targeted by Clb5-CDK1. In vivo, cyclins demonstrate considerable redundancy as a deletion of 2 of the three G1 cyclins generates viable mutants. Similarly, deletion experiments with B-type cyclins show that a single B cyclin, either Clb1 or Clb6, when overexpressed, is sufficient to trigger all essential events during the cell cycle[15, 78, 90]. Sic1 serves as a model for how increased CDK1 activity may trigger a response that is not elicited at low CDK1 activity levels. Sic1 contains a cluster of CDK1 sites. Increasing CDK1 activity phosphorylates more sites within this cluster and it thus acts as a sensor that is responsive to the level of CDK1 activity and targets Sic1 for degradation only above a certain threshold [102].

However, on-time appearance of the cyclins is required to maintain normal timing between the events of the cell cycle. The G1 cyclins Cln1 and Cln2 normally trigger polarization of the actin cytoskeleton and bud formation at the site specified during G1, duplication of the SPB and render the cell insensitive to mating pheromones[23, 103-105]. Clb5 and Clb6 in turn trigger timely initiation of DNA replication at origins that have assembled a PreRC and simultaneously inhibit assembly of further PreRCs[26, 87, 106]. Onset of DNA replication additionally requires phosphorylation by the Dbf4 dependent kinase (DDK) Cdc7 which associates with origins and promotes conversion from a Pre-RC to a Pre-IC. Analogous to the activation of CDK1 by cyclins, Cdc7 kinase levels are constant but the activating cofactor Dbf4 is a target of the APC/C and accumulates only after CDK1-dependent inactivation of Cdh1-APC in S phase[26, 107-115]. It was suggested that Dbf4 serves to target Cdc7 to origins[116-118]. Clb3 and Clb4 trigger spindle assembly and are required for spindle polarity by maintaining asymmetry of the SPBs[15, 37, 44, 86, 87]. Clb1 and Clb2 are the final B cyclins to be expressed and they are required for progression through and completion of mitosis after spindle assembly, including Cohesin cleavage and ultimately B-type cyclin destruction by Cdc20-APC. In addition they randomize actin polarity, switching back from polarized to isotropic bud growth. Cyclin B destruction at anaphase re-focuses the actin cytoskeleton and vesicular traffic towards the bud neck, the site of future cytokinesis[15, 23, 79, 119-121].

Expression of cyclins is regulated firstly by transcription of sequential regulons and secondly by ubiquitin mediated proteolysis through the SCF and APC/C ubiquitin ligases. Cln1 and Cln2 as well as Clb5 and Clb6 are part of the late G1 regulon while Clb2 is part of the Clb2 regulon, transcribed at the end of S-phase. Positive feedback loops and feedback inhibition of earlier regulons are thought to drive a switch-like transition from one regulon to the next, and thereby into the next cell cycle stage, while simultaneously suppressing the previous[92, 122-127]. Ubiquitin mediated destruction has an important role during two major, irreversible transitions in the cell cycle: commitment to mitosis at the G1/S transition and anaphase onset at the M/G1 transition. During G1, the ubiquitin ligase APC/C (anaphase promoting complex/cyclosome) with its co-activator Cdh1 targets B cyclins for destruction. An exception is Clb5 that is not a target of Cdh1-APC/C[128-130]. Simultaneously, Clb-CDK1s are suppressed by the Clb-CDK1 inhibitor Sic1 in G1[131-134]. Expression of Cln1 and Cln2 at the end of G1 allows Cln-CDK1 dependent phosphorylation of Sic1, which targets it for destruction by the SCF ubiquitin ligase[103, 133, 135]. Decreasing Clb-CDK1 inhibition permits Cdh1 phosphorylation by CDK1 releasing it from the APC/C and thereby shuts off B-type cyclin proteolysis. This stabilizes B-type cyclins and permits progression into S and M phase. After chromosomes have been replicated and bioriented on the mitotic spindle, silencing of the spindle assembly checkpoint (SAC) permits the APC/C to use a second co-activator, Cdc20, to target its substrates[120]. Intriguingly, Cdc20 binding to APC/C requires CDK1 phosphorylation and thereby cyclins set the stage for their own destruction[120, 136]. In addition to B-type cyclins, Cdc20-APC/C targets the Separase inhibitor Securin for destruction[137-139]. Separase in turn is a protease that cleaves the kleisin subunit of the Cohesin complex, resolving sister chromatid cohesion[65, 140]. Cleavage of the kleisin is the only event required to trigger anaphase in budding yeast. However stabilization of the spindle during anaphase B, mitotic exit and reentry into G1 requires destruction of cyclins and reversal of CDK1 phosphorylation by the phosphatase Cdc14[91, 141]. Cyclin destruction during mitotic exit proceeds in two steps, an initial phase that is mediated by Cdc20-APC/C and a later phase mediated by the G1 APC/C, Cdh1-APC/C[120]. Similarly, release of the CDK1-antagonizing phosphatase Cdc14 from the nucleolus proceeds in two phases. Partial early release through the FEAR pathway (Cdc14 early release) and the later full release through the mitotic exit network (MEN)[142, 143]. Like Cdc20-APC/C activity, Cdc14 release by the FEAR pathway requires CDK1 activity. Cdc14 is sequestered in the nucleolus, bound to Net1. CDK1 phosphorylates Net1 to liberate Cdc14 but this is suppressed by the phosphatase PP2A until anaphase onset. When the SAC is silenced and Separase is liberated from Securin, it downregulates PP2A mediated dephosphorylation of Net1 by a mechanism distinct of its protease activity and thereby permits CDK1 to release Cdc14[144]. Were the FEAR pathway and Cdc20-APC the only mediators of mitotic exit, falling CDK1 activity would quickly deactivate both, re-sequestering Cdc14 into the nucleolus and removing Cdc20 from APC/C, leading to a failure to exit mitosis. Cdh1-APC/C and MEN allow cyclin B destruction and reversal of CDK1 phosphorylation in absence of CDK1 activity. Cdc14-dephosphorylated Cdh1 can bind to APC/C and target B-cyclins for destruction[120]. Further the MEN triggers full, CDK1 independent Cdc14 release in response to a number of stimuli, which in part consist of signals generated by correct spindle positioning along the mother-bud axis thereby forming the spindle-positioning checkpoint. The GTPase-like protein Tem1 is placed at the apex of this pathway and is thought to sense positional information from the spindle. It is asymmetrically localized to the daughter-bound SPB and thought to be activated once it enters the bud, triggering Cdc14 release through a signaling cascade consisting of cdc15 kinase and the Mob1/Dbf2 kinase complex which ultimately effects Cdc14 release[143-145]. Falling CDK1 activity also allows the transcription factor Swi5 to re-enter the nucleus and initiate Sic1 expression, contributing to Clb-CDK1 inactivation and allowing reentry into G1[146, 147].

2.4 The spindle assembly checkpoint

Chromosomes that have not correctly bioriented block the onset of anaphase through a pathway termed the spindle assemble checkpoint (SAC). This is generally vital for survival as disengaging sister chromatids before each one has become targeted to their respective pole will lead to missegregation and a loss of genomic stability. Budding yeast represents one exception to this rule. Here the SAC is not essential because its early spindle assembly allows kinetochores to attach before DNA replication is complete. Therefore, in an unperturbed cell cycle, budding yeast will have bioriented its chromosomes long before chromosome segregation is attempted[148]. The intact SAC is able to block anaphase in the face of a single unattached kinetochore[149-151]. While the simplistic view is that a single kinetochore generates an anaphase inhibitor potent enough to postpone anaphase indefinitely or until apoptosis is triggered in response to a prolonged arrest, multiple inhibitory mechanisms exist within the SAC. Further, a number of cases in which cells arrest either only transiently or only in response to multiple unattached kinetochores have been reported. One prominent example for this is found in the highly aneuploid HeLa cell line which is prone to initiate anaphase when few chromosomes are unattached but robustly arrests when all are unattached[152]. This would suggest that instead of a single inhibitory pathway generating an "all or nothing"-response to a chromosome that has not bioriented, multiple pathways serve to inhibit anaphase onset. A number of SAC proteins have initially been identified in budding yeast and subsequently been found conserved in animals. These are Mad1, Mad2, Bub1, Bub3 and Mps1 as well as Mad3 which in animals has fused to a Bub1 related kinase domain and is therefore referred to as BubR1. Bub1, Mps1 and BubR1 are all active kinases[72, 148, 153-169]. A deviation from this general statement is found in C.elegans, which possesses a Mad3 homologue that does not have any kinase domain and does not possess any Mps1 related kinase[170].

2.4.1 The SAC blocks anaphase by inhibiting Cdc20-APC/C

The transition from metaphase to anaphase requires activation of Cdc20-APC and the degradation of its targets, Securin and B-type cyclins. The SAC blocks this transition by inhibiting Cdc20-APC/C. Among the core checkpoint proteins, 3 inhibitory mechanisms are known. Bub1 is able to phosphorylate Cdc20 directly which inhibits Cdc20-APC/C in vitro. This phosphorylation is however not required for a SAC arrest in vivo[171]. The related BubR1 kinase also phosphorylates Cdc20, this is however not inhibitory[172]. Both BubR1^{Mad3} and Mad2 can bind to different sites on Cdc20 individually and act as a stoichiometric Cdc20-APC inhibitor. Inhibition of Cdc20-APC/C by Mad2 and BubR1^{Mad3} is synergistic and both binding of Mad2 or BubR1^{Mad3} enhances binding of the other[172-177]. The mechanism of Cdc20-APC inhibition by BubR1^{Mad3} is well defined. It supplies degron motifs that compete with bona-fide Cdc20-APC/C substrates for recognition. Additionally it promotes APC/C mediated ubiquitination and destruction of Cdc20, and it has been suggested that it either acts to position Cdc20 as an APC/C substrate or that its degron sequences act in trans[178-182]. It is important to note that an active SAC is a steady state in which both Cdc20 and SAC proteins are continuously synthesized and destruction of Cdc20 serves to tip the balance towards an arrest[183]. The ability of Cdc20 to bind to both, Mad2 and BubR1^{Mad3} has fostered the idea of a mitotic checkpoint complex (MCC) to be the soluble inhibitor generated by unattached kinetochores. This complex consists of Mad2 bound to Cdc20 and a complex of BubR1^{Mad3} and Bub3 that binds to a second independent site on Cdc20 via BubR1^{Mad3} [184-186]. The recent crystal structure of the fission yeast MCC corroborates BubR1^{Mad3}'s function as pseudo-substrate inhibitor and demonstrates additionally that the full MCC shifts the position of Cdc20 of the APC/C, disrupting a second, composite, degron receptor site[187]. However it should be noted that a number of investigators have reported BubR1^{Mad3}-Cdc20 and Mad2-Cdc20 stoichiometries which are inconsistent with a single entity, the MCC, formed as the product of a linear pathway. Most interesting, the amount of Mad2-Cdc20 relative to BubR1^{Mad3}-Cdc20 appears related to the nature of SAC arrest[174, 180, 188, 189]. In Taxol arrested cells which are generally presumed to be arrested because of low tension, the amount of Mad2 associated with a Cdc20-BubR1^{Mad3} complex is lower than in a Nocodazole arrest where all kinetochores are unattached[190]. Thus, the MCC, while isolatable from arrested cells and reconstitutable in vitro, may either be a dynamic entity i.e. different subunits join and leave at different timepoints or in response to different stimuli or alternatively it may be one of multiple checkpoint complexes.

2.4.2 Activating the SAC

How do kinetochores sense mal-attachment and activate the SAC? Mechanistically this is not well understood. Firstly it is known that the MCC assembles before mitosis in absence of functional kinetochores, as soon as Cdc20 is expressed. To reconcile this with the idea of a kinetochore generated signal it has been proposed that the MCC is assembled kinetochore-independent in interphase to give a baseline timer, a minimum duration of mitosis. Kinetochore-directed MCC assembly then extends this timer if it senses erroneous attachment by synthesizing additional MCC[185, 189, 191]. In this vein, loss of Mad2, BubR1^{Mad3} or the Mps1 kinase, which is required for MCC assembly in both interphase and mitosis, significantly decrease the duration of mitosis while loss of Mad1, Bub1 or Bub3 do not[191, 192]. To generate a SAC signal based on the MCC, kinetochores would have to catalytically facilitate MCC assembly. Indeed an interesting catalytic mechanism has been partially delineated over the past years. Mad2 can adopt either of two conformer states, open or closed (O-Mad2 and C-Mad2), which slowly interconvert with a half life of about 9h in vitro. Only C-Mad2 binds Cdc20 with high affinity and promotes BubR1^{Mad3} binding. A tetramer Mad1/C-Mad2 is recruited to unattached kinetochores and the C-Mad2 in the tetramer is able to recruit additional O-Mad2. By an undefined mechanism that requires Mps1 kinase activity, the Mad1-C-Mad2 complex promotes the conversion of bound O-Mad2 to Cdc20 binding C-Mad2[193]. In this model, unattached kinetochores would promote binding of Mad2 to Cdc20 and subsequently BubR1^{Mad3} would join the complex from the cytoplasm, supported by the fact that while BubR1^{Mad3} is required for a SAC response, a cytoplasmic fragment containing Cdc20 binding regions is sufficient[194]. While in vitro isolated chromosomes amplify Cdc20-APC inhibition only through Mad2 but not through BubR1, it is questionable if Mad2-directed MCC assembly is the only active mechanism due to a number of reasons[174, 195]. Firstly, Mad1 and Mad2 leave the kinetochore as soon as it becomes end-on attached. In experiments in which microtubule dynamics were perturbed by decreasing the temperature to 23°C, cells arrest dependent on BubR1 and Mad2 for up to 80min although both Mad1 and Mad2 were absent from the kinetochore[196]. Further, while in budding yeast the assembly of the MCC in vivo seems linear insofar as Mad1 is required for Mad2 binding to Cdc20 and Mad2 is required for Mad3 binding to Cdc20 but itself is independent of Mad3, in D.melanogaster BubR1 or Mad2 can bind to Cdc20 in the absence of the respective other[177, 184]. More important a loss of Mad2 in D.melanogaster fails initial establishment of a SAC but when arrested by a proteasome inhibitor and released into Nocodazole later, a sustained BubR1 dependent checkpoint is active[197]. Lastly, when one assays the turnover kinetics of checkpoint proteins on vertebrate kinetochores, one observes that BubR1 and Cdc20, in contrast to Mad2, show a similar biphasic recovery from photobleaching and for Cdc20 this is dependent on BubR1[198]. The slower recovery phase of BubR1 and Cdc20 is similar to Mad2 recovery and this has been equated to the event of MCC formation. The fast phase in contrast may equate to Cdc20 recruitment by BubR1. Cdc20 recruitment by BubR1 has been directly demonstrated in D.melanogaster and appears likely in vertebrates where the localization pattern of Cdc20 parallels that of BubR1. In detail, appearances of BubR1 and Cdc20 on the kinetochore coincide temporally. While Mad2 is lost on attachment, BubR1 and Cdc20 decrease only when tension is applied but persist at lower levels at kinetochores through anaphase[177, 198-200]. Thus it is debatable if generation of Mad2-Cdc20 at unattached kinetochores is the only pathway to synthesize MCC or if, for example, attached tensionless kinetochores that have lost Mad2 may achieve this through an alternate pathway involving an initial BubR1^{Mad3}-Cdc20 complex that is later joined by cytoplasmic Mad2. A further possibility is the assembly of the entire MCC at the kinetochore, suggested by the fact that SAC proteins upstream of BubR1^{Mad3} and Mad2, namely Bub3 which binds Bub1 and BubR1^{Mad3}, the Mad2 receptor Mad1 and Bub1, form a complex upon activation of the SAC that contains neither Mad2 nor BubR1^{Mad3} and could act as an assembly platform[155, 201]. The function of this complex however is unknown. Lastly the APC/C localizes to unattached kinetochores. It localizes independently of Cdc20 and it has been argued that the APC itself may need to be sensitized for inhibition by the checkpoint at the kinetochore [172, 199, 202].

2.5 The mitotic spindle

2.5.1 Microtubule dynamics and regulation by MT associated proteins

Microtubules are the basic building blocks of a mitotic spindle[203-205]. These are tube-shaped self assembling biopolymers formed from α/β-tubulin heterodimers[206-213]. Within a MT, tubulin heterodimers make head to tail longitudinal contacts forming elongated protofilaments while lateral bonds between dimers serve to generate sheets of 13 protofilaments that close into tubules[214-223]. MTs display both structural and dynamic polarity[224]. They grow preferentially and faster at one end, defined as the +end, while the -end requires a higher tubulin concentration to initiate growth[225-228]. MTs differ from equilibrium polymers as polymerization does not simply proceed until free subunit concentration drops below the critical concentration. Rather they switch stochastically between polymerization and depolymerization. This property is termed dynamic instability and is a result of tubulins' GTPase activity and the conformational change it undergoes after hydrolyzing its bound nucleotide[229, 230]. A GTP-tubulin heterodimer consists of two globular domains connected at an angle that increases on hydrolysis[231-234]. In solution tubulin can exchange its nucleotide while when incorporated into the MT lattice, exchange is blocked[235, 236]. After assembly into MTs, GTP tubulin converts to GDP tubulin. This renders its conformation less compatible with the extended MT structure. Incorporated into the MT, a preferentially curved protofilament is forced into an elongated conformation, which changes the lattice spacing of the MT and stores elastic energy in the structure in the form of lattice strain[230, 237, 238]. Upon depolymerization this energy is released as lateral bonds are broken and GDP-protofilaments assume their preferred conformation, curling back from the shortening end[231]. The stored elastic energy can be used to work, a shortening MT can pull two particles together if they are stably anchored to opposite ends. Conversely the decrease of free energy that drives polymerization allows a growing MT to push on particles located in its path[239-242]. Because there is a lag between incorporation into the lattice and hydrolysis of GTP, polymerizing MTs retain a region of GTP-tubulin crowing the growing end, a GTP cap[243-245]. Further, MTs grow by closure of a leading, polymerizing tubulin sheet[214, 246, 247]. Both structures, the GTP cap and the leading sheet, are believed to be stabilizing structures. The cap because its lateral bonds can hold the tips of protofilaments together against their tendency to curl apart, the sheet because its curvature is closer to that of an individual protofilament than a closed MT. A growing MT switches to shrinkage when hydrolysis catches up with polymerization and the GTP cap is lost. A fast rate of sheet closure may lead to a catastrophe as this stabilizing structure is lost. Very recently it has been reported that MTs have an intrinsic aging mechanism and that longer MTs are more prone to undergo catastrophe. Catastrophe requires at least three destabilizing events, possibly the acquisition of lattice defects or structural changes in the polymerizing +end[248]. In vivo, dynamic instability is observable but MT dynamics are regulated by a plethora of microtubule associated proteins. Generally mitotic microtubules are more dynamic than interphase microtubules[141, 249, 250]. Growth rate in vivo is faster than expected based on the cellular tubulin concentration alone and at growth rates where one observes virtually no catastrophes in vitro, they are frequent in vivo[251-254]. Moreover, MTs are locally regulated, nucleated at specific subcellular structures during mitosis, i.e. centrosomes or chromsomes, selectively stabilized when they make contact with some structures, such as the kinetochore, or destabilized when contacting other structures such as the bud neck in yeast[255]. Lastly, motor proteins and nonmotor proteins serve to crosslink MTs into bundles and sort them into a defined fusiform structure, the mitotic spindle.

The γ-tubulin ring complex (γ-TuRC) is a well-established MT nucleator[256]. The γ-TuRC contains the α/β-tubulin related γ-tubulin[257]. γ-Tubulin is thought to oligomerize into one turn of a helix corresponding to the lattice spacing of a MT and allow assembly of α/β-tubulin on top, providing a MT template and capping the -end to stabilize it against depolymerization[258-260]. Budding yeast contains only a subcomplex of the γ-TuRC, the γ-tubulin small complex (γ-TuSC) which is thought to function similar to the γ-TuRC[256, 261].

MT +end dynamics and interaction with subcellular structures or surfaces is thought to be primarily regulated by a number of MT +end localizing proteins or +tips[262-264]. The prime +tip, the calponin homology domain protein EB1, is able to autonomously track polymerizing +ends by recognizing the GTP-cap of growing MTs. By interaction with other +tips, EB1 allows them to track +ends[265-268]. In itself EB1 promotes dynamic instability. It binds to two adjacent protofilaments, promoting polymerization, increasing growth rate and preventing lattice defects. However, because it expedites leading sheet closure, this stabilizing structure is shortened, rendering MTs prone to catastrophe[268-270]. Clip170 is a second well characterized but non-autonomous +tip. It requires EB1 and tyrosinated α-tubulin, the C-termini of both form a composite binding site for Clip170 at MT +ends[267, 271-274]. Clip170 in turn recruits p150^{glued} of the Dynactin complex, rendering recruitment of Dynein/Dynactin to +ends dependent on both EB1 and Clip170[275-280].

The XMAP215/Dis1- and the CLASP- families are established MT polymerases[281-286]. Both catalyze the addition of tubulin heterodimers to the +end. Under certain conditions XMAP215 can also catalyze the reverse reaction in vitro, removal of tubulin from ends. It increases both growth and shrinkage rate of MTs and thereby renders them more dynamic[287-289]. Kinetochore-localized CLASP has been demonstrated to promote the incorporation of tubulin at the +end of kMTs and it may do so specifically under tension, allowing a switch to kMT growth in response to applied tension[290, 291]. CLASPs bound to MT walls are thought to promote rescue if a depolymerizing MT +end passes by while XMAP215 decreases the frequency of rescues[284, 288].

Depolymerases induce MT shrinkage. OP18^{Stathmin} may act by either sequestering tubulin dimers or inducing catastrophe by increasing protofilament curvature at +ends. It's mechanism of action is pH dependent[292-295]. The kinesin-13 family has no motor activity and induces depolymerization from either +end or -end. A kinesin-13 utilizes its ATPase activity to trigger a catastrophe by inducing a GDP-tubulin protofilament like bend into the GTP-protofilaments at the +end. This turns catastrophe into a one-step event[248, 296-299]. In contrast, members of the kinesin-8 familiy are +end directed motors[41, 248, 300-302]. They are thought to walk along a MT until they reach the +end where they stop. When reached by following kinesin-8 motors, they are bumped off the tip, taking only one or two tubulin dimers with them. This slows MT growth and promotes aging, inducing a catastrophe through the MT inherent multistep process. Kinesin-8 family members are processive +end directed motors and longer MTs recruit higher amounts of kinesin-8. Thus they act as length-dependent, +end specific depolymerases.

Lastly, the assembly of a structure such as the mitotic spindle requires sorting and crosslinking of MTs. This is accomplished by a number of nonmotor MT crosslinkers such as APC (Adenomatous polyposis coli), NuMA, NuSAP, TPX2, HURP and molecular motors, some of which have intrinsic crosslinking activity[303-313]. HURP has the notable ability to promote polymerization of an additional, stabilizing sheet of tubulin around a MT +end but it is not clear if this is an in vitro effect entirely[314]. The tetrameric +end directed kinesin-5 motors are bipolar with two motor heads at either end. Although this conformation alone allows them to crosslink MTs, additional non-motor MT binding domains have been recently identified[315-317]. The dimeric -end directed kinesin-14 family requires both the motor and the additional N-terminal nonmotor MT binding sites to crosslink MTs[318-324]. Kinesin-12 is dimeric, +end directed and may be able to crosslink MTs when in complex with TPX2[325, 326]. The -end directed Dynein in turn binds to the Dynactin complex, which serves as a cargo adaptor and enhances processivity of Dynein[327, 328]. In addition a complex of Lis1 and NudE/L associates with Dynein/Dynactin and strengthens Dynein´s MT binding during its ATP cycle, which is thought to adapt it for high loads[329-331]. The largest subunit of the Dynactin complex, p150^{glued}, has non-motor MT binding and crosslinking activity[332, 333].

2.5.2 Spindle assembly and kinetochore attachment in yeast and animals

A spindle contains up to three distinct populations of MTs that emanate from each of its two poles with their +ends pointing outwards [334-336]. Interpolar MTs (ipMTs) emanate from either pole and overlap in the spindle midzone, kinetochore MTs (kMTs) connect each sister kinetochore to one pole. Astral MTs (aMTs) are present only in astral spindles in which poles are organized by MTOCs while they are absent from anastral meiotic spindles or mitotic spindles of higher plants[337]. aMTs project away from the spindle, radial in centrosome-containing spindles and as a bundle from yeast SPBs. They can mediate interaction with the cortex, facilitating spindle positioning within the cell.

Both spindle assembly and structure are considerably more complex in metazoa compared to budding yeast. Metazoan spindles may contain hundreds of MTs while budding yeast contains only about 40, 32 kMTs for each of the 32 sister chromatids and about 8 ipMTs [338-340]. Further, animal spindles assemble by two superimposed pathways; one driven by centrosomes and one driven by chromosomes, while yeast only utilizes a single MTOC driven pathway[341-343].

Classical MTOC driven spindle assembly begins in prophase, when two microtubule organizing centers (MTOCs), centrosomes in animals or SPB's in budding yeast, form a central spindle by interdigitating ipMTs. In budding yeast this is accomplished by three balanced forces. SPBs nucleate cytoplasmic aMTs and ipMTs through y-TuSC tethered to receptors at both their cytoplasmic and nuclear face[344]. Kinesin-5 is activated by CDK1, crosslinks and pushes anti-parallel overlapping ipMTs apart, separating the SPBs. Kinesin-14 in turn crosslinks ipMTs and provides a resisting force, counteracting spindle elongation[345-349]. Astral pulling forces generated by Dynein are able to rescue mutants defective in kinesin-5 driven spindle elongation but Dyneins role in spindle elongation is likely limited to anaphase B where it serves mainly to pull the two nuclei into either mother or bud[50]. Once chromosomes have bioriented, kinetochores are placed under tension drawing poles inward, evidenced by the stretched centromeric chromatin during normal metaphase and the elongated spindles observed when kinetochores are defective[52, 350].

In animal spindles a similar collection of balanced forces drives spindle assembly. Initially, centrosomes nucleate microtubules via y-TuRC and begin separation during prophase, which may not complete before NEBD, through transport along the Dynein-enriched NE[351-353]. In human cells kinesin-5 assists prophase separation by anti-parallel MT sliding[354-361]. At

NEBD kinesin-14 is liberated from the nucleus and provides a resisting force against spindle elongation by kinesin-5[318, 360, 362-366]. However, in contrast to yeast, Dynein/Dynactin localized to +ends through Clip170, supplies the dominant collapsing force to counteract kinesin-5 in vertebrates.[318, 360, 361, 367]. In addition kinesin-12 functions in parallel with kinesin-5 to push poles apart[368]. With the release of nuclear spindle assembly factors the balance of forces changes and if centrosomes have not separated sufficiently during prophase, they will collapse into a monopolar spindle. Recently, a kinetochore derived pushing force has been shown to promote bipolar spindle assembly specifically when centrosome separation does not complete before NEBD. This force is generated by continuous growth of the kMT +end anchored to the kinetochore which pushes the kMT -end outward[369]. Like their yeast counterparts, bioriented chromosomes in animal cells will ultimately be placed under tension, resulting in a force resisting spindle elongation. Additionally, animal chromosomes are under the influence of polar ejection forces, which derive from growing ipMTs impinging on chromatin and chromatin bound +end directed kinesins[370-373]. The budding yeast SPB is a relatively compact structure, where Microtubules are tethered, via intervening proteins, to a central plaque consisting of a 2-dimensional crystalline lattice of Spc42[14, 374]. Animal spindle poles, centrosomal or acentrosomal, rely on active mechanisms that crosslink MT -ends to focus them into poles and attach them to centrosomes if present. They may fracture under abnormal traction or if a loss of spindle crosslinkers perturbs their integrity, yielding multipolar spindles[375, 376].

In prometaphase chromosomes are captured and bioriented on the spindle. Dynamic MTOC-nucleated MTs probe the cyto- or nucleoplasm for kinetochores, a mechanism termed search and capture[377, 378]. If a single MT contacts a KT, the chromosome is transported poleward, its kinetochore laterally attached to the MT wall[379]. Budding yeast utilizes kinetochore-bound kinesin-14 for this form of transport. Upon lateral attachment, kinesin-8 is released from the kinetochore and, in complex with Stu2 of the XMAP215/Dis1 family of MT polymerases, walks to the plus end and promotes rescue of this MT[380, 381]. It may however undergo catastrophe and depolymerize until it reaches the KT, whereupon either lateral attachment is converted to an end-on attachment or the MT undergoes a Stu2 dependent rescue[382]. Although this event can be observed when kinetochores are conditionally activated, it is unclear to what extent search and capture takes place during unperturbed yeast mitosis as centromeres replicate early and there is only a very transient detachment from SPB nucleated MTs which in budding yeast persist throughout the cell cycle[45, 382]. Animal chromosomes undergo search and capture after NEBD during normal mitosis, although poleward movement after lateral attachment is mediated by kinetochore-tethered Dynein[379, 383, 384]. Once at the pole, the close proximity facilitates end-on attachment of one kinetochore, yielding a monoriented chromosome. In animals the monoriented chromosome can then be pulled towards the spindle midzone by kinetochore tethered Kinesin-7 (CENP-E) where the likelihood of an end-on attachment by MTs from the opposite pole is increased[385, 386]. End-on attached kMTs are selectively stabilized, once both kinetochores of a chromosome have attached, the chromosome is bioriented and congresses to the spindle equator where it remains stably attached until anaphase onset. Budding yeast exclusively utilizes this classical pathway for chromosome attachment, adding one twist: it can nucleate and tether +end distal MTs at its kinetochores, independent of the y-TuSC, which then interact with spindle MTs and are transported polewards to assist biorientation. These MTs are lost once the +end of a SPB nucleated MT attaches[387].

Animal cells employ a second pathway for spindle assembly, which is chromosome rather than centrosome driven[341-343, 388, 389]. Here, upon NEBD, MTs are nucleated with random orientation in the vicinity of chromosomes. Subsequently, they become sorted and crosslinked into two bundles with their +ends overlapping in the vicinity of the chromosomes and their -ends projecting away, focused into two anastral poles lacking MTOCs. Chromosomal spindle assembly is initiated by two independent pathways, a RanGTP gradient emanating from chromosomes and the chromosomally located Aurora B kinase [390-393]. Aurora B kinase localizes to chromatin and locally downregulates kinesin-13 and OP18/stathmin, permitting MT assembly[394-396]. A RanGTP gradient centered on chromatin is generated by the chromosome bound Ran-GEF RCC1[393, 397]. RanGTP in turn effects localized release of kinesin-14, NuMA, NuSAP, HURP and TPX2 from Importin [306, 307, 310, 312, 398-402]. During chromosomal spindle assembly kinetochores are major MT nucleating sites and bundles of kMTs termed kFibers direct spindle assembly[377, 403]. A local accumulation of RanGTP at the kinetochore induces nucleation of microtubules through the kinetochore-localized nuclear pore Nup107-160 complex which tethers and activates y-TuRC in response to RanGTP[403, 404]. RanGTP at the centromere is quickly hydrolyzed after MT nucleation by recruitment of the nuclear export receptor Crm1 in complex with RanBP2 and RanGAP1, which promotes local RanGTP hydrolysis and shuts off nucleation. Chromatin nucleated MTs are amplified by microtubule dependent microtubule nucleation. The augmin complex tethers y-TuRC to existing MT walls and promotes further nucleation[405]. The +end of a subpopulation of kinetochore-nucleated MTs will become embedded into the kinetochore and form kMTs. One may speculate that an outer kinetochore localized +end motor, such as CENP-E, could assist herein. The +end MT crosslinker HURP, which is required for the formation of kFibers, associates with kMTs and they elongate as tubulin is incorporated into their plus end by CLASPs[152, 291, 311, 312, 369, 403]. kMTs form depolymerization resistant, highly crosslinked bundles, termed kFibers[406-408]. HURP is found in a complex, termed EXTAH, containing in addition TPX2, XMAP215, Aurora A and kinesin-5. It has been suggested that, because this complex contains crosslinking, polymerase and sliding capabilities, it would be ideally suited to promote assembly of a bipolar spindle, coupling MT elongation with outward movement of kMTs[311]. However it is currently unclear if HURP is exclusively active on kFibers. While overexpression of HURP induces ectopic cold-stable kFiber-like bundles, the EXTAH complex was identified as a factor that promotes bipolar spindle assembly on chromatin coated beads devoid of kinetochores[311, 312]. No structural component of the kinetochore is currently known to recruit HURP although it does show kinetochore specific localization, slightly distal from the core kinetochore microtubule binding site, the KMN network. A second crosslinker, APC (Adenomatous polyposis coli) localizes internal to the KMN network. [409, 410].

Sorting and assembly of chromosomally nucleated MTs into a spindle is mediated by a similar set of factors involved in astral spindle assembly. Kinesin-5 preferentially generates anti-parallel bundles and slides -ends apart but stalls once it reaches the +end. Kinesin-14, which slides +ends apart, preferentially generates asters where -ends are clustered and +ends lie distal[356, 411-413]. As is the case with spindle elongation, Dynein functions in parallel with kinesin-14 and in anastral spindles of Xenopus provides the major pole focussing activity[413]. To generate a focused pole that can resist the applied forces the Dynein-Dynactin complex, which itself has intrinsic crosslinking ability additionally transports the crosslinkers TPX2 and NuMA polewards to support a stable structure [305, 414-418].

RanGTP and Aurora B generate anastral meiotic spindles, but they function superimposed on the dominant MTOC-driven mechanism during mitosis. Chromosomally nucleated kMTs are threaded into the spindle that assembles between the two centrosomes by Dynein dependent poleward transport along ipMTs anchored at the centrosomes[377, 403, 419, 420]. Both pathways cooperate, centrosomal MT nucleation is enhanced by the RanGTP pathway and centrosomal MTs show directional growth towards chromatin suggesting that MT stabilizing gradients of RanGTP and Aurora B downregulated depolymerases act as a guidance system[377, 393, 421-423].

2.5.3 Poleward flux, kFibers and anaphase A

Considerable differences exist between the spindle dynamics of budding yeast and animals. One is the formation of kFibers mentioned in the preceding paragraph. In budding yeast only a single kMt attaches to each kinetochore[13, 49]. -Ends are silenced, stably anchored to the y-TuSC at the SPB and only +ends are dynamic[424]. kMT dynamics during metaphase and anaphase are more complex within the kFibers of animal cells. Firstly, kMTs and indeed all spindle MTs undergo poleward flux[425, 426]. Poleward flux describes a net movement of tubulin towards spindle poles and can in principle arise from two processes, either the motor dependent transport of entire MTs towards the pole or simultaneous polymerization of a MT +end and depolymerization at its –end, allowing tubulin to flux through the polymer. Both processes are active but the extent of their contribution to flux of kMts and ipMTs differs. Anastral meiotic spindles contain a high number of ipMTs which flux dependent on kinesin-5. It is thought that they are nucleated in the vicinity of chromosomes, then pushed out of the midzone by kinesin-5, pulled polewards by Dynein and fed into the pole-localized kinesin-13 depolymerases MCAK and Kif2a[427-432]. Dynein itself transports Kif2a poleward and thereby is responsible for pole focusing, MT transport and the localization of depolymerase activity to the pole[430]. In spindles in which ipMTs are less abundant, one observes a motor independent flux that likely derives from kFibers fluxing by +end growth and depolymerization of -ends anchored at the pole[385]. In line with this, most ipMTs are non-continuous and are thought to form a tiling array while most kMTs are continuous between pole and kinetochore[339, 340, 433]. However it can't be excluded currently that ipMT and kMT flux may occur by overlapping mechanisms[434].

kFibers are an integral structural component of the mitotic spindle and some of their roles have already been mentioned. They push on incompletely separated centrosomes during spindle assembly[369]. Furthermore when spindles are placed under pressure, they elongate and this elongation seems to be driven by pushing kFibers. When pressure is decreased, kFibers resist a collapse of the spindle to its original size[435]. This creates a conceptual problem. kFibers are thought to elongate when under tension and shrink in its absence[436]. A dominant role in pushing poles apart would however require them to elongate in the absence of tension. It is unknown how such a switch may be regulated. In addition kFibers display significant autonomy. When severed from the pole and removed from the spindle, they maintain constant length and continue to flux[437]. A possible factor that allows them to flux when disconnected from poles is Kif2a. Dynein-mediated poleward transport along kFibers places it at the right location to promote kFiber -end depolymerization and thereby flux[430].

During anaphase A, budding yeast chromatids must move via a Pacman mechanism in which kinetochores remain stably attached to depolymerizing +ends, dragging them towards the pole because they do not exhibit flux and -end directed motors are not required for anaphase A[424]. Animal spindles in turn can utilize flux to power chromosome movement. There are extreme cases in which kFibers continue to polymerize at the +end, while being reeled in by depolymerization of pole anchored kFiber -ends[438]. Human cells use both flux and Pacman movement, a Pacman-flux mechanism, in which the kFiber shortens from both ends. However, flux based anaphase A movement constitutes only a minor component of poleward movement in human cells[439]. Three models explain how a kinetochore may remain attached to a shrinking MT +end and harness the energy stored in the microtubule lattice to power chromosome movement. Biased diffusion posits that the force coupler is free to diffuse along the MT lattice but a high energy barrier prevents it from falling off the +end. A shortening MT +end will bias 1-dimensional diffusion towards the MT -end[440]. The hill sleeve is a special case of biased diffusion and assumes closely spaced linear arranged tubulin binding sites in the linker. The initial model was based on a sleeve encircling the MT. Thermal motion will allow the MT to penetrate into the sleeve and every additional tubulin-sleeve bond that is formed will decrease the free energy of the system. Therefore the sleeve has a tendency to move towards the -end. However because for each additional bond to be formed the entire sleeve must move along the MT, which requires all existing bonds to be broken, there is a limit to how deep the MT can penetrate before the MT-sleeve bonds become to stable to be broken by thermal energy. A hill sleeve coupler would therefore track both growing and shrinking +ends and not diffuse freely along the MT[441]. Lastly the forced walk model suggests that protofilaments curling back from the depolymerizing +end of a shrinking MT impinge on the force coupler, pushing it backward along the MT[442].

2.5.4 Chromosome oscillation during animal prometaphase and metaphase

Budding yeast kinetochores immediately undergo transient separation following biorientation. During transient separation kinetochores move uncoordinated, coupled to the +end dynamics of their individual kMT[424]. However, rarely does one kinetochore cross over into the other half spindle. It is thought that a spatial catastrophe gradient is active and the frequency of catastrophe increases with distance to the pole. At the same time, attached kinetochores under tension promote rescue and elongation of their kMT. Thus, whenever a kMT grows toward the spindle equator, it is prone to catastrophe while when shrinking to close to the pole it will undergo a tension dependent rescue[443]. The kinesin-8 Kip3 would be an ideal candidate to generate such a catastrophe gradient. Surprisingly it appears to be the kinesin-5 Cin8, which in yeast is distributed in a gradient along spindle MTs and facilitates length dependent depolymerization of kMTs[444]. Kip3 in turn suppresses kMT plus end dynamics ensuring KT clustering between the spindle midzone and pole, a role that is also emerging for animal kinesin-8[445]. During anaphase A however Kip3 may be shortening kMTs as a loss of Kip-3 leads to lagging chromosomes[446].

In contrast to the uncoordinated movements in budding yeast, animal kinetochores undergo coordinated oscillations. Oscillation is observed on monoriented chromosomes and on bioriented chromosomes in spindles that display a low flux rate. It has been suggested that at high flux rates tension is sufficient to switch both kinetochores to permanent polymerization. However at lower flux rates polymerization from one kinetochore is sufficient to balance the net loss of tubulin polymer to pole localized depolymerases. In this case one of the two sister kinetochores is attached to a polymerizing kFiber while the other kFiber is depolymerizing and the two kinetochores switch between growth and shrinkage coordinately, leading to chromosome oscillation back and forth on the metaphase plate [436, 447, 448]. During one oscillation period the centromere remains stretched, but the magnitude of this stretch increases and the shrinking kFiber at the leading KT undergoes rescue when stretch is maximal, suggesting that at this point tension has increased far enough to switch both KTs to polymerization. The trailing KT switches to depolymerization after a short lag, when tension has sufficiently decreased[449, 450]. If both kinetochores have an equal probability to switch to depoylmerization when tension is low, one would expect directional movement, on average, to cancel out and the chromosome to oscillate around a relatively stable position. A number of factors have been identified that affect oscillation and some of them, such as Sgo2 and MCAK, accumulate specifically on the leading kinetochore while CENP-I accumulates on the trailing kinetochore [451, 452]. Thus, oscillation may be molecularly controlled rather than just a stochastic switch between growth and shrinkage of the kFibers. Principally, oscillation appears to be driven by two motors. The two kinesin-13s, MCAK and Kif2b, promote oscillation. The kinesin-8 Kif18A in turn dampens oscillations, which contrasts with the established role of kinesin-8s as depolymerases[453-457]. Kif2b and MCAK are temporally controlled, Kif2b is only active in prophase while MCAKs activity is restricted to metaphase[458, 459]. The observed temporal regulation of Kif2b and MCAK is likely a response to applied tension and therefore not globally restricted to prometaphase or metaphase but rather regulated at individual kinetochores in response to attachment state [458-462].

2.6 The kinetochore

The kinetochore integrates many of the mitotic functions described including spindle assembly, SAC signaling and chromosome congression. It may not be surprising then that animal kinetochores are complex machines thought to contain over 100 different components[463-466]. The repeat subunit model states that the large animal kinetochores are compound structures formed by multiplication of autonomous core structures which are functionally equivalent[467]. Budding yeast kinetochores are thought to constitute a single copy of this core structure for a number of reasons: budding yeast kinetochores only attach to a single microtubule while human kinetochores attach to ~25. Animal kinetochores can fracture but retain core functions, such as the ability to bind MTs and align on the metaphase plate, demonstrating that they can be subdivided[467]. Additionally, not only are the identities of core kinetochore components conserved, but their relative stoichiometry and localization within the kinetochore are too[468-471]. Classical electron micrographs depict the animal kinetochore as a trilaminar structure, two electron dense circular layers separated by an electron-translucent layer. One of the two electron dense layers, the inner plate, abuts the chromatin, while kMTs terminate in the outer plate. Corona fibers project distal from the outer plate[472]. This appearance is an artifact of chromosome dehydration during conventional sample preparation and new techniques visualize the outer plate as a mat-like structure abutting the centromere, embedded in a clear ribosome free zone surrounding the outer plate[473]. Fibrils emanating from this mat contact kMTs directly, but there is no apparent repetitive motif that would correspond to a core structure[474]. Although an artifact, the classical plate structure serves well for comparative localization studies and descriptive purposes as it illustrates an important point. Kinetochores assemble in a hierarchical manner during the animal cell cycle and a chromatin-bound base recruits microtubule binding components to interact with the spindle. The structural kinetochore can conceptually be split into 3 parts, the chromatin proximal CCAN (constitutively centromere associated network), which is recruited by the CENP-A containing centromeric nucleosome, the KMN network (Knl1-Mis12-Ndc80), which provides the core microtubule binding site within the kinetochore required for end-on attachment and additional outer kinetochore/corona proteins that facilitate initial lateral and the conversion to end-on attachment, many of which are recruited by the KMN network[475]. It is important to note that this model is an oversimplification, as multiple examples for a bypass of this hierarchy exist, the formin mDia3 for example binds directly to both, centromeric histones and microtubules[476, 477]. It does, however, present a convenient framework for discussion. While the KMN network is conserved between yeast and animals, further outer kinetochore/corona proteins are not. Recently, Dr.Alexander Schleiffer was able to demonstrate new, albeit distant, homologies among the budding yeast Ctf19 complex, the fission yeast Sim4 complex and the vertebrate CCAN suggesting that this supermolecular network may too be conserved almost entirely between yeast and human.

2.6.1 The KMN network

Because of the central position of the well-investigated KMN network within the kinetochore and its role as core microtubule binding site, it is well suited as an entry point for this discussion[478]. It consists of two complexes, the Ndc80 complex (NDC80C) and the Mis12 complex (MIS12C) and additionally the protein Knl1. Budding yeast Mtw1 and MTW1C will be referred to as ScMis12 and ScMIS12C, budding yeast Spc105 as ScKnl1. NDC80C is a 4 protein complex consisting of Ndc80, Nuf2, Spc24 and Spc25. Ndc80 and Nuf2 both contain CH-domains at their N-termini and dimerize via their C-terminal coiled coil (CC) regions. The C-termini of Spc24 and Spc25 fold into a globular domain that contains a groove lined with conserved hydrophobic residues. N-terminal CC-domains of Spc24 and Spc25 allow tetramerization with the CC domains of Nuf2/Ndc80 generating an elongated complex in which the two globular heads formed by Ndc80/Nuf2 and by Spc24/25 are separated by an elongated flexible rod domain[479-484]. An internal loop disrupts Ndc80's CC domain and introduces a kink into the rod close to the Ndc80/Nuf2 head[485]. The Spc24/25 head connects the NDC80C to the rest of the KMN network while the Ndc80/Nuf2 head binds microtubules directly[478, 486-488]. MT binding requires a number of conserved lysine residues in both CH domains as well as a short tail domain extending N-terminally from the Ndc80 CH domain[489]. Human NDC80C binds MTs cooperatively and is able to oligomerize on the MT lattice. In electron-tomographic reconstructions the Ndc80 CH domain can be observed to contact the gap between α- and β-tubulin monomers, both within and between dimers. The Nuf2 head does not directly contact the lattice but might be involved in electrostatic interactions with the lattice. Additionally it was suggested that the Ndc80 tail mediates oligomerization of NDC80C on the lattice by interaction with a Nuf2 head of an adjacent NDC80C[490, 491]. Oligomerization of Ndc80/Nuf2 heads on the MT lattice is an important feature, as it may explain how a filamentous mat-like kinetochore reorganizes in response to kMT attachment and may provide multiple linearly arranged tubulin binding sites, forming a pliable hill sleeve which on the one hand needs to closely appose tubulin binding sites to the MT wall but on the other hand must adapt to the curling end of a shrinking kMT[442, 492]. Because the Ndc80 CH domain contacts the gaps between tubulin monomers, it´s binding to MTs is conformation sensitive. This has been suggested to be the basis of NDC80C´s biased diffusion. Rather than the progressive loss of Ndc80 binding sites by loss of tubulin dimers at the +end of a depolymerizing MT, protofilament curling progressively occludes binding sites[491]. In contrast to the NDC80C, little structural information is available on Knl1. Its C-terminus is required for localization to the kinetochore and binds to the MIS12C[478]. NDC80C and Knl1 target to kinetochores independently in budding yeast and humans but NDC80C localization is dependent on Knl1 in C.elegans [493-496]. Importantly, like NDC80C, Knl1 has intrinsic MT-binding activity[478, 493]. The final KMN subcomplex is the heterotetrameric MIS12C complex, consisting of Mis12, Dsn1, Nnf1 and Nsl1, which has the shape of an asymmetric dumbbell. The structural contributions of the individual components in MIS12C are less clearly defined as for NDC80C, but the larger globular domain of the dumbbell is composed of Dsn1, Mis12 and Nsl1, the latter of which extends into the smaller globular domain together with Nnf1[497]. MIS12C binds both the c-terminal region of Knl1 and the Spc24/25 head of the NDC80C. Crosslinking experiments suggest that a Dsn1/Nsl1 dimer binds to Spc24/25 while Mtw1/Nnf1 in turn connects the KMN network to the kinetochore[475, 488]. Affinity purification of an epitope tagged ScDsn1 yields a supercomplex of ScNDC80C, ScMIS12C, ScKnl1 and Kre28, a protein that has been suggested to be the yeast homologue of Zwint-1. This supercomplex is equi-stoichometric, containing one copy of each, ScNDC80C, ScMIS12C and ScKnl1, which suggests that the KMN network may comprise a linking fiber that is recruited to the kinetochore en bloc[493, 498]. A similar supercomplex is present in Xenopus cell lysates, supporting this idea[499]. Thus, in a model of the KMN network, the Mtw1 complex serves to connect the microtubule binding NDC80C and Knl1 to the inner kinetochore, which is consistent with NDC80C localizing to the outer plate and MIS12C localizing to the central plate in vertebrate kinetochores[500, 501].

2.6.2 Outer kinetochore and corona components

A number of proteins that are either recruited by the KMN network or, at least in part, by the underlying CCAN localize to the outer plate and corona fibers of the kinetochore. These serve to facilitate initial lateral attachment, kinetochore mobility on the microtubule wall and subsequently the conversion to end-on attachment by the KMN network. Lateral attachment and poleward transport of an animal chromosome is facilitated by kinetochore-tethered Dynein[379, 383, 384]. Dynein and Dynactin recruitment requires the KMN network, the RZZ complex (Rod1-ZW10-Zwilch), Spindly and Zwint-1[502-509]. Zwint-1 may have up to 3 contact points on the KMN network, binding to NDC80C, MIS12C and Knl-1 and it recruits the RZZ via a direct interaction with ZW10[496, 504, 506, 510-513]. It thereby links the RZZ complex to the KMN network, which in turn recruits Dynein and Dynactin. Because ZW10 interacts with both p50$^{\text{dynamitin}}$ of the Dynactin complex and the Dynein intermediate chain, it is likely responsible for their independent recruitment to unattached kinetochores. However, multiple pools of Dynein may exist at kinetochores[460, 507, 514]. Spindly recently was identified as an additional factor required for Dynein/Dynactin recruitment and demonstrated to require the RZZ complex for localization[508, 509, 515]. Because direct interactions between the RZZ and both Dynein and Dynactin have been described, it is not yet clear if Spindly simply provides an additional link between RZZ and Dynein/Dynactin or if it has a regulatory role in Dynein/ Dynactin recruitment. The RZZ complex has been suggested to suppress KMN network microtubule binding as loss of Spindly leads to a severe end-on attachment defect that can be partially rescued by the loss of the RZZ complex[515]. Once a kinetochore is able to support tension, Dynein/Dynactin are no longer recruited and stream away along the kFiber, stripping the RZZ complex and SAC proteins from the kinetochore in the process. In contrast to poleward transport of chromosomes, stripping of outer kinetochore/corona proteins by Dynein does require Dynactin[516-520]. Removal of the RZZ complex requires Spindly and is thought to activate the KMN network, facilitating a hand over from lateral to end-on attachment. A second Dynein recruitment pathway rests on CENP-F. CENP-F recruitment is independent from the NDC80C but requires Knl1, Bub1, which is recruited to Knl1 and possibly CENP-H/I/K of the underlying CCAN although the latter is disputed. Because Bub1 does not require CENP-H/I/K to localize, these may be two individual requirements.[521-524]. CENP-F has MT binding activity and recruits Lis1, Nde1 and Ndel1. Nde1 is required for Dynein recruitment and Dynein mediated stripping[525, 526]. CENP-F, like the RZZ complex, is stripped by Dynein following end-on attachment[527]. Monooriented chromosomes can congress to the metaphase plate through the kinetochore bound +end directed kinesin-7 CENP-E[385, 386]. Human CENP-E appears to be recruited to kinetochores through interaction with NDC80C and to a lesser extent through interaction with BubR1. It contains a SUMO interacting motif required for its localization and both Nuf2 and BubR1 are SUMOylated[528].

Additional requirements for CENP-E recruitment have been described, such as the kinetochore localized Septin-7 and CENP-F, which is partially required for CENP-E localization and interacts with CENP-E[149, 529-531]. Like the RZZ, Spindly, CENP-F, and SAC proteins, CENP-E is stripped by Dynein from end-on attached kinetochores[516].

None of the discussed outer kinetochore/corona components are present at the budding yeast kinetochore[532]. Instead, it recruits two kinesin motors. The kinesin-14 Kar-3 may be linked to the MTW12C via Cik1 and allows poleward transport of laterally attached KTs analogous to Dynein in animal systems. The kinesin-8 Kip3 transports Stu2 to MT +ends promoting a rescue event[381, 446, 533]. An interactor for Kip3 at the kinetochore has not yet been suggested.

2.6.3 The Dam1 and Ska complexes

NDC80C is critical for end-on attachment and recruits two complexes that are similarly required for end-on attachment and that have been suggested to be functional but not evolutionary homologues, the animal Ska complex (SKA-C), composed of Ska1-3, and the yeast specific heterodecameric Dam1 complex (DAM1C)[532, 534-544]. End-on attachment and recruitment of both complexes requires the Ndc80 internal loop[381, 485, 545]. Both SKA-C and DAM1C can couple beads to depolymerizing MT +ends facilitating movement[534, 546, 547]. While both SKA-C and DAM1C oligomerize on the MT lattice, the structure of a DAM1C oligomer is much more striking as it forms ring or helix like structures on a MT wall[534, 548, 549]. This has inspired the idea that it may serve to act as a force coupler, either through biased diffusion or by forced walk, remaining connected to the kinetochore via NDC80C[242, 440, 442, 550, 551]. DAM1C and ScNDC80C interact and bind microtubules cooperatively[552, 553]. ScNDC80C binding to microtubules is highly sensitive to physiological salt concentrations and shows no specificity for +ends. Further, ScNDC80C only weakly binds to the DAM1C. However, in presence of microtubules and the DAM1C, ScNDC80C-MT interaction is strongly enhanced and NDC80C in complex with DAM1C is now able to track shrinking +ends. Interaction with DAM1C may obviate the need for ScNDC80C oligomerization in budding yeast.

2.6.4 The constitutive chromatin associated network (CCAN)

The Constitutive Centromere Associated CCAN network defines a group of 16 proteins recently identified in vertebrate kinetochores by their co-purification with the centromeric nucleosome[554-558]. These proteins localize internal to the KMN network and remain at the kinetochore during interphase in contrast to outer kinetochore and corona components[501, 559]. Earlier genetic studies and more recent biochemical studies in budding yeast identified the 12 kinetochore proteins of the Ctf19 complex and in a number of publications sequence homologies between the budding yeast Ctf19 complex, the fission yeast Sim4 complex and the vertebrate CCAN have accumulated, most recently expanded by Dr. Alexander Schleiffer[463, 532, 560-571]. The full list of putative orthologues is given in Table1. ScCENP-W is included in this list for clarity although its identification and characterization is undertaken and described later in this work. Notably, CCAN proteins with the exception of CENP-C have not been found in D.melanogaster or C.elegans[572]. Vertebrate CCAN proteins were assigned to groups depending on the requirements for their centromere localization, biochemical interactions and their requirement for cell viability. In vertebrate cells, many CCAN proteins are essential, though loss of some members of the CCAN has a less severe effect on viability. CENP-C and the CENP-T/W complex target kinetochores independently but require the centromeric nucleosome for localization. Chicken cells that have lost either CENP-C or CENP-T/W stop proliferating after 36-48 hrs and undergo apoptosis[556, 573-577].

Table 1: CCAN protein orthologues in vertebrates, budding and fission yeast

	Vertebrate	S.cerevisiae	S.pombe
CENP-C:	CENP-C	Mif2	Cnp3
CENP-T/W:	CENP-T	Cnn1	Cnp20
	CENP-W	Wip1	SPAC17G8.15
CENP-H/I/K:	CENP-I	Ctf3	Mis6
	CENP-H	Mcm16	Fta3
	CENP-K	Mcm22	Sim4
CENP-N/M/L:	CENP-N	Chl4	Mis15
	CENP-M		
	CENP-L	Iml3	Fta1
CENP-Q/U/P/O/R:	CENP-Q	Okp1	Fta7
	CENP-U	Ame1	Mis17
	CENP-P	Ctf19	Fta2
	CENP-O	Mcm21	Mal2
	CENP-R		
CENP-S/X:	CENP-S	YOL086W-A	SPBC2D10.16
	CENP-X	YDL160C-A	SPCC576.12c
Unassigned:		Nkp1	Fta4
		Nkp2	Cnl2
			Fta5
			Fta6

Sources for the assigned orthologues are: Schleiffer et al, 2012, McClelland et al, 2007, Meraldi et al 2006

Further downstream the CENP-H/I/K and the CENP-L/M/N group of proteins localize to kinetochores interdependently. CENP-K, CENP-H and CENP-I knockouts impact viability severely with cells ceasing to proliferate after 36-48hrs while CENP-M knockouts are less severe and cells stop proliferating after 72 hrs[556, 578]. Interestingly, it has been shown that CENP-H/I/K is required for centromere localization of CENP-C during interphase but not mitosis[573]. Conversely, during kinetochore assembly onto frog sperm chromatin, which likely represents a de novo kinetochore assembly onto the centromeric nucleosome, CENP-C is required to recruit CENP-H/I/K[579]. In fission yeast localization of both, CENP-L/M/N and CENP-H/I/K group proteins, depends partially on CENP-C and CENP-T, suggesting a two-pronged recruitment pathway[580]. Similarly, both CENP-T and CENP-C depletion lead to a loss of CENP-H from HeLa centromeres and CENP-N can be recruited by ectopically tethering the N-terminus of either CENP-T or CENP-C to a chromosomal site[577]. Lastly, both CENP-H/I/K and CENP-L/M/N are required for recruitment of the CENP-S/X complex and the CENP-Q/U/O/P/R complex, which localize independently of one another. Chicken cells that have lost CENP-Q/U/O/P/R components are viable and continue to proliferate at an increased generation time. An apparent cell type specific difference has been observed for loss of CENP-S/X, which in chicken cells only leads to minor mitotic defects while strong congression defects are observed in HeLa cells[581]. As a rule, if any of the members of a given group or complex is lost, all members of the respective group as well as the downstream groups/complexes are lost from the centromere. Exceptions to these localization requirements are CENP-M, which in chicken DT40 cells but not in human cells additionally requires the CENP-Q/U/P/O/R complex but is not required for CENP-L localization, as well as CENP-R, which can be lost from the CENP-Q/U/P/O/R complex without delocalizing the other members from the centromere [555, 556, 582]. Supporting localization data, the CENP-T/W, CENP-S/X and the CENP-Q/U/P/O/R complexes have been biochemically demonstrated to form stable complexes[576, 581, 582]. CENP-T/W are histone fold proteins, as are CENP-S/X[11, 576, 581]. CENP-C is a DNA binding protein[583-585]. ScCENP-U was initially described as an actin-related protein (Arp100)[586]. CENP-C and CENP-N have additionally been demonstrated to bind directly to centromeric nucleosomes[587, 588]. All investigated vertebrate CCAN proteins localize to the inner kintochore, between centromeric nucleosomes and the KMN network, suggesting a DNA proximal structure possibly corresponding to the inner plate[470, 501, 559]. The only known exception to this is CENP-T. While its histone fold is located at the inner kinetochore, its flexible N-terminal domain stretches towards the outer kinetochore[501]. In budding yeast subcomplex identity may be conserved, but recruitment dependency and the loss-of-function impact on viability seems to have been turned upside down with respect to the vertebrate and fission yeast CCAN. ScCENP-Q/U, whose vertebrate counterparts have a mild effect on cell viability when lost, are the only essential

CCAN proteins in budding yeast[568, 589]. The nonessential members of ScCCAN were identified initially in genetic screens for factors that are required for faithful chromosome transmission. It appears that ScCENP-P/O mutants have the most severe defect in chromosome segregation, while an intermediate defect is observed for ScCENP-N and a relatively weak defect for ScCENP-H/I/K and ScCENP-L[590]. A quadruple deletion of ScCENP-P and ScCENP-H/I/K, which is expected to remove all ScCCAN components except ScCENP-Q/U, is viable and shows no additive phenotypes[566, 567, 590]. ScCENP-Q and ScCENP-U are interdependent for centromere localization and required for targeting of ScCENP-O/P. ScCENP-Q/U and ScCENP-O/P have been suggested to form dimeric subcomplexes and to associate into a ScCENP-Q/U/P/O complex following transition of START[463, 569, 591]. Some of these observations parallel those in vertebrates. In both, vertebrates and budding yeast, depletion of CENP-Q also affects CENP-U protein levels while a loss of CENP-O affects CENP-P protein levels[463, 582]. ScCENP-Q/U is the most upstream complex within the budding yeast CCAN and requires the CBF3 complex as the most upstream factor in budding yeast kinetochore assembly. The CBF3 complex is required for localization of the centromeric nucleosome and ScCENP-C and indeed all other known components of the yeast kinetochore. The evolutionary origins of the CBF3 complex are mysterious, but, because it is only found in budding yeasts where it plays a pivotal role in kinetochore assembly, its appearance may underlie the change in CCAN recruitment hierarchy[532]. ScCENP-C in turn is required for recruitment of CENP-P. As ScCENP-P/O are lost in ScCENP-Q/U mutants it seems reasonable to propose that ScCENP-C is required for CENP-Q/U recruitment[568, 591, 592]. ScCENP-O/P are required to localize ScCENP-N/L and both ScCENP-O and ScCENP-N are required to target ScCENP-I to kinetochores. ScCENP-N may be in complex with ScCENP-L because the latter requires ScCENP-N to localize and this if conserved would be equivalent to the vertebrate CENP-N/M/L group. ScCENP-I has been suggested to form a complex with ScCENP-H and ScCENP-K by yeast two hybrid analysis, the putative budding yeast equivalent of the vertebrate CENP-H/I/K group[566, 567, 593]. When epitope-tagged ScCCAN proteins are purified from budding yeast, they are isolated in a complex named the Ctf19 complex, after one of its components, ScCENP-O$^{\mathrm{Ctf19}}$. The Ctf19 complex does not contain ScCENP-C but does contain ScCENP-Q/U/P/O, also known as COMA complex, ScCENP-N/L, ScCENP-H/I/K and additionally Nkp1 and Nkp1 for which no homologies have been established. Additionally, affinity-purified Ctf19 complex contained ScMis12 as the only KMN member. Conversely, affinity-purified ScMis12 proteins co-purify ScCCAN members and ScCENP-C[569, 592, 594]. This would suggest that either the ScCCAN interacts with the KMN network or that the established subcomplex architecture is not absolute and kinetochore proteins may exist in multiple distinct assemblies. Similar to the vertebrate CCAN, the Ctf19 complex and ScCENP-C co-purifiy with the centromeric nucleosome[595]. Recently, Dr. Alexander Schleiffer proposed budding yeast Cnn1 and the products of the uncharacterized ORFs YDL086W-A and Yol160C-A to be homologous to CENP-T, CENP-S and CENP-X respectively. This led us to believe that most of the vertebrate CCAN was conserved in budding yeast and we renamed the Ctf19 complex to ScCCAN, incorporating the novel homologues. However while ScCENP-T^{Cnn1} has been localized to the kinetochore, ScCENP-T, ScCENP-S and ScCENP-X had not yet been detected in association with the Ctf19 complex[11, 463]. Furthermore, for reasons explained in the results section, a budding yeast CENP-W orthologue eluded identification by a bioinformatics approach.

2.6.5 The CCAN as a recruitment platform for outer kinetochore assembly

With the CCAN located between centromeric nucleosome and the outer kinetochore, it seems plausible that one of its functions would be to supply a binding platform for outer kinetochore components including the KMN network. Loss of function studies, however, have yielded ambiguous results. A number of publications argue CENP-C, CENP-T, CENP-S, CENP-H/I/K and CENP-M depletions to have an effect on centromere targeting of KMN components. Specifically CENP-C depletions lead to a corresponding loss of MIS12C with a less pronounced effect on NDC80C[573]. Conversely, CENP-T, CENP-S and CENP-H/I/K depletions strongly, but not fully, loose NDC80C localization but have a weak effect on MIS12C localization. Knl1 kinetochore localization is decreased when either CENP-C, CENP-T/W or CENP-H/I/K is depleted [524, 577, 581, 596]. This asymmetry in KMN network recruitment is also observed when either CENP-C, which recruits high amounts of MIS12C and Knl1, or CENP-T, which recruits high amounts of Ndc80, are force-localized to ectopic chromosomal loci and argues against recruitment of the KMN network as a single entity. CENP-I depletions further lose Mps1 and Mad1 and Mad2 from the kinetochore. This is not unexpected as Mps1 requires NDC80C to localize while Mad1 and Mad2 require NDC80C to be retained at kinetochores against Dynein mediated stripping. CENP-I is also required to recruit Dynactin and possibly CENP-F but not Bub1 or BubR1 and surprisingly not the RZZ complex or CENP-E which do require NDC80C. CENP-C in turn is required CENP-E and to a lesser extent NDC80C as well as both Mad1, Mad2, Bub1 and BubR1. Note that Mad1, Mad2 and BubR1 require Bub1 for localization. CENP-C is furthermore required for RZZ complex and Dynactin recruitment[451, 524, 579, 596]. CENP-I recruitment weakly depends on MIS12C only during mitosis, which is interesting as the major MIS12C recruitment factor, CENP-C, depends on CENP-I for localization only during interphase but not mitosis[573, 579, 596-599]. One study in budding yeast suggests that ScCCAN, ScMTW12C and ScNDC80 target to kinetochores independently on the grounds that temperature sensitive ScNdc80, ScMis12 or ScCENP-Q do not loose localization of the respective other complexes[463]. Another study suggests interdependence; ScMIS12C is lost in the absence of ScCENP-Q and vice versa. ScNDC80C in turn requires ScMIS12C for kinetochore localization[600].

2.6.6 Recruitment and tension/attachment sensitivity of kintochore-bound kinases

A number of kinases localize to kinetochores and regulate kinetochore assembly, attachment state and SAC signaling. These include Aurora B, Mps1 and Bub1 in budding yeast and additionally Polo-like kinase 1 (Plk1), BubR1, CDK1 and Nek2a in animals. Localization of many of these kinases is strongly interdependent in animals, connected by multiple feedback loops in which one kinase increases either activity or localization of the other. In yeast however, a relatively simple linear recruitment pathway has been delineated. Here Mps1 is likely recruited to NDC80C. Phosphorylation of unattached NDC80C by Aurora B may promote but not be required for Mps1 recruitment, as is the case in vertebrates. [601-603]. Mps1 in turn phosphorylates Knl1, which allows binding of Bub1[604, 605]. This linear pathway may be conserved in animals as some studies suggest that NDC80C is required to recruit Mps1, Aurora B accelerates but is not required for recruitment of Mps1 to unattached kintochores and Bub1 is not required for Mps1 recruitment. Mps1, NDC80C, Aurora B and Knl1 in turn would be required to recruit Bub1[191, 496, 523, 531, 603, 606, 607]. However, significant discord exists on this subject as other studies argue Bub1 localization to be codependent with Mps1 in Xenopus extract or independent of either NDC80C or Mps1 in human cell lines. Furthermore, Bub1 persists at kinetochores into anaphase while Mps1 needs to be released before anaphase onset[191, 531, 602, 608-612]. It is possible that additional localization pathways exist, that localization dependency changes during the course of mitosis or that feedback loops obscure results. In animals three feedback loops have been identified that allow Bub1, Mps1, Plk1 and Haspin kinase to potentiate Aurora B localization and activity. Aurora B localizes in a complex termed the centromeric passenger complex (CPC) including Survivin, Borealin, INCENP and Aurora B itself[613]. The CPC recognizes two histone phosphorylation marks, namely phosphorylated H3T3, which is generated by Haspin kinase and read by Survivin, and Bub1 phosphorylated H2A, in humans on T120, read by Shugoshin which in turn binds to Survivin[614-619]. Because Haspin is recruited to Cohesin by Pds5, its H3pT3 mark is placed along the long axis of condensing chromsosomes while the Bub1 placed H2ApT130 spans the inner centromere, the chromatin between two kinetochores. It is thought that the CPC localizes to the intersection of these two marks at the inner centromere. The animal CPC can amplify its own localization by a feedback loop in which it phosphorylates Haspin, increasing its activity, by a feedback loop in which Mps1 promotes Bub1 mediated formation of H2ApT130 and a feedback loop including Plk1 which enriches the CPC on unaligned chromosomes in a Plk1 and Aurora B dependent manner[620-622]. The latter Plk1 feedback loop may also be reasonably direct as Plk1 is phosphorylated and activated by Aurora B[623]. Mps1 can further phosphorylate Borealin, enhancing Aurora B activity and phosphorylation of the CPC by CDK1 is required for it to bind Shugoshin[610, 617]. Subtle hints suggest that there may be additional factors active in targeting animal CPC. A construct that contains a full length Survivin but only the N-termini of INCENP and Borealin does not target centromeres, suggesting an involvement of Borealins C-terminus[624]. Furthermore under tension the CPC partially re-localizes from the centromere to the inner kinetochore and a second binding site has been invoked to explain this[625]. In contrast to animals and fission yeast, budding yeast CPC localization appears to be controlled by none of the described pathways. Neither Haspin nor Bub1 are needed for its recruitment to centromeres. However, budding yeast Survivin binds directly to the Ndc10 subunit of CBF3 [532, 626]. Because INCENP and Aurora B but not Survivin are lost from centromeres when ScCENP-U is absent a second interaction between ScCENP-U and the CPC, distinct from the interaction between CBF3 and Survivin, has been suggested.[627].

Plk1 appears on animal centromeres before Aurora B. It binds phosphoepitopes via its polo-box binding domain. These epitopes are either generated by proline-directed kinases such as CDK1 or by Plk1 itself. The latter is known as self-primed recruitment and thought to amplify the localization of Plk1 via a product activated feed-forward mechanism while non-self-priming recruitment by CDK1 would be responsible for initial recruitment[628, 629]. CDK1 primed binding sites are found on INCENP, Bub1 and on BubR1 while self primed binding sites are found on CENP-U and the Dynein/Dynactin associated NudC[630-635]. A loss of NudC has been described to lose focused localization of Plk1 to the centromere while a loss of CENP-U leads to a loss of Plk1 from interphase centromeres but only to a decrease from mitotic centromeres. While BubR1 does not appear to be generally required for Plk1 recruitment, a loss of Bub1 reduces Plk1 at the centromere and INCENP has been described as absolutely required for Plk1 recruitment.

Similarly to Bub1, the requirements for kinetochore recruitment of BubR1^{Mad3} are debated. It is generally agreed upon that recruitment of BubR1 requires Bub1, Bub3 and Knl1. However, results conflict, even in the same cell line, as to whether Mps1 and Aurora B are required for its recruitment[160, 192, 496, 522, 530, 531, 606, 608, 610, 636-639].

Lastly, in animals, CDK1 localizes to kinetochores via cyclinB1. No binding partner at the kinetochore is known, but it requires the NDC80C and surprisingly Mad2, which is thought to have no role in attachment besides SAC signaling[640, 641].

Some of the introduced kinases demonstrate either tension or attachment sensitive behavior. This behavior manifests either in the tension or attachment dependent phosphorylation of substrates or in tension or attachment dependent localization. Bub1 and BubR1 display tension sensitivity and their levels decrease as kinetochores come under tension. Bub1, additionally, is attachment sensitive and is partially lost from kinetochores upon attachment. CDK1 and Mps1 are attachment sensitive and lost from attached kinetochores[611, 641]. Tension sensitive phosphorylation is established for both Aurora B and Plk1. Aurora B phosphorylates, among others, NDC80C in response to a lack of tension while these phosphoepitopes are lost when tension is applied[642, 643]. Although not all of its targets are phosphorylated in a tension dependent manner, Plk1 generates the 3F3/2 epitope on BubR1 which is lost under tension[633, 644-647]. The basis of Aurora B's tension sensitivity is well investigated. Within the CPC, Aurora B is bound to the C-terminal IN box of INCENP, while the N-terminus of INCENP forms a three helix bundle with Survivin and Borealin, required for the centromere localization of the CPC. INCENP is thought to form a long flexible bridge between kinase activity and centromere targeting activity of the CPC and thereby to act as a "nanoruler". It tethers Aurora B to the centromere and limits its range. Once tension is applied to the kinetochore it stretches, moving Aurora B substrates out of Aurora B's range[466, 569, 624, 648-652]. The basis of Plk1’s tension sensitivity is not known yet.

2.6.7 Regulation of kMT dynamics, attachment and error correction

The kinetochore components introduced above facilitate and regulate attachment, kMT dynamics and error correction. Error correction is an important component of a system that relies on stochastic encounters of microtubules with kinetochores to achieve biorientation of chromosomes. The error correction mechanism reverses failed, syntelic, attachments in which both kinetochores are attached to a single pole. It discriminates between correctly and incorrectly attached kinetochores by their ability to support tension. Only amphitelic attachment, in which each kinetochore is pulled to one of the opposing poles, is stabilized. Syntelic attachments are destabilized by the tension sensitive Aurora B kinase [638, 653-662]. This entails phosphorylation of KMN components, the N-terminus of Ndc80 implicated in MT binding and oligomerization on the MT lattice, the MT binding domain of Knl1 and the Dsn1 subunit of the MIS12C, decreasing the KMN networks' affinity for MTs[478, 569, 643, 663]. In budding yeast Aurora B additionally phosphorylates DAM1C, severing its link to NDC80C and thereby to the kinetochore[552, 569, 652, 664, 665]. The animal SKA-C is phosphorylated by Aurora B and this inhibits its KMN dependent accumulation at kinetochores, suggesting a similar mechanism controlling interactions between the KMN network and Ska complex[666]. Under tension, DAM1C/SKA-C and the KMN network are stretched away from the inner kinetochore and separated from Aurora B kinase, stabilizing the amphitelic attachment.

Cells that attach multiple kMTs to their kinetochores, such as animal cells or fission yeast, face an additional problem, merotelic attachments, in which one kinetochore is attached to both poles. To overcome this they employ additional error correction mechanisms. Release of kMTs from the KMN network is a specific response to tension. Merotelic attachments in contrast generate significant tension as two portions of the KT are stretched to opposite poles, rendering them invisible to the SAC [667]. Thus, the stimulus that activates merotelic error correction is currently ill defined. In addition to mere release of a kMT, animal cells are able to induce kMT depolymerization, either of an entire kFiber or of individual kMTs within a kFiber. The first is observerved for syntelic chromosome attachments, which, after moving to the pole, depolymerize an entire kFiber, freeing the kinetochore for MT capture from the other pole[668]. The second may be a continuous process in which individual kMTs are released from the KT and then re-grow, while the rest of the bundle remains attached, resulting in net turnover of the stable kFiber +end[669]. kFiber +ends show a high turnover in prometaphase, a lower turnover in metaphase which then abruptly decreases further at anaphase onset[458, 670]. Prometaphase turnover has been ascribed to the kinesin-13 Kif2b, while the slower metaphase turnover has been ascribed to the activity of MCAK[459]. Because a loss of Kif2b leads to a failure to correct syntelic attachments, an error that presumably arises early during prometaphase, Kif2b is thought to facilitate the destabilization of an entire kFiber. In contrast, a loss of MCAK allows correction of syntelic attachments but leads to an accumulation of merotelic attachments and therefore MCAK is thought to be active during a less stringent error correction phase later in prometaphase congression[456, 459, 671]. It is questionable if the error correction mechanism actively senses merotelic attachments. Aurora B is enriched at merotelic attached KTs and recruits additional MCAK, however because both MCAK and the CPC recruiting Sgo2 are also enriched at leading KTs of bioriented chromosomes this may not be a specific effect[452, 672]. One may speculate that a nonselective turnover of individual kMTs by MCAK allows the abnormally stretched and distorted kinetochore to reorient slowly under the applied tension until one of the two kFibers "wins out", generating either a amphitelic or syntelic attached chromosome[457]. Kinesin-13 based error correction remains under control of Aurora B. Kif2b is evicted under tension by astrin and astrin localization in turn is negatively regulated by Aurora B in absence of tension[458, 460]. Aurora B phosphorylation further inhibits MCAK activity and MCAK relocalizes from the centromere to the inner kinetochore under tension, potentially escaping inhibition by Aurora B[461, 673]. Therefore, Aurora B regulates a tension dependent switch to an error correction phase that deals mainly with merotelic attachment. It is interesting to note that the two kinesin-13s implicated in error correction are those that drive chromosome oscillation. Oscillation may be a result of MT turnover by Kif2b and MCAK and a manifestation of error correction. As only a subset of chromosomes oscillate, those located centrally in the spindle, there appears to be no requirement for oscillation per se[450, 487, 657, 674]. Mps1 is involved in error correction and biorientation in both yeast and man. In vertebrate cells Mps1 operates upstream of Aurora B and displays a similar loss of function phenotype, the inability to correct syntelic attachments. Thus it may act via its feedback pathway on Aurora B[607].

Beyond error correction, a number of factors promote the formation of stable kFibers and stable attachments. These include components of the SAC, Bub1, Bub3 and BubR1^{Mad3}, structural components of the kinetochore, such as the KMN network and the CCAN as well as MAPs such as EB1, APC and CLASPs. Although relations among these components are not well defined, some regulatory pathways are beginning to emerge.

Among structural kinetochore components, the NDC80C is absolutely required for kFiber formation and loss of MIS12C or Knl1 decreases the number of stable kFibers, in line with their requirement for end-on attachment[496, 500, 675, 676]. An Ndc80 mutant that is immune to Aurora B phosphorylation and error correction displays dampened chromosome oscillations while antibody injections against Ndc80 abolish oscillation and lead to increased tension, suggesting that attachment stability increases when NDC80C cannot be released from kMTs[487, 625]. Loss of the CCAN groups CENP-H/I/K and CENP-L/M/N, which have a role in but are not absolutely required for NDC80C recruitment, surprisingly leads to the opposite phenotype, hyperstable kFibers[451]. Therefore, CENP-H/I/K and CENP-L/M/N appear to have destabilizing function on kFibers. When CENP-O is depleted, kFibers indeed become unstable, dependent on CENP-H/I/K and CENP-L/N/M[570]. If this was due to an effect on NDC80C, CENP-O could inhibit CENP-H/I/K's and CENP-L/N/M's action on the NDC80C. Supporting this idea, vertebrate CENP-U is degraded by ubiquitin mediated destruction before the onset of anaphase in response to CENP-U phosphorylation by Plk1[582, 632]. This could conceptually be a regulatory mechanism affecting kFiber dynamics. This line of argument, however, is troubled by the fact that while CENP-O depletions do show increased NDC80C recruitment to the kinetochore that is dependent on CENP-H/I/K and CENP-L/M/N and both CENP-H and CENP-U have been shown to interact with Ndc80, Ndc80 contains the MT binding domain of the NDC80C, not its kinetochore localization domain and an increase of NDC80C on a kinetochore would be predicted to increase, rather than decrease, kMT stability[570, 677-679]. Because a loss of CENP-H had no effect on recruitment of kinetochore components known to affect kMT stability such as Aurora B, Shugoshin, MCAK, Bub1, BubR1, Kif18a or CENP-F and because CENP-Q was demonstrated to bind MTs directly, it has been suggested that the CCAN's effect on kFiber stability may be direct rather than mediated through the KMN network or other kinetochore proteins. However, not all kinetochore localized potential MT regulators have been exhaustively tested yet[451, 596].

While kMT destabilizing mechanisms have been described, i.e. release and depolymerization, mechanisms that promote stabilization are still very much speculative. Conceptually, this could happen by simply escaping the error correction mechanism when tension is applied. Furthermore, classical theoretical biochemistry demonstrates that applying traction to a MT +end promotes growth and disfavors shrinkage[239]. Molecularly, the kinesin CENP-E can promote ATP-dependent MT growth, while CLASPs and the yeast Dam1 complex support MT elongation under tension[290, 291, 680, 681]. Although this would explain stable attachment and polymerization under tension, together with current models of error correction it does not account for a range of effects. Firstly, in absence of attachment, the KMN network should be Aurora B phosphorylated and initial MT capture therefore should be suppressed. The kinase Nek2a has recently been described as a factor that increases NDC80C affinity for MT by phosphorylation and may allow NDC80C attachment to MTs despite being phosphorylated by Aurora B. However upstream regulators of Nek2A are so far unknown[682]. Secondly, the observed kFiber pushing on poles as well as the maintenance of stable kFibers attached to kinetochores on monopolar spindles or after severing kFibers from poles should, according to current models, not exist. In the absence of tension these structures should undergo Aurora B based error correction and be released from the KT.

An emerging pathway that opposes Aurora B mediated kFiber destabilization and promotes stable kFibers rests on BubR1, Bub1 and Bub3, the latter two being required for localization of BubR1. In absence of either the occurrence of lateral attachments increases over the observed end-on attachments to stable kMTs. Aurora B has been demonstrated to operate antagonistic to BubR1 as inhibition of Aurora B rescues unstable kFibers in BubR1 depleted cells[683-687]. BubR1 receives upstream input and its kinase activity has been reported to be enhanced by multiple factors, by binding of CENP-E, weakly by a CDK1 priming phosphorylation and strongly by the Plk1 phosphorylation following priming phosphorylation by CDK1 [633, 688]. Therefore Bub1, Bub3 and BubR1 may integrate multiple signals to stabilize kFibers and they are well positioned within the kinetochore to do so. Bub1 and BubR1^{Mad3} bind to Knl1 and interact individually with Bub3[496, 689]. One recently identified mechanism by which BubR1 opposes Aurora B mediated kFiber destabilization operates by counteracting Aurora B phosphorylation via Plk1 and Protein phosphatase 2A (PP2A). Like a loss of Bub1, Bub3 and BubR1, a loss of Plk1 leads to increased lateral attachments and BubR1 phosphorylation by Plk1 is required for chromosome alignment [690-692]. Plk1 phosphorylates the kinetochore attachment regulator domain (KARD) of BubR1 that promotes PP2A recruitment, leading to dephosphorylation of Aurora B substrates in the KMN and placing the kinetochore in an attachment competent state. This work also questioned the long established kinase activity of BubR1 and suggested it to be a pseudokinase that, although it retains a catalytic triad in humans, has lost its kinase activity. BubR1's previously described kinase activity may be entirely due to contaminating kinases and its scaffold function may be more important[693, 694]. Indeed the involvement of BubR1's possible kinase activity has been debated for some time. Surprisingly, PP2A depletion can be rescued by inhibiting Plk1 and PP2A reciprocally controls Plk1 localization to the kinetochore, likely by dephosphorylating PBDs. The role of this apparent feedback inhibition remains to be investigated but suggests upstream components in this pathway[693]. BubR1 additionally interacts with CENP-E via its kinase domain and both are found in complex with the kinesin-8 Kif18a[688, 695]. Furthermore BubR1, Bub1 and Bub3 are found in complex with APC and BubR1 is required for APC recruitment. APC is a highly specific substrate for phosphorylation by Bub1 and possibly BubR1 although the mentioned recent evidence against BubR1's kinase activity now questions the latter[696, 697]. APC in turn interacts with EB1 and the formin mDia3 and all three bind MTs directly. On top of that, mDia3 binds to the centromeric nucleosome by direct interaction with CENP-A[477, 698]. No comprehensive study to date investigates the relationship among all of these components. It is therefore unclear if they are part of the Plk1-BubR1-PP2A kFiber stabilizing pathway or act in parallel. APC, EB1 and BubR1 were initially described to be active in the same kFiber-stabilizing pathway, but a recent study demonstrates that in absence of APC, kFibers become hyperstable, counterintuitive, given APC's crosslinking and MT stabilizing function in vitro and in vivo at the cell cortex[669, 696, 698-701]. This may be explainable by APC’s association with MCAK in Xenopus, although in human cells over-expression of Kif2b, but not MCAK, rescues hyperstable kFibers[410, 669].

Animal kinases regulate not only error correction and kFiber stability but also the recruitment and ejection of kinetochore proteins in response to attachment state. Mps1 is required for the initial localization of the RZZ complex but not its maintenance at unattached kinetochores. CENP-E recruitment requires Bub1 and is partially dependent on BubR1 while Mps1 requirement is debated [530, 531, 606, 607, 609, 683, 688, 702-706]. Bub1 is also required for recruitment of CENP-F[522, 531]. Aurora B is required for recruitment of both CENP-E and the RZZ complex, which is not surprising, as it localizes Mps1 and Bub1. However it has a direct role in at least the recruitment of the RZZ complex as Aurora B phosphorylation of Zwint-1 is required for recruitment of RZZ and, downstream, of Dynein and Dynactin[531, 638, 707]. Aurora B's role in the recruitment of MCAK and Kif2b has been mentioned previously[460, 673]. In addition, Plk1 is required for Kif2b localization and activation[708]. Furthermore, Plk1 phosphorylates Dynein, decreasing its affinity for ZW10 and promoting binding to Dynactin, inducing Dynein mediated stripping of kinetochore components[514, 520].

Taking these observations together, one may imagine a mechanism in which a Plk1 based early and an Aurora B based late pathway regulates kMT attachment. Initially, Plk1 places Dynein/Dynactin in a stripping competent state, promotes kFiber attachment and stabilization to the KMN network by antagonizing Aurora B via BubR1 and PP2A as well as early error correction via Kif2b. Following initial end-on attachment, Dynein stripping commences, removing BubR1 and permitting Aurora B phosphorylation. Aurora B inhibits further loading of RZZ in response to tension, deactivates Kif2b mediated error correction by permitting astrin to localize to the kinetochore and activates MCAK and KMN dependent error correction.

The work demonstrating CENP-H/I/K's involvement in kFiber dynamics additionally showed that kFibers were not only hyperstable following a loss of CENP-H, but that kFiber flux was entirely absent[451]. While +end kFiber turnover and kinetochore movement speed was increased, chromosomes ceased coordinated oscillations. Similarly, loss-of-flux and loss of oscillation phenotypes have been described for a number of factors active in error correction, some of which do interact with the CCAN. Aurora B is required for flux and oscillation and in its absence kFibers become hyperstable[657]. A loss of Shugoshin leads to unstable kFibers, which may be explained by one of its additional roles, recruitment of PP2A[674, 693, 709]. Antibody injection against Shugoshin produced a phenotype very similar to Aurora B/MCAK or CENP-H depletions, a loss of oscillation, hyperstable kFibers and an absence of flux. Loss of MCAK or Kif2b leads to a loss of kMT turnover and oscillations. More specifically loss of Kif2b leads to an absence of oscillations of mono-oriented chromosomes, while a loss of MCAK has been described to decrease KT movement speed and to interfere with oscillation of bioriented chromosomes because kinetochores become unable to sustain poleward movement[427, 453, 456]. Interestingly, MCAK and Sgo2 display kinetochore localization reciprocal to CENP-I during oscillation, concentrating at the leading kinetochore while CENP-I is increased at the trailing kinetochore[451, 452]. If both MCAK and CENP-H/I/K have kFiber destabilizing activity, this would suggest that in order for chromosomes to move or oscillate, leading and trailing kFibers need to be differentially destabilized. An alternate mechanism for oscillation would be for all MTs of a kFiber to switch coordinately between growth and shrinkage, allowing the entire kFiber at the leading KT to shrink while the kFiber at the trailing KT grows. Such a mechanism has become untenable with the demonstration that two thirds of the kMTs within a kFiber are depolymerizing even when a kFiber grows and an alternative model suggests that a subpopulation of kMTs needs to be detached from kinetochores to permit oscillation[457, 710].

Although the CCAN´s influence on kFiber stability has been suggested to be independent of Aurora B and downstream effectors such as MCAK and NDC80C, direct interactions between CENP-H and both Ndc80C and MCAK have been demonstrated[677]. As mentioned previously, when tension is applied to a kinetochore, Aurora B and MCAK delocalize from the centromere to the inner kinetochore and a second binding site has been suggested. Because MCAK relocalization requires dephosphorylation of Aurora B generated phosphoepitopes this positional shift is not simply a response to kinetochore stretching under tension[452, 461]. Speculatively, the vertebrate CCAN may play a role in relocalization of MCAK and/or Aurora B to the kinetochore but not be absolutely required for its localization to the centromere. This is based on an observation in budding yeast. Here as, previously mentioned, the CBF3 complex is absolutely required and ScCENP-U is partially required for CPC recruitment. ScCENP-O in turn has been suggested to promote the timely eviction of the CPC from the centromere in response to Cdc14 release by the FEAR. Ndc10 of the CBF3 complex, ScSurvivin and ScCENP-O are SUMOylated. SUMOylation of ScCENP-O is not required for kinetochore recruitment of the CPC but may rather play a role in its eviction at anaphase, hinting at a possible SUMOylation pathway that includes the ScCCAN and regulates CPC localization[711-713]. Similarly, Boralin in human cells is SUMOylated by RanBP2, though a role for this modification is not clear[714]. The human CCAN, specifically CENP-I and -H are SUMOylated, however a loss of SUMOylation leads to a loss of CENP-H/I/K from the kinetochore and the expected gross kinetochore assembly defect[715].

Lastly, the effect a loss of CCAN complexes has on kFiber stability affects the force balance required to form a bipolar spindle. The appearance of multipolar spindles by centrosome fragmentation has been described for depletions of CENP-H/I/K and CENP-M, as is often observed when traction on kFibers is high enough to shatter centrosomes [554, 556, 578, 597, 716]. The opposite phenotype arises in CENP-Q/U/P/O/R complex depletions. A loss of CENP-P or CENP-O induces monopolar spindles. A depletion of either the CENP-H/I/K or the CENP-L/M/N group rescues not only unstable kFibers but also the monopolar spindle phenotype, underscoring the antagonistic relationship between CENP-Q/U/P/O/R and both CENP-H/I/K and CENP-L/M/N. The bipolarization defect resulting from a CENP-O depletion arises from an inability to generate kFiber pushing during prometaphase to separate centrosomes and is not specific to CENP-O, as it is also observed when NDC80C, CENP-E or both MCAK and Kif2a are lost. As double depletion of Kif2a and MCAK abolish flux, flux is thought to be required for prometaphase centrosome separation. Flux is however not required for chromosome oscillation[369, 375, 439]. Thus, the activity that destabilizes kFibers and induces monopolar spindles rests on CENP-H/I/K and CENP-L/M/N. The multipolar spindle phenotype in CENP-H/I/K and CENP-L/M/N group depletions also suggests either an underlying or independent activity responsible for spindle pole shattering possibly due to traction[570, 717].

Together these observations present a complex and incompletely defined interaction network regulating attachment and detachment of animal kinetochores. Budding yeast chromosome dynamics are less complex and many of the factors active at animal kinetochores are either not conserved or not present on yeast kinetochores[532]. Specifically, many kinetochore components that mediate early attachment, conversion to end-on attachment and oscillation in animals, including CENP-E, CENP-F, Nde1, Lis1, Dynein/Dynactin, Polo-like kinase, APC, Kif2b and MCAK are absent from budding yeast kinetochores. This may be due to its simplified prometaphase in which kinetochores are captured shortly after centromere replication as well as the requirement for only a simple error correction mechanism for syntelic attachments. Yet, in addition to kMT capture and biorientation promoted by the KMN network and DAM1C and its regulation by Aurora B, a second pathway has been suggested to act independently of Aurora B through Bub1, Shugoshin and Mps1. A hint at how Mps1 would promote biorientation is provided by the observation that Mps1 is required to "lock" the DAM1C onto kMT +ends, but it is not known if this is an activity of Mps1 alone or the entire pathway. In addition to ScBub1, loss of ScBub3 and ScMad3 leads to a chromosome transmission fidelity defect. It will be interesting to determine whether the role of ScBub1, ScBub3 and ScMad3 in chromosome segregation is in any way reminiscent of that of Bub1, Bub3 and BubR1 in animals[718-721]. The role of the budding yeast CCAN in chromosome biorientation is not well investigated. Initial characterization demonstrates that all nonessential ScCCAN proteins show chromosome transmission fidelity defects when lost[561-564, 566]. Loss of ScCENP-Q/U leads to a biorientation and error correction defect explained by ScCENP-U's role in budding yeast CPC recruitment[627]. More recently a weak biorientation defect upon loss of ScCENP-P has been demonstrated. The basis for this is a defect in centromeric loading of Cohesin observed upon loss of ScCENP-O/P or ScCENP-L/N, which then likely leads to misorientation of sister kinetochores[590, 722].

2.6.8 Involvement of the structural kinetochore in SAC activation.

Although recruitment of SAC proteins to kinetochores is often used as a proxy for SAC activity in the literature, it cannot be directly equated with a SAC arrest. Mad1 and Mad2 leave the kinetochore before anaphase while Bub1 and BubR1 persist at low levels into anaphase[196, 612, 723]. Kinetochore recruitment of SAC proteins depends firstly on upstream binding partners within the kinetochore and regulating kinases such as Aurora B and secondly is, by incompletely defined mechanisms, sensitive to attachment state and tension on the kinetochore. The observation that, in animals, kinetochore localization of Mad1 and Mad2 is responsive to attachment while localization of Bub1, Bub3 and BubR1 is responsive to tension has sparked a debate over whether the SAC is silenced by attachment or tension[724, 725]. An enticingly simple model states that the SAC proper only recognizes unattached kinetochores[663]. The error correction mechanism in turn stabilizes kinetochore-microtubule attachments that support tension while it severs microtubule attachments to kinetochores that do not support tension and thereby coverts them back into their unattached state in which they generate a SAC signal. Mad1 and Mad2 display a localization behavior that is consistent with this idea, they are lost upon attachment even if tension on the kinetochore is reduced by treatment with Taxol. Alternatively, the SAC may be able to sense both, unattached and tensionless kinetochores, directly. In line with this idea, BubR1 is partially lost from the kinetochore when under tension but remains at high at attached, tensionless kinetochores. Bub1 and Bub3 in turn have been described as both attachment and tension sensitive as their kinetochore localization decreases moderately upon attachment and strongly when tension is applied[166, 167, 196, 612, 703, 723, 726-730].

How would localization of SAC proteins be rendered responsive to the attachment state? One possibility is an attachment or tension sensitive recruitment to kinetochores. Aurora B is a candidate factor for this regulated recruitment. Mps1 as one upstream SAC kinase may be able to sense unattached kinetochores independently, possibly by binding to NDC80C, because although its recruitment is accelerated by Aurora B, Aurora B is not absolutely required for its localization. Bub1, the second upstream SAC kinase, localizes to kinetochores independent of Aurora B in yeast but possibly dependent on Aurora B in animals. Because of the recruitment of Bub1 through Mps1 phosphorylation on Knl1 in yeast, Aurora B may have an indirect effect on Bub1 recruitment through Mps1 here but in animals requirement of Mps1 for Bub1 recruitment is still debated[531, 601-603, 607, 655]. Localization requirements of the SAC proteins Bub3 and BubR1 are not fully clear. It is generally agreed upon that Bub1 and Bub3 are required to recruit BubR1 to the kinetochore, however, like for Bub1, a requirement for Mps1 in vertebrate BubR1 recruitment is debated. Furthermore, Bub3 may recruit Bub1 or conversely be either co-dependent or fully dependent on Bub1 for recruitment[160, 191, 423, 522, 530, 609, 636, 637, 685, 689, 704, 731]. The recruitment dependency of Bub1 and BubR1 on Aurora B suggested by some authors could prove to be a tension sensitive mechanism rooted on the CPC. Supporting this, tension dependent phosphorylation of ScMad3 by ScAurora B is required for a tension dependent SAC arrest in budding yeast. However a substantial amount of authors argue against a requirement for Aurora B in Bub3 and BubR1 recruitment in animals[636, 638, 639, 732, 733]. An alternative explanation would be a loss of these proteins in response to tension. BubR1 is stripped from the kinetochore by Dynein, Bub3 has been found to interact with dynein light chain 3 and both BubR1$^{\text{Mad3}}$ and Bub3 have been found in complex with Spindly[515, 516, 734]. Notably, in fission yeast but not animals, Bub3 is not required to establish a SAC arrest but has a role in silencing the SAC after chromosome alignment[735]. A third mechanism rendering the SAC responsive to tension that is not based on localization has been suggested, following the observation that, under tension, NDC80C and Knl1 shift their relative position. Here it is thought that a signaling complex consisting of Bubs bound to Knl1 and other SAC proteins, such as Mad1, Mad2 and Mps1, bound to NDC80C is turned off as the two KMN components separate under tension[736]. Although Bub1 is known to phosphorylate Mad1 and a complex of Bub1, Bub3 and Mad1 has been described, the binding partners of Mad1 and Mad2 at the kinetochore are far from clear[155, 201]. While a yeast two-hybrid interaction between Mad1 and Ndc80 has been described, NDC80C is, at least, not its only recruitment factor in vivo because a loss of NDC80C does not lead to a failure of Mad1 and Mad2 to localize. Rather, in absence of NDC80C, Mad1 and Mad2 are not retained against Dynein-mediated stripping which initially created the impression that it was lost from kinetochores[523, 737]. A second possible recruiting factor for Mad1 and Mad2 is the RZZ complex as its absence leads to a loss of Mad2 from vertebrate kinetochores [506, 738]. Because RZZ localization requires NDC80C and Mad2 localizes in absence of NDC80C, the RZZ complex again is either not a direct interaction partner or not the only one[490]. A third possibility is Mad1´s and Mad2's interaction with the nuclear pore subcomplexes (NPC). During interphase, Mad1 and 2 localize to NPCs, which in yeast requires the Nic96 complex containing Nic96, Nup53, Nup59, Nup157, Nup170, Nup188 as well as a nuclear basket complex consisting of Mlp1, Mlp2, Nup1, Nup2, Nup60. Mad1 and Mad2 are found associated with Nic96 complex members in co-immunoprecipitations. The nuclear export receptor Crm1, which in animals is required for kinetochore loading of the Nup107-160 complex, as well as RanGTP and a nuclear exclusion sequence on Mad1 are required to load Mad1 onto unattached yeast kinetochores. A Mad1 NES mutant however retains an active SAC, despite Mad1's inability to localize to kinetochores, underscoring that SAC protein localization does not absolutely correlate with SAC activation[739-743]

Both Mad1 and Mad2 require Mps1 and Bub1 for their recruitment and Mps1 is required for O-Mad2/C-Mad2 turnover[164, 191, 522, 523, 531, 609, 637, 702, 704]. While Mps1 localizes to unattached kinetochores and is required to recruit Mad1 and Mad2 it does not need to be at the kinetochore to accomplish this[523, 601, 603]. When Mps1 is rendered cytoplasmic by Aurora B inhibition, Mad2 appears at KTs after a delay and the initial onset of cyclin B degradation is halted, producing a stable SAC arrest. Mps1 overexpression induces a SAC arrest despite correct attachment of all chromosomes and can do so in absence of kinetochores. Mps1 is activated by trans-autophosphorylation and leaves the kinetochore swiftly, dependent on its own kinase activity. Thus, in response to a lack of attachment, Aurora B concentrates Mps1 at kinetochores to expedite its activation, though it may autoactivate slowly at unattached kinetochores or in the cytoplasm[603, 611, 744-746]. Based on this, recruitment and release of Mps1 has been suggested to supply the cytoplasm with active Mps1 in response to SAC activation, potentially providing a SAC signal upstream of MCC assembly [202].

Recruitment of SAC proteins to the KMN network would suggest that it is, together with the KMN recruiting CCAN network, required for SAC signaling. However, while a loss of NDC80C and Knl1 in both yeast and animals abolishes the SAC, a loss of MIS12C only impairs the SAC and cells arrest if all kinetochores detach but fail to maintain arrest[51, 493, 496, 594, 597, 675, 676, 747]. The requirement of CCAN proteins for SAC signaling has been extensively mapped in budding yeast[479, 480, 675, 748]. Surprisingly, not a single ScCCAN protein, not even ScCENP-C, has been found to be required for a SAC arrest although the employed temperature sensitive alleles may be hypomorphic in this respect. The only known kinetochore proteins that abolish SAC signaling in budding yeast when lost are ScNDC80C, ScKnl1 and the CBF3 complex. To observe a loss of SAC signaling in response to loss of Ndc80C components in budding yeast, one needs to either inactivate Spc24 or Spc25 or both Nuf2 and Ndc80. This may be either due to residual or redundant function of the remaining NDC80C components. It has, however, been reported that ScCENP-U mutants display a defect in maintaining a robust arrest[591]. During general characterization of vertebrate CCAN proteins, no CCAN protein was found absolutely required for a SAC arrest, although a loss of CENP-C or Plk1 phosphosites on CENP-U impaired the SAC[555, 556, 558, 576, 582]. Closer investigation demonstrated a SAC arrest to be impaired in CENP-O and CENP-I depletions. CENP-O displays a loss of SAC only under very stringent depletion while under CENP-I depletion, the SAC is unable to arrest mitosis during an unperturbed cell cycle but does so when all kinetochores are detached by Nocodazole treatment. It appears that after depletion of CENP-I, cells become polyploid during the first failed mitosis, accumulating sufficient chromosomes, and thereby kinetochores, to arrest robustly the subsequent mitosis[521, 717].

2.7 Centromere inheritance in animals and budding yeast

When the budding yeast centromere was isolated and defined as a ~125bp genomic DNA element that was sufficient to direct kinetochore assembly, it was speculated that animal centromeres may similarly be genetically defined[749]. 30 years later this appears highly unlikely as no animal centromere-defining sequence has been found, although low efficiency kinetochore assembly is observed on human type α-I satellite DNA[750-753]. The genetically defined centromere of budding yeast appears to be a relatively recent evolutionary acquisition and an exception to the rule[532]. In animals the location of a centromere is predominantly epigenetically defined. This is firstly evidenced by the occurrence of neocentromeres on chromosomal loci that have no significant similarity to the repetitive DNA sequences found at animal centromeres. While these neocentromeres are functional, inherited over multiple generations and recruit all proteins expected for an active centromere, including centromeric nucleosomes, CCAN proteins, KMN components and SAC proteins, the original centromere locus is silent and recruits none of these factors[754-759]. A second well established system in which epigenetic effects on centromere activity are observed is fission yeast. Here, when the genomic centromere sequence is abbreviated, centromeres switch between active and inactive states and inherit the current state over a number of generations[760].

Assembly of a kinetochore on a centromere that is defined by sequence is conceptually very simple. A DNA binding protein may recognize the centromeric sequence and recruit downstream kinetochore components. Budding yeast kinetochores assemble in such a manner. Its ~125bp centromeric consensus sequence is subdivided into 3 linearly arranged elements, CDEI, CDEII and CDEIII[761]. The 26bp CDEIII sequence is absolutely essential for kinetochore function and is recognized by CBF3, which directs downstream kinetochore assembly. The CBF3 complex consists of Ndc10, Cep3, Ctf13 and Skp1 and is a recent acquisition of a family of budding yeasts, including S.cerevisiae, which have evolved genetically defined point centromeres. CBF3 is the most upstream factor in kinetochore assembly and required for recruitment of all other kinetochore proteins including the centromeric nucleosome[480, 568, 762-767]. While CDEIII is essential for kinetochore formation, it requires in addition at least a fragment of the AT rich CDEII element which is located between CDEI and CDEIII[768]. A body of evidence indicates that CDEII is bound by the single centromeric nucleosome present in yeast kinetochores[769-772]. The 8bp CDEI element is recognized by the homodimeric bHLH family transcription factor CBF1. Its exact role at the centromere is unclear but an effect on nucleosome positioning, DNA topology and a direct interaction between CBF1 and the CDEIII binding CBF3 complex have been demonstrated[773-782]. The latter implies the CDEII element to form a loop around the centromeric nucleosome that is secured by interaction of CBF1 and CBF3.

Although CBF3 is critical for kinetochore assembly, thus far no interactions with structural components of the kinetochore have been described. Its role has recently become clearer with the identification of the HJURP/Scm3 protein family. HJURP/Scm3 family proteins are histone chaperones that facilitate loading of the centromeric nucleosome at the centromere[783-787]. Scm3 and CBF3 interact and thereby CBF3 may facilitate sequence specific targeting and loading of centromeric nucleosomes during S-phase[788]. Subsequently, structural kinetchore components would assemble on top of this nucleosome as it is the case in vertebrates, where the centromeric nucleosome is the most upstream factor for kinetochore assembly[596]. Vertebrate CENP-C and CENP-N have been demonstrated to interact with the centromeric nucleosome and this may be the first step in CCAN assembly at the kinetochore[587, 588]. The budding yeast centromeric nucleosome is required for recruitment of at least ScCENP-C, which is in turn required for localization of ScCENP-O[592].

Epigenetic inheritance requires a mark other than DNA to define centromere location. The prime candidate to provide this mark is CENP-A, the centromeric histone found to replace canonical Histone H3 in centromeric nucleosomes[789-792]. Animals and most yeast do not possess a CBF3 complex and here CENP-A is the most upstream factor in kinetochore protein recruitment. Kinetochore assembly on sperm chromatin vividly illustrates its presumed function as a mark. In frog and bovine spermatogenesis canonical nucleosomes are stripped from the genome and replaced with protamines. CENP-A however is quantitatively retained and after fertilization directs assembly of a kinetochore[579, 793].

An epigenetic mark would require a mechanism to direct its own persistence and inheritance. In contrast to budding yeast, CENP-A levels at the vertebrate centromere decrease by 50%

following DNA replication and are subsequently replenished, replication independent, during early G1[794-796]. Thus a mechanism for a cell cycle specific deposition of CENP-A exists. Identification of factors involved in deposition of CENP-A in model systems other than budding yeast suggest that it is a three step process that encompasses licensing, loading and maintenance of CENP-A in G1. Fission yeast Mis18 has two vertebrate orthologs, Mis18α and Mis18β. Mis18α and Mis18β together with Mis18BP1 form the vertebrate Mis18 complex (Mis18C)[796-799]. Mis18BP1 is absent in fission yeast and only Mis18BP1 is present in C.elegans. Mis18C localizes to kinetochores at telophase, slightly before HJURP. Mis18C is believed to prime the centromere for subsequent loading of CENP-A by HJURP and force localizing of either HJURP or Mis18α to ectopic sites can induce kinetochore assembly[800, 801]. Two additional Histone chaperones may be involved in loading, RbAp46/48 which bind H4 and Nucleophosmin 1 which binds to all core histones[784, 786, 799, 802]. The priming event may include histone modifications as a deacetylase inhibitor or a centromere tethered histone acetylase domain are able to rescue loss of vertebrate Mis18C but not HJURP[797, 801]. Later factors in CENP-A deposition are the remodeling and spacing factor (Rsf) and MgcRacGAP. Rsf localizes to centromeres at mid G1, MgcRacGAP at late G1. A loss of Rsf1 appears to lead to a defect not in recruitment but in loading of CENP-A as it becomes more amenable to salt extraction. MgcRacGAP, a GTPase activating protein appears to act late in G1 and is required to maintain loaded CENP-A. It's likely target at the centromere is Cdc42 and a loss of Cdc42 mimiks the decrease of CENP-A when MgcRacGAP is depleted[803, 804].

What is the role of the CCAN in epigenetic centromere inheritance? In addition to these priming, loading and maintenance factors, the vertebrate and fission yeast CCAN are required for CENP-A deposition. Vertebrate CENP-N and CENP-C bind directly to centromeric nucleosomes. CENP-A binding by CENP-N is required to load CENP-A. Additionally, vertebrate CENP-H/I/K and CENP-M as well as fission yeast CENP-I have been demonstrated to be necessary for CENP-A loading[556, 587, 805]. Interestingly the CCAN in fission yeast defines a specialized chromatin domain that spreads over introduced sequences, between heterochromatin boundaries at both sides, in sum suggesting that the CCAN governs temporally and spatially restricted loading of CENP-A onto the centromere [799, 806, 807]. Although budding yeast directs CENP-A loading to the centromere via CBF3 during S-phase, the ScCCAN may retain a vestigial function in CENP-A deposition. Cells that loose ScCENP-N are defective in activating a conditional centromere but capable of propagating previously activated centromeres over multiple generations[568, 808, 809].

CENP-N binds to the CENP-A targeting domain(CATD). CENP-A is related to Histone H3 and when the CATD is grafted onto H3, this chimeric histone localizes to the centromere and directs kinetochore assembly in absence of CENP-A[810-813]. Other proteins have been found to bind the CATD as well, including the HJURP/Scm3 family and Psh1, an E3 ubiquitin ligase that targets ectopic CENP-A for degradation[595, 814-818]. In contrast to CENP-A loading by HJURP, ubiquitination of CENP-A by Psh1 evicts CENP-A from ectopic chromosomal loci. Thus the centromeric locus may be defined by targeted loading of CENP-A via HJURP/Scm3 and via local protection of CENP-A from global degradation as recently suggested for C.albicans[819]. The CCAN may collaborate with HJURP/Scm3, as centromere localization in fission yeast requires CENP-K and CENP-I[786]. Furthermore in vertebrates CENP-C modulates Mis18BP1 recruitment to the centromere. More specifically it interacts directly with Mis18BP1 and is required to recruit Mis18BP1 to the centromere at telophase and to inhibit recruitment of Mis18BP1 to the centromere in interphase[820]. Extending this to the known requirement of CENP-H/I/K for recruitment of CENP-C to interphase but not mitotic centromeres and the requirement of CENP-H/I/K for CENP-N localization, which in turn decreases by 80% during the course of mitosis up until metaphase, one may speculate about an indirect role of CENP-H/I/K in controlling CENP-A loading by regulating localization of the two CENP-A binding CCAN components, CENP-C and CENP-N[570, 573]. It is interesting to note that organisms in which no CCAN components other than CENP-C have been identified, D.melanogaster and C.elegans, also possess no known HJURP/Scm3 homologues[532, 783, 821, 822]. Although the budding yeast centromere is defined by DNA sequence, one epigenetic effect has been noted, the loading of Cohesin. The budding yeast centromere acts as an enhancer of Cohesin loading. This requires ScCENP-A, ScCENP-C, ScMIS12C, ScCENP-O/P, ScCENP-N/L and possibly ScCENP-H/I/K. Furthermore it requires the Smc2/4 Cohesin loader complex to localize to centromeres and localization of Smc2/4 is impaired in ScCENP-O mutants. ScCENP-A, ScCENP-C or Ndc10 mutants cause decreased Cohesin loading at newly activated centromeres, but not established centromeres[57, 67, 68, 590, 722, 823, 824].

3. Results

3.1 In vivo characterization of the budding yeast CCAN

To investigate interactions among ScCCAN subcomplexes and between ScCCAN subcomplexes and other kinetochore components, I employed two parallel strategies. Firstly I constructed yeast strains in which one member of the ScCCAN was fused to a tandem affinity tag at its genomic locus. TAP-tag fusions were constructed for a representative member of each putative ScCCAN subcomplex as well as for all newly assigned proteins. Following strain construction and verification of correct integration of the tag, I purified each bait protein from 24l of exponentially growing liquid culture. Subsequently the affinity-purified samples were analyzed by our in-house mass-spectrometry facility in order to identify co-purifying kinetochore proteins and posttranslational modifications. Similar experiments have been performed previously, but only with single ScCCAN members and not systematically[569, 592]. I reasoned that by comparison, one may observe differential association of kinetochore proteins with ScCCAN subcomplexes, which in turn would provide clues to their overall connectivity. Because I did not observe a convincing association of the putative CENP-T homologue with any kinetochore protein under standard conditions, this initial experimental approach was expanded and I performed a second set of purifications of all bait proteins under lower ionic strength. Thus, each of the 6 bait proteins was purified twice, in presence of either 100mM or 300mM NaCl. In a second approach, I expressed ScCCAN subcomplexes from a polycistronic bacterial vector in order to purify sufficient amounts of recombinant protein to perform direct binding assays. Because cloning into this vector is sequential, the possible orders in which one can perform the construction of a full vector with reasonable effort are limited. I chose the proteins to tag in vivo according to their compatibility with the cloning process for bacterial expression so that I would be able to tag and purify the same bait proteins in both approaches, yielding comparable data. A schematic description of the bait proteins and their position within the putative ScCCAN subcomplexes is given in Figure 1. Figure 2B shows a silver stained SDS-PAGE for each ScCCAN purification performed. 15µl of the three elutions performed for each purified native ScCCAN protein as well as 7.5µl of boiled beads after elution were applied to the Gel. Figure 2A shows a comparative SDS-PAGE of the entire remaining bead fraction, 77.5µl for each purification. While this is not representative for the samples analyzed by mass spectrometry, as these bead samples were collected after elution, it does allow comparison of remaining band patterns on the same scale. The inset shows the tentatively assigned band identities. The strongest band in each sample was assumed to be the bait protein while the remaining untagged proteins were assigned according to molecular weight in case of ScCENP-I, ScCENP-K and ScCENP-L and their relative migration distance in relation to ScCENP-U, inferred from recombinant protein in the case of ScCENP-Q, ScCENP-P and ScCENP-O.

Figure1. Purification rationale

Budding yeast CCAN:

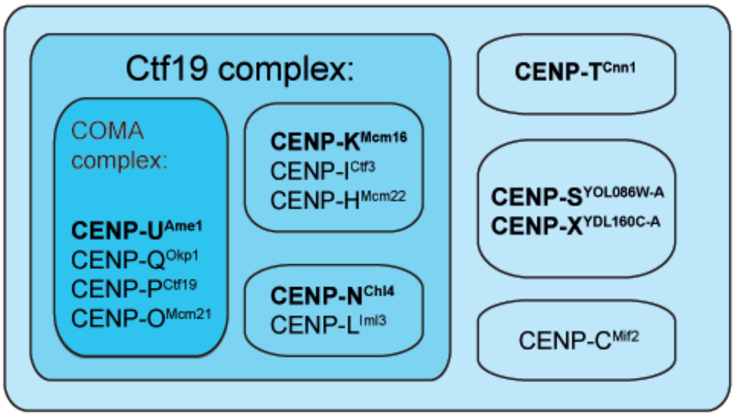
Ctf19 complex:
COMA complex:
CENP-U^{Ame1}
CENP-Q^{Okp1}
CENP-P^{Ctf19}
CENP-O^{Mcm21}
CENP-K^{Mcm16}
CENP-I^{Ctf3}
CENP-H^{Mcm22}
CENP-N^{Chl4}
CENP-L^{Iml3}
CENP-T^{Cnn1}
CENP-S$^{YOL086W-A}$
CENP-X$^{YDL160C-A}$
CENP-C^{Mif2}

Figure 1) This figure displays the putative grouping of budding yeast CCAN proteins into subcomplexes based on published interactions of both yeast and vertebrate CCAN proteins and assuming conservation of subcomplex architecture. The corresponding yeast gene is denoted in superscript, the emboldened protein names denote all constructed TAP-tag fusions.

Figure 2. SDS-PAGE of tandem affinity purifications

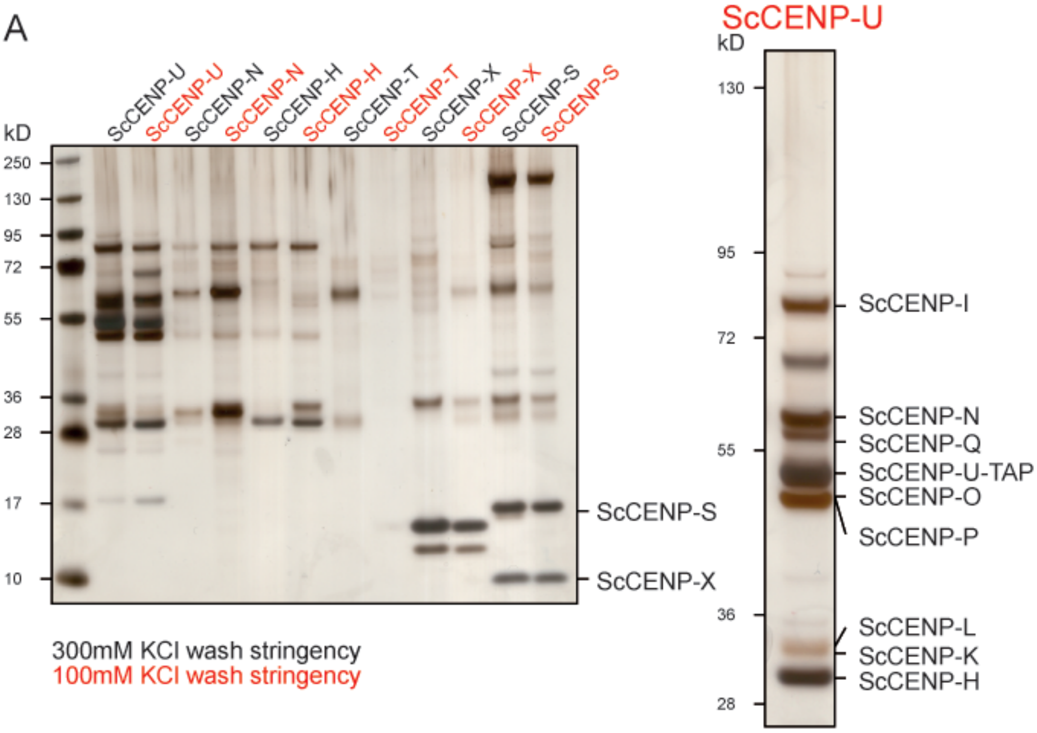
A
ScCENP-U
ScCENP-U
ScCENP-N
ScCENP-N
ScCENP-H
ScCENP-H
ScCENP-T
ScCENP-T
ScCENP-X
ScCENP-X
ScCENP-S
ScCENP-S
kD
250
130
95
72
55
36
28
17
10
ScCENP-S
ScCENP-X
300mM KCl wash stringency
100mM KCl wash stringency
ScCENP-U
kD
130
95
72
55
36
28
ScCENP-I
ScCENP-N
ScCENP-Q
ScCENP-U-TAP
ScCENP-O
ScCENP-P
ScCENP-L
ScCENP-K
ScCENP-H

Figure 2A) This figure displays a SDS-PAGE of the contents remaining on beads after tandem affinity purification and elution. It allows comparison of the major bands found in each sample but is not representative for the samples analyzed by mass spectrometry. These are shown in Figure 2B.

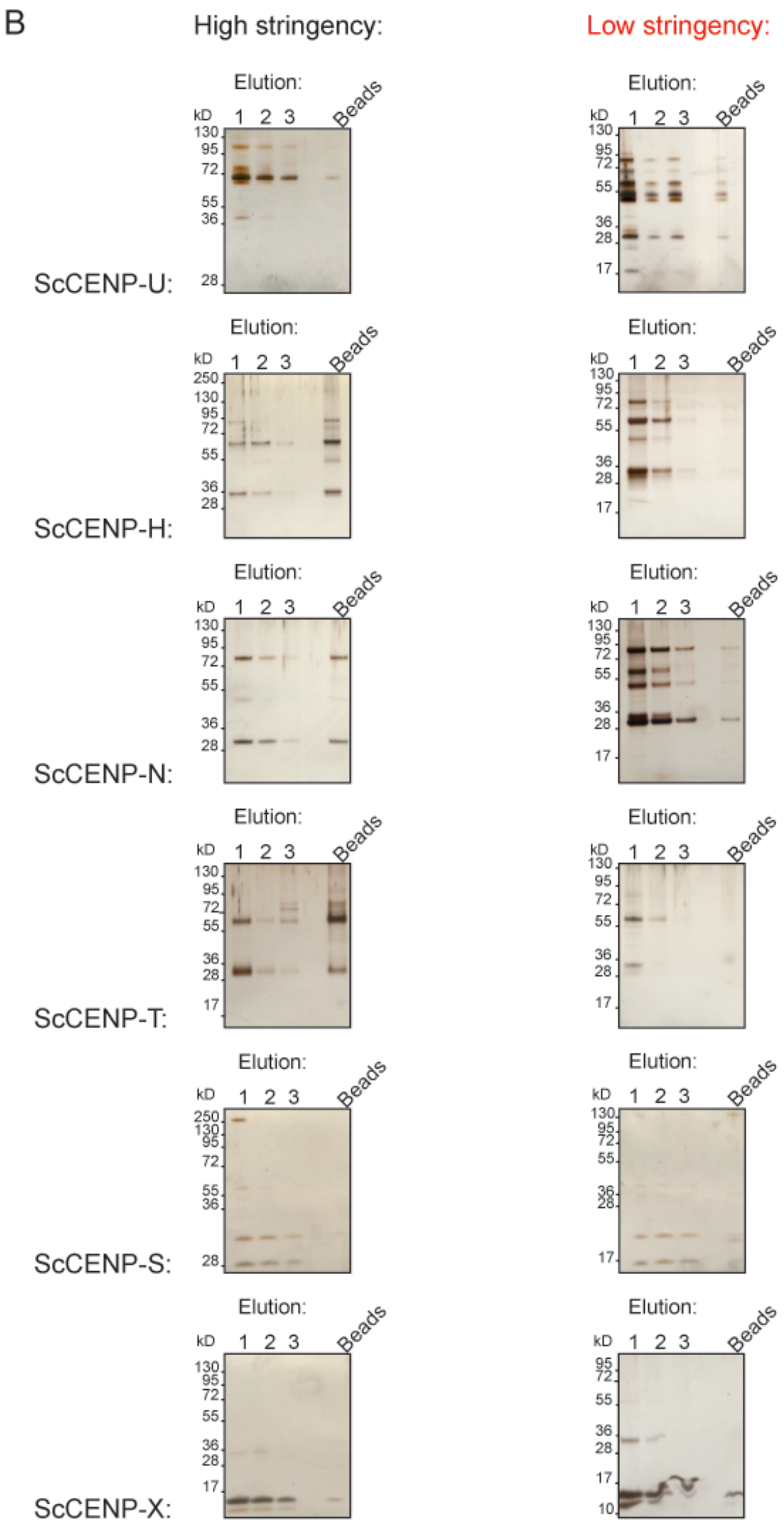
B
High stringency:
Low stringency:
Elution:
kD
1 2 3
Beads
ScCENP-U:
ScCENP-H:
ScCENP-N:
ScCENP-T:
ScCENP-S:
ScCENP-X:
250
130
95
72
55
36
28
17
10

Figure 2B) After purification, each sample was eluted three times in 60µl 0,1M Glycine pH 2. 15µl of each elution were loaded onto the gel while the remaining 45µl were analyzed by mass spectrometry. Following the third elution, 7,5 µl beads were boiled and the 4 samples, 3 elutions and the remaining bead bound protein were analyzed by SDS-PAGE to judge suitability for mass spectrometry and elution efficiency.

Protein identification data for all analyzed samples is summarized in Figure 3. Figure 3A displays structural kinetochore proteins that co-purify with the respective CCAN proteins. A few relationships are readily apparent. Firstly, the KMN network components do not co-purify as a single entity. Rather the ScMIS12C is found to associate with all established, but not the novel ScCCAN components while ScNDC80C and low levels of ScKnl1 are exclusively found associated with ScCENP-T. Secondly, as in previous publications, the ScCCAN components ScCENP-U, ScCENP-H and ScCENP-N purify as a tight complex, containing all of the established ScCCAN proteins, allowing no further conclusion about their subcomplex architecture from presence or absence alone. Thirdly the putative ScCENP-T is found in association with most established ScCCAN proteins but only under low purification stringency. These purifications also identified a candidate protein for the budding yeast homologue of CENP-W, the product of a small, uncharacterized open reading frame YDR374W-A, which we have subsequently termed Wip1. Furthermore the putative ScCENP-X co-purifies with a substantial number of ScCCAN proteins under low stringency, suggesting a weak or transient interaction with the established ScCCAN components. The results for the putative yeast CENP-S homologue are less clear as it only associates with ScCENP-U and ScCENP-T. Note that both, ScCENP-S and ScCENP-X associate with each other and are found in low stringency ScCENP-T purifications. Remarkably, ScCENP-C is found only in high, not low stringency ScCENP-T samples while the only other ScCCAN protein that co-purifies ScCENP-C, ScCENP-U does so regardless of the stringency applied. Lastly, while all three established ScCCAN components, ScCENP-U, ScCENP-N and ScCENP-H associate with all core histones and the CENP-A ubiquitin ligase Psh1, ScCENP-A itself is only found in ScCENP-U purifications.

Additional proteins of interest that copurify with ScCCAN components are summarized in Figure 3B. Note that exclusively the putative ScCENP-S homologue associates with three proteins involved in DNA repair Mph1, Msh2 and Msh3. Mph1 is a DEAH-box DNA helicase and a homologue of human FANCM, part of the Fanconi anemia complex[825, 826]. FANCM/Mph1has been suggested to promote replication fork regression and recombinatorial repair after the fork stalls due to replicational stress[827-832]. Reasons for replication fork stalling are varied but include lack of nucleotides or interstrand crosslinks[833]. Importantly however, FANCM associates with CENP-S/X (also known as MHF1&2) which promote FANCM DNA binding and replication fork regression[834]. Thus, although only ScCENP-X displays association with the ScCCAN and only ScCENP-S associates with Mph1/FANCM we believe this corroborates conservation of CENP-S/X between human and yeast. The reason for the differential association of ScCENP-S/X in this experiment is not known but it is possible that multiple pools of CENP-S/X exist and that tagging either of the two discriminates between these two pools.

Of the nuclear pore complex proteins identified in these purifications, Nup60 is interesting as it is part of the nuclear basket complex that associates with Mad1. Additionally RanGTPase (Gsp1) and the exportin Crm1 were detected. However other NPC proteins were present in the ScCCAN purifications that are components of NPC subcomplexes that have not previously been implicated in Mad1/2 recruitment. Therefore it is likely that these proteins constitute contaminations rather than a specific association[742]. Lastly a number of potentially regulatory kinases are found to co-purify with ScCCAN proteins. This includes the Dbf4/Cdc7 DDK kinase complex found to associate with ScCENP-H and ScCENP-N, Clb5-CDK1 found to associate with ScCENP-T and Cka1/Ckb1 of the casein kinase II complex found to associate with ScCENP-U and ScCENP-N.

Although all established ScCCAN proteins purified in a tight complex, precluding any inference to ScCCAN subcomplex architecture, the established ScCCAN bait proteins ScCENP-U, ScCENP-H and ScCENP-N did appear to enrich for peptides corresponding to proteins of the suggested subcomplexes. Label-free quantitative mass spectrometry has emerged as an alternative to SILAC, ITRAQ or similar label based quantification. While it is currently not possible to predict signal strength of a given protein based on its primary sequence, some of the parameters measured during protein identification correlate with protein concentration. Among these, the total number of acquired spectra, demonstrates a very good linear correlation with relative protein abundance (r^2=0,9997)[835]. Although in absence of standards no absolute quantification is possible, a relative quantification in multiple samples, such as those resulting from my purifications, is. It needs to be said however that applying this method would, strictly speaking, firstly require validation with a protein complex of known assembly and secondly would have to be performed in replicates to determine the magnitude of error involved. Both are beyond the scope of this work and thus the following analysis serves only to visualize the relative abundance of peptide spectra for a given protein, which in turn may serve as a rough guide for potential relations within the ScCCAN that may be fruitful to investigate by more precise assays.

For a relative quantification of kinetochore proteins in the samples analyzed, the number of peptide spectra acquired per protein in a given sample was normalized to the total number of peptide spectra acquired for all proteins in that sample. Then, pooling the data from either high or low stringency purifications, the normalized peptide number of a given protein in one purification was divided by the sum of the normalized peptide numbers of a given protein in all three purifications, ScCENP-U, ScCENP-H and ScCENP-N. This yields an enrichment factor (EF) describing the enrichment for peptides of a given co-purifying protein when purifying one of the three baits. An exemplary calculation for the enrichment factor of a given bait protein "x" in the purification of ScCENP-U is given in equation 1.

Figure 3. Summary of protein identification

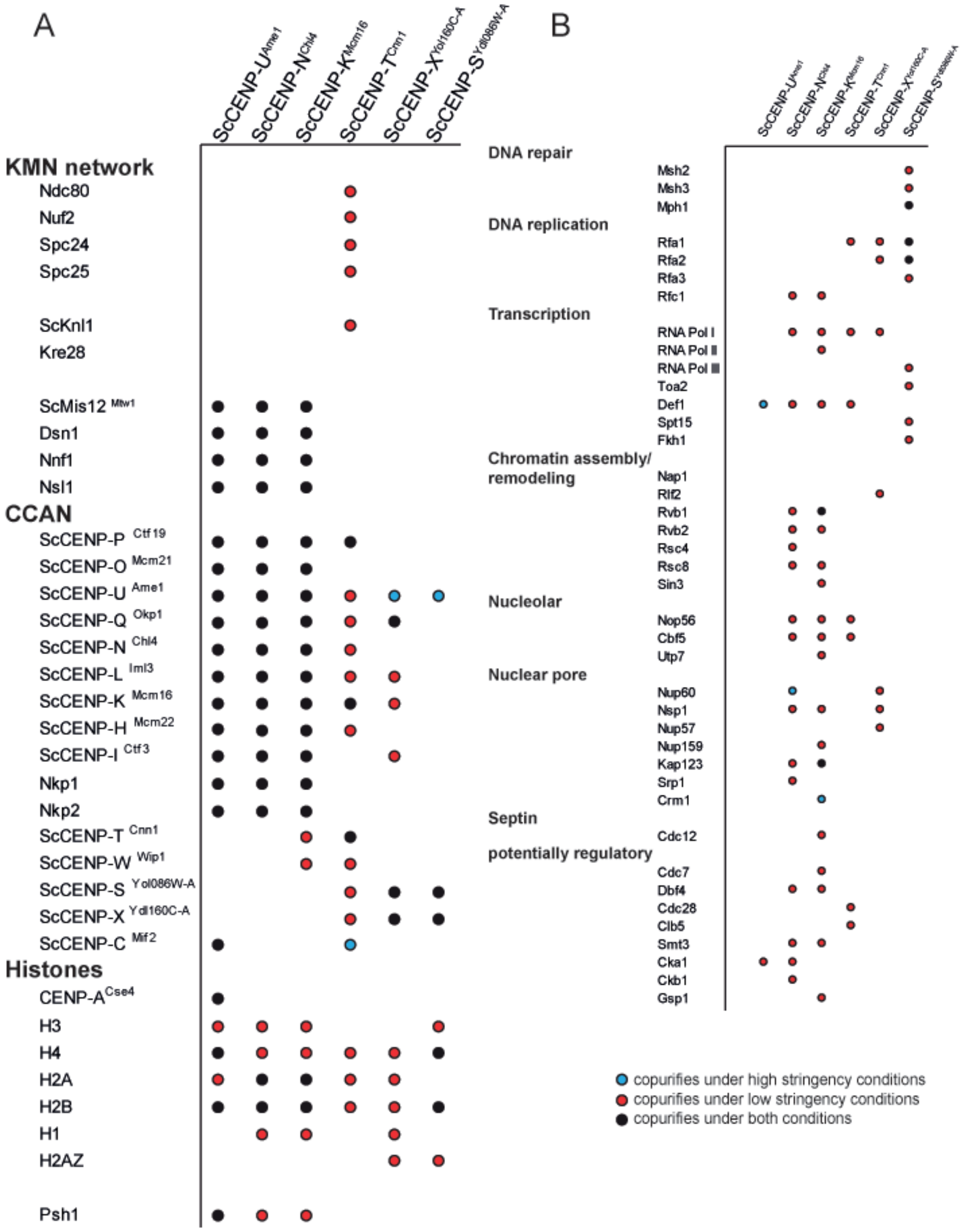

A

	ScCENP-U^{Ame1}	ScCENP-N^{Chl4}	ScCENP-K^{Mcm16}	ScCENP-T^{Cnn1}	ScCENP-X$^{Ydl160C-A}$	ScCENP-S$^{Yol086W-A}$
KMN network						
Ndc80				🔴		
Nuf2				🔴		
Spc24				🔴		
Spc25				🔴		
ScKnl1				🔴		
Kre28						
ScMis12^{Mtw1}	⚫	⚫	⚫			
Dsn1	⚫	⚫	⚫			
Nnf1	⚫	⚫	⚫			
Nsl1	⚫	⚫	⚫			
CCAN						
ScCENP-P^{Ctf19}	⚫	⚫	⚫	⚫		
ScCENP-O^{Mcm21}	⚫	⚫	⚫			
ScCENP-U^{Ame1}	⚫	⚫	⚫	🔴	🔵	🔵
ScCENP-Q^{Okp1}	⚫	⚫	⚫	🔴	⚫	
ScCENP-N^{Chl4}	⚫	⚫	⚫	🔴		
ScCENP-L^{Iml3}	⚫	⚫	⚫	🔴	🔴	
ScCENP-K^{Mcm16}	⚫	⚫	⚫	⚫	🔴	
ScCENP-H^{Mcm22}	⚫	⚫	⚫	🔴		
ScCENP-I^{Ctf3}	⚫	⚫	⚫		🔴	
Nkp1	⚫	⚫	⚫			
Nkp2	⚫	⚫	⚫			
ScCENP-T^{Cnn1}			🔴	⚫		
ScCENP-W^{Wip1}			🔴	🔴		
ScCENP-S$^{Yol086W-A}$				🔴	⚫	⚫
ScCENP-X$^{Ydl160C-A}$				🔴	⚫	⚫
ScCENP-C^{Mif2}	⚫			🔵		
Histones						
CENP-A^{Cse4}	⚫					
H3	🔴	🔴	🔴			🔴
H4	⚫	🔴	🔴	🔴	🔴	⚫
H2A	🔴	⚫	⚫	🔴	🔴	
H2B	⚫	⚫	⚫	🔴	🔴	⚫
H1		🔴	🔴		🔴	
H2AZ					🔴	🔴
Psh1	⚫	🔴	🔴			

B

		ScCENP-U^{Ame1}	ScCENP-N^{Chl4}	ScCENP-K^{Mcm16}	ScCENP-T^{Cnn1}	ScCENP-X$^{Ydl160C-A}$	ScCENP-S$^{Yol086W-A}$
DNA repair	Msh2						🔴
	Msh3						🔴
	Mph1						⚫
DNA replication	Rfa1				🔴	🔴	⚫
	Rfa2					🔴	⚫
	Rfa3						🔴
	Rfc1		🔴	🔴			
Transcription	RNA Pol I		🔴	🔴	🔴	🔴	
	RNA Pol II			🔴			
	RNA Pol III						🔴
	Toa2						🔴
	Def1	🔵	🔴	🔴	🔴		
	Spt15						🔴
	Fkh1						🔴
Chromatin assembly/ remodeling	Nap1						
	Rlf2					🔴	
	Rvb1		🔴	⚫			
	Rvb2		🔴	🔴			
	Rsc4		🔴				
	Rsc8		🔴	🔴			
	Sin3			🔴			
Nucleolar	Nop56		🔴	🔴	🔴		
	Cbf5		🔴	🔴	🔴		
	Utp7			🔴			
Nuclear pore	Nup60		🔵			🔴	
	Nsp1		🔴	🔴		🔴	
	Nup57					🔴	
	Nup159			🔴			
	Kap123		🔴	⚫			
	Srp1		🔴				
	Crm1			🔵			
Septin	Cdc12			🔴			
potentially regulatory	Cdc7			🔴			
	Dbf4		🔴	🔴			
	Cdc28				🔴		
	Clb5				🔴		
	Smt3		🔴	🔴			
	Cka1	🔴	🔴				
	Ckb1		🔴				
	Gsp1			🔴			

🔵 copurifies under high stringency conditions
🔴 copurifies under low stringency conditions
⚫ copurifies under both conditions

Figure 3A/B) Summary of proteins found to co-purify with ScCCAN bait proteins. The color code denotes identification in samples that were obtained after purification under high stringency (300mM NaCl), low stringency (100mM NaCl) or both. **Figure 3A** focuses on structural kinetochore proteins while **Figure 3B** focuses on proteins involved in replication, chromatin assembly as well as potentially regulatory proteins.

$$EF(x)_{ScCENP-U} = \frac{\dfrac{PS_{ScCENP-U}(x)}{PS_{ScCENP-U}(total)}}{\dfrac{PS_{ScCENP-U}(x)}{PS_{ScCENP-U}(total)} + \dfrac{PS_{ScCENP-N}(x)}{PS_{ScCENP-N}(total)} + \dfrac{PS_{ScCENP-H}(x)}{PS_{ScCENP-H}(total)}} \qquad (1)$$

Equation 1) Exemplary calculation of the enrichment factor for protein X in a tandem affinity purification using ScCENP-U as bait. X is a given co-purifying protein, $EF(x)_{ScCENP-U}$ is the enrichment factor for X in a purification sample using ScCENP-U as a bait. $PS_{ScCENP-U}(x)$ is the number of recorded peptide spectra for X from a ScCENP-U purification sample while $PS_{ScCENP-U}(total)$ is the sum of all peptide spectra recorded for a ScCENP-U purification sample.

This approach assumes an average amount of a co-purifying protein to be present in purifications of the ScCCAN, regardless if ScCENP-U, ScCENP-H or ScCENP-N are used as a bait. Any increase above or decrease below this average amount reflects a stronger or weaker association with the bait protein in question. The enrichment factor thus describes peptide enrichment of a co-purifying protein by association of one of the bait proteins. To sum up individual contributions of bait proteins to enrichment, a coordinate system was generated using three unit vectors that represent an association with one of the three bait proteins as basis. To place a co-purifying protein in this coordinate system, each of the three enrichment factors was multiplied with the corresponding bait unit vector and the three resulting vectors were added together. The resulting coordinates for both stringency conditions are shown in Figure 4. The positions within these coordinate systems neither describe a spatial relation nor suggest direct interactions. They are merely a comparative measure for the relative increase of identified peptides, which is presumed to be due strength of association of an individual co-purifying protein with one of the three bait proteins. Note the similarity of both independent data sets. The components of ScCENP-N/L and ScCENP-H/I/K cluster closely. Similarly, all subunits of the established four protein ScMIS12C cluster together. There appears to be little association of ScMIS12C and ScCENP-N/L while ScMIS12C, especially ScNnf1 associates strongly with ScCENP-U and to a lesser extent with ScCENP-H.

Figure 4. Illustration of peptide spectra enrichment

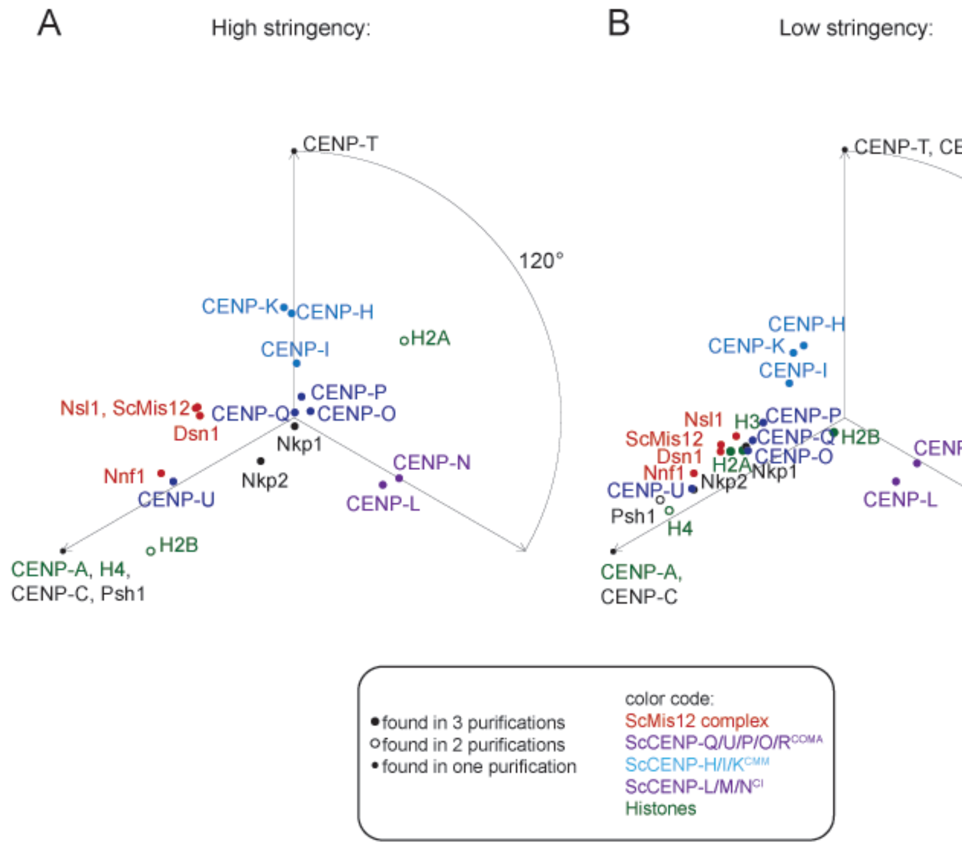

Figure 4) A vector representation, illustrating the relative association of a co-purifying protein with one of the three bait proteins, ScCENP-U,-H and -N. Note that, as mentioned in the text, this serves only to illustrate increased peptide spectra specific to a bait protein and does not necessarily reflect a structural assembly or direct interaction. Each of the dots denotes the end of a vector beginning at the center of the coordinate system, generated by adding the three vectors that result from multiplying the bait unit vector with the corresponding enrichment factor. Small dots denote proteins that were detected co-purifying with only one bait protein and thus are found at the end of the respective bait unit vector. Circles denote proteins that were found in two purifications and are thus located on a vertex connecting the ends of the two bait protein unit vectors. Large dots denote proteins that were found to associate with all 3 bait proteins. Known and putative subcomplexes were color-coded as a visual aid. **Figure 4A** uses data from three independent purifications of ScCENP-U, ScCENP-H and ScCENP-N performed at high stringency (300mM NaCl). **Figure 4B** uses data from independent low stringency purifications (100mM NaCl) of ScCENP-U, ScCENP-H and ScCENP-N.

3.2 Identification of Wip1 as the budding yeast CENP-W homologue.

As mentioned in the preceding paragraph I identified the product of a small, uncharacterized open reading frame, YDR374W-A as co-purifying with ScCENP-T as well as ScCENP-H. At this time Dr. Alexander Schleiffer had proposed yeast homologues for CENP-T, CENP-S and CENP-X based on distant sequence homology to the vertebrate proteins. A potential yeast CENP-W homologue however eluded these efforts. Using YDR374W-A as a candidate Dr. Schleiffer demonstrated it to be a CENP-W related histone fold protein which we named Wip1 (W-like protein)[11]. Figure 5 displays a multiple sequence alignment of Wip1 with CENP-W orthologues. Secondary structure prediction suggests three consecutive helices, characteristic of a histone fold. Helix 1 is divergent in budding yeast, which explains why purely bioinformatical methods failed to identify Wip1.

Figure 5. Multiple sequence alignment of Wip1 with CENP-W orthologues

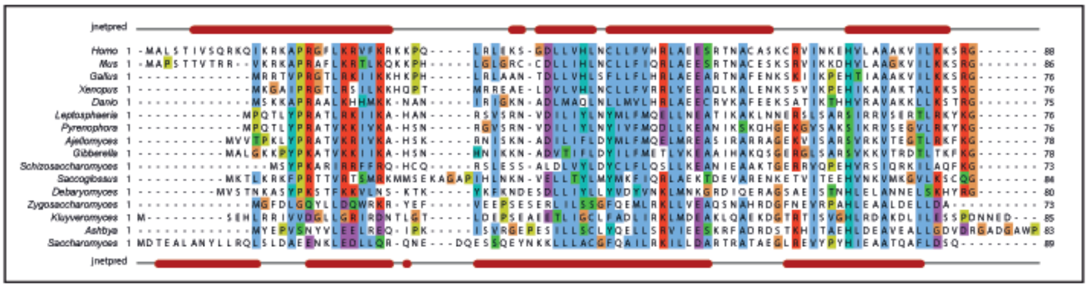

Figure 5) Multiple sequence alignment of Wip1, the putative budding yeast CENP-W homologue by Dr. Alexander Schleiffer. Note the predicted three helices, characteristic for a histone fold. Also observe the low sequence conservation of Wip1 in helix 1 which impeded identification by bioinformatic means.

If Wip1 is indeed the budding yeast CENP-W ortholog, two predictions can be made. Firstly, that it should be a kinetochore protein. Secondly, because the two vertebrate histone fold proteins CENP-W and CENP-T form a dimeric complex and are interdependent for localization to the kinetochore, a similar relation should be observable in yeast[576]. Figure 6 demonstrates both predictions to be true. A GFP tagged Wip1 expressed from its native locus localizes to the kinetochore throughout the cell cycle as evidenced by co-localization with the kinetochore marker Nuf2. Furthermore localization requires ScCENP-T as it is abolished in a ScCENP-T deletion strain. A recent publication suggests ScCENP-T copy number at the kinetochore to increase from 6 to 20 during anaphase. I have not noticed increase of the Wip1-GFP signal between different cell cycle stages, however I did not perform any quantification of fluorescence intensity[836].

Figure 6. Localization of ScCENP-W^{Wip1} and dependence on ScCENP-T^{Cnn1}

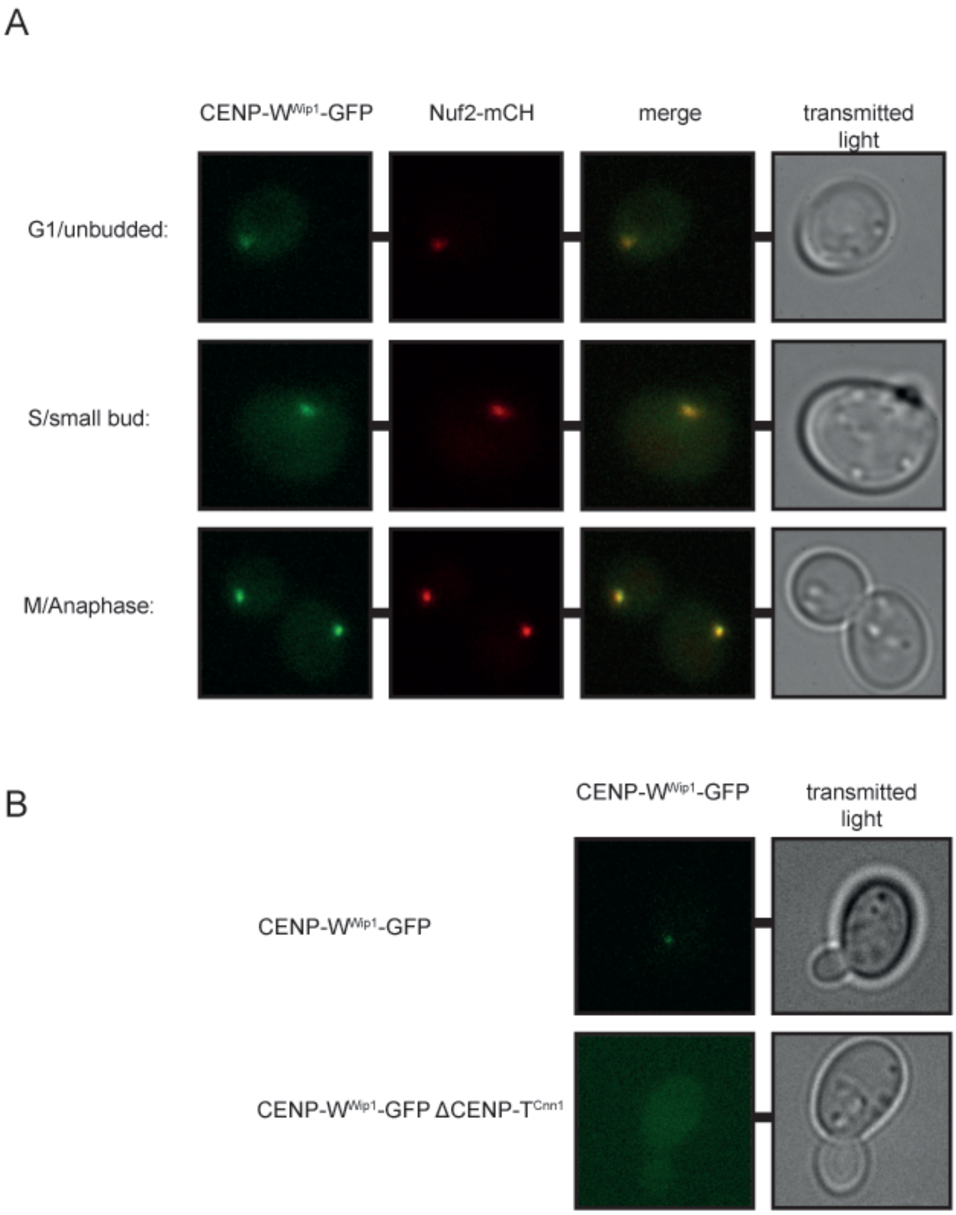
A
CENP-W^{Wip1}-GFP
Nuf2-mCH
merge
transmitted light
G1/unbudded:
S/small bud:
M/Anaphase:
B
CENP-W^{Wip1}-GFP
transmitted light
CENP-W^{Wip1}-GFP
CENP-W^{Wip1}-GFP ΔCENP-T^{Cnn1}

Figure 6A) GFP fused ScCENP-W^{Wip1} was found to co-localize with Nuf2 at the kinetochore throughout the cell cycle. **Figure 6B)** Localization of ScCENP-W^{Wip1} depends on ScCENP-T^{Cnn1} and is abolished when ScCENP-T^{Cnn1} is deleted.

3.3 Cloning of ScCCAN subcomplexes for bacterial expression

To generate recombinant proteins with which I could perform in vitro binding assays I chose to clone the established ScCCAN proteins into two different co-expression systems, preserving the putative subcomplex composition. I aimed to co-express all components of the putative ScCENP-Q/U/P/O, ScCENP-N/L or ScCENP-H/I/K complexes, each from an individual vector. The components of ScCENP-Q/U/P/O and those of ScCENP-H/I/K were cloned into individual polycistronic pST39 vectors with the tagged protein taking up the last cassette, allowing for an easy change of the tag type[837]. Multiple tagged versions were generated, according to the schematic in Figure 7A-D. Expression required an intron in ScCENP-O to be removed. This was accomplished by reverse transcription of TRIzol® extracted total RNA and subsequent PCR amplification of the cDNA using ScCENP-O specific primers. The resulting construct was cloned into pET3aTr. Subcloning of ScCENP-O and ScCENP-H required removal of two EcoRI restriction sites in ScCENP-P and one SacI site in ScCENP-H (See materials and methods).

The components of the ScCENP-N/L complex were cloned into a pCOLADuet-1 dual expression vector according to Figure 7E-F[838]. Kanamycin resistance of the pCOLADuet-1-ScCENP-N/L vector allows co-transfection and expression with either pST39-ScCENP-Q/U/P/O or pST39-ScCENP-H/I/K vectors. The final constructs with their respective tags are listed in Figure 7G. Two different tags on each complex allow CoIP experiments with any combination of complexes. Lastly I planned the cloning strategy in such a way that the construction of a composite vector containing all 9 proteins according to Figure 7H was possible. While the size of the vector approaches technical limits, the DAM1C has been cloned onto a single vector using a similar strategy and yielding a vector in a similar size range[548]. This composite vector could however not be completed due to the limited time. For reasons unknown, the efficiency by which the pCOLADuet-1-CENP-L/N vector could be isolated by Miniprep was so low that it was only barely visible on an ethidium bromide gel. However this vector and all other described vectors were sequenced and found to contain the desired genes. Furthermore the CENP-L/N vector expresses efficiently as demonstrated later.

Figure 7. Cloning strategy for ScCCAN subcomplexes

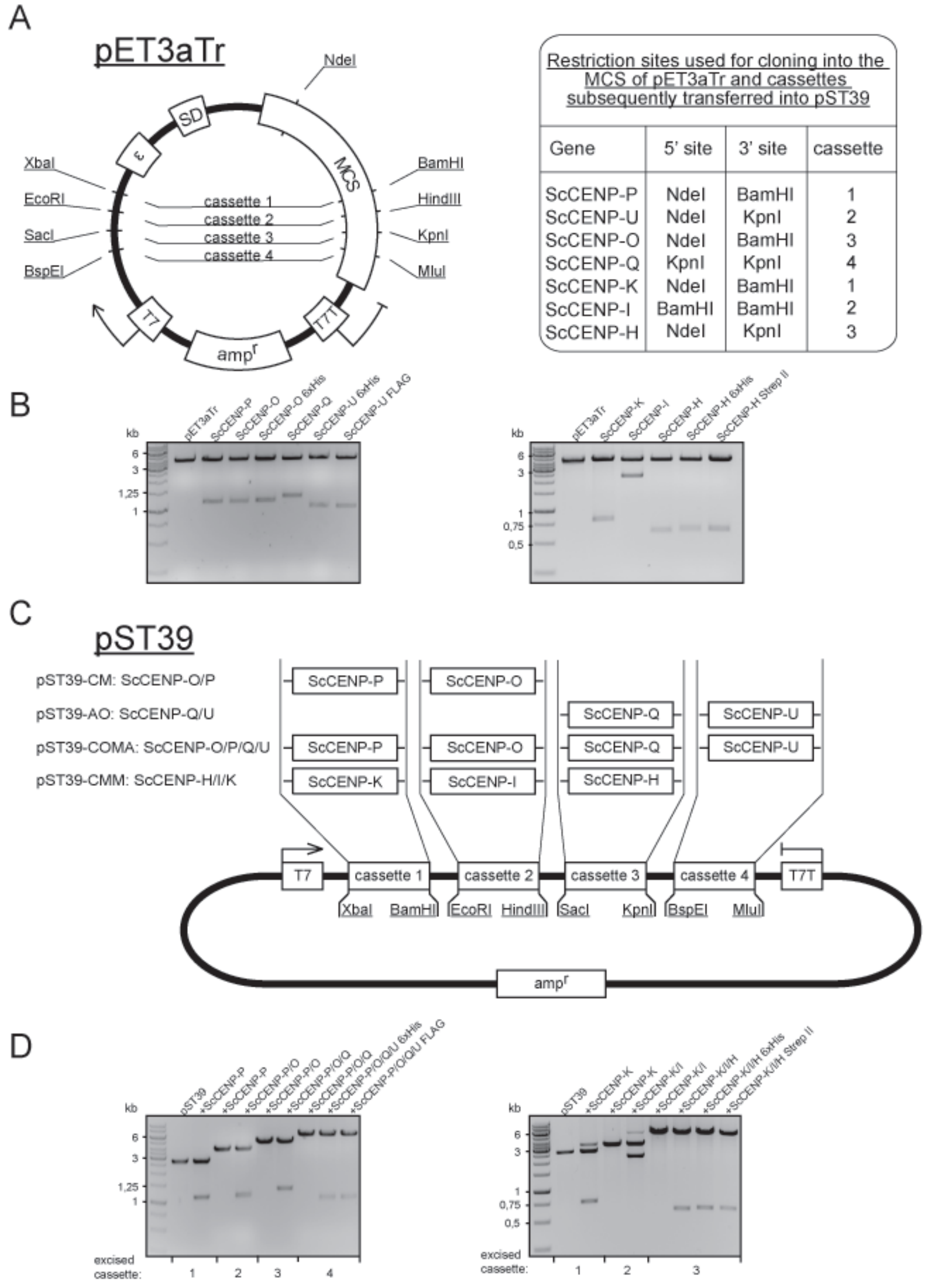
A
pET3aTr
NdeI
SD
ε
MCS
XbaI
EcoRI
SacI
BspEI
BamHI
HindIII
KpnI
MluI
cassette 1
cassette 2
cassette 3
cassette 4
T7
T7T
amp^r
B
kb
6
3
1,25
1
pET3aTr
ScCENP-P
ScCENP-O
ScCENP-O 6xHis
ScCENP-Q
ScCENP-U 6xHis
ScCENP-U FLAG
kb
6
3
1
0,75
0,5
pET3aTr
ScCENP-K
ScCENP-I
ScCENP-H
ScCENP-H 6xHis
ScCENP-H Strep II
C
pST39
pST39-CM: ScCENP-O/P
pST39-AO: ScCENP-Q/U
pST39-COMA: ScCENP-O/P/Q/U
pST39-CMM: ScCENP-H/I/K
ScCENP-P
ScCENP-O
ScCENP-Q
ScCENP-U
ScCENP-K
ScCENP-I
ScCENP-H
T7
cassette 1
cassette 2
cassette 3
cassette 4
T7T
XbaI
BamHI
EcoRI
HindIII
SacI
KpnI
BspEI
MluI
amp^r
D
kb
6
3
1,25
1
pST39
+ScCENP-P
+ScCENP-P
+ScCENP-P/O
+ScCENP-P/O
+ScCENP-P/O/Q
+ScCENP-P/O/Q
+ScCENP-P/O/Q/U 6xHis
+ScCENP-P/O/Q/U FLAG
excised cassette:
1
2
3
4
kb
6
3
1
0,75
0,5
pST39
+ScCENP-K
+ScCENP-K
+ScCENP-K/I
+ScCENP-K/I
+ScCENP-K/I/H
+ScCENP-K/I/H 6xHis
+ScCENP-K/I/H Strep II
excised cassette:
1
2
3

Restriction sites used for cloning into the MCS of pET3aTr and cassettes subsequently transferred into pST39

Gene	5' site	3' site	cassette
ScCENP-P	NdeI	BamHI	1
ScCENP-U	NdeI	KpnI	2
ScCENP-O	NdeI	BamHI	3
ScCENP-Q	KpnI	KpnI	4
ScCENP-K	NdeI	BamHI	1
ScCENP-I	BamHI	BamHI	2
ScCENP-H	NdeI	KpnI	3

Figure 7A) Schematic representation of the transfer vector pET3aTr and the restriction sites used to clone each of the 7 genes described here into one individual vector. **Figure 7B)** Analytical digestion of all constructed transfer vectors. **Figure 7C)** Scheme illustrating the composition of the constructed polycistronic complex expression vectors. **Figure 7D)** Analytical digestion of the constructed polycistronic complex expression vectors.

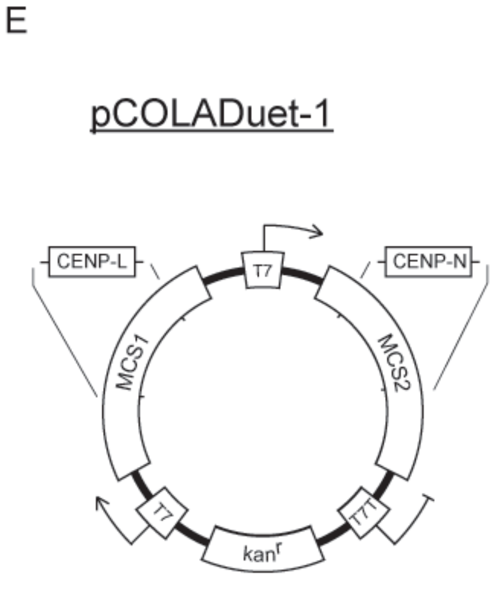
E
pCOLADuet-1
CENP-L
T7
CENP-N
MCS1
MCS2
T7
kanr
T7T

F

Restriction sites used to clone into pCOLADuet-1			
Gene	5' site	3' site	cassette
ScCENP-L	NcoI	BamHI	1
ScCENP-N	NdeI	XhoI	2

G

Expressable complex:	Tagged Protein: (one per construct)
ScCENP-P/O	ScCENP-O-6xHis
ScCENP-Q/U	ScCENP-U-6xHis
ScCENP-Q/U/P/O	ScCENP-U-6xHis
	ScCENP-U-FLAG
ScCENP-H/I/K	ScCENP-H-6xHis
	ScCENP-H-StrepII
ScCENP-N/L	ScCENP-N-FLAG
	ScCENP-N-6xHN

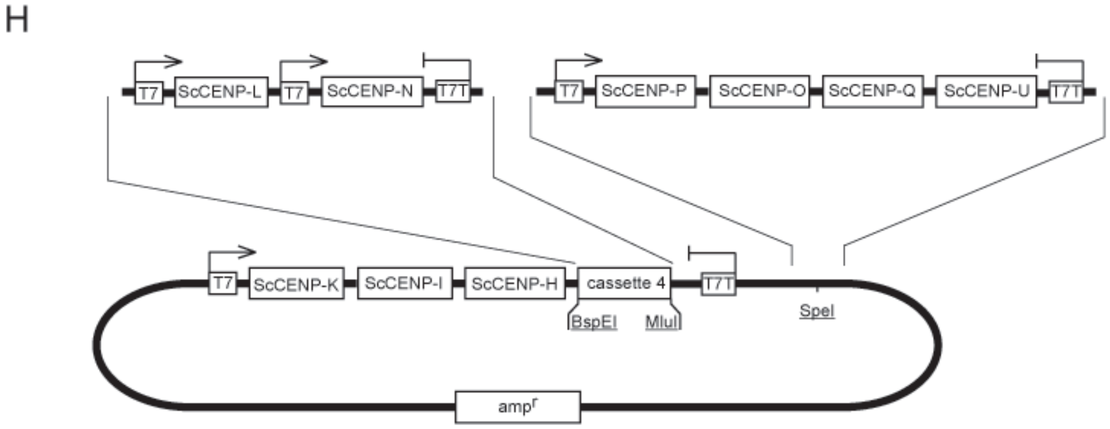
H
T7
ScCENP-L
T7
ScCENP-N
T7T
T7
ScCENP-P
ScCENP-O
ScCENP-Q
ScCENP-U
T7T
T7
ScCENP-K
ScCENP-I
ScCENP-H
cassette 4
T7T
BspEI
MluI
SpeI
ampr

Figure 7E/F) Schematic representation of the pCOLADuett-1 vector and the restriction sites used to construct a ScCENP-N/L expression vector. **Figure 7G)** List of the generated expression vectors encoding CCAN subcomplexes and the respective tag variants**. Figure 7H)** Planned, uncompleted composite expression vector encoding all established ScCCAN proteins. Vector maps were adapted from Song Tan, 2001(pET3aTr/pST39) and the product brochure (pCOLADuet-1; Merck)

3.4 Determining expression conditions

During initial bacterial expression it was noted that while ScCENP-P/O, ScCENP-Q/U, ScCENP-Q/U/P/O and ScCENP-L/N could be expressed, ScCENP-H/I/K could not. Furthermore bacterial cultures in which ScCENP-Q/U/P/O expression was induced over night at 18°C, according to a standard protocol, would often cease growth. To investigate this and to find suitable expression conditions for ScCENP-H/I/K, I screened through different expression times and temperatures (Figure 8). For this screen, an exponentially grown pre-culture was split into smaller cultures. Expression was induced and the cultures were incubated at 4 different temperatures, 18°C, 24°C, 30°C and 37°C. At three timepoints, after 3h, 6h and 12h, samples were taken, sonicated and the soluble protein remaining in the supernatant after centrifugation was analyzed by western blotting. For the blots, ScCENP-O and ScCENP-U were probed with Anti-6xHis antibodies, ScCENP-N was probed with an Anti-FLAG antibody and CENP-H was probed with a Strep-Tactin HRP conjugate. Note that expression of ScCENP-Q/U/P/O and ScCENP-P/O decreases growth rate significantly and at higher rates appears to be toxic. A shorter expression of 5 hours at 24°C was adopted. Expression of ScCENP-Q/U or CENP-L/N did not have any adverse effects on growth and could be induced at 37°C for 6 hrs. Lastly no condition was found at which ScCENP-H/I/K were expressed efficiently. The blot in Figure 8D shows a weak signal from the Strep-Tactin HRP conjugate, appearing 12 hrs after induction of ScCENP-H/I/K-StrepII expression. This may be non-specific as in contrast to the other blots, which were exposed for seconds, this signal appeared only after a minute of exposure. Furthermore I attempted a small scale purification of 6xHis tagged ScCENP-H/I/K which did not specifically enrich for any protein. Lastly if the complex were expressed, ScCENP-I should produce a characteristic high molecular weight band of about 84kD, which was never observed (data not shown). Thus work on ScCENP-H/I/K was postponed.

Initial NiNTA bead batch purification of the ScCENP-Q/U/P/O complex suggested that it could be purified at high yield and high purity. Figure 9A shows a purification scheme for the ScCENP-Q/U/P/O complex and the inset shows the same sample run on a longer Gel as the central ScCENP-O and ScCENP-U bands often did not separate on a standard 10cm Gel. Band identity was established by cutting out the individual bands and identifying the corresponding protein by mass spectrometry. Although resolvable by large gels, these tended to smear and thus in many cases were not informative. Because this issue could not be resolved, only small gels will be shown. In these small gels, when ScCENP-O and ScCENP-U do not resolve, ScCENP-P acts as a proxy for the amount of ScCENP-O and ScCENP-Q acts a proxy for the amount of ScCENP-U. This is valid because when analyzing either, the ScCENP-Q/U/P/O complex or the two subcomplexes ScCENP-P/O and ScCENP-Q/U, there was always an equi-stoichiometric 1:1 relation between ScCENP-P and ScCENP-O as well as ScCENP-Q and ScCENP-U (compare Figure 18A).

Figure 8. Expression condition screen

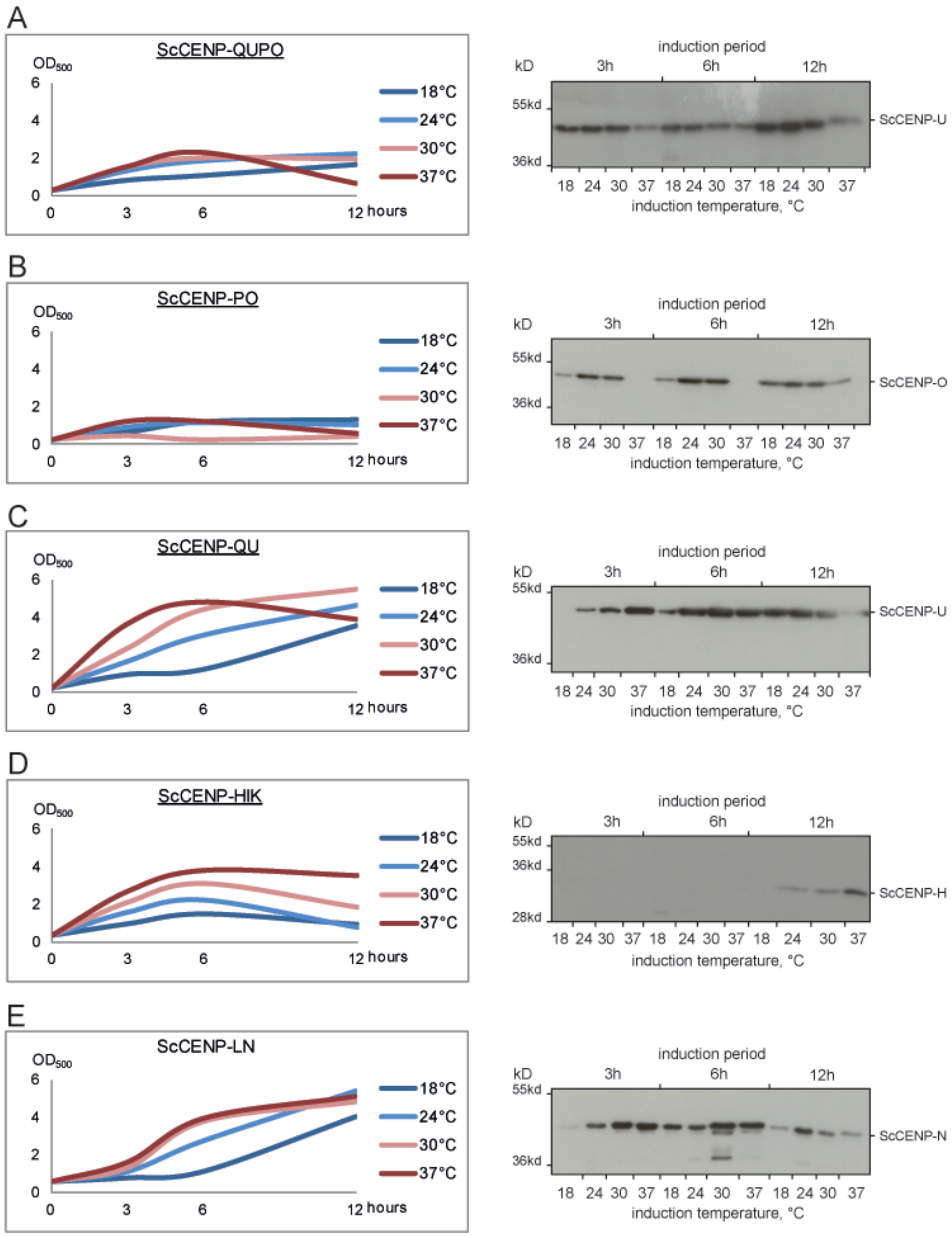

Figure 8) Expression analysis for the constructed ScCCAN subcomplex expression vectors. Each putative complex was expressed at 4 different temperatures and samples were taken at three timepoints. OD_{500} measurements are summarized by the graphs on the left while soluble protein from these samples is analyzed by western blots on the right. Results are displayed in **A)** for ScCENP-Q/U/P/O, in **B)** for ScCENP-P/O, in **C)** for ScCENP-Q/U, in **D)** for ScCENP-H/I/K and in **E)** for ScCENP-L/N.

3.5 Establishment of a purification protocol suitable for isolation of recombinant ScCENP-Q/U/P/O, ScCENP-Q/U, ScCENP-P/O and ScCENP-L/N

The ScCENP-Q/U/P/O complex after size exclusion chromatography appears equi-stoichiometric (Figure 9A). During size exclusion chromatography the entire ScCENP-Q/U/P/O peak migrated in the void volume, indicating either a large assembly or precipitated complex. Because no visible precipitation occurred in the sample and ScCENP-P, ScCENP-Q and ScCENP-U localize chromatin proximal, I reasoned that this effect could be caused by nonspecific binding to bacterial DNA[469]. To investigate this I loaded purified ScCENP-Q/U/P/O onto an ethidium bromide stained agarose gel and indeed observed a smear of what presumably was DNA (Figure 9A). The ScNDC80C purified according to the same NiNTA standard protocol serves as a negative control, demonstrating that this is not an artifact of the purification process itself. Similarly a purified ScCENP-L/N complex co-purifies what presumably is DNA (Figure 9B).

To further investigate the co-purifying nucleic acid I performed a TRIzol® extraction of the purified ScCCAN-CENP-Q/U/P/O. Although one may assume that DNA is the contaminant, classical and modern work demonstrates RNA as a component of the vertebrate inner kinetochore plate during mitosis and a band connecting the two co-oriented kinetochores during meiosis[839-841]. A role for RNA at the vertebrate kinetochore has been described. Human centromeric α-satellite DNA is highly transcribed by RNA-Pol2 and α-satellite RNA stabilizes CENP-C binding to DNA. Furthermore alpha satellite RNA is required for CENP-C, Boralin and INCENP but not Survivin to localize to the centromere. This is interesting in light of the fact that vertebrate CENP-I is required for CENP-C recruitment in interphase and that budding yeast looses ScBorealin and ScINCENP but not ScSurvivin from the kinetochore when ScCENP-U is lost[842, 843]. Therefore it is not innately clear that the CENP-Q/U/P/O complex is DNA binding rather than RNA binding although the contamination by bacterial nucleic acid suggests that binding is rather unspecific.

A TRIzol® extraction allows to discriminate between DNA and RNA as RNA partitions to the aqueous phase while DNA can be recovered from the organic phase after extraction. To ensure that the extraction was successful, an additional step was applied, the digestions of extracted DNA or RNA by DNAseI or RNAse A. Figure 10A shows an ethidium bromide stained agarose gel displaying the results of this experiment. The vector pET3aTr was used as control DNA, while control RNA was taken from an in situ hybridization kit available in the laboratory. It appears that the major fraction of the contaminating nucleic acid is found in the RNA-phase and contamination by carry over is unlikely as it is isolated from the top aqueous phase. Unfortunately subsequent digestion is not conclusive as our RNAse A shows activity against the control DNA. Thus, I could not unequivocally identify the contaminant. Because the contaminant is of bacterial origin and likely not representative for an actual interaction occurring in budding yeast I instead focused on removing it from the ScCENP-Q/U/P/O complex rather than further investigating it. It is however interesting to note that a different research group performing similar experiments found a bacterially expressed CENP-Q/O/P heterotrimer to be contaminated by nucleic acid and contamination could only be removed by RNAse A, not DNAse I or Benzonase[844].

Following the results displayed in Figure 10A, I attempted to remove the contaminant by digestion. I was unsuccessful in using DNAseI and the higher pH and temperature required for a micrococcal nuclease digestion precipitated the complex. Digestion by RNAse A had limited success and allowed purification of contaminant free ScCENP-Q/U/P/O, however the yield dropped significantly as much of the protein precipitated during the procedure and the remaining complex appeared inseparably bound to what is likely the bacterial DnaJ chaperone (data not shown). Thus a different purification protocol was needed. Figure 10B displays an initial attempt to use a high ionic strength buffer, 500mM NaCl, to dissociate complex and contaminant during size exclusion chromatography. While separation is evident, the resolution is insufficient to yield pure samples and one observes dissociation of the ScCENP-Q/U and ScCENP-O/P subcomplexes. After multiple different buffer additives and attempted ion exchange chromatography either failed to generate pure complex or dissociated the two subcomplexes, I performed a parallel screen, testing multiple ionic strength buffers in order to find conditions under which the complex would remain stable but the contaminant would be removed.

To find a suitable washing buffer I set up a large-scale batch purification from 24l of liquid culture in a standard low salt lysis buffer and split the ScCENP-Q/U/P/O bound Ni-NTA beads into equal fractions. These beads where then washed twice by incubation and agitation in a specific washing buffer. Each washing buffer had the same composition as the initial lysis buffer save for the salt concentration. A series of wash buffers was used, containing increasing concentrations of either KCl, NaCl, $MgCl_2$ or $CaCl_2$. I succeeded at removing the contaminant from ScCENP-Q/U/P/O 6xHis bound to NiNTA beads with both KCl and NaCl. While KCl was suitable to remove the contaminant and preserve subunit stoichiometry, NaCl did so at lower concentrations and therefore a 600mM NaCl was subsequently used for purification (Figure 11A). It is important to note that the high salt wash buffer was not added at the lysis step but only applied after two initial washes in low salt lysis buffer (150mM NaCl). Furthermore in later large-scale purifications each washing step was standardized and consisted of 10min agitation of the beads in wash buffer. It is not possible to give a standard number of washing steps. Rather, one needs to collect the wash buffer after washing and monitor 260nm and 280nm extinction at each washing step, continuing until completion, i.e. until protein and DNA signal in the wash buffer decrease to noise level.

Even low levels of remaining contaminant are sufficient to move most of the complex into the void volume during size exclusion chromatography.

Figure 9. Contamination of recombinant ScCCAN subcomplexes by bacterial DNA

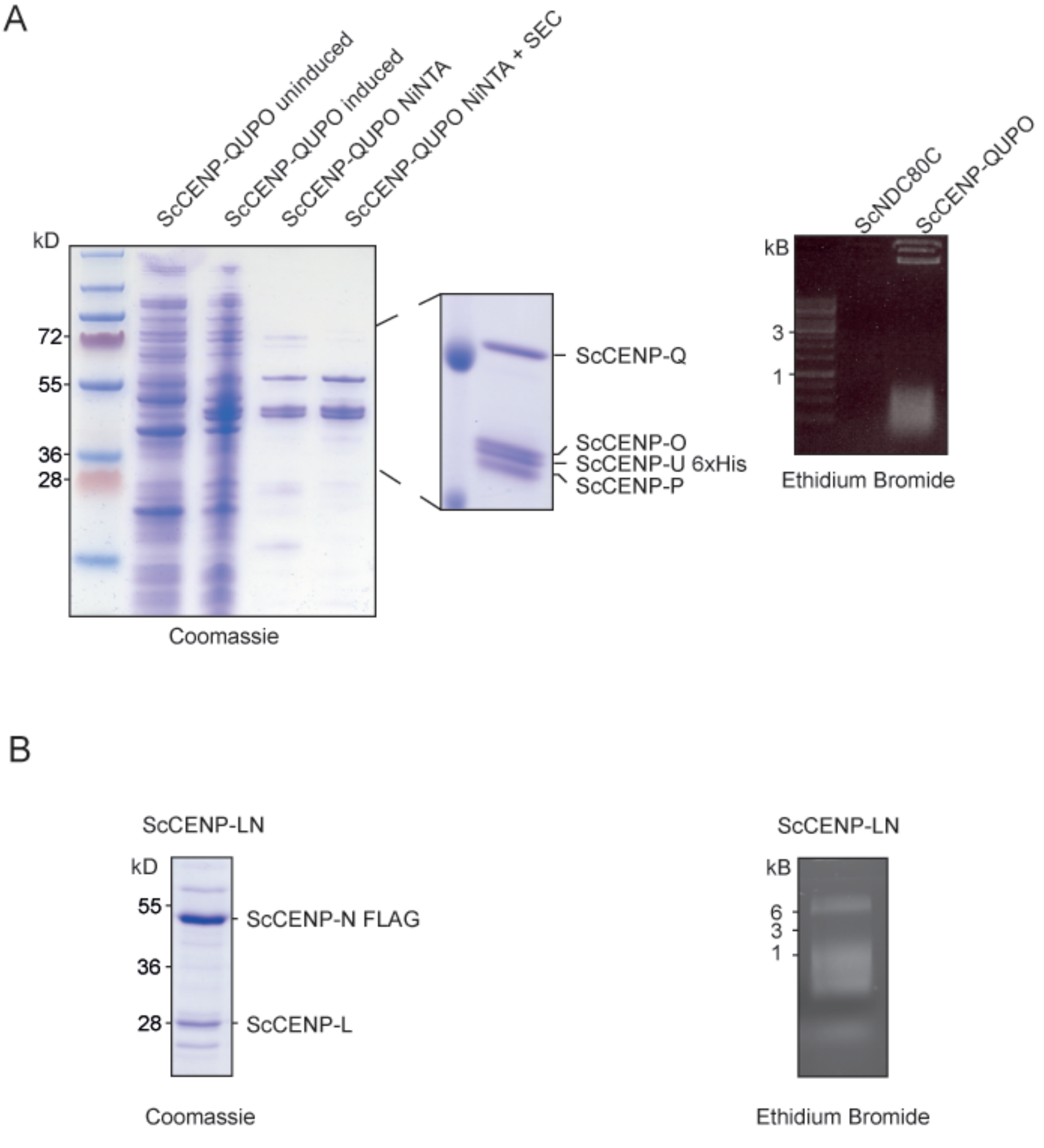
A
ScCENP-QUPO uninduced
ScCENP-QUPO induced
ScCENP-QUPO NiNTA
ScCENP-QUPO NiNTA + SEC
kD
72
55
36
28
ScCENP-Q
ScCENP-O
ScCENP-U 6xHis
ScCENP-P
Coomassie
ScNDC80C
ScCENP-QUPO
kB
3
1
Ethidium Bromide
B
ScCENP-LN
kD
55
36
28
ScCENP-N FLAG
ScCENP-L
Coomassie
ScCENP-LN
kB
6
3
1
Ethidium Bromide

Figure 9A) Expression and purification strategy for ScCENP-Q/U/P/O 6xHis by NiNTA affinity purification and size exclusion chromatography. The final complex migrated in the void volume during chromatography. To test for nonspecific DNA binding, a sample of the complex was analyzed on an ethidium bromide stained Agarose Gel. ScNDC80C served as control and in contrast to ScCENP-Q/U/P/O is not contaminated by DNA. **Figure 9B**) Similarly to the CENP-Q/U/P/O complex, FLAG-tag affinity purified ScCENP-L/N migrated in the void volume during size exclusion chromatography and was contaminated by DNA.

Figure 10. Analysis of the contaminant

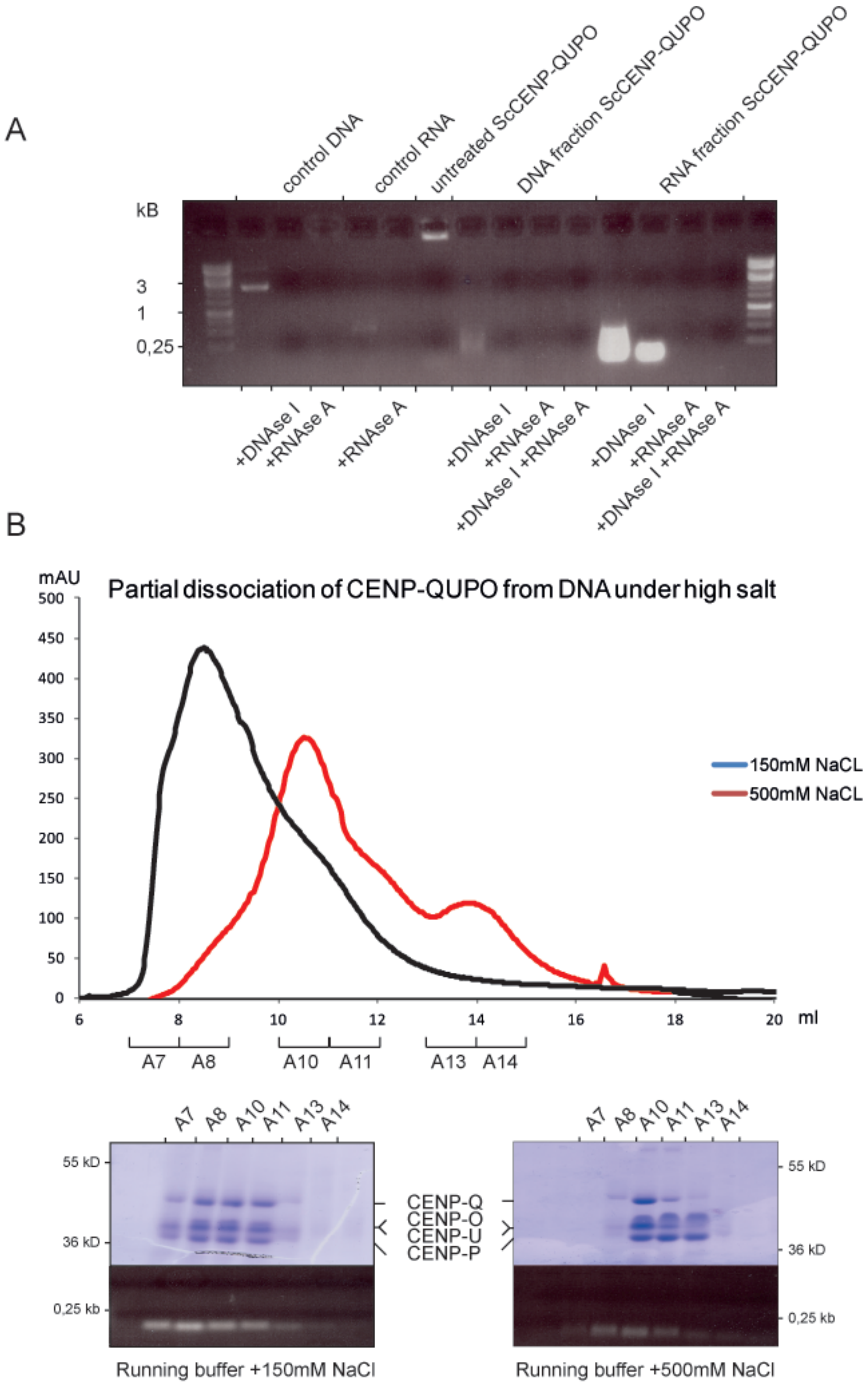

Figure 10A) To analyze the contaminant found in recombinant ScCENP-Q/U/P/O complex, DNA and RNA from a sample of the complex were extracted with the Trizol® reagent. DNA and RNA fractions were further analyzed by digestion with DNAseI or RNAse A, respectively, to confirm extraction results. Note that our RNAse A was active against DNA as evidenced by degradation of the control DNA (pET3A). The majority of the contaminant remains in the RNA fraction. Note lane 6, CENP-Q/U/P/O that has not been extracted with TRIzol® and remains in complex with the contaminant retains it in the Gel-pocket. **Figure 10B** demonstrates an initial attempt to separate complex and contaminant by increasing ionic strength in the buffer. ScCENP-Q/U/P/O was subjected to size exclusion chromatography in a running buffer containing either 150mM or 500mM NaCl. While the complex peak does separate from the contaminant peak in high salt, during chromatography the complex itself dissociates and peak separation is not sufficient to isolate pure samples.

Although salt washes removed the contaminant, the pure CENP-Q/U/P/O complex after elution was very unstable and tended to precipitate shortly after elution. Thus I set up a secondary systematic screen in the hope to find conditions that would stabilize the contaminant-free complex. The approach was similar to the initial screen. A large-scale purification from 24l was performed and washed as described. Following washing, beads were split into equal volumes and eluted with buffer that was equal to the lysis buffer save for the 300mM imidazole required for elution and one varied parameter, ionic strength, pH or additive. I screened a series of pH variations, a series of ionic strength variations and a number of ionic additives. 5mM of divalent cations known to be complexed with some proteins, Mg^{2+}, Zn^{2+} and Ca^{2+} were tested. Because divalent cations may have precipitating effect on proteins, one buffer containing 50mM of both EGTA and EDTA was tested. While EDTA has a preference for Mg^{2+} and EGTA has a preference for Ca^{2+}, both generally complex divalent cations and thus this buffer, with a relatively high concentration of chelators, would be expected to remove all divalent cations from solution. Lastly Heparin was tested. Heparin is highly negatively charged and though to remove DNA from DNA binding proteins by competition for the often basic binding site. Figure 11B shows the results of the pH and additive screen, the ionic concentration screen is omitted because only a minor effect on complex stability was observed. Note that the ScCENP-U and ScCENP-O bands have not been separated on these gels. Thus complex integrity was judged by intensity of ScCENP-P relative to ScCENP-Q. Observe that in the bottom gel of Figure 11B addition of EGTA/EDTA affects stoichiometry negatively, as the ScCENP-P band is entirely absent. Addition of 5mM Ca^{2+} in contrast provides best preservation of stoichimetry although some ScCENP-O/P is lost and subsequently separates from ScCENP-Q/U/P/O during size exclusion chromatography. In the following large-scale purifications, the concentration of Ca^{2+} was reduced to 1mM to minimize possible adverse effects of this chaotropic ion. The top gel displays the effects of varying pH in the elution buffer. While not significant, it appears that a slightly lower pH between 6.6 and 7 is beneficial, although, because no Ca^{2+} was present in these elution buffers, complex stoichiometry is significantly disrupted.

Using the conditions established in this screen the first large scale purification was performed from 6l liquid culture. The purification scheme in Figure 12 demonstrates its success. The contaminant is present in the complex eluted from beads before the washing steps but absent after washing. Concentrated ScCENP-Q/U/P/O complex loaded onto a size exclusion chromatography column separates sufficiently to obtain pure samples (Figure 12B). The pure ScCENP-Q/U/P/O complex is followed by a complex that co-migrates with a high amount of putative chaperone and later by what appears to be disrupted dimeric complex, predominantly ScCENP-Q/U. The yield is relatively low, about 1,5mg of total protein per 6l culture, sufficient only for a few assays, but the complex behaves well during size exclusion chromatography as shown in Figure 14 A.

All three dimeric subcomplexes ScCENP-Q/U, ScCENP-O/P and ScCENP-L/N, when expressed individually, were found to be contaminated with bacterial DNA. I successfully applied this protocol to purify in addition the ScCENP-Q/U complex (Figure 13). The yield of a ScCENP-Q/U purification is significantly higher with about 11mg per 6l culture. Dr. Peter Hornung successfully used this protocol to purify both ScCENP-O/P and ScCENP-L/N complexes. One may deviate from the ScCENP-Q/U/P/O protocol by using salt concentrations of 1M and 1,5M for the purification of ScCENP-Q/U and ScCENP-P/O respectively, to expedite washing. Both dimeric complexes are extremely salt stable, the CENP-Q/U complex did not dissociate when NaCl concentration was gradually increased up to 5M, suggesting a hydrophobic interaction between ScCENP-Q and ScCENP-U (data not shown).

Figure 11. Systematic screen for suitable ScCENP-Q/U/P/O wash and elution buffers

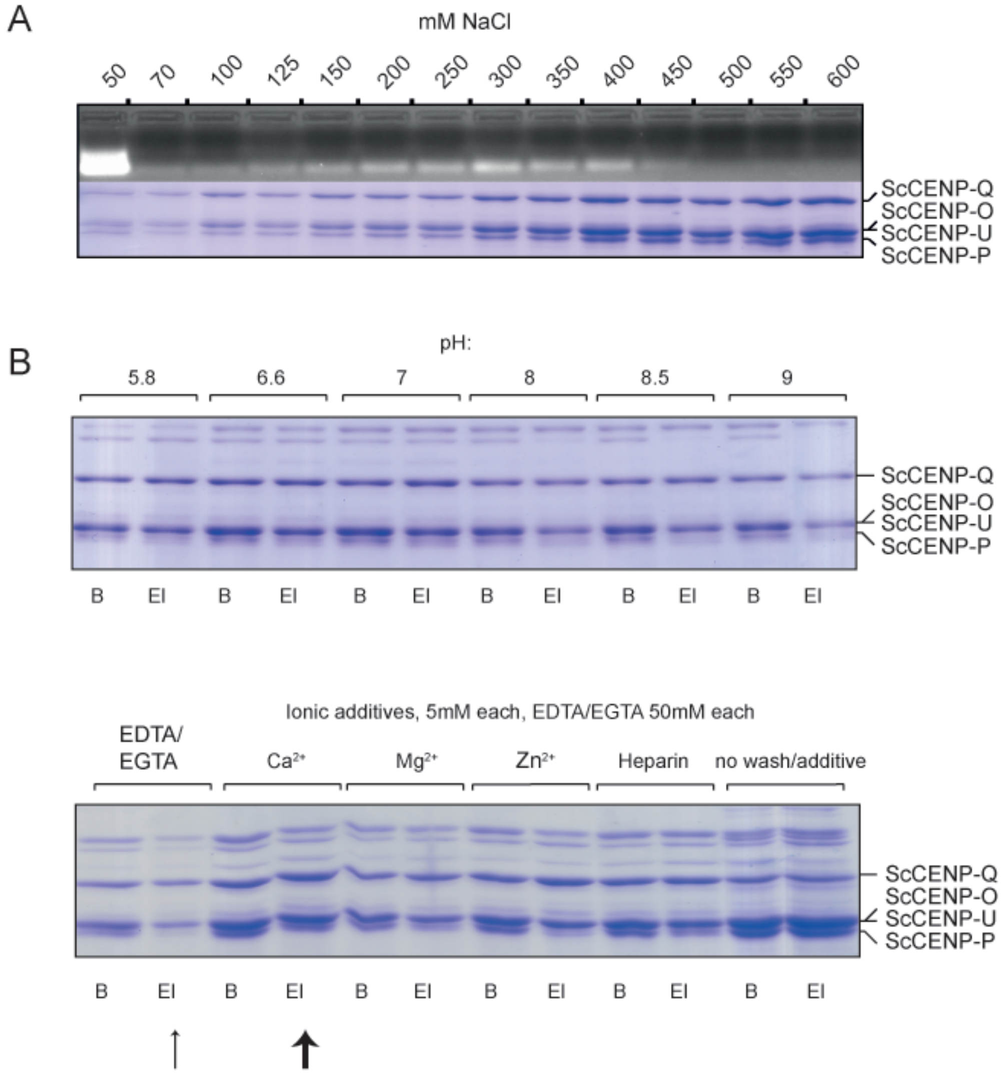
A
mM NaCl
50
70
100
125
150
200
250
300
350
400
450
500
550
600
ScCENP-Q
ScCENP-O
ScCENP-U
ScCENP-P
B
pH:
5.8
6.6
7
8
8.5
9
ScCENP-Q
ScCENP-O
ScCENP-U
ScCENP-P
B El B El B El B El B El B El
Ionic additives, 5mM each, EDTA/EGTA 50mM each
EDTA/
EGTA
Ca2+
Mg2+
Zn2+
Heparin
no wash/additive
ScCENP-Q
ScCENP-O
ScCENP-U
ScCENP-P
B El B El B El B El B El B El

Figure 11A) displays the results of the NaCl concentration series in a screen to find a suitable wash buffer that would remove the contaminant but retain complex stoichiometry. The contaminant is lost with increasing salt strength retaining complex integrity up to 600mM NaCl. Beyond 600mM NaCl, complex stoichiometry was significantly disrupted (not shown). **Figure 11B)** displays the results of the subsequent screen for an elution buffer that would stabilize the contaminant-free complex. Note the absence of ScCENP-P from the complex when EGTA/EDTA is supplemented (small arrow). Addition of 5mM Ca^{2+} in turn provided best conservation of ScCENP-P in the ScCENP-Q/U/P/O complex that was purified through a 6xHis tag on ScCENP-U.

Figure 12. Purification of ScCENP-Q/U/P/O

A. Batch purification

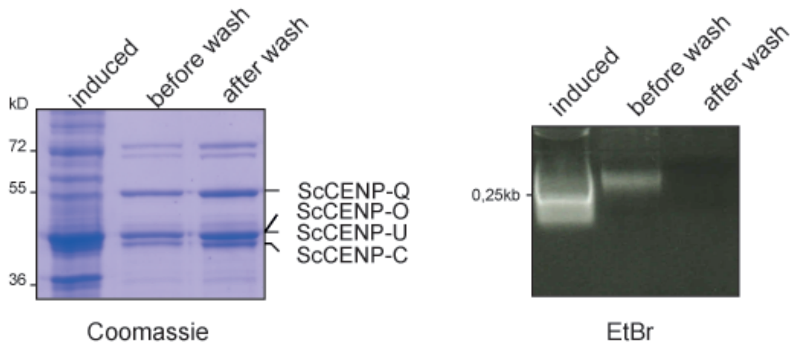
induced
before wash
after wash
kD
72
55
36
ScCENP-Q
ScCENP-O
ScCENP-U
ScCENP-C
Coomassie
induced
before wash
after wash
0,25kb
EtBr

B. Size exclusion chromatography

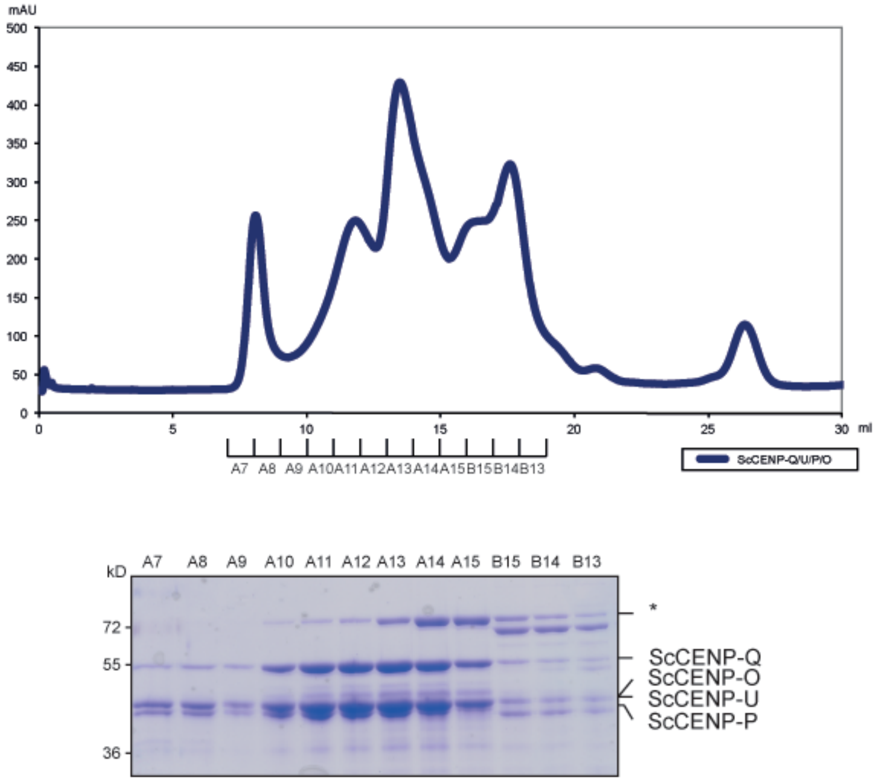

Figure 12A) Large scale batch purification of ScCENP-Q/U/P/O. Comparative SDS-PAGE and ethidium bromide agarose gels demonstrate that the contaminant is lost by washing and complex stoichiometry remains intact. **Figure 12B)** Size exclusion chromatography of ScCENP-Q/U/P/O. Note the pure complex in fraction A10-13 followed by a contaminating chaperone band (*) in fraction A14-15 and dimeric ScCENP-Q/U in A14-A15.

Figure 13. Purification strategy for ScCENP-Q/U

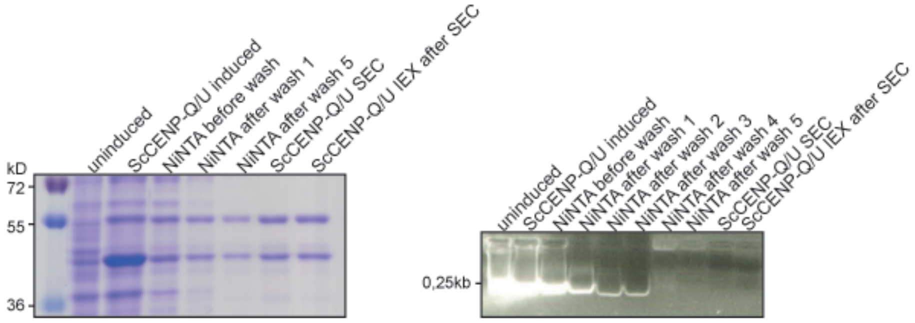
kD
72
55
36
uninduced
ScCENP-Q/U induced
NiNTA before wash
NiNTA after wash 1
NiNTA after wash 5
ScCENP-Q/U SEC
ScCENP-Q/U IEX after SEC
0,25kb
uninduced
ScCENP-Q/U induced
NiNTA before wash
NiNTA after wash 1
NiNTA after wash 2
NiNTA after wash 3
NiNTA after wash 4
NiNTA after wash 5
ScCENP-Q/U SEC
ScCENP-Q/U IEX after SEC

Figure 13) Purification scheme of recombinant ScCENP-Q/U. After initial adsorption of the complex onto beads, the complex was washed 5 times in 1M NaCl containing wash buffer. The complex was further purified by size exclusion chromatography. An ion exchange chromatography step following SEC did not yield a significant increase in purity.

3.6 Interactions of the ScCENP-Q/U/P/O complex.

With the recombinant ScCENP-Q/U/P/O complex in hand I was able to perform in vitro binding assays. Three candidates were investigated. Firstly the ScMIS12C, as it is unclear how it is recruited to kinetochores in yeast, but its localization is impaired in ScCENP-Q mutants[600]. Secondly, binding to microtubules was tested, as a vertebrate CENP-Q interaction with microtubules had been shown[451]. Thirdly, the interaction with DNA was tested, as the complex was contaminated with bacterial DNA/RNA. Starting out with the ScMIS12C, I tested for a potential interaction with the ScCENP-Q/U/P/O complex by a binding assay in which I mixed both complexes in solution and analyzed complex formation by size exclusion chromatography. The chromatogram in Figure 14A demonstrates co-elution of the two complexes after mixing and a notable shift of the elution profile to a lower volume which is accompanied by an increase of the Stokes radius as both complexes associate. This interaction was confirmed by Dr. Peter Hornung by both size exclusion chromatography and CoIP and has since been published[488]. The corresponding SDS-PAGE analysis in Figure 14B shows the shift and the effect of binding on complex stoichiometry. Currently we are not certain why some ScCENP-O appears to remain in the higher elution volume. However in the topmost gel, lane A11, it appears that some ScCENP-O may exist free from the COMA complex in this sample. Some of our unpublished binding assays suggest that it is the CENP-Q/U complex, likely CENP-U, that binds to either ScMis12 or ScNnf1 which is supported by Figure 4. This would explain why free ScCENP-O is incompetent to bind ScMIS12C (Dr. Peter Hornung, personal communication).

Figure 14. In vitro reconstitution of an interaction between ScCENP-QUPO and ScMTW12C

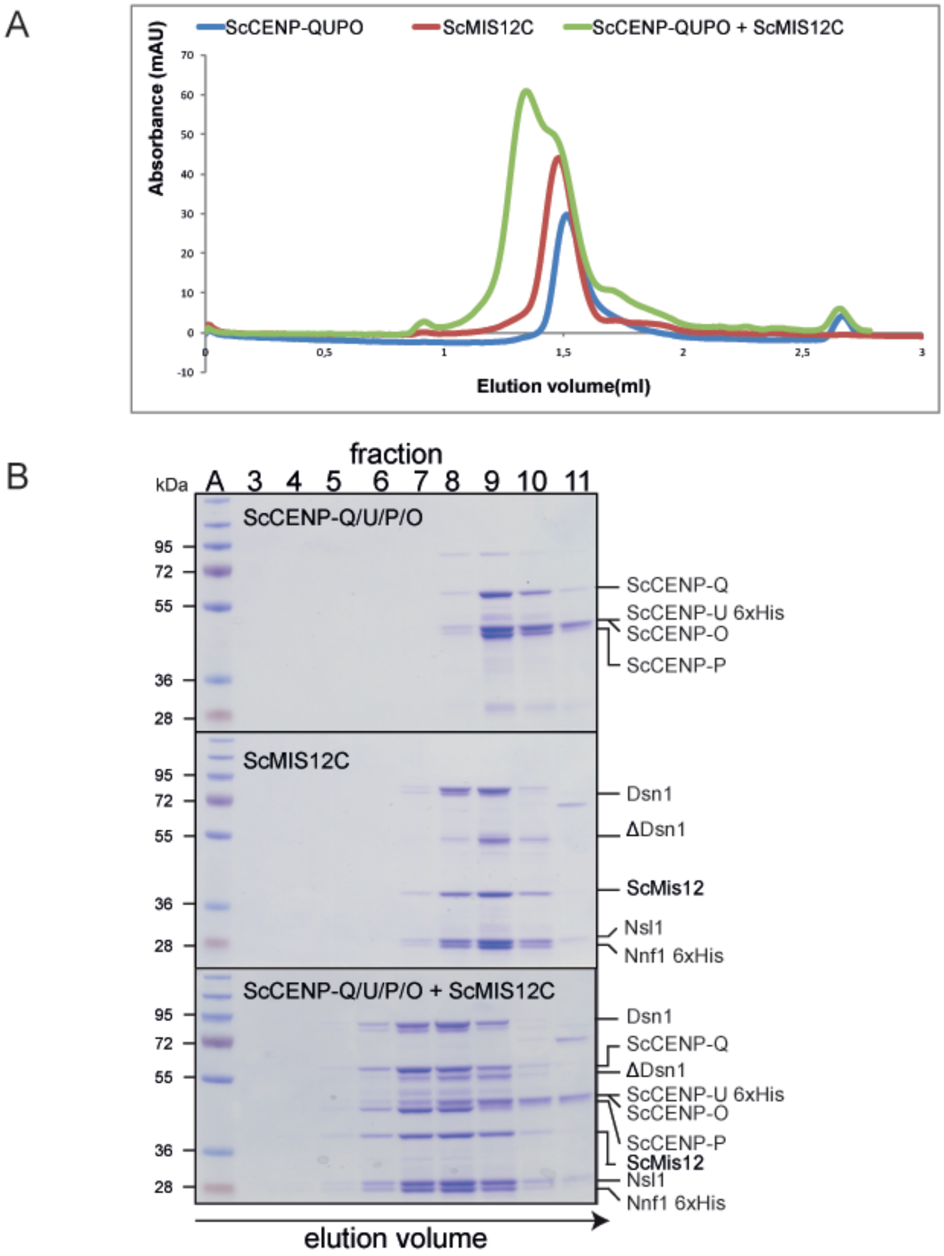

Figure 14) In vitro reconstitution of an interaction between ScMIS12C and ScCENP-Q/U/P/O. **A)** Overlay of the chromatograms resulting from analytical size exclusion chromatography of ScCENP-Q/U/P/O, ScMIS12C and the ScMIS12C-ScCENP-Q/U/P/O complex formed by pre-incubation. **B)** Consecutive fractions eluted during analytical SEC. Note that some ScCENP-O retains a low elution volume and does not associate with the complex.

Having demonstrated interaction between ScCENP-Q/U/P/O and ScMIS12C I investigated the interaction of ScCENP-Q/U/P/O with microtubules. For this I initially employed a standard microtubule co-sedimentation assay (MTBA) in which microtubules are assembled in vitro, stabilized by Taxol, incubated with the protein complex in question, then separated from the supernatant by centrifugation. The microtubule pellet and the remaining supernatant are then analyzed for the relative amount of sedimenting complex. The standard assay uses conditions that are detrimental to the solubility of ScCENP-Q/U/P/O, namely a low salt buffer and no Ca^{2+}. I was able to supplement 150mM NaCl but omit Ca^{2+}, which depolymerizes microtubules, and thereby reduce the fraction of ScCENP-Q/U/P/O that sedimented in absence of microtubules. Figure 15A displays an initial MTBA using standard conditions. Note the strong, microtubule independent sedimentation of ScCENP-Q/U/P/O. Figure 15B displays a microtubule binding assay in the presence of 150mM NaCl in the binding buffer. Some microtubule-independent sedimentation of ScCENP-Q/U/P/O remains but no microtubule concentration dependent increase in sedimentation is evident. Thus, ScCENP-Q/U/P/O does not bind microtubules in my hands.

Figure 15. ScCENP-Q/U/P/O microtubule binding assay

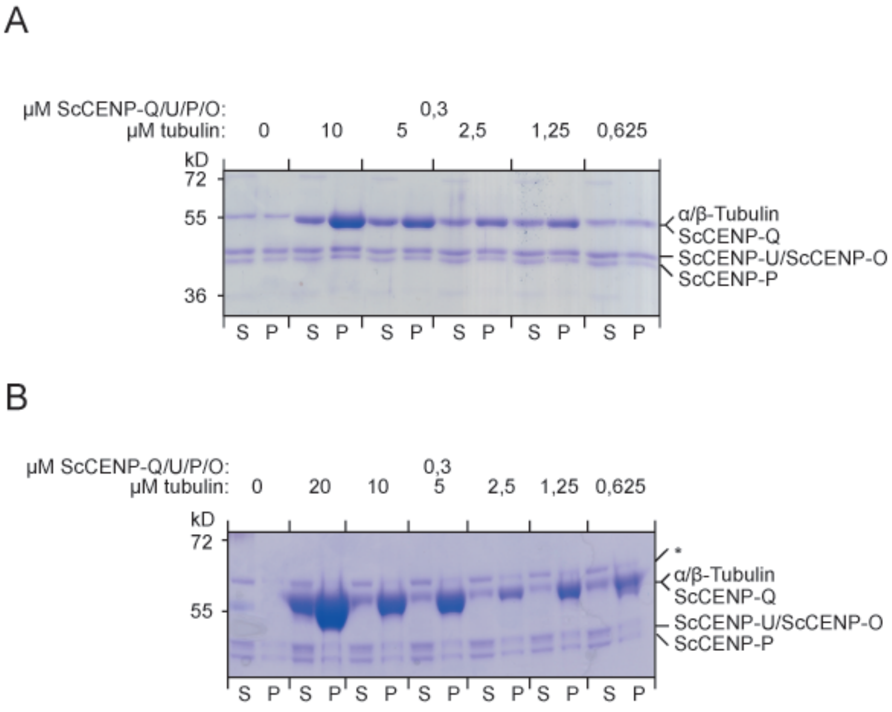
A
µM ScCENP-Q/U/P/O: 0,3
µM tubulin: 0 10 5 2,5 1,25 0,625
kD
72
55
36
α/β-Tubulin
ScCENP-Q
ScCENP-U/ScCENP-O
ScCENP-P
S P S P S P S P S P S P
B
µM ScCENP-Q/U/P/O: 0,3
µM tubulin: 0 20 10 5 2,5 1,25 0,625
kD
72
55
*
α/β-Tubulin
ScCENP-Q
ScCENP-U/ScCENP-O
ScCENP-P
S P S P S P S P S P S P S P

Figure 15) Microtubule binding assays for ScCENP-Q/U/P/O. **A)** The ScCENP-Q/U/P/O complex sediments on its own under standard MTBA buffer conditions. **B)** Supplementing 150mM NaCl reduces ScCENP-Q/U/P/O sedimentation. Under these conditions, no interaction with microtubules is observed, as there is no tubulin-dependent increase of sedimenting ScCENP-Q/U/P/O.

Lastly I attempted to demonstrate DNA binding activity of the ScCENP-Q/U/P/O complex. For this I adopted a simple electrophoretic mobility shift assay (EMSA) in which I used a yeast centromeric sequence that was incubated with ScCENP-Q/U/P/O for thirty minutes. Upon binding, I expected a decreased mobility of only the centromere-containing DNA in a Polyacrylamid Gel if ScCENP-Q/U/P/O bound the centromere with sequence specificity and decreased mobility for both centromeric and non-centromeric control DNA if binding was nonspecific.

Figure 16. EMSA for ScCENP-Q/U/P/O

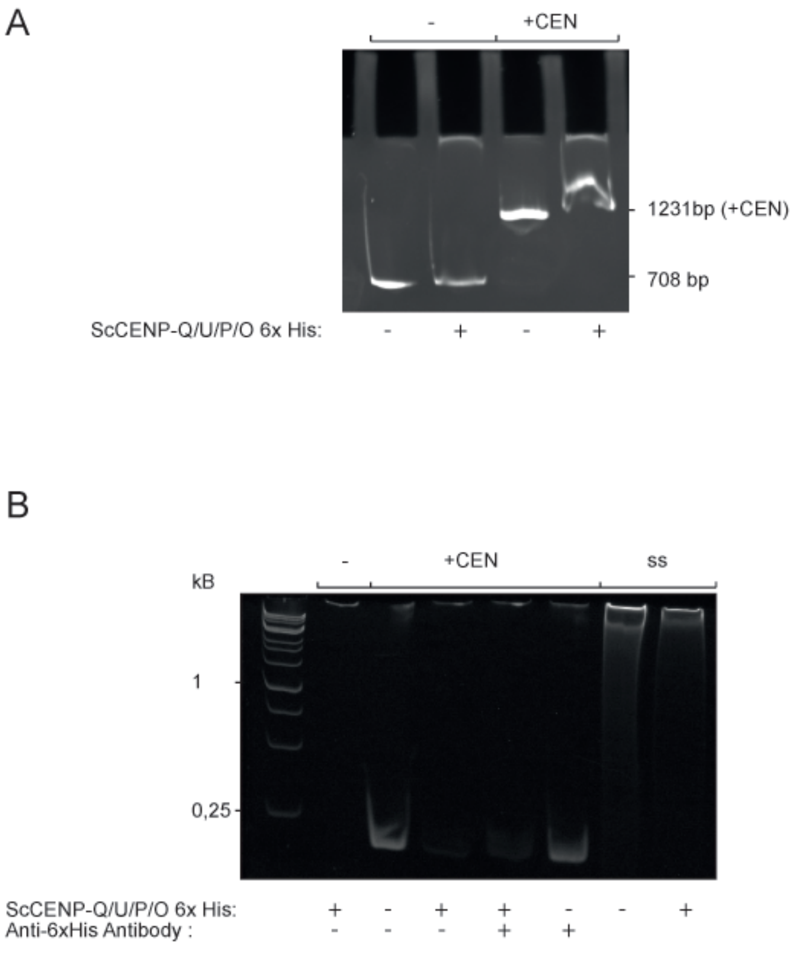
A
-
+CEN
1231bp (+CEN)
708 bp
ScCENP-Q/U/P/O 6x His: - + - +
B
-
+CEN
ss
kB
1
0,25
ScCENP-Q/U/P/O 6x His: + - + + - - +
Anti-6xHis Antibody : - - - + +

Figure 16A) EMSA using recombinant ScCENP-Q/U/P/O, a CEN6-ARSH4 containing fragment excised from pRS313 and the corresponding CEN6-ARSH4 free fragment excised from the parent vector pRS303. **Figure 16B**) EMSA using CEN6 amplified from pRS313 and salmon sperm as a CEN-free control.

Figure 16A displays an initial attempt. Here a fragment containing CEN6-ARSH4 of pRS313 was excised using restriction enzymes ScaI and AfeI, yielding a CEN6 containing DNA fragment of 1231bp length. The same region was excised from the parent vector, pRS303, lacking both yeast CEN6 and ARSH4, to yield a 708bp fragment devoid of a centromere. Both sequences were tested for binding to ScCENP-Q/U/P/O. Mobility of only the CEN6 containing sequence is decreased when incubated with ScCENP-Q/U/P/O complex. In an attempt to further refine this assay I used a smaller construct, a single CEN6 sequence amplified by PCR (Figure 16B). To increase the mobility shift, I added anti-Hisx6 antibodies to one ScCENP-Q/U/P/O-CEN6 binding reaction in the hope of supershifting the complex on the polyacrylamide gel. Results of these EMSAs were not conclusive. The ScCENP-Q/U/P/R samples used in these initial experiments were purified by RNAse digestion, not by salt washes and retained some bacterial DNA. Rather than unambiguously decreasing DNA mobility, ScCENP-Q/U/P/O appeared prone to retain additional CEN6 DNA in the gel pocket. Note however that lane 4, which includes the anti-Hisx6 antibody, displays a band that is smeared upwards. Dr. Peter Hornung was more successful using agarose gels to demonstrate a mobility shift (not show, unpublished)

3.7 Phosphorylation-site analysis of the budding yeast CCAN.

We decided to map phosphorylation sites on all ScCCAN proteins to be able to investigate potential phospho-regulation. To this end the samples I generated during my tandem affinity purifications of native yeast ScCCAN proteins were not only subjected to protein identification but also to identification of phosphorylation sites by mass spectrometry. Figure 17 displays the collection of all phosphosites detected in vivo. Among others, we detected multiple phosphosites conforming to the CDK1 minimum consensus sequence [S/T][P]. It has previously been established that ScCENP-T is a specific target of Clb5-CDK1[95]. Vertebrate CENP-U and CENP-T have been demonstrated to contain multiple CDK-phosphorylated residues[582]. ScCENP-U contains a cluster of phosphorylated CDK1 consensus sites close to its amino terminus (Figure 17B). Clusters of CDK1 consensus sites are predictive for in vivo phosphorylation and finding a phosphorylated cluster here identifies an interesting, possibly functionally regulated region of ScCENP-U[845]. In order to confirm the results obtained from native kinetochore proteins I employed an in vitro phosphorylation assay. Both ScCENP-Q/U/P/O subcomplexes, ScCENP-Q/U and ScCENP-O/P were tested for phosphorylation by either Clb2-CDK1 or Clb5-CDK1. As demonstrated in Figure 18, ScCENP-U, ScCENP-Q and ScCENP-O are in vitro targets for CDK1. ScCENP-U displays a prominent mobility shift during SDS-PAGE after CDK1 phosphorylation (Figure 18A).

Figure 17. ScCCAN phosphorylation sites in vivo

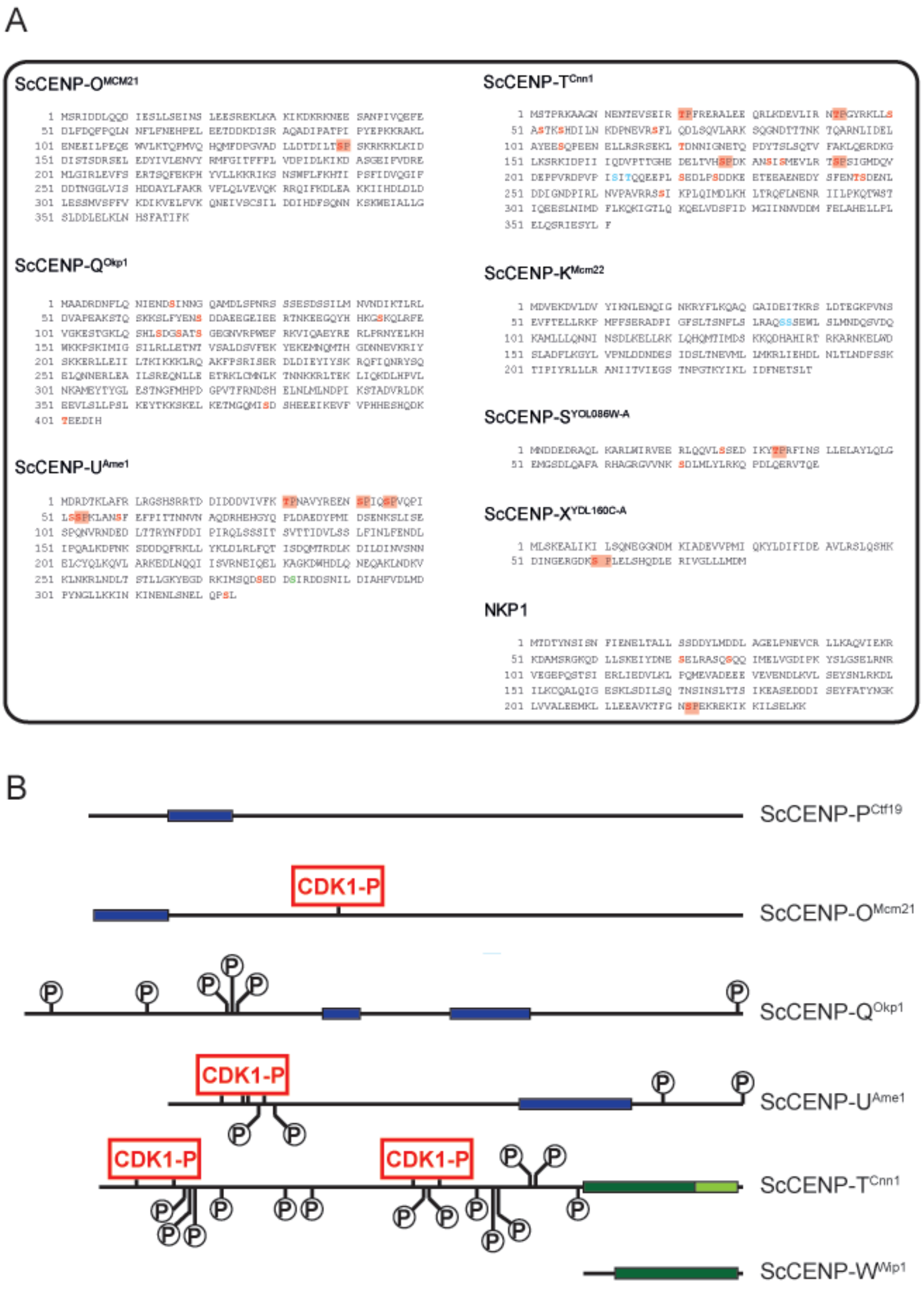
A
ScCENP-O^{MCM21}
1 MSRIDDLQQD IESLLSEINS LEESREKLKA KIKDKRKNEE SANPIVQEFE
51 DLFDQFPQLN NFLFNEHPEL EETDDKDISR AQADIPATPI PYEPKKRAKL
101 ENEEILPEQE WVLKTQPMVQ HQMFDPGVAD LLDTDILTSP SKRKRKLKID
151 DISTSDRSEL EDYIVLENVY RMFGITFFPL VDPIDLKIKD ASGEIFVDRE
201 MLGIRLEVFS ERTSQFEKPH YVLLKKRIKS NSMFLFKHTI PSFIDVQGIF
251 DDTNGGLVIS HDDAYLFAKR VFLQLVEVQK RRQIFKDLEA KKIIHDLDLD
301 LESSMVSFFV KDIKVELFVK QNEIVSCSIL DDIHDFSQNN KSKMEIALLG
351 SLDDLELKLN HSFATIFK
ScCENP-Q^{Okp1}
1 MAADRDNFLQ NIENDSINNG QAMDLSPNRS SSESDSSILM NVNDIKTLRL
51 DVAPEAKSTQ SKKSLFYENS DDAEEGEIEE RTNKEEGQYH HKGSKQLRFE
101 VGKESTGKLQ SHLSDGSATS GEGNVRPWEF RKVIQAEYRE RLPRNYELKH
151 WKKPSKIMIG SILRLLETNT VSALDSVFEK YEKEMNQMTH GDNNEVKRIY
201 SKKERLLEII LTKIKKKLRQ AKFPSRISER DLDIEYIYSK RQFIQNRYSQ
251 ELQNNERLEA ILSREQNLLE ETRKLCMNLK TNNKKRLTEK LIQKDLHPVL
301 NKAMEYTYGL ESTNGFMHPD GPVTFRNDSH ELNLMLNDPI KSTADVRLDK
351 EEVLSLLPSL KEYTKKSKEL KETMGQMISD SHEEEIKEVF VPHHESHQDK
401 TEEDIH
ScCENP-U^{Ame1}
1 MDRDTKLAFR LRGSHSRRTD DIDDDVIVFK TPNAVYREEN SPIQSPVQPI
51 LSSPKLANSF EFPITTNNVN AQDRHEHGYQ PLDAEDYPMI DSENKSLISE
101 SPQNVRNDED LTTRYNFDDI PIRQLSSSIT SVTTIDVLSS LFINLFENDL
151 IPQALKDFNK SDDDQFRKLL YKLDLRLFQT ISDQMTRDLK DILDINVSNN
201 ELCYQLKQVL ARKEDLNQQI ISVRNEIQEL KAGKDWHDLQ NEQAKLNDKV
251 KLNKRLNDLT STLLGKYEGD RKIMSQDSED DSIRDDSNIL DIAHFVDLMD
301 PYNGLLKKIN KINENLSNEL QPSL
ScCENP-T^{Cnn1}
1 MSTPRKAAGN NENTEVSEIR TPFRERALEE QRLKDEVLIR NTPGYRKLLS
51 ASTKSHDILN KDPNEVRSFL QDLSQVLARK SQGNDTTTNK TQARNLIDEL
101 AYEESQPEEN ELLRSRSEKL TDNNIGNETQ PDYTSLSQTV FAKLQERDKG
151 LKSRKIDPII IQDVPTTGHE DELTVHSPDK ANSISMEVLR TSPSIGMDQV
201 DEPPVRDPVP ISITQQEEPL SEDLPSDDKE ETEEAENEDY SFENTSDENL
251 DDIGNDPIRL NVPAVRRSSI KPLQIMDLKH LTRQFLNENR IILPKQTWST
301 IQEESLNIMD FLKQKIGTLQ KQELVDSFID MGIINNVDDM FELAHELLPL
351 ELQSRIESYL F
ScCENP-K^{Mcm22}
1 MDVEKDVLDV YIKNLENQIG NKRYFLKQAQ GAIDEITKRS LDTEGKPVNS
51 EVFTELLRKP MFFSERADPI GFSLTSNFLS LRAQSSSEWL SLMNDQSVDQ
101 KAMLLLQNNI NSDLKELLRK LQHQMTIMDS KKQDHAHIRT RKARNKELWD
151 SLADFLKGYL VPNLDDNDES IDSLTNEVML LMKRLIEHDL NLTLNDFSSK
201 TIPIYRLLLR ANIITVIEGS TNPGTKYIKL IDFNETSLT
ScCENP-S$^{YOL086W-A}$
1 MNDDEDRAQL KARLMIRVEE RLQQVLSSED IKYTPRFINS LLELAYLQLG
51 EMGSDLQAFA RHAGRGVVNK SDLMLYLRKQ PDLQERVTQE
ScCENP-X$^{YDL160C-A}$
1 MLSKEALIKI LSQNEGGNDM KIADEVVPMI QKYLDIFIDE AVLRSLQSHK
51 DINGERGDKS PLELSHQDLE RIVGLLLMDM
NKP1
1 MTDTYNSISN FIENELTALL SSDDYLMDDL AGELPNEVCR LLKAQVIEKR
51 KDAMSRGKQD LLSKEIYDNE SELRASQGQQ IMELVGDIPK YSLGSELRNR
101 VEGEPQSTSI ERLIEDVLKL PQMEVADEEE VEVENDLKVL SEYSNLRKDL
151 ILKCQALQIG ESKLSDILSQ TNSINSLTTS IKEASEDDDI SEYFATYNGK
201 LVVALEEMKL LLEEAVKTFG NSPEKREKIK KILSELKK
B
ScCENP-P^{Ctf19}
CDK1-P
ScCENP-O^{Mcm21}
P
P
P
P
P
P
ScCENP-Q^{Okp1}
CDK1-P
P
P
P
P
ScCENP-U^{Ame1}
CDK1-P
CDK1-P
P
P
P
P
P
P
P
P
P
P
P
P
P
P
ScCENP-T^{Cnn1}
ScCENP-W^{Mip1}

Figure 17A) Mapped in vivo phosphorylation sites on ScCCAN proteins. Red letters denote phosphorylated sites. Red-shaded letters mark phosphorylated CDK1 consensus sites. Pairs of blue letters denote that at least one residue of the pair is phosphorylated but it is uncertain which. The green serine within the sequence of ScCENP-U denotes a site conforming to a polo like kinase consensus sequence not found to be phosphorylated. **Figure 17B)** Schematic depiction of phosphorylation sites on proteins of the ScCENP-Q/U/P/O complex as well as on the ScCENP-T/W complex. Phosphorylation sites conforming to a minimal CDK1 consensus are marked in red, all other phosphorylation sites in black. The colored segments denote structural elements identified by Dr. Alexander Schleiffer. Blue represents a predicted coiled coil while green represents a histone fold. Light green marks a C-terminal domain unique to CENP-T orthologues.

ScCENP-Q/U and ScCENP-P/O were in vitro phosphorylated using ATPγ^{32}P and either Clb2-CDK1 or Clb5-CDK1. The autoradiographs in Figure 18B demonstrate that ScCENP-U is strongly phosphorylated by Clb2-CDK1 but not by Clb5-CDK1. Similarly, ScCENP-O is strongly phosphorylated by Clb2-CDK1 but only weakly Clb5-CDK1. As Clb2-CDK1 displayed a higher activity towards both, ScCENP-Q/U and ScCENP-P/O, I performed two additional in vitro phosphorylation reactions of both complexes using Clb2-CDK1 and ATP. The residues phosphorylated in vitro were subsequently identified by mass spectrometry. As was the case in vivo, no in vitro phosphorylated residues were detected on ScCENP-P. Recombinant ScCENP-Q was in vitro phosphorylated by Clb2-CDK1 but none of the phosphorylated residues matched those identified on the native protein. In contrast the CDK1 consensus site on ScCENP-O S139 was phosphorylated both in vivo and in vivo. The CDK1 phosphorylated N-terminal cluster found on ScCENP-U in vivo was confirmed by in vitro phosphorylation. T31, S41, S45 and S53 were phosphorylated in both experiments. Phosphorylation of the adjacent S58 was only detected in vivo while phosphorylation of the CDK1 consensus at S101 was only detected in vitro.

The animal kinetochore undergoes extensive assembly and disassembly during the cell cycle. The CPC, the KMN network, Zwint-1, CENP-E, CENP-F, Bub1 and BubR1 localize to the kinetochore between late G2 and prophase while the RZZ complex, Spindly, Mad1&2 and Dynein/Dynactin localize to the kinetochore shortly before or after NEBD. SAC proteins and the CPC leave the kinetochore before anaphase onset while the KMN network leaves at telophase[503, 515, 531, 577, 596, 612, 738, 846]. CCAN proteins remain at the centromere throughout most of the cell cycle but recent higher resolution assays demonstrate subtle cell cycle specific changes[570, 632, 717, 795]. In contrast, budding yeast kinetochores appear competent to assemble at any point during the cell cycle as long as ScCENP-A has been deposited at the centromere during S-Phase. However more subtle changes of kinetochore assembly or, as reported for purified kinetochore particles, changes in microtubule affinity may take place over the cell cycle[465, 788, 847]. The prime candidate for the regulation of cell cyle dependent kinetochore assembly would be a cyclin dependent kinase. Supporting the idea of a CDK regulated kinetochore assembly, it has recently been demonstrated that CDK1 phosphorylation- mimicking vertebrate CENP-T recruits NDC80C to ectopic foci while a CDK1 phosphorylation negative CENP-T does not[577]. However to date no essential CDK phosphorylation at the kinetochore has been described. Confirming a CDK1 cluster on the essential ScCENP-U, together with its interaction with the ScMIS12C suggested its essential function may be regulated by CDK1.

In order to test this, I employed the anchor away technique in a yeast strain in which conditional nuclear depletion of ScCENP-U was possible. In short this technique relies on the high affinity dimerization of human FKBP12 and the FRB domain of human mTOR that is induced in presence of rapamycin. FKBP12 is fused to the ribosmal RPL13A in the anchor away parent strain used, while a FRB domain can be fused to the protein targeted for depletion from the nucleus. Upon addition of rapamycin, RPL-13A-FKBP12 and FRB-ScCENP-U dimerize and the flux of ribosomal proteins out of the nucleus sequesters FRB-ScCENP-U into the cytoplasm. Because the nuclear envelope never breaks down, this technique is applicable to deplete a nuclear protein during budding yeast mitosis[848]. The anchor away FRB-ScCENP-U strain was a kind donation of Dr. Christine Mieck. As demonstrated in Figure 19, this strain fails to grow when ScCENP-U depletion is induced on rapamycin containing YPD-plates while the parent strain is viable. To investigate the functional significance of the identified CDK1 cluster, ScCENP-U was cloned into pRS306. I included 284bp upstream sequence preceeding the start codon and 234bp downstream of the stop codon to preserve the native promoter and 3'UTR, so expression of episomal ScCENP-U would be regulated to levels close to those of genomic ScCENP-U. CDK1-phosphonegative ScCENP-U was generated by a Quikchange® site directed mutagenesis kit, mutating T31, S41, S45, S53 and S101 of pRS306-ScCENP-U to alanine. The FRB-ScCENP-U anchor away strain was then transformed with either pRS306-ScCENP-U or pRS306-ScCENP-U 5A linearized with AfeI and selection for the Ura$^+$ marker allowed isolation of clones containing either ScCENP-U or ScCENP-U 5A integrated into the URA3 locus. If CDK1 phosphorylation of ScCENP-U regulated an essential process, one would expect ScCENP-U to rescue a depletion of genomic ScCENP-U while ScCENP-U 5A should not be able to do so.

As evident in Figure 19, both, ScCENP-U and ScCENP-U 5A are competent to rescue the lethality of a conditional ScCENP-U depletion. Three clones resulting from transformation with either pRS306-ScCENP-U or pRS306-ScCENP-U were tested. While this may be surprising, it is consistent with results in vertebrates. Here, changing 16 CDK1 phosphorylation sites of CENP-U to alanine did not have an observable phenotype[582].

Figure 18. In vitro phosphorylation of ScCENP-Q/U/P/O

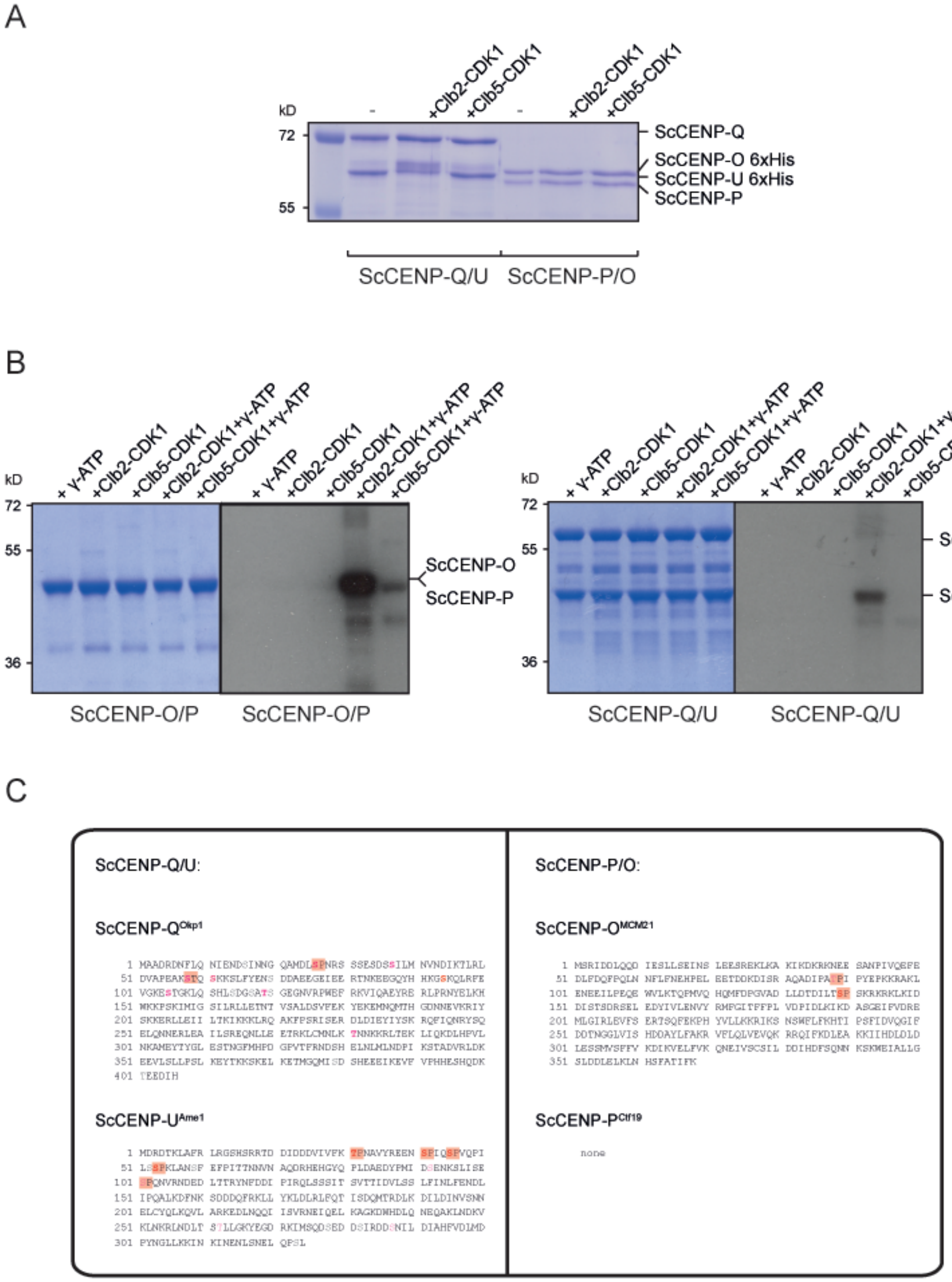

ScCENP-Q/U:

ScCENP-Q^{Okp1}

```
  1 MAADRDNFLQ NIENDSINNG QAMDLSPNRS SSESDSSILM NVNDIKTLRL
 51 DVAPEAKSTQ SKKSLFYENS DDAEEGEIEE RTNKEEGQYH HKGSKQLRFE
101 VGKESTGKLQ SHLSDGSATS GEGNVRPWEF RKVIQAEYRE RLPRNYELKH
151 MKKPSKIMIG SILRLLETNT VSALDSVFEK YEKEMNQMTH GDNNEVKRIY
201 SKKERLLEII LTKIKKKLRQ AKFPSRISER DLDIEYIYSK RQFIQNRYSQ
251 ELQNNERLEA ILSREQNLLE ETRKLCMNLK TNNKKRLTEK LIQKDLHPVL
301 NKAMEYTYGL ESTNGFMHPD GPVTFRNDSH ELNLMLNDPI KSTADVRLDK
351 EEVLSLLPSL KEYTKKSKEL KETMGQMISD SHEEEIKEVF VPHHESHQDK
401 TEEDIH
```

ScCENP-U^{Ame1}

```
  1 MDRDTKLAFR LRGSHSRRTD DIDDDVIVFK TPNAVYREEN SPIQSPVQPI
 51 LSSPKLANSF EFPITTNNVN AQDRHEHGYQ PLDAEDYPMI DSENKSLISE
101 SPQNVRNDED LTTRYNFDDI PIRQLSSSIT SVTTIDVLSS LFINLFENDL
151 IPQALKDFNK SDDDQFRKLL YKLDLRLFQT ISDQMTRDLK DILDINVSNN
201 ELCYQLKQVL ARKEDLNQQI ISVRNEIQEL KAGKDWHDLQ NEQAKLNDKV
251 KLNKRLNDLT STLLGKYEGD RKIMSQDSED DSIRDDSNIL DIAHFVDIMD
301 PYNGLLKKIN KINENLSNEL QPSL
```

ScCENP-P/O:

ScCENP-O^{MCM21}

```
  1 MSRIDDLQQD IESLLSEINS LEESREKLKA KIKDKRKNEE SANPIVQEFE
 51 DLFDQFPQLN NFLFNEHPEL EETDDKDISR AQADIPATPI PYEPKKRAKL
101 ENEEILPEQE WVLKTQPMVQ HQMFDPGVAD LLDTDILTSP SKRKRKLKID
151 DISTSDRSEL EDYIVLENVY RMFGITFFPL VDPIDLKIKD ASGEIFVDRE
201 MLGIRLEVFS ERTSQFEKPH YVLLKKRIKS NSWFLFKHTI PSFIDVQGIF
251 DDTNGGLVIS HDDAYLFAKR VFLQLVEVQK RRQIFKDLEA KKIIHDLDLD
301 LESSMVSFFV KDIKVELFVK QNEIVSCSIL DDIHDFSQNN KSKMEIALLG
351 SLDDLELKLN HSFATIFK
```

ScCENP-P^{Ctf19}

none

Figure 18A) In vitro phosphorylation of ScCENP-Q/U and ScCENP-P/O with either Clb2-CDK1 or Clb5-CDK1. Note the mobility shift of ScCENP-U upon phosphorylation. This figure also displays the 1:1 stoichiometry of ScCENP-Q/U and ScCENP-O/P and demonstrates that band identity ascribed earlier by mass spectrometric protein identification is correct. **Figure 18B)** Autoradiograms of ScCENP-Q/U and ScCENP-P/O phosphorylated by either Clb2-CDK1 or Clb5-CDK1 with ATPγ^{32}P. **Figure 18C)** Clb2-CDK1 in vitro phosphosites identified on ScCENP-O/P and ScCENP-Q/U**.** Phosphorylated residues identified both in vitro and in vivo are colored red, phosphorylated residues only found in vitro are colored pink. Phosphorylated minimum CDK1 sites are shaded red.

Figure 19. ScCENP-U CDK1 sites are not essential

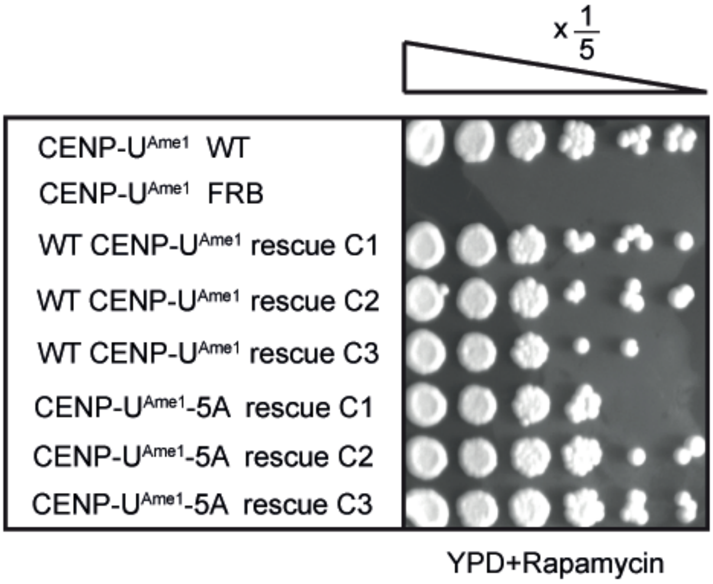
x $\frac{1}{5}$
CENP-U^{Ame1} WT
CENP-U^{Ame1} FRB
WT CENP-U^{Ame1} rescue C1
WT CENP-U^{Ame1} rescue C2
WT CENP-U^{Ame1} rescue C3
CENP-U^{Ame1}-5A rescue C1
CENP-U^{Ame1}-5A rescue C2
CENP-U^{Ame1}-5A rescue C3
YPD+Rapamycin

Figure 19) A Rapamycin induced, conditional nuclear depletion of ScCENP-U fused to a FRB-domain in an anchor away strain is lethal but can be rescued by expression of ScCENP-U integrated into the URA3 locus. Mutating the 5 CDK1 phosphosites identified in vitro to alanine does not impair the ability of integrated ScCENP-U mutants to rescue viability.

4. Discussion

In this work I have investigated interactions of the budding yeast ScCCAN with other kinetochore components and thereby corroborated our claim that this supramolecular assembly located at the chromatin base of the kinetochore is a KMN network assembly platform conserved between yeast and vertebrates. The principal findings are firstly the conserved identity and function of CCAN subcomplexes. Secondly I have begun to delineate subcomplex architecture in the budding yeast CCAN and investigated interactions of the ScCENP-Q/U/P/O complex.

4.1 Conservation of CENP-T/W and CENP-S/X complexes in budding yeast

In my tandem affinity purifications, I found ScCENP-T^{Cnn1} to associate with ScNDC80C and ScKnl1. Furthermore I identified a candidate yeast CENP-W homologue, Wip1, confirmed it as a kinetochore protein and showed that its localization depends on ScCENP-T^{Cnn1}. This closely parallels the situation in vertebrates. Identification of ScCENP-W^{Wip1} allowed later successful co-expression and purification of a recombinant ScCENP-T/W dimer by Dr. Stefan Westermann, which was demonstrated to directly bind ScNDC80C via ScCENP-T's extended flexible N-terminus. While this work was ongoing, an interaction between vertebrate CENP-T and NDC80C was demonstrated[11, 577]. Taken together this strongly suggests a conserved function for ScCENP-T/W in ScNDC80C recruitment.

I failed to observe co-localization of GFP-tagged ScCENP-S/X with Nuf2 as a marker for the kinetochore. By tandem affinity purification however, ScCENP-X prominently associates with the ScCCAN while ScCENP-S associates with the FANCM related Mph1, interactions previously described for vertebrate CENP-S/X. I found both to co-purify with ScCENP-T, again paralleling the findings in vertebrates[581, 834]. Therefore CENP-S/X are conserved in budding yeast and appear to associate with other centromere proteins. We do not know why I was unable to observe localization of either ScCENP-X-GFP or ScCENP-S-GFP to the kinetochore. A trivial explanation may be that the GFP fusion proteins are not functional. Alternatively we suspect that its localization may be very transient during S-phase when centromeres are replicated. Kinetochores may pose a replication block to a DNA polymerase encountering them. Indeed, the brief detachment of kinetochores during S-phase requires replication and is thus unlikely to be regulated by the outer kinetochore. Interestingly, during detachment, ScCENP-P is lost from the kinetochore suggesting that the encounter of a replication fork with a kinetochore induces its disassembly[45]. It is conceivable that some ScCCAN proteins, including ScCENP-S/X, mediate disassembly of the ScCCAN during replication if they encounter an active replisome. FANCM/Mph1 promotes replication fork regression and recombination repair under replication stress, when the DNA polymerase stalls. It is possible that FANCM/Mph1 stabilizes replication forks encountering a kinetochore and thereby assists replication through the centromere. This would however not be an essential mechanism as neither ScCENP-S/X nor FANCM/Mph1 are essential.

4.2 Conservation of the CENP-Q/U/P/O/R complex and the CENP-L/M/N group in yeast

Distant sequence homology of CENP-Q/U/P/O/R and ScCENP-Q/U/P/O^{COMA} as well as CENP-L/M/N and ScCENP-N/L^{Chl4,Iml3} suggests these two groups are also conserved in budding yeast. Indeed I was able to purify recombinant ScCENP-Q/U/P/O^{COMA}. As the existence of a vertebrate CENP-Q/U/P/O/R complex is established, this supports conservation of this complex as complex as a defined molecular identity. We do, however, not know if the complex is functionally conserved. ScCENP-Q/U are essential, which might be explained by their interaction with ScMIS12C. Reports on the vertebrate CENP-Q/U/P/O/R conflict and most suggest that its loss leads to only a minor mitotic defect[555, 556, 717]. Furthermore no effect on vertebrate MIS12C localization has been described upon loss of CENP-Q/U/P/O/R. Thus, binding of ScCENP-Q/U/P/O to ScMIS12 may be specific to yeast but it will be interesting to investigate this possible interaction in vertebrates. Time limited the characterization of the ScCENP-N/L^{Chl4,Iml3} complex. All we can currently say is that the two recombinant proteins, ScCENP-N and ScCENP-L, do form a stable complex even after bacterial DNA has been removed (Dr. Peter Hornung, personal communication). Complex formation for the vertebrate CENP-L/M/N has not yet been demonstrated. We lack a homologue for CENP-M in both budding and fission yeast (Table 1). It is interesting to note here that a loss of vertebrate CENP-M, in contrast to a loss of CENP-L or CENP-N, has a milder but still substantial effect on cell viability. Lastly, the existence of a complex formed by the ScCENP-H/I/K group of proteins still needs to be investigated in both budding yeast and human cells. For reasons unknown, I was unable to express recombinant ScCENP-H/I/K in bacteria. I speculate that either ScCENP-H/I/K may require other components of the ScCCAN to be co-expressed in order to fold correctly or that it is posttranslationally modified. Vertebrate CENP-H/I/K is SUMOylated during S-Phase and it has been suggested that this modification is required for stability[715]. It may be therefore possible to express ScCENP-H/I/K in eukaryotic expression systems such as insect cells.

4.3 Interactions of the ScCENP-Q/U/P/O^{COMA} complex with ScMIS12C, microtubules and DNA

Two interactions between the ScCCAN complex and the KMN network could be demonstrated. A direct interaction between ScCENP-Q/U/P/O and MIS12C in this work and, following this work, a direct interaction between ScCENP-T and NDC80C by Dr. Stefan Westermann[11, 488]. As MIS12C binds NDC80C, I suggest at that least two independent populations of NDC80C exist at the kinetochore, one recruited by ScCENP-T/W and one recruited by ScCENP-Q/U/P/O via the ScMIS12 complex. It is unclear if this interaction is conserved between budding yeast and man as depletion of vertebrate CENP-Q/U/P/O/R does in most cases not lead to severe defects. Alternatively animal MIS12 has been demonstrated to bind CENP-C, which has not been described for budding yeast[598, 599]. It will be interesting to delineate if vertebrates and yeast possess three shared recruitment pathways for NDC80C or if budding yeast utilizes ScCENP-Q/U/P/O/R while vertebrates utilize CENP-C for MIS12C recruitment and both recruit additional NDC80C via CENP-T. It will also be necessary to resolve the position of Knl-1 within this network. One may suspect that Knl1 is recruited to MIS12C and not to ScCENP-T. However I find low amounts of ScKnl1 exclusively in ScCENP-T tandem affinity purifications. It has been demonstrated that a loss of the Ndc80 internal loop leads to a loss of a subpopulation of Knl1 from vertebrate kinetochores. In C.elegans, CeMIS12C has been suggested not to be required for CeNDC80C recruitment. In depletions of CeMIS12C, CeNDC80C is recruited to kinetochores, albeit delayed, dependent on CeKnl-1 and CeKnl-3, a protein essential for C.elegans kinetochore assembly that has no currently known homologues. Given that CENP-T is not conserved in C.elegans, this may have been due to incomplete depletion of

CeMis12C, yet, recruitment of CeNdc80C is dependent on CeKnl1. Furthermore in budding yeast, absence of either, ScNDC80C or ScKnl1, the respective other demonstrates decreased kinetochore localization. It is thus possible that ScNDC80C and ScKnl1 form a complex that is recruited by ScCENP-T independently of ScMIS12C or that ScKnl1 recruitment partially depends on the ScCCAN proteins present in this purification[498, 849, 850]. Recent measurement of budding yeast kinetochore protein stoichiometry however does not support a ScMIS12 independent ScKnl1 population at the kinetochore as their copy number closely match. Yet ScNDC80C is present in excess over ScMIS12C, each kinetochore contains ~19 and ~15 copies respectively. Postulating the remaining 4 copies of NDC80C to be recruited by ScCENP-T/W would explain this discrepancy. Similarly, ScMIS12C is present in excess over both, ScCENP-C (4 copies) and ScCENP-P (6 copies). Dual recruitment of ScMIS12C by ScCENP-C and ScCENP-Q/U/P/O may explain how more ScMIS12 is recruited than could be accommodated by a single species of kinetochore receptors[471, 851]. This model may however not sufficiently take into account the dynamics of structural ScCCAN and ScKMN network components as ScCENP-T has been reported to increase, from a copy number of 6 up to a copy number of 20 during anaphase[836].

Vertebrate CENP-Q has previously been demonstrated to interact with microtubules[451]. I could not observe microtubule binding of the ScCENP-Q/U/P/O complex. It is possible that the increased salt, 150mM, in the MTBA prohibits this interaction. It is also possible that microtubule binding of CENP-Q is vertebrate specific. Alternatively the observed microtubule binding could be an artifact of using an isolated protein that is normally part of an obligate CENP-Q/U complex in both yeast and vertebrate cells. ScCENP-Q/U, SeCENP-O/P, ScCENP-Q/U/P/O and ScCENP-N/L were all contaminated by bacterial nucleic acid after purification while ScNDC80C was not. It appears that each dimeric subcomplex, ScCENP-Q/U, ScCENP-O/P and ScCENP-N/L contains either DNA or RNA binding activity. I was unable to unambiguously identify the contaminant as either RNA or DNA but I suspect it may be both. I envision these complexes to bind randomly throughout the bacterial nucleoid and, on purification, to co-purify fragments of the nucleoid that are actively engaged in transcription to explain what is possibly contaminating bacterial RNA. I attempted to establish a polyacryl-amide gel based EMSA protocol that would allow me to unequivocally demonstrate ScCENP-Q/U/P/O interaction with DNA, with limited success. The complex appears to bind DNA but the results were not sufficiently reproducible and often the tester DNA would simply be retained in the pocket when mixed with ScCENP-Q/U/P/O. Dr. Peter Hornung had more success using an agarose gel based EMSA, likely because of the larger pore size of these gels. It is however important to note that we do detect an interaction of the ScCENP-Q/U/P/O complex with DNA but not microtubules. This suggests that it is not a nonspecific interaction due to complex charge as both microtubules and DNA are negatively charged at physiological pH. It appears in Figure 16A that ScCENP-Q/U/P/O binds to the centromere containing fragment but not to the centromere free fragment but I have obtained no evidence that the binding would be sequence specific. Rather it is possible that ScCENP-Q/U/P/O has a preference for AT-rich sequences such as that found in the CDEII element. Consistent with this idea, some yeast CENP-U or –Q proteins are predicted to contain “AT-Hooks“ (Dr. Schleiffer, personal communication)

4.4 Regulation of and by the budding yeast CCAN

We mapped phosphorylation sites of ScCCAN proteins in vivo and demonstrated that Clb2-CDK1 directly phosphorylates the ScCENP-Q/U/P/O complex in vitro. The most striking feature was a CDK1-phosphocluster that we found in the N-terminus of ScCENP-U. A 5A phospho-negative mutant however shows no impaired viability. I did not investigate the effect of a phospho-mimicking mutant. Thus it is still possible that not phosphorylation but de-phosphorylation of this cluster is essential. We suspect CDK1 to have a role in kinetochore assembly or regulation. Even though the budding yeast kinetochore appears to remain intact throughout the cell cycle, save for a short period when the centromere is replicated, there may be subtle changes in kinetochore assembly or a cell cyle dependent suppression/activation of some of its functions[592]. As we find at least two KMN network anchor points in the budding yeast CCAN, it is possible that this phospho-cluster is redundant. We have not yet investigated more subtle phenotypes that may have arisen due to deletion of this cluster such as increased benymol sensitivity or slower progression through the cell cycle. Alternatively, loss of the cluster may only produce a pronounced phenotype when redundant KMN anchors such as ScCENP-T are deleted.

Beyond CDK1 regulation, there is another interesting kinase I identified in my tandem affinity purifications of ScCENP-N and ScCENP-H, namely the DDK kinase complex. This complex is implicated in a number of functions in addition to initiation of DNA replication, including the formation of the synaptonemal complex during meiosis, translesion DNA synthesis and loading of Cohesin during replication in X.laevis[110, 114, 116, 852-855]. Association of DDK with CCAN proteins could be artifactual as it targets origins of replication and at least CEN12 is, in addition to a centromere, an active origin of replication[856, 857]. However, I find no components of the origin recognition complex in my tandem affinity purifications. Another possibility is that DDK promotes cohesion loading at the centromere. As mentioned in the introduction, a number of ScCCAN proteins participate in the loading of Cohesin and ScCENP-O participates in recruitment of the cohesion loader complex Smc2/Smc4. X.laevis DDK is found in complex with Smc2/Smc4 and is required for its recruitment to origins of replication. A similar relation may hold true for budding yeast and the ScCCAN may enhance cohesion loading via DDK and Smc2/Smc4[858].

In tandem affinity purifications of ScCENP-U, ScCENP-H and ScCENP-N I further find Psh1, the CENP-A ubiquitin ligase[595]. Arguably it should be everywhere else along the chromosome to evict ectopic centromeric nucleosomes, but not at the centromere itself. ScCENP-A did only appear in purifications of ScCENP-U. An interaction between ScCENP-N or ScCENP-C and ScCENP-A has not yet been demonstrated. However an interaction between ScCENP-Q/U/P/O and ScCENP-A has. Specifically, ScCENP-P binds to a short region on the N-terminal tail of ScCENP-A, termed the end-domain. The end-domain contains a methylated arginine, R37. Methylation of R37 is necessary for recruitment of wild type levels of ScMIS12C and ScCENP-P but not to recruit wild type levels of ScCENP-A itself. Association of ScCENP-Q/U/P/O with both ScCENP-A and Psh1 tempts me to speculate that one of the functions of the CCAN may be to provide CENP-A binding sites that are protected from Psh1, possibly by negatively regulating it. As ScCENP-A R37 methylation is not required to localize normal ScCENP-A levels, protection of ScCENP-A would at least not require this modification. However, the end-domain is essential while neither ScCENP-P or R37 methylation are, suggesting additional functions of the complete domain[859-862].

Lastly, I find neither, the CBF3 complex or the CPC which has been shown to bind to the CBF3 complex and partially require CENP-U/Q for kinetochore localization in my tandem affinity purifications. I attempted preliminary binding assays between the ScCENP-Q/U/P/O complex and a ScINCENP/ScAurora B dimer readily available in the laboratory but did not observe an interaction. An interaction between CPC and ScCENP-Q/U/P/O may however require Boralin and/or Survivin, which were not present in my CPC derivative. Especially since a loss of ScCENP-U leads to the absence of ScBorealin, ScINCENP and ScAurora B but not ScSurvivin from the kinetochore[627]. Alternatively an interaction between the CPC and ScCENP-Q/U/P/O may require posttranslational modification as the localization of the CPC is controlled by phosphorylation[863, 864]. Therefore an interaction between ScCENP-Q/U/P/O and the CPC needs to be reinvestigated.

4.5 Model and future directions

I have described two distinct pathways by which the budding yeast CCAN may recruit the KMN network and allows re-evaluation of older results. Firstly it explains conflicting observations when investigating recruitment dependencies. A purely hierarchical recruitment would be expected to lose all downstream components and functions, such as the KMN network and the SAC, when upstream components, such as CENP-C, are lost. Although we don’t yet know if CENP-Q/U/P/O/R in vertebrates is able to recruit MIS12C and conversely if ScCENP-C is able to recruit ScMIS12C, there appear to be at least two independent anchor points for the KMN network in both.

With this in mind it is clear why some vertebrate KMN components strongly loose kinetochore localization on depletion of CENP-C while others do not. NDC80C simply is recruited by an additional pathway, including CENP-T/W and likely CENP-H/I/K. This also explains why the SAC is active when MIS12C is lost in vertebrates and yeast but abolished when NDC80C is lost. It would further explain why vertebrate cells that lose either, CENP-I or MIS12C, show an inability to stably arrest in the first mitosis when only a few kinetochores are unattached. The SAC may monitor attachment of NDC80C to MTs regardless of the kinetochore receptor it is recruited to. Reducing the amount of NDC80C by depletion of either, CENP-I or MIS12C, would decrease but not abolish NDC80C recruitment to the kinetochore. These impaired kinetochores may generate less MCC when unattached or not under tension due to the decreased amount of NDC80C and thus be unable to block anaphase when only one or a few kinetochores are mal-attached. Rather the SAC signal from these kinetochores may be sufficient for an arrest only when multiple kinetochores are mal-attached. Therefore these cells would be unable to arrest in the first cell cycle due to a weak signal from the few unattached signaling impaired kinetochores. However, as ploidy increases in subsequent cell cycles due to missegregation, so does the number of impaired unattached kinetochores and thereby their ability to arrest the cell[51, 490, 493, 594, 597, 675, 747, 748, 865].

Why would two distinct recruitment pathways have evolved? Clearly it is simpler to just amplify recruitment by a single pathway, although evolution is not necessarily in search of the simplest approach. It is possible that the vertebrate NDC80C recruitment pathway via CENP-T supplements the recruitment pathway via CENP-C and MIS12. The outer plate of the kinetochore, which can be tentatively equated with NDC80C, is in many cases entirely absent when CENP-T is lost, while it is discontinuous in absence of CENP-C[500, 576, 596]. Therefore the core kinetochore in vertebrates may consist of the centromeric nucleosome and a CENP-C-MIS12C-NDC80C recruitment pathway. This core kinetochore may exist in multiple copies and the space between CENP-A nucleosomes may be filled by CENP-T/W dimers, as suggested by super-resolution microscopy, recruiting additional NDC80 in order to form the stable inner and outer plate structures[866]. In this case CENP-T/W would simply serve to “squeeze” as much NDC80C as possible onto a centromere in order to make attachments as stable as possible. A more enticing idea is that NDC80Cs recruited by either CENP-T or MIS12C are actually functionally divergent. In line with this idea, vertebrate NDC80C is required to recruit the RZZ complex and CENP-E. Similarly CENP-C is required to recruit these components but CENP-I is not[490, 511, 596, 867]. A vertebrate cell may use different populations of NDC80C and Knl1, recruited by either CENP-T/W or MIS12C, to localize defined subsets of outer kinetochore proteins, MAPs and motors. In theory this could constitute functionally different linking structures connecting centromeric DNA and microtubules. These linking structures may be subject to differential regulation by kinases, which may be a key to understand the interplay of Aurora B, Mps1, Plk1 and BubR1. Functionally differentiated linkers based on CENP-T/W and CENP-C could mediate distinct attachment phases, lateral or end-on and the conversion between both, as suggested in Figure 20B. While this is in principle also possible in budding yeast, the relatively mild defects observed when ScCENP-T is deleted suggests that a ScCENP-T based linker is less important compared to other linkers in the yeast kinetochore or a CENP-T based linker in vertebrates.

Figure 20A displays a model for the yeast kinetochore. ScNDC80C is recruited either by association with ScCENP-T or ScMIS12C. ScMIS12C in turn is recruited via ScCENP-Q/U/P/O. We do not yet know if budding yeast also recruits ScMIS12C via ScCENP-C. Furthermore we do not know the exact relation of ScCENP-Q/U/P/O and ScCENP-C. Although loss-of-function experiments suggest that ScCENP-C is required for ScCENP-Q/U/P/O recruitment, the recruitment dependency of the budding yeast CCAN remains confusing. As mentioned localization ScCENP-P and therefore likely the localization of the entire ScCENP-Q/U/P/O complex depends on ScCENP-C. Recruitment of the ScCENP-L/N complex in turn depends on ScCENP-O. Surprisingly ScCENP-T/W recruitment depends on ScCENP-N but not ScCENP-P. However loss of ScCENP-P dislodges ScCENP-O from the kinetochore[11, 463, 567, 592]. Furthermore, ScNDC80 depletions lead to a complete loss of attachment phenotype, which can be mimicked by deleting ScCENP-T in combination with ScCENP-C, ScCENP-Q/U or ScMIS12, corroborating dual recruitment. The fact that loss of ScCENP-C or ScCENP-Q/U alone does not lead to complete detachment suggests that CENP-T/W is still present at the centromere[11, 463]. Therefore it may localize independent of ScCENP-C and ScCENP-Q/U/P/O as is the case in vertebrates and fission yeast. Closer investigation into ScCCAN recruitment dependency may be able to resolve these issues and yield results transposable into the vertebrate system.

Figure 20B illustrates my speculation on the role of multiple subpopulations of NDC80C and Knl1 recruited by different kinetochore receptors using a vertebrate kinetochore as an example. The loss of the RZZ complex and Dynactin in absence of CENP-C or MIS12C suggests that these two components may be recruited exclusively to a KMN network anchored to the kinetochore by CENP-C while ScCENP-T/W recruited NDC80C does not participate in this process. Figure 20B also illustrates an inhibition of this CENP-C recruited KMN network by the RZZ complex during lateral attachment before it is stripped by Dynein. CENP-T/W anchored NDC80C may be free and assist lateral attachment during the motor based movement of kinetochores along the microtubule wall. Once at the MT +end, the CENP-C recruited KMN network is activated by Dynein mediated stripping of the RZZ complex which allows hand over to end-on attachment.

Anchoring two independently regulated populations of NDC80C at the kinetochore has potential benefits. It may allow asymmetric regulation of a specific set of attachment fibers during error correction and chromosome oscillation. As an example, if both kFibers are differentially destabilized during oscillation and error correction, CENP-H/I/K may facilitate this on the trailing kinetochore, acting only on a subpopulation of NDC80C, that is recruited by CENP-T/W, while Aurora B and MCAK may act on a different, CENP-C recruited subpopulation on the leading kinetochore. Alternatively I would like to suggest a role of the CENP-T/W recruited NDC80C subpopulation in increasing attachment stability of a bioriented chromosome in metaphase or a single segregating chromatid in anaphase. CENP-T/W recruited NDC80C could be activated in response to tension. Once a kinetochore attaches end-on to a kFiber via CENP-C recruited KMN network and is able to support tension, additional CENP-T/W recruited NDC80C may be activated, increasing attachment stability. Hyperstable kFibers in ScCENP-H/I/K depletions would corroborate both ideas if CENP-H/I/K indeed destabilizes kFibers by negatively regulating CENP-T/W recruited NDC80C.

My results suggest that kinetochore assembly is not absolutely hierarchical. While there are centromere proximal components that recruit centromere distal components, there are multiple pathways for the CCAN to recruit KMN components. Results from fission yeast demonstrate the ability of centromeric chromatin, defined by the CCAN, to spread along DNA between heterochromatin boundaries. I envision the CCAN to coat DNA as a copolymer that consists of defined repetitive elements, some of which mediate recruitment of microtubule binding proteins such as the KMN network while others organize the centromere in space, in animals crosslinking centromeric DNA into the inner plate structure. With this in mind, more detailed investigation into interactions between CCAN subunits and other kinetochore proteins and more exhaustive loss of function studies of single CCAN proteins will be necessary to define exactly which outer kinetochore proteins and microtubule associated factors are recruited by which CCAN subcomplex. Furthermore it will be necessary to define a temporally ordered sequence of CCAN assembly throughout the cell cycle in order to interpret recruitment dependencies. Because they appear to change during the cell cycle this may be the origin of some conflicting reports. The budding yeast CCAN will be instrumental for this as many relationships among proteins appear conserved, and biochemical reconstitutions of interactions are feasible.

Figure 20. Model of kinetochore architecture

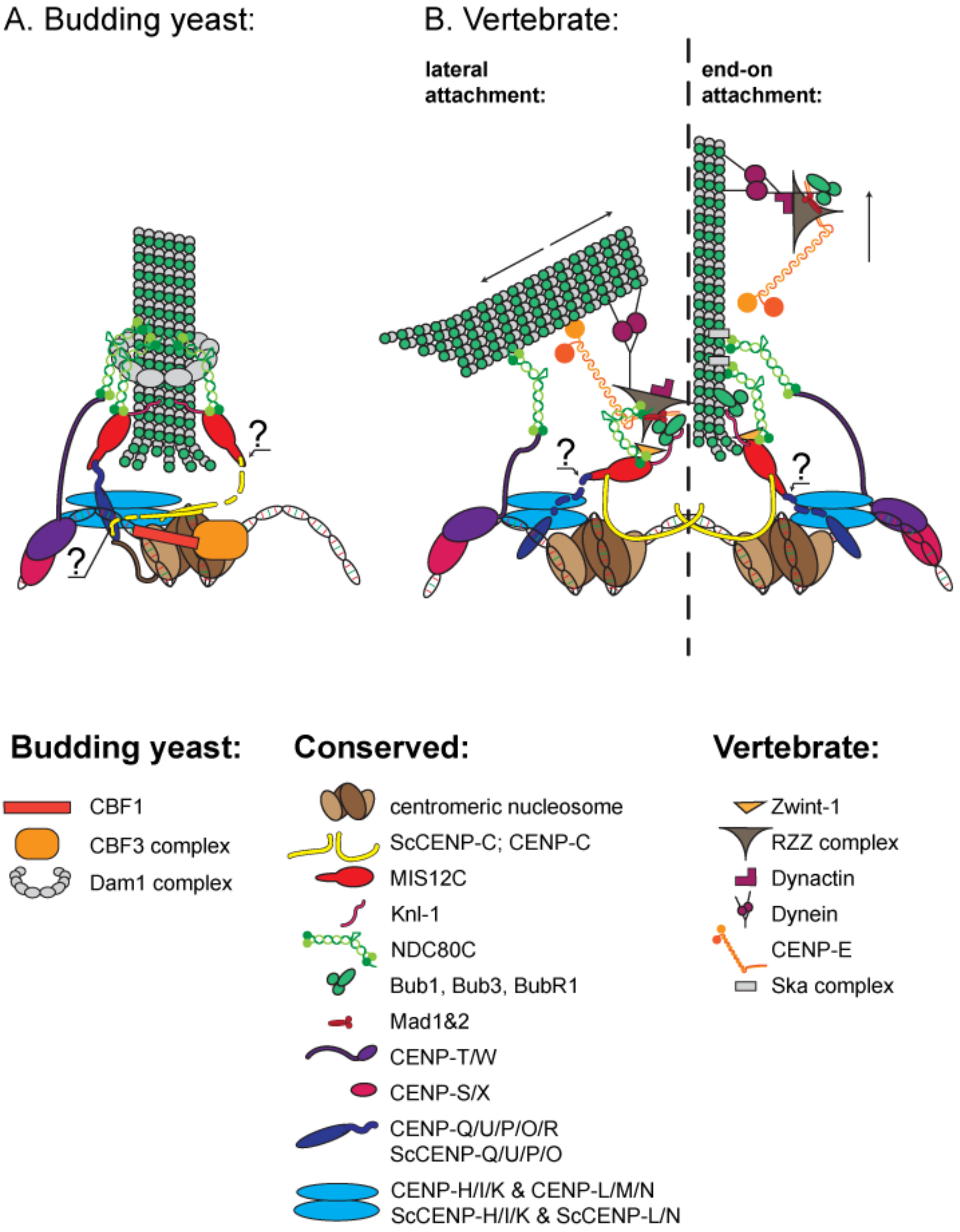
A. Budding yeast:
B. Vertebrate:
lateral attachment:
end-on attachment:
?
?
?
?
Budding yeast:
CBF1
CBF3 complex
Dam1 complex
Conserved:
centromeric nucleosome
ScCENP-C; CENP-C
MIS12C
Knl-1
NDC80C
Bub1, Bub3, BubR1
Mad1&2
CENP-T/W
CENP-S/X
CENP-Q/U/P/O/R
ScCENP-Q/U/P/O
CENP-H/I/K & CENP-L/M/N
ScCENP-H/I/K & ScCENP-L/N
Vertebrate:
Zwint-1
RZZ complex
Dynactin
Dynein
CENP-E
Ska complex

Figure 20A) A model of budding yeast kinetochore architecture. ScNDC80C is recruited by both ScMIS12C and ScCENP-T/W. ScMIS12 additionally recruits ScKnl1. There is currently no reason to believe that different populations of ScNDC80C interact differently with the DAM1C. ScMIS12C is recruited by ScCENP-Q/U/P/O and possibly ScCENP-C. ScCENP-C may recruit ScCENP-Q/U/P/O although this complex interacts with ScCENP-A. ScCENP-T/W is likely recruited by additional ScCCAN proteins, specifically ScCENP-N. CBF1 and CBF3 have no direct role in the structural assembly of the kinetochore but may establish it by loading of the ScCENP-A containing centromeric nucleosome and CBF3 mediated recruitment of the CPC may regulate attachment through the error correction mechanism (not depicted) **Figure 20B)** Model of vertebrate kinetochore architecture. Like in budding yeast, NDC80C is recruited by CENP-T/W and NDC80 and Knl1 are recruited by MIS12C. MIS12C is recruited by CENP-C, a recruitment by CENP-Q/U/P/O/R is not established. While in budding yeast the centromeric nucleosome, CENP-C and CENP-N are required to recruit CENP-T, in vertebrates CENP-T is required to recruit the remaining CCAN proteins, of which CENP-H/I/K are required to load the centromeric nucleosome. This shift in recruitment dependency could be due to the evolution of sequence specific loading of the centromeric nucleosome by CBF3, obviating the need for the self-propagation of a centromeric chromatin domain defined by the CCAN. Subpopulations of NDC80 in vertebrates may be differentially regulated. The RZZ complex could localize to and inhibit only MIS12C recruited NDC80C while CENP-T/W recruited NDC80C is free to assist in lateral attachment assisting motor based movement of the kinetochore on the MT wall. Once the kinetochore reaches the +end of a MT, MIS12C recruited NDC80C is activated as Dynein removes the RZZ complex and depleted the kinetochore of motors, including itself and CENP-E.

5. Materials and methods

5.1 Strain and plasmid construction

Plasmid construction

All plasmids used, whether based on pET3aTr, pST39, pCOLADuet-1 or pRS306 were maintained in E.coli DH5α and isolated using a Qiagen QIAprep spin Miniprep kit. For molecular cloning of genes, the respective fragments were amplified from yeast genomic DNA using a Finnzymes Phusion® high fidelity PCR kit and extended primers to add the desired restriction sites. Restriction enzyme digestion of both plasmid and insert were performed with Fermentas FastDigest® enzymes with the exception of digestions by MluI and BspEI for which NEB restriction enzymes were used. The restriction sites used for cloning into expression vectors are given in Figure 7, the sites used for cloning of Ame1 into pRS306 in the text (5'XbaI and 3'XhoI). Inserts and plasmids were purified by electrophoresis in an agarose gel, subsequent isolation of the correct bands and elution from the agarose gel using a Qiagen QIAquick Gel extraction Kit®. Purified insert and plasmid were subjected to analytical electrophoresis to judge concentration in the sample and subjected to ligation in approximate ratios of 3:1 and 10:1. Ligation was performed using a Fermentas T4 DNA ligase.

PCR protocol (Fermentas Phusion)

Reaction mix:

H_2O		35µl
Buffer		10µl
dNTP's	10mM	1µl
Primer 1	20µM	1,25µl
Primer 2	20µM	1,25µl
Template		1µl
Phusion Polymerase		0,5µl

		50µl

Cycles:

98°C	30s	x1
----------	----------	----------
98°C	10s	
54°C	30s	
72°C	60s per 1kb	x30
----------	----------	----------
72°C	10min	x1

Primers used for insert amplification

	5'	3'
pET3aTr:		
(ScCENP-P) Ctf19	oPH97	oPH98
(ScCENP-O) Mcm21	oPH100	oPH101
(ScCENP-O) Mcm21 + 6xHis Tag	oPH100	oMM32
(ScCENP-Q) Okp1	oPH111	oPH113
(ScCENP-U) Ame1 + 6xHis Tag	oPH102	oPH108
(ScCENP-U) Ame1 + FLAG Tag	oPH102	oPH107
(ScCENP-K) Mcm22	oMM1	oMM2
(ScCENP-I) Ctf3	oMM3	oMM31
(ScCENP-H) Mcm16 N-term	oMM5	oMM6
(ScCENP-H) Mcm16 C-term	oMM7	oMM8
(ScCENP-H) Mcm16 C-term + 6xHis Tag	oMM7	oMM23
(ScCENP-H) Mcm16 C-term + Strep II Tag	oMM7	oMM10
(ScCENP-H) Mcm16 FL	oMM5	oMM8
(ScCENP-H) Mcm16 FL + 6xHis Tag	oMM5	oMM23
(ScCENP-H) Mcm16 FL + Strep II Tag	oMM5	oMM10
pCOLADuet:		
(ScCENP-L) Iml3	oMM27	oMM12
(ScCENP-N) Chl4	oMM19	oMM34
(ScCENP-N) Chl4 + HN Tag	oMM19	oMM35
(ScCENP-N) Chl4 + FLAG Tag	oMM19	oMM36
pRS306:		
(ScCENP-U) Ame1 +284bp upstream, +234bp downstream	oMM83	oMM82

Overlap extension PCR to construct (ScCENP-H) Mcm16 inserts

To remove an internal SacI site in Mcm16 and allow for subcloning into pST39, an overlap extension PCR using mismatch primers was employed. Two overlapping fragments of Mcm16, N-terminal and C-terminal were amplified. oMM5/6 were used for the N-terminal fragment. oMM7 was used together with either, oMM8, oMM23 or oMM10 to generate one tag free, one 6xHis tagged and one Strep II tagged c-terminal fragment. The internal primers oMM6/7 are complementary and both contain a base change at position 300, C to G. To generate the full length constructs, second PCR reactions were prepared in which both N-terminal fragment and either of the C-terminal fragments were added as template. Primers were omitted in the first three cycles to allow annealing and elongation of the two fragments. Subsequently oMM5 and either, oMM8, oMM23 or oMM10 were added to the reaction to allow amplification of the fusion construct.

Restriction enzyme digestion protocol

Insert:

Fast Digest buffer	3µl
PCR product after purification	6µl
Restriction enzyme 1	1µl
Restriction enzyme 2	1µl
H_2O	19µl

Plasmid:

Fast Digest buffer	3µl
Plasmid after purification	15µl
Restriction enzyme 1	1µl
Restriction enzyme 2	1µl
H_2O	11µl

Digestions were carried out on 37°C for 60 minutes

Ligation protocol

Ligase buffer	2µl
Insert + vector, ratio 3:1 or 10:1, dissolved in H_2O	17µl
T4 Ligase	1µl

Ligation mixtures were incubated for 30 minutes at room temperature or at 16°C over night.

Quikchange® site directed mutagenesis

This site directed mutagenesis protocol utilizes mismatch dsDNA primers to amplify a linear derivate of an isolated template plasmid in a PCR reaction that contains the desired point mutation. The template is subsequently digested using DpnI endonuclease which is specific for methylated DNA. Following digestion, the linear derivate is transformed into bacteria where it is circularized and maintained as a circular plasmid. If the desired point mutations are in close proximity, one may employ single primers containing multiple mismatches. One may further use multiple primers in single reaction as long as their target sequences do not overlap. Quikchange® mutagenesis was employed to remove two EcoRI sites in ScCENP-O$^{\mathrm{Ctf19}}$ cloned into the pET3aTr vector to allow subsequent subcloning into pST39. Furthermore it was used to generate the ScCENP-U$^{\mathrm{Ame1}}$ 5A mutant in a pRS306 vector. Mutagenesis of ScCENP-O$^{\mathrm{Ctf19}}$ was achieved in a single reaction using oPH16 encoding both silent T to C mutations at positions 27 and 45. Construction of ScCENP-U$^{\mathrm{Ame1}}$ 5A required two reactions. In the first reaction mutations A to G at position 91 and mutations T to G at positions 133 and 301 were introduced using oMM90, oMM92 and oMM94. The 3A mutant was identified among a number of sequenced clones following transformation with the product of this first reaction. The vector was isolated and subjected to a second round of mutagenesis, utilizing oMM91 and oMM93 to introduce T to G mutations at positions 121 and 157. Successful mutagenesis for both ScCENP-O$^{\mathrm{Ctf19}}$ in pET3aTr and ScCENP-U$^{\mathrm{Ame1}}$ in pRS306 was confirmed by sequencing.

Quikchange protocol:

Reaction mix:

H_2O		to 25µl
Buffer		2,5µl
dNTP's	10mM	1µl
Primer	20µM	0,3µl each
Template		1,2µl
Quikchange Pfu Turbo DNA Pol		1µl

		25µl

Cycles:

95°C	30s	x1

95°C	30s	
55°C	60s	
68°C	8min	x18

DpnI digestion:

Add 1µl of DpnI supplied with the kit to the reaction mixture after PCR and incubate 1h at 37°C.

Transformation:

Standard bacterial transformation protocol as given below, using however the supplied ultra-competent XL1-Blue cells instead of DH5α.

Generation of yeast genomic integration constructs

Yeast strains containing genomic TAP fusion tags were constructed by transforming yeast cells with the respective integration construct. These constructs were generated by PCR amplification from a pKW804 template plasmid containing the respective tag-ORF using primers containing plasmid specific sequences and additional ~50bp extensions homologous to the targeted genomic region, allowing for integration. pKW804 encodes a modified TAP-tag in which a S-tag and a ZZ-tag are separated by a TEV cleavage site[542]. The TAP-Tag construct contains a KanMX resistance cassette. The full list of plasmid and primer combinations is given below. Integration constructs were generated by application of the standard PCR protocol given above.

TAP-tag integration constructs:

Gene&Tag:	Primers:	Plasmid template:
ScCENP-U^{Ame1}-TAP	oMM44; oMM45	pKW804
ScCENP-H^{Mcm16}-TAP	oMM17; oMM26	pKW804
ScCENP-N^{Chl4}-TAP	oMM13; oMM24	pKW804
ScCENP-S$^{YOL086W-A}$-TAP	oMM51; oMM52	pKW804
ScCENP-X$^{YDL160C-A}$-TAP	oMM55; oMM56	pKW804

Strain construction

Transformation protocol, E.coli

Chemically competent DH5α were thawed on ice. 5µl of the ligation product was added to 100µl thawed DH5α liquid culture and incubated 30 minutes on ice. This was followed by a 30 second heat shock at 42°C and a 2 minute incubation on ice before 400µl SOC medium was added and the cells were allowed to recover for 60 minutes at 37°C. Following recovery, cells were plated on selection medium.

Transformation protocol, budding yeast

Log phase cells were harvested, washed in MonoQ H_2O, then washed and resuspend in 1ml TE/LiAc (10mM Tris-HCl, 1mM EDTA, 100mM LiAc, pH7.5). 50µl of yeast supension were mixed with 1µg transforming DNA and 50µg single stranded salmon sperm carrier DNA. 300µl of PEG 4000 solution was added (10mM Tris-HCl, 1mM EDTA, 100mM LiAc, 40% PEG 4000, pH7.5). Transformation mixes were incubated under agitation at 30°C for 30min and then heat shocked at 42°C for 15min. Following heat shock, cells were washed in MonoQ H_2O and plated on the appropriate medium. To select for resistance markers, cells were initially plated on YPD and replica plated onto antibiotic containing plates after 1-2 days.

5.2 Biochemistry

Tandem affinity purification protocol:

Harvest yeast cells from liquid culture at OD_{600}=1.2 and drop freeze in liquid N_2.
Lyse by grinding pellets, immersed in liquid N_2, in a Warring blender into powder.
(In low stringency purifications, frozen cell pellets were lysed in a freezer mill)

Thaw and dissolve 60g of powder in 60ml of 2xHyman buffer with added phosphatase inhibitors (+2,4ml 1M ß-glycerol phosphate; +8ml phosphatase inhibitor cocktail)

Add protease inhibitors before powder has thawed (1.2ml PMSF, 1.2ml protease inhibitor cocktail, Calbiochem)

Incubate in warm water bath to expedite thawing

Add 12,5ml 10% TritonX-100, sonicate for 30s

Sediment insoluble fraction by centrifugation in SA-600 rotor at 10.000rpm for 25min

Aspirate supernatant and sediment remaining insoluble components by ultracentrifugation in a Ti-70 rotor at 45.000rpm for 30min

Pre-clear supernatant by passing it through a 12ml CL-6B Sepharose column, pre-equilibrated with 1xHyman buffer.

Wash 0,65ml IgG Sepharose slurry in a disposable column with 10ml TST, 1ml 0,5M NH_4OAc (pH 3,4), 5ml TST, 1ml 0,5M NH_4OAc (pH 3,4), 5ml TST, 5ml 1xHyman buffer or 5ml 1xHyman buffer +300mM KCl, depending on desired purification stringency.

For high stringency purification add sufficient 2,5M KCl to the pre-cleared supernatant to achieve a final concentration of 300mM. Omit this step in low stringency purifications.

Add washed IgG Sepharose beads to supernatant and rock at 4°C for 3hrs

Remove supernatant from IgG beads in a disposable column, wash with 15ml 1xHyman buffer for low stringency purification or 15ml 1xHyman buffer +300mM KCl for high stringency purification

Wash IgG beads with 25ml 1xHyman (+300mM KCl for high stringency purifications) +1mM DTT +0,1% Tween 20

Resuspend IgG beads in 1,5ml 1xHyman (+300mM KCl for high stringency purifications) +1mM DTT +0,1% Tween 20

Add 40µl of purified TEV protease (supplied in house) and keep rocking 4hrs at 4°C

Add 50µl of purified TEV protease and keep rocking over night at 4°C

Remove beads and collect supernatant in a disposable column. Wash with an additional 1ml of 1xHyman (+300mM KCl for high stringency purifications) +1mM DTT +0,1% Tween 20 and collect eluate.

Add 85µl S-protein agarose slurry (washed with 1xHyman buffer 3 times) to the pooled supernatant and eluate and rock at 4°C for 3h

Elute 3 times by incubation of the beads in 60µl 0,1M Glycine pH 2 for 30mins. Keep beads agitated.

Buffers and Reagents for tandem affinity purification:

1xHyman Buffer:
50mM Bis-Tris Propane (pH 7)
100mM KCl
5mM EDTA
5mM EGTA
10% Glycerol

TST:
50mM Tris-HCl (pH 7,4)
150mM NaCl
0,1% Tween 20

Phosphtase inhibitor cocktail 15x:
50ml H_2O
1,65g Sodium pyrophosphate
244mg Sodium azide
315mg Sodium fluoride
55mg Sodium orthovanadate

Expression:

All recombinant protein was expressed in Rosetta 2 cells. Expression was induced by addition of 0,2mM IPTG.

Standard protein purification from bacteria, 6xHis-tag

Harvest Bacteria, wash in PBS (freezing optional) and centrifuge 10min at 6000g

Resuspend pellet in cold lysis buffer (5-10 pellet Vol; 30 mM HEPES pH 7, with 150 mM NaCl and 30mM Imidazole). Add 1 tablet of Complete EDTA-free protease inhibitor per 50ml, 1/100 PMSF, Lysozyme 1/200 (100mg/ml stock) and DNAse if to viscous

Sonicate 30s on ice, incubate 10 min

Centrifuge homogenous lysate 15 min at 15-17k rpm (SS-34 rotor)

Wash NiNTA resin three times in lysis buffer (approx. 1ml of resin per 10g of cell pellet dry weight were used) before adding it to the supernatant. Rock 1h at 4°C.

Remove supernatant and wash resin with lysis buffer until supernatant remains clear

Elute 3 times. Remove supernatant and add elution buffer (30 mM HEPES pH 7, with 150mM NaCl and 300mM Imidazole), rock 30min at 4°C before aspirating the eluate.

Modification of 6xHis purification protocol for ScCCAN complexes

Lyse cells in 30 mM HEPES pH 7, with 150 mM NaCl, 30mM Imidazole and additionally 1mM $CaCl_2$ if required by the complex (ScCENP-O/P, ScCENP-Q/U/P/O). Add 1 tablet of complete EDTA-free protease inhibitor per 50ml, 1/100 PMSF, Lysozyme 1/200 (100mg/ml stock) and DNAse if to viscous.

Sonicate 30s on ice, incubate 10 min.

DNAse is required for ScCENP-O/P, ScCENP-Q/U, ScCENP-Q/U/P/O and ScCENP-N/L complexes as expression produces a very viscous lysate that requires DNAse digestion, possibly before and during sonication.

Centrifuge homogenous lysate 15 min at 15-17k rpm (SS-34 rotor)

Wash NiNTA resin three times in lysis buffer (approx. 1ml of resin per 10g of cell pellet dry weight were used) before adding it to the supernatant. Rock 1h at 4°C.

Perform two initial washing steps of the protein bound resin with the low salt lysis buffer.

For DNA binding ScCCAN complexes, perform all further washing steps with high salt wash buffers. Wash buffers are similar in composition to the lysis buffer, containing 30mM HEPES pH 7, 30mM Imidazole and 1mM $CaCl_2$ if required. Salt concentrations in the wash buffers depend on the target complex. I have used 600mM NaCl to wash DNA from the ScCENP-Q/U/P/O complex, 1M NaCl to wash DNA from the ScCENP-Q/U complex and up to 1.5M NaCl to wash DNA from the ScCENP-O/P complex. These higher salt concentrations are not necessary but decrease the number of required washing steps. As mentioned in the text, the number of required washing steps is variable. I monitor the decrease of absorption at 260 and 280 nm in the wash buffer after each wash step and continue washing until the values reach noise level.

After exhaustive washing, elute 3 times. Remove supernatant and add elution buffer (30 mM HEPES pH 7, with 150mM NaCl, 300mM Imidazole and 1mM $CaCl_2$ if required), rock 30min at 4°C before aspirating the eluate.

Protein purification from Bacteria, FLAG-tag

Harvest Bacteria, wash in PBS (freezing optional) and centrifuge 10min at 6000g

Resuspend pellet in cold lysis buffer (5-10 pellet Vol; 50 mM Tris HCl pH 7.4, with 150 mM NaCl), add 1 tablet of Complete EDTA-free protease inhibitor per 50ml, add 1/100 PMSF, Lysozyme 1/200 (100mg/ml stock) and DNAse if to viscous

Sonicate 30s on ice, add 0,5% Triton X100 and incubate 10 min

Centrifuge homogenous lysate 15 min at 15-17k rpm (SS-34 rotor)

Rinse FLAG-resin in disposable column with TBS. Wash resin 3x with 0,1 M Glycine pH 3.5, then wash resin with 5 Vol. TBS

Add resin to supernatant, rotate 1h at 4°C, then sediment resin by centrifugation at 1000g and remove supernatant.

Wash resin with TBS until supernatant remains clear. To elute place resin in disposable column, drain supernatant and elute with TBS +100µg/ml FLAG-peptide. Elute 3-4 times.

Preparative size exclusion chromatography

Preparative size exclusion chromatography was performed to further purify recombinant ScCCAN complexes. Depending on the amount of protein, either a 120ml Superdex 200 HiLoad 16/60 or a 24ml Superose 6 10/300 GL column (GE Healthcare) were used. Running buffers were either 30mM HEPES pH 7 for NiNTA purified complexes or 50mM Tris HCl pH 7.4 for αFLAG antibody purified complexes. Either buffer contained 150mM NaCl and additionally 1mM $CaCl_2$ if a protein complex containing ScCENP-O/P was purified.

ScCENP-Q/U/P/O - ScMIS12C binding assay and analytical size exclusion chromatography

Samples of ScCENP-Q/U/P/O and ScMIS12C were mixed in a binding buffer containing 30mM HEPES pH 7, 150mM NaCl and 1mM $CaCl_2$ and left at 4°C for 30 minutes. Subsequently samples were subjected to analytical size exclusion chromatography in binding buffer on a 2.4 ml Superose 6 PC 3.2/30 column.

Microtubule binding assay

Microtubules were assembled in vitro from 60µM purified bovine brain tubulin in G-PEM buffer (80mM K-Pipes pH 6.8, 1mM EGTA, 1mM $MgCl_2$, 1mM GTP)+ 25% Glycerol. After 30min incubation at 35°C for MT assembly, 20µM Taxol was added to stabilize MTs. MTs were diluted in PEM (80mM K-Pipes pH 6.8, 1mM EGTA, 1mM $MgCl_2$, 1mM GTP) +10µM Taxol. Recombinant ScCENP-Q/U/P/O was dialyzed into PEM and 0.3 mg/ml of ScCENP-Q/U/P/O was added to variable concentrations of assembled tubulin (20µM-6µM). After 20min incubation on room temperature, MTs were sedimented by ultracentrifugation for 20min at 70.000rpm. Supernatant and pellets were separated and analyzed on gel. Improved ScCENP-Q/U/P/O MTBA's contained an additional 150mM NaCl in both G-PEM and PEM.

EMSA

50µl of ScCENP-Q/U/P/O complex samples were mixed with tester DNA or RNA and incubated 30minutes on 4°C. Subsequently, samples were loaded onto a nondenaturing 5% polyacrylamid gel, pH 7. After electrophoresis, gels were stained with ethidium bromide.

In vitro phosphorylation

Clb2-TAP and Clb5-TAP were purified according to the given TAP protocol. 3µl of kinase were incubated with 2µl of the ScCCAN subcomplex samples and 5µM ATP (γ-$[P^{32}]$ATP for radioassays) in CDK1 buffer (25mM HEPES pH 7.6, 100mM KCl, 2mM $MgCl_2$, 1mM DTT, 1mM EGTA, 5% glycerol, 20mM β-glycerolphosphate) for 30min at 25ºC. The γ-$[P^{32}]$ATP-phosphorylated products were separated by SDS-PAGE, the gels dried and exposed to a autoradiography film. To map in vitro CDK1 phosphorylation sites ATP phosphorylated samples were handed to mass spectrometry for in solution digestion and analysis.

5.3 Mass spectrometry

Susanne Opravil, Richard Imre, Otto Hudecz

Information supplied by IMP/IMBA protein chemistry core facility

The nano-HPLC system used in all experiments was an UltiMate 3000 Dual Gradient HPLC system (Dionex), equipped with a Proxeon nanospray source (Proxeon), coupled to an LTQ Velos Orbitrap mass spectrometer (Thermo Fisher Scientific), operated in data-dependent mode using a full scan in the ion cyclotron resonance cell followed by tandem mass spectrometry (MS/MS) scans of the 12 most abundant ions in the linear ion trap. MS/MS spectra were acquired in the multistage activation mode, where subsequent activation was performed on fragment ions resulting from the neutral loss of −98, −49 or −32.6 *m*/*z* for potential follow-up phosphorylation site analysis. Precursor ions selected for fragmentation were put on a dynamic exclusion list for 180 s. Monoisotopic precursor selection was enabled.

Analysis of MS data. For peptide identification, all MS/MS spectra were searched using Mascot 2.2.04 (Matrix Science) and Sequest (Thermo Scientific) against the yeast SGD protein sequence database (6,717 sequences; 3,020,761 residues). The following search parameters were used: carbamidomethylation or methyl methylthiomethyl sulphoxide respectively on cysteine was set as a fixed modification; oxidation on methionine was set as variable modification. Monoisotopic masses were searched within unrestricted protein masses for tryptic, chymotryptic and unspecific (subtilisin digest) peptides. The peptide mass tolerance was set to ±5 ppm and the fragment mass tolerance to ±0.5 Da. The maximal number of missed cleavages was set to 2. Using a Thermo Proteome Discoverer 1.3.0.339 (Thermo Scientific), the results of both search engines were combined and filtered to 1% false discovery rate using an integrated Percolator algorithm. Furthermore, high-quality criteria filters such as peptide rank 1 and minimum 2 peptides per protein were applied.

5.4 Live cell fluorescence microscopy

Unsynchronized cells expressing Nuf2-mCH and Wip1-GFP with or without a ScCENP-T deletion (yMM550, yMM551) were grown in synthetic medium and placed on a Concanavalin A coated cover slip. Cells representative of morphologically identifiable cell cycle stages (G1, S, M) were imaged by Deltavision deconvolution microscopy (AppliedPrecision) on an Olympus IX-71 microscope controlled by Softworx and equipped with a PlanApo 100x 1.4NA objective (Olympus) and a Coolsnap HQ camera (Photometrics) at 25ºC.

6. References

1. Flemming, W., *Zellsubstanz, Kern und Zelltheilung*. 1882: Vogel.
2. Weaver, B.A., et al., *Aneuploidy acts both oncogenically and as a tumor suppressor.* Cancer Cell, 2007. **11**(1): p. 25-36.
3. Hassold, T. and P. Hunt, *To err (meiotically) is human: the genesis of human aneuploidy.* Nat Rev Genet, 2001. **2**(4): p. 280-91.
4. Boveri, T., *Zellenstudien. II.* 1888.
5. Boveri, T., *Die Blastomerenkerne von Ascaris megalocephala und die Theorie der Chromosomenindividualität*. 1909: Universität Leipzig.
6. Sutton, W.S., *The Chromosomes in Heredity.* Biol Bull, 1903. **4**(5): p. 231-250.
7. Morgan, T.H., *Chromosomes and heredity* The American Naturalist, 1910(44): p. 449–496.
8. Morgan, T.H., *The Mechanism of Mendelian heredity*. 1915: H. Holt and company.
9. Beneden, E.v., *Recherches sur la maturation de l'oeuf, la fécondation, et la division cellulaire*. 1883: H. Engelcke.
10. Henderson, S.A., R.B. Nicklas, and C.A. Koch, *Temperature-induced orientation instability during meiosis: an experimental analysis.* J Cell Sci, 1970. **6**(2): p. 323-50.
11. Schleiffer, A., et al., *CENP-T proteins are conserved centromere receptors of the Ndc80 complex.* Nat Cell Biol. **14**(6): p. 604-13.
12. Peterson, J.B. and H. Ris, *Electron-microscopic study of the spindle and chromosome movement in the yeast Saccharomyces cerevisiae.* J Cell Sci, 1976. **22**(2): p. 219-42.
13. Robinow, C.F. and J. Marak, *A fiber apparatus in the nucleus of the yeast cell.* J Cell Biol, 1966. **29**(1): p. 129-51.
14. Jaspersen, S.L. and M. Winey, *The budding yeast spindle pole body: structure, duplication, and function.* Annu Rev Cell Dev Biol, 2004. **20**: p. 1-28.
15. Fitch, I., et al., *Characterization of four B-type cyclin genes of the budding yeast Saccharomyces cerevisiae.* Mol Biol Cell, 1992. **3**(7): p. 805-18.
16. Berlin, V., C.A. Styles, and G.R. Fink, *BIK1, a protein required for microtubule function during mating and mitosis in Saccharomyces cerevisiae, colocalizes with tubulin.* J Cell Biol, 1990. **111**(6 Pt 1): p. 2573-86.
17. Dechant, R. and M. Glotzer, *Centrosome separation and central spindle assembly act in redundant pathways that regulate microtubule density and trigger cleavage furrow formation.* Dev Cell, 2003. **4**(3): p. 333-44.
18. Glotzer, M., *The molecular requirements for cytokinesis.* Science, 2005. **307**(5716): p. 1735-9.
19. Mitchison, J.M., *The Biology of the Cell Cycle.* 1971.
20. Hartwell, L.H., *Saccharomyces cerevisiae cell cycle.* Bacteriol Rev, 1974. **38**(2): p. 164-98.
21. Adams, A.E. and J.R. Pringle, *Relationship of actin and tubulin distribution to bud growth in wild-type and morphogenetic-mutant Saccharomyces cerevisiae.* J Cell Biol, 1984. **98**(3): p. 934-45.
22. Kilmartin, J.V. and A.E. Adams, *Structural rearrangements of tubulin and actin during the cell cycle of the yeast Saccharomyces.* The Journal of Cell Biology, 1984. **98**(3): p. 922-933.

23. Lew, D.J. and S.I. Reed, *Morphogenesis in the yeast cell cycle: regulation by Cdc28 and cyclins.* J Cell Biol, 1993. **120**(6): p. 1305-20.

24. Cid, V.J., et al., *Molecular basis of cell integrity and morphogenesis in Saccharomyces cerevisiae.* Microbiol Rev, 1995. **59**(3): p. 345-86.

25. Diffley, J.F., et al., *Two steps in the assembly of complexes at yeast replication origins in vivo.* Cell, 1994. **78**(2): p. 303-16.

26. Sclafani, R.A. and T.M. Holzen, *Cell cycle regulation of DNA replication.* Annu Rev Genet, 2007. **41**: p. 237-80.

27. Blow, J.J. and R.A. Laskey, *A role for the nuclear envelope in controlling DNA replication within the cell cycle.* Nature, 1988. **332**(6164): p. 546-8.

28. Bucking-Throm, E., et al., *Reversible arrest of haploid yeast cells in the initiation of DNA synthesis by a diffusible sex factor.* Exp Cell Res, 1973. **76**(1): p. 99-110.

29. Hereford, L.M. and L.H. Hartwell, *Sequential gene function in the initiation of Saccharomyces cerevisiae DNA synthesis.* J Mol Biol, 1974. **84**(3): p. 445-61.

30. Winey, M. and E.T. O'Toole, *The spindle cycle in budding yeast.* Nat Cell Biol, 2001. **3**(1): p. E23-7.

31. Moor, H., *Endoplasmic reticulum as the initiator of bud formation in yeast (S. cerevisiae).* Arch Mikrobiol, 1967. **57**(2): p. 135-46.

32. Sentandreu, R. and D.H. Northcote, *The formation of buds in yeast.* J Gen Microbiol, 1969. **55**(3): p. 393-8.

33. Hartwell, L.H., et al., *Genetic control of the cell division cycle in yeast.* Science, 1974. **183**(4120): p. 46-51.

34. Chant, J. and J.R. Pringle, *Patterns of bud-site selection in the yeast Saccharomyces cerevisiae.* J Cell Biol, 1995. **129**(3): p. 751-65.

35. Yeh, E., et al., *Spindle dynamics and cell cycle regulation of dynein in the budding yeast, Saccharomyces cerevisiae.* J Cell Biol, 1995. **130**(3): p. 687-700.

36. Mulholland, J., et al., *Ultrastructure of the yeast actin cytoskeleton and its association with the plasma membrane.* J Cell Biol, 1994. **125**(2): p. 381-91.

37. Huisman, S.M. and M. Segal, *Cortical capture of microtubules and spindle polarity in budding yeast - where's the catch?* J Cell Sci, 2005. **118**(Pt 3): p. 463-71.

38. Tkacz, J.S. and J.O. Lampen, *Wall replication in saccharomyces species: use of fluorescein-conjugated concanavalin A to reveal the site of mannan insertion.* J Gen Microbiol, 1972. **72**(2): p. 243-7.

39. Pearson, C.G. and K. Bloom, *Dynamic microtubules lead the way for spindle positioning.* Nat Rev Mol Cell Biol, 2004. **5**(6): p. 481-92.

40. Karpova, T.S., et al., *Role of actin and Myo2p in polarized secretion and growth of Saccharomyces cerevisiae.* Mol Biol Cell, 2000. **11**(5): p. 1727-37.

41. Gupta, M.L., Jr., et al., *Plus end-specific depolymerase activity of Kip3, a kinesin-8 protein, explains its role in positioning the yeast mitotic spindle.* Nat Cell Biol, 2006. **8**(9): p. 913-23.

42. Shaw, S.L., et al., *Nuclear and spindle dynamics in budding yeast.* Mol Biol Cell, 1998. **9**(7): p. 1627-31.

43. Shaw, S.L., et al., *Astral microtubule dynamics in yeast: a microtubule-based searching mechanism for spindle orientation and nuclear migration into the bud.* J Cell Biol, 1997. **139**(4): p. 985-94.

44. Liakopoulos, D., et al., *Asymmetric loading of Kar9 onto spindle poles and microtubules ensures proper spindle alignment.* Cell, 2003. **112**(4): p. 561-74.

45. Kitamura, E., et al., *Kinetochore microtubule interaction during S phase in Saccharomyces cerevisiae.* Genes Dev, 2007. **21**(24): p. 3319-30.

46. Guacci, V., E. Hogan, and D. Koshland, *Chromosome condensation and sister chromatid pairing in budding yeast.* J Cell Biol, 1994. **125**(3): p. 517-30.

47. Mundkur, B., *Electron microscopical studies of frozendried yeast. II. The nature of basophile particles and vesicular nuclei in Saccharomyces.* Exp Cell Res, 1961. **25**: p. 1-23.

48. Straight, A.F., et al., *Mitosis in living budding yeast: anaphase A but no metaphase plate.* Science, 1997. **277**(5325): p. 574-8.

49. O'Toole, E.T., et al., *Three-dimensional analysis and ultrastructural design of mitotic spindles from the cdc20 mutant of Saccharomyces cerevisiae.* Mol Biol Cell, 1997. **8**(1): p. 1-11.

50. Woodruff, J.B., D.G. Drubin, and G. Barnes, *Dynein-driven mitotic spindle positioning restricted to anaphase by She1p inhibition of dynactin recruitment.* Mol Biol Cell, 2009. **20**(13): p. 3003-11.

51. Goshima, G. and M. Yanagida, *Establishing biorientation occurs with precocious separation of the sister kinetochores, but not the arms, in the early spindle of budding yeast.* Cell, 2000. **100**(6): p. 619-33.

52. He, X., S. Asthana, and P.K. Sorger, *Transient sister chromatid separation and elastic deformation of chromosomes during mitosis in budding yeast.* Cell, 2000. **101**(7): p. 763-75.

53. Michaelis, C., R. Ciosk, and K. Nasmyth, *Cohesins: chromosomal proteins that prevent premature separation of sister chromatids.* Cell, 1997. **91**(1): p. 35-45.

54. Toth, A., et al., *Yeast cohesin complex requires a conserved protein, Eco1p(Ctf7), to establish cohesion between sister chromatids during DNA replication.* Genes Dev, 1999. **13**(3): p. 320-33.

55. Uhlmann, F. and K. Nasmyth, *Cohesion between sister chromatids must be established during DNA replication.* Curr Biol, 1998. **8**(20): p. 1095-101.

56. Haering, C.H., et al., *Molecular architecture of SMC proteins and the yeast cohesin complex.* Mol Cell, 2002. **9**(4): p. 773-88.

57. Nasmyth, K., *Cohesin: a catenase with separate entry and exit gates?* Nat Cell Biol, 2011. **13**(10): p. 1170-7.

58. Waizenegger, I.C., et al., *Two distinct pathways remove mammalian cohesin from chromosome arms in prophase and from centromeres in anaphase.* Cell, 2000. **103**(3): p. 399-410.

59. Sumara, I., et al., *The dissociation of cohesin from chromosomes in prophase is regulated by Polo-like kinase.* Mol Cell, 2002. **9**(3): p. 515-25.

60. McGuinness, B.E., et al., *Shugoshin prevents dissociation of cohesin from centromeres during mitosis in vertebrate cells.* PLoS Biol, 2005. **3**(3): p. e86.

61. Riedel, C.G., et al., *Protein phosphatase 2A protects centromeric sister chromatid cohesion during meiosis I.* Nature, 2006. **441**(7089): p. 53-61.

62. Kitajima, T.S., et al., *Shugoshin collaborates with protein phosphatase 2A to protect cohesin.* Nature, 2006. **441**(7089): p. 46-52.

63. Tang, Z., et al., *PP2A is required for centromeric localization of Sgo1 and proper chromosome segregation.* Dev Cell, 2006. **10**(5): p. 575-85.

64. Lima-de-Faria, A., *The division cycle of the kinetochore.* Hereditas, 1955. **41**(1-2): p. 238-240.

65. Uhlmann, F., et al., *Cleavage of cohesin by the CD clan protease separin triggers anaphase in yeast.* Cell, 2000. **103**(3): p. 375-86.

66. Marston, A.L., et al., *A genome-wide screen identifies genes required for centromeric cohesion.* Science, 2004. **303**(5662): p. 1367-70.

67. Eckert, C.A., D.J. Gravdahl, and P.C. Megee, *The enhancement of pericentromeric cohesin association by conserved kinetochore components promotes high-fidelity chromosome segregation and is sensitive to microtubule-based tension.* Genes Dev, 2007. **21**(3): p. 278-91.

68. Tanaka, T., et al., *Identification of cohesin association sites at centromeres and along chromosome arms.* Cell, 1999. **98**(6): p. 847-58.

69. Lew, D.J., *The morphogenesis checkpoint: how yeast cells watch their figures.* Curr Opin Cell Biol, 2003. **15**(6): p. 648-53.

70. Foiani, M., et al., *DNA damage checkpoints and DNA replication controls in Saccharomyces cerevisiae.* Mutat Res, 2000. **451**(1-2): p. 187-96.

71. Melo, J. and D. Toczyski, *A unified view of the DNA-damage checkpoint.* Curr Opin Cell Biol, 2002. **14**(2): p. 237-45.

72. Hoyt, M.A., L. Totis, and B.T. Roberts, *S. cerevisiae genes required for cell cycle arrest in response to loss of microtubule function.* Cell, 1991. **66**(3): p. 507-17.

73. Reed, S.I., J.A. Hadwiger, and A.T. Lorincz, *Protein kinase activity associated with the product of the yeast cell division cycle gene CDC28.* Proc Natl Acad Sci U S A, 1985. **82**(12): p. 4055-9.

74. Piggott, J.R., R. Rai, and B.L. Carter, *A bifunctional gene product involved in two phases of the yeast cell cycle.* Nature, 1982. **298**(5872): p. 391-3.

75. Kishimoto, T. and H. Kondo, *Extraction and preliminary characterization of maturation-promoting factor from starfish oocytes.* Exp Cell Res, 1986. **163**(2): p. 445-52.

76. Reed, S.I. and C. Wittenberg, *Mitotic role for the Cdc28 protein kinase of Saccharomyces cerevisiae.* Proc Natl Acad Sci U S A, 1990. **87**(15): p. 5697-701.

77. Murray, A.W. and M.W. Kirschner, *Cyclin synthesis drives the early embryonic cell cycle.* Nature, 1989. **339**(6222): p. 275-80.

78. Enserink, J.M. and R.D. Kolodner, *An overview of Cdk1-controlled targets and processes.* Cell Div, 2010. **5**: p. 11.

79. Nasmyth, K., *At the heart of the budding yeast cell cycle.* Trends Genet, 1996. **12**(10): p. 405-12.

80. Draetta, G. and D. Beach, *Activation of cdc2 protein kinase during mitosis in human cells: cell cycle-dependent phosphorylation and subunit rearrangement.* Cell, 1988. **54**(1): p. 17-26.

81. Brizuela, L., G. Draetta, and D. Beach, *Activation of human CDC2 protein as a histone H1 kinase is associated with complex formation with the p62 subunit.* Proc Natl Acad Sci U S A, 1989. **86**(12): p. 4362-6.

82. Draetta, G., et al., *Cdc2 protein kinase is complexed with both cyclin A and B: evidence for proteolytic inactivation of MPF.* Cell, 1989. **56**(5): p. 829-38.

83. Wittenberg, C. and S.I. Reed, *Control of the yeast cell cycle is associated with assembly/disassembly of the Cdc28 protein kinase complex.* Cell, 1988. **54**(7): p. 1061-72.

84. Pavletich, N.P., *Mechanisms of cyclin-dependent kinase regulation: structures of Cdks, their cyclin activators, and Cip and INK4 inhibitors.* J Mol Biol, 1999. **287**(5): p. 821-8.

85. Hadwiger, J.A., et al., *A family of cyclin homologs that control the G1 phase in yeast.* Proc Natl Acad Sci U S A, 1989. **86**(16): p. 6255-9.

86. Richardson, H., et al., *Cyclin-B homologs in Saccharomyces cerevisiae function in S phase and in G2.* Genes Dev, 1992. **6**(11): p. 2021-34.

87. Schwob, E. and K. Nasmyth, *CLB5 and CLB6, a new pair of B cyclins involved in DNA replication in Saccharomyces cerevisiae.* Genes Dev, 1993. **7**(7A): p. 1160-75.

88. Epstein, C.B. and F.R. Cross, *CLB5: a novel B cyclin from budding yeast with a role in S phase.* Genes Dev, 1992. **6**(9): p. 1695-706.

89. Richardson, H.E., et al., *An essential G1 function for cyclin-like proteins in yeast.* Cell, 1989. **59**(6): p. 1127-33.

90. Cross, F.R., *Cell cycle arrest caused by CLN gene deficiency in Saccharomyces cerevisiae resembles START-I arrest and is independent of the mating-pheromone signalling pathway.* Mol Cell Biol, 1990. **10**(12): p. 6482-90.

91. Ghiara, J.B., et al., *A cyclin B homolog in S. cerevisiae: chronic activation of the Cdc28 protein kinase by cyclin prevents exit from mitosis.* Cell, 1991. **65**(1): p. 163-74.

92. Tyers, M., G. Tokiwa, and B. Futcher, *Comparison of the Saccharomyces cerevisiae G1 cyclins: Cln3 may be an upstream activator of Cln1, Cln2 and other cyclins.* EMBO J, 1993. **12**(5): p. 1955-68.

93. Bailly, E., et al., *Differential cellular localization among mitotic cyclins from Saccharomyces cerevisiae: a new role for the axial budding protein Bud3 in targeting Clb2 to the mother-bud neck.* J Cell Sci, 2003. **116**(Pt 20): p. 4119-30.

94. Miller, M.E. and F.R. Cross, *Distinct subcellular localization patterns contribute to functional specificity of the Cln2 and Cln3 cyclins of Saccharomyces cerevisiae.* Mol Cell Biol, 2000. **20**(2): p. 542-55.

95. Loog, M. and D.O. Morgan, *Cyclin specificity in the phosphorylation of cyclin-dependent kinase substrates.* Nature, 2005. **434**(7029): p. 104-8.

96. Woodbury, E.L. and D.O. Morgan, *Cdk and APC activities limit the spindle-stabilizing function of Fin1 to anaphase.* Nat Cell Biol, 2007. **9**(1): p. 106-12.

97. Schuyler, S.C., J.Y. Liu, and D. Pellman, *The molecular function of Ase1p: evidence for a MAP-dependent midzone-specific spindle matrix. Microtubule-associated proteins.* J Cell Biol, 2003. **160**(4): p. 517-28.

98. Khmelinskii, A., et al., *Cdc14-regulated midzone assembly controls anaphase B.* J Cell Biol, 2007. **177**(6): p. 981-93.

99. Khmelinskii, A., et al., *Phosphorylation-dependent protein interactions at the spindle midzone mediate cell cycle regulation of spindle elongation.* Dev Cell, 2009. **17**(2): p. 244-56.

100. Archambault, V., et al., *Two-faced cyclins with eyes on the targets.* Cell Cycle, 2005. **4**(1): p. 125-30.

101. Oikonomou, C. and F.R. Cross, *Rising cyclin-CDK levels order cell cycle events.* PLoS One. **6**(6): p. e20788.

102. Koivomagi, M., et al., *Cascades of multisite phosphorylation control Sic1 destruction at the onset of S phase.* Nature. **480**(7375): p. 128-31.

103. Dirick, L., T. Bohm, and K. Nasmyth, *Roles and regulation of Cln-Cdc28 kinases at the start of the cell cycle of Saccharomyces cerevisiae.* EMBO J, 1995. **14**(19): p. 4803-13.

104. Oehlen, L.J. and F.R. Cross, *G1 cyclins CLN1 and CLN2 repress the mating factor response pathway at Start in the yeast cell cycle.* Genes Dev, 1994. **8**(9): p. 1058-70.

105. Haase, S.B., M. Winey, and S.I. Reed, *Multi-step control of spindle pole body duplication by cyclin-dependent kinase.* Nat Cell Biol, 2001. **3**(1): p. 38-42.

106. Dahmann, C., J.F. Diffley, and K.A. Nasmyth, *S-phase-promoting cyclin-dependent kinases prevent re-replication by inhibiting the transition of replication origins to a pre-replicative state.* Curr Biol, 1995. **5**(11): p. 1257-69.

107. Hollingsworth, R.E., Jr. and R.A. Sclafani, *DNA metabolism gene CDC7 from yeast encodes a serine (threonine) protein kinase.* Proc Natl Acad Sci U S A, 1990. **87**(16): p. 6272-6.

108. Hartwell, L.H., *Three additional genes required for deoxyribonucleic acid synthesis in Saccharomyces cerevisiae.* J Bacteriol, 1973. **115**(3): p. 966-74.

109. Jackson, A.L., et al., *Cell cycle regulation of the yeast Cdc7 protein kinase by association with the Dbf4 protein.* Mol Cell Biol, 1993. **13**(5): p. 2899-908.

110. Bahman, M., et al., *Characterisation of the CDC7 gene product of Saccharomyces cerevisiae as a protein kinase needed for the initiation of mitotic DNA synthesis.* Biochim Biophys Acta, 1988. **951**(2-3): p. 335-43.

111. Kitada, K., et al., *Temperature-sensitive cdc7 mutations of Saccharomyces cerevisiae are suppressed by the DBF4 gene, which is required for the G1/S cell cycle transition.* Genetics, 1992. **131**(1): p. 21-9.

112. Chapman, J.W. and L.H. Johnston, *The yeast gene, DBF4, essential for entry into S phase is cell cycle regulated.* Exp Cell Res, 1989. **180**(2): p. 419-28.

113. Johnston, L.H. and A.P. Thomas, *A further two mutants defective in initiation of the S phase in the yeast Saccharomyces cerevisiae.* Mol Gen Genet, 1982. **186**(3): p. 445-8.

114. Jazwinski, S.M., *CDC7-dependent protein kinase activity in yeast replicative-complex preparations.* Proc Natl Acad Sci U S A, 1988. **85**(7): p. 2101-5.

115. Yoon, H.J., S. Loo, and J.L. Campbell, *Regulation of Saccharomyces cerevisiae CDC7 function during the cell cycle.* Mol Biol Cell, 1993. **4**(2): p. 195-208.

116. Dowell, S.J., P. Romanowski, and J.F. Diffley, *Interaction of Dbf4, the Cdc7 protein kinase regulatory subunit, with yeast replication origins in vivo.* Science, 1994. **265**(5176): p. 1243-6.

117. Duncker, B.P. and G.W. Brown, *Cdc7 kinases (DDKs) and checkpoint responses: lessons from two yeasts.* Mutat Res, 2003. **532**(1-2): p. 21-7.

118. Sclafani, R.A., et al., *Differential regulation of the yeast CDC7 gene during mitosis and meiosis.* Mol Cell Biol, 1988. **8**(1): p. 293-300.

119. Surana, U., et al., *The role of CDC28 and cyclins during mitosis in the budding yeast S. cerevisiae.* Cell, 1991. **65**(1): p. 145-61.

120. Peters, J.M., *The anaphase promoting complex/cyclosome: a machine designed to destroy.* Nat Rev Mol Cell Biol, 2006. **7**(9): p. 644-56.

121. Rahal, R. and A. Amon, *Mitotic CDKs control the metaphase-anaphase transition and trigger spindle elongation.* Genes Dev, 2008. **22**(11): p. 1534-48.

122. Dirick, L. and K. Nasmyth, *Positive feedback in the activation of G1 cyclins in yeast.* Nature, 1991. **351**(6329): p. 754-7.

123. Cross, F.R. and A.H. Tinkelenberg, *A potential positive feedback loop controlling CLN1 and CLN2 gene expression at the start of the yeast cell cycle.* Cell, 1991. **65**(5): p. 875-83.

124. Nasmyth, K. and L. Dirick, *The role of SWI4 and SWI6 in the activity of G1 cyclins in yeast.* Cell, 1991. **66**(5): p. 995-1013.

125. Skotheim, J.M., et al., *Positive feedback of G1 cyclins ensures coherent cell cycle entry.* Nature, 2008. **454**(7202): p. 291-6.

126. Wittenberg, C. and S.I. Reed, *Cell cycle-dependent transcription in yeast: promoters, transcription factors, and transcriptomes.* Oncogene, 2005. **24**(17): p. 2746-55.

127. Amon, A., et al., *Mechanisms that help the yeast cell cycle clock tick: G2 cyclins transcriptionally activate G2 cyclins and repress G1 cyclins.* Cell, 1993. **74**(6): p. 993-1007.

128. Irniger, S., et al., *Genes involved in sister chromatid separation are needed for B-type cyclin proteolysis in budding yeast.* Cell, 1995. **81**(2): p. 269-78.

129. Visintin, R., S. Prinz, and A. Amon, *CDC20 and CDH1: a family of substrate-specific activators of APC-dependent proteolysis.* Science, 1997. **278**(5337): p. 460-3.

130. Schwab, M., A.S. Lutum, and W. Seufert, *Yeast Hct1 is a regulator of Clb2 cyclin proteolysis.* Cell, 1997. **90**(4): p. 683-93.

131. Donovan, J.D., et al., *P40SDB25, a putative CDK inhibitor, has a role in the M/G1 transition in Saccharomyces cerevisiae.* Genes Dev, 1994. **8**(14): p. 1640-53.

132. Mendenhall, M.D., *An inhibitor of p34CDC28 protein kinase activity from Saccharomyces cerevisiae.* Science, 1993. **259**(5092): p. 216-9.

133. Schwob, E., et al., *The B-type cyclin kinase inhibitor p40SIC1 controls the G1 to S transition in S. cerevisiae.* Cell, 1994. **79**(2): p. 233-44.

134. Schneider, B.L., Q.H. Yang, and A.B. Futcher, *Linkage of replication to start by the Cdk inhibitor Sic1.* Science, 1996. **272**(5261): p. 560-2.

135. Petroski, M.D. and R.J. Deshaies, *Function and regulation of cullin-RING ubiquitin ligases.* Nat Rev Mol Cell Biol, 2005. **6**(1): p. 9-20.

136. Hershko, A., et al., *Components of a system that ligates cyclin to ubiquitin and their regulation by the protein kinase cdc2.* J Biol Chem, 1994. **269**(7): p. 4940-6.

137. Yamamoto, A., V. Guacci, and D. Koshland, *Pds1p, an inhibitor of anaphase in budding yeast, plays a critical role in the APC and checkpoint pathway(s).* J Cell Biol, 1996. **133**(1): p. 99-110.

138. Cohen-Fix, O., et al., *Anaphase initiation in Saccharomyces cerevisiae is controlled by the APC-dependent degradation of the anaphase inhibitor Pds1p.* Genes Dev, 1996. **10**(24): p. 3081-93.

139. Ciosk, R., et al., *An ESP1/PDS1 complex regulates loss of sister chromatid cohesion at the metaphase to anaphase transition in yeast.* Cell, 1998. **93**(6): p. 1067-76.

140. Uhlmann, F., F. Lottspeich, and K. Nasmyth, *Sister-chromatid separation at anaphase onset is promoted by cleavage of the cohesin subunit Scc1.* Nature, 1999. **400**(6739): p. 37-42.

141. Higuchi, T. and F. Uhlmann, *Stabilization of microtubule dynamics at anaphase onset promotes chromosome segregation.* Nature, 2005. **433**(7022): p. 171-6.

142. Stegmeier, F., R. Visintin, and A. Amon, *Separase, polo kinase, the kinetochore protein Slk19, and Spo12 function in a network that controls Cdc14 localization during early anaphase.* Cell, 2002. **108**(2): p. 207-20.

143. Piatti, S., et al., *The spindle position checkpoint in budding yeast: the motherly care of MEN.* Cell Div, 2006. **1**(1): p. 2.

144. Queralt, E. and F. Uhlmann, *Cdk-counteracting phosphatases unlock mitotic exit.* Curr Opin Cell Biol, 2008. **20**(6): p. 661-8.

145. Bardin, A.J. and A. Amon, *Men and sin: what's the difference?* Nat Rev Mol Cell Biol, 2001. **2**(11): p. 815-26.

146. Moll, T., et al., *The role of phosphorylation and the CDC28 protein kinase in cell cycle-regulated nuclear import of the S. cerevisiae transcription factor SWI5.* Cell, 1991. **66**(4): p. 743-58.

147. Knapp, D., et al., *The transcription factor Swi5 regulates expression of the cyclin kinase inhibitor p40SIC1.* Mol Cell Biol, 1996. **16**(10): p. 5701-7.

148. Li, R. and A.W. Murray, *Feedback control of mitosis in budding yeast.* Cell, 1991. **66**(3): p. 519-31.

149. Bomont, P., et al., *Unstable microtubule capture at kinetochores depleted of the centromere-associated protein CENP-F.* EMBO J, 2005. **24**(22): p. 3927-39.

150. Rieder, C.L., et al., *The checkpoint delaying anaphase in response to chromosome monoorientation is mediated by an inhibitory signal produced by unattached kinetochores.* J Cell Biol, 1995. **130**(4): p. 941-8.

151. Zhang, D. and R.B. Nicklas, *'Anaphase' and cytokinesis in the absence of chromosomes.* Nature, 1996. **382**(6590): p. 466-8.

152. Wong, J. and G. Fang, *HURP controls spindle dynamics to promote proper interkinetochore tension and efficient kinetochore capture.* J Cell Biol, 2006. **173**(6): p. 879-91.

153. Roberts, B.T., K.A. Farr, and M.A. Hoyt, *The Saccharomyces cerevisiae checkpoint gene BUB1 encodes a novel protein kinase.* Mol Cell Biol, 1994. **14**(12): p. 8282-91.

154. Weiss, E. and M. Winey, *The Saccharomyces cerevisiae spindle pole body duplication gene MPS1 is part of a mitotic checkpoint.* J Cell Biol, 1996. **132**(1-2): p. 111-23.

155. Seeley, T.W., L. Wang, and J.Y. Zhen, *Phosphorylation of human MAD1 by the BUB1 kinase in vitro.* Biochem Biophys Res Commun, 1999. **257**(2): p. 589-95.

156. Winey, M., et al., *MPS1 and MPS2: novel yeast genes defining distinct steps of spindle pole body duplication.* J Cell Biol, 1991. **114**(4): p. 745-54.

157. Lauze, E., et al., *Yeast spindle pole body duplication gene MPS1 encodes an essential dual specificity protein kinase.* EMBO J, 1995. **14**(8): p. 1655-63.

158. Poch, O., et al., *RPK1, an essential yeast protein kinase involved in the regulation of the onset of mitosis, shows homology to mammalian dual-specificity kinases.* Mol Gen Genet, 1994. **243**(6): p. 641-53.

159. Chan, G.K., B.T. Schaar, and T.J. Yen, *Characterization of the kinetochore binding domain of CENP-E reveals interactions with the kinetochore proteins CENP-F and hBUBR1.* J Cell Biol, 1998. **143**(1): p. 49-63.

160. Taylor, S.S., E. Ha, and F. McKeon, *The human homologue of Bub3 is required for kinetochore localization of Bub1 and a Mad3/Bub1-related protein kinase.* J Cell Biol, 1998. **142**(1): p. 1-11.

161. Chan, G.K., et al., *Human BUBR1 is a mitotic checkpoint kinase that monitors CENP-E functions at kinetochores and binds the cyclosome/APC.* J Cell Biol, 1999. **146**(5): p. 941-54.

162. Chen, R.H., *BubR1 is essential for kinetochore localization of other spindle checkpoint proteins and its phosphorylation requires Mad1.* J Cell Biol, 2002. **158**(3): p. 487-96.

163. He, X., et al., *Mph1, a member of the Mps1-like family of dual specificity protein kinases, is required for the spindle checkpoint in S. pombe.* J Cell Sci, 1998. **111 (Pt 12)**: p. 1635-47.

164. Abrieu, A., et al., *Mps1 is a kinetochore-associated kinase essential for the vertebrate mitotic checkpoint.* Cell, 2001. **106**(1): p. 83-93.

165. Pangilinan, F., et al., *Mammalian BUB1 protein kinases: map positions and in vivo expression.* Genomics, 1997. **46**(3): p. 379-88.

166. Logarinho, E., et al., *Different spindle checkpoint proteins monitor microtubule attachment and tension at kinetochores in Drosophila cells.* J Cell Sci, 2004. **117**(Pt 9): p. 1757-71.

167. Chen, R.H., et al., *Spindle checkpoint protein Xmad1 recruits Xmad2 to unattached kinetochores.* J Cell Biol, 1998. **143**(2): p. 283-95.

168. Li, Y. and R. Benezra, *Identification of a human mitotic checkpoint gene: hsMAD2.* Science, 1996. **274**(5285): p. 246-8.

169. Jin, D.Y., F. Spencer, and K.T. Jeang, *Human T cell leukemia virus type 1 oncoprotein Tax targets the human mitotic checkpoint protein MAD1.* Cell, 1998. **93**(1): p. 81-91.

170. Essex, A., et al., *Systematic analysis in Caenorhabditis elegans reveals that the spindle checkpoint is composed of two largely independent branches.* Mol Biol Cell, 2009. **20**(4): p. 1252-67.

171. Tang, Z., et al., *Phosphorylation of Cdc20 by Bub1 provides a catalytic mechanism for APC/C inhibition by the spindle checkpoint.* Mol Cell, 2004. **16**(3): p. 387-97.

172. Fang, G., *Checkpoint protein BubR1 acts synergistically with Mad2 to inhibit anaphase-promoting complex.* Mol Biol Cell, 2002. **13**(3): p. 755-66.

173. Tang, Z., et al., *Mad2-Independent inhibition of APCCdc20 by the mitotic checkpoint protein BubR1.* Dev Cell, 2001. **1**(2): p. 227-37.

174. Kulukian, A., J.S. Han, and D.W. Cleveland, *Unattached kinetochores catalyze production of an anaphase inhibitor that requires a Mad2 template to prime Cdc20 for BubR1 binding.* Dev Cell, 2009. **16**(1): p. 105-17.

175. Wassmann, K. and R. Benezra, *Mad2 transiently associates with an APC/p55Cdc complex during mitosis.* Proc Natl Acad Sci U S A, 1998. **95**(19): p. 11193-8.

176. Fang, G., H. Yu, and M.W. Kirschner, *The checkpoint protein MAD2 and the mitotic regulator CDC20 form a ternary complex with the anaphase-promoting complex to control anaphase initiation.* Genes Dev, 1998. **12**(12): p. 1871-83.

177. Li, D., et al., *Recruitment of Cdc20 to the kinetochore requires BubR1 but not Mad2 in Drosophila melanogaster.* Mol Cell Biol, 2010. **30**(13): p. 3384-95.

178. King, E.M., S.J. van der Sar, and K.G. Hardwick, *Mad3 KEN boxes mediate both Cdc20 and Mad3 turnover, and are critical for the spindle checkpoint.* PLoS One, 2007. **2**(4): p. e342.

179. Burton, J.L. and M.J. Solomon, *Mad3p, a pseudosubstrate inhibitor of APCCdc20 in the spindle assembly checkpoint.* Genes Dev, 2007. **21**(6): p. 655-67.

180. Nilsson, J., et al., *The APC/C maintains the spindle assembly checkpoint by targeting Cdc20 for destruction.* Nat Cell Biol, 2008. **10**(12): p. 1411-20.

181. Mansfeld, J., et al., *APC15 drives the turnover of MCC-CDC20 to make the spindle assembly checkpoint responsive to kinetochore attachment.* Nat Cell Biol, 2011. **13**(10): p. 1234-43.

182. Elowe, S., et al., *Uncoupling of the spindle-checkpoint and chromosome-congression functions of BubR1.* J Cell Sci, 2009. **123**(Pt 1): p. 84-94.

183. Pan, J. and R.H. Chen, *Spindle checkpoint regulates Cdc20p stability in Saccharomyces cerevisiae.* Genes Dev, 2004. **18**(12): p. 1439-51.

184. Hwang, L.H., et al., *Budding yeast Cdc20: a target of the spindle checkpoint.* Science, 1998. **279**(5353): p. 1041-4.

185. Sudakin, V., G.K. Chan, and T.J. Yen, *Checkpoint inhibition of the APC/C in HeLa cells is mediated by a complex of BUBR1, BUB3, CDC20, and MAD2.* J Cell Biol, 2001. **154**(5): p. 925-36.

186. Herzog, F., et al., *Structure of the anaphase-promoting complex/cyclosome interacting with a mitotic checkpoint complex.* Science, 2009. **323**(5920): p. 1477-81.

187. Chao, W.C., et al., *Structure of the mitotic checkpoint complex.* Nature. **484**(7393): p. 208-13.

188. Poddar, A., P.T. Stukenberg, and D.J. Burke, *Two complexes of spindle checkpoint proteins containing Cdc20 and Mad2 assemble during mitosis independently of the kinetochore in Saccharomyces cerevisiae.* Eukaryot Cell, 2005. **4**(5): p. 867-78.

189. Fraschini, R., et al., *Bub3 interaction with Mad2, Mad3 and Cdc20 is mediated by WD40 repeats and does not require intact kinetochores.* EMBO J, 2001. **20**(23): p. 6648-59.

190. Westhorpe, F.G., et al., *p31comet-mediated extraction of Mad2 from the MCC promotes efficient mitotic exit.* J Cell Sci, 2011. **124**(Pt 22): p. 3905-16.

191. Meraldi, P., V.M. Draviam, and P.K. Sorger, *Timing and checkpoints in the regulation of mitotic progression.* Dev Cell, 2004. **7**(1): p. 45-60.

192. Tighe, A., O. Staples, and S. Taylor, *Mps1 kinase activity restrains anaphase during an unperturbed mitosis and targets Mad2 to kinetochores.* J Cell Biol, 2008. **181**(6): p. 893-901.

193. Luo, X. and H. Yu, *Protein metamorphosis: the two-state behavior of Mad2.* Structure, 2008. **16**(11): p. 1616-25.

194. Malureanu, L.A., et al., *BubR1 N terminus acts as a soluble inhibitor of cyclin B degradation by APC/C(Cdc20) in interphase.* Dev Cell, 2009. **16**(1): p. 118-31.

195. Maldonado, M. and T.M. Kapoor, *Constitutive Mad1 targeting to kinetochores uncouples checkpoint signalling from chromosome biorientation.* Nat Cell Biol, 2011. **13**(4): p. 475-82.

196. Shannon, K.B., J.C. Canman, and E.D. Salmon, *Mad2 and BubR1 function in a single checkpoint pathway that responds to a loss of tension.* Mol Biol Cell, 2002. **13**(10): p. 3706-19.

197. Orr, B., H. Bousbaa, and C.E. Sunkel, *Mad2-independent spindle assembly checkpoint activation and controlled metaphase-anaphase transition in Drosophila S2 cells.* Mol Biol Cell, 2007. **18**(3): p. 850-63.

198. Howell, B.J., et al., *Spindle checkpoint protein dynamics at kinetochores in living cells.* Curr Biol, 2004. **14**(11): p. 953-64.

199. Acquaviva, C., et al., *The anaphase promoting complex/cyclosome is recruited to centromeres by the spindle assembly checkpoint.* Nat Cell Biol, 2004. **6**(9): p. 892-898.

200. Kallio, M., et al., *Mammalian p55CDC mediates association of the spindle checkpoint protein Mad2 with the cyclosome/anaphase-promoting complex, and is involved in regulating anaphase onset and late mitotic events.* J Cell Biol, 1998. **141**(6): p. 1393-406.

201. Brady, D.M. and K.G. Hardwick, *Complex formation between Mad1p, Bub1p and Bub3p is crucial for spindle checkpoint function.* Curr Biol, 2000. **10**(11): p. 675-8.

202. Musacchio, A. and E.D. Salmon, *The spindle-assembly checkpoint in space and time.* Nat Rev Mol Cell Biol, 2007. **8**(5): p. 379-93.

203. Robbins, E. and N.K. Gonatas, *The Ultrastructure of a Mammalian Cell during the Mitotic Cycle.* J Cell Biol, 1964. **21**: p. 429-63.

204. Harris, P., *Electron microscope study of mitosis in sea urchin blastomeres.* J Biophys Biochem Cytol, 1961. **11**: p. 419-31.

205. Roth, L.E. and E.W. Daniels, *Electron microscopic studies of mitosis in amebae. II. The giant ameba Pelomyxa carolinensis.* J Cell Biol, 1962. **12**: p. 57-78.

206. Grimstone, A.V. and A. Klug, *Observations on the Substructure of Flagellar Fibres.* Journal of Cell Science, 1966. **1**(3): p. 351-362.

207. Bryan, J. and L. Wilson, *Are cytoplasmic microtubules heteropolymers?* Proc Natl Acad Sci U S A, 1971. **68**(8): p. 1762-6.

208. Eipper, B.A., *Rat brain microtubule protein: purification and determination of covalently bound phosphate and carbohydrate.* Proc Natl Acad Sci U S A, 1972. **69**(8): p. 2283-7.

209. Mohri, H., *Amino-acid composition of "Tubulin" constituting microtubules of sperm flagella.* Nature, 1968. **217**(5133): p. 1053-4.

210. Borisy, G.G. and E.W. Taylor, *The mechanism of action of colchicine. Binding of colchincine-3H to cellular protein.* J Cell Biol, 1967. **34**(2): p. 525-33.

211. Borisy, G.G. and E.W. Taylor, *The mechanism of action of colchicine. Colchicine binding to sea urchin eggs and the mitotic apparatus.* J Cell Biol, 1967. **34**(2): p. 535-48.

212. Feit, H., L. Slusarek, and M.L. Shelanski, *Heterogeneity of tubulin subunits.* Proc Natl Acad Sci U S A, 1971. **68**(9): p. 2028-31.

213. Weisenberg, R.C., *Microtubule formation in vitro in solutions containing low calcium concentrations.* Science, 1972. **177**(54): p. 1104-5.

214. Chretien, D., S.D. Fuller, and E. Karsenti, *Structure of growing microtubule ends: two-dimensional sheets close into tubes at variable rates.* J Cell Biol, 1995. **129**(5): p. 1311-28.

215. Shelanski, M.L., F. Gaskin, and C.R. Cantor, *Microtubule assembly in the absence of added nucleotides.* Proc Natl Acad Sci U S A, 1973. **70**(3): p. 765-8.

216. Nogales, E., et al., *High-resolution model of the microtubule.* Cell, 1999. **96**(1): p. 79-88.

217. Gaskin, F., C.R. Cantor, and M.L. Shelanski, *Turbidimetric studies of the in vitro assembly and disassembly of porcine neurotubules.* J Mol Biol, 1974. **89**(4): p. 737-55.

218. Ledbetter, M.C. and K.R. Porter, *Morphology of Microtubules of Plant Cell.* Science, 1964. **144**(3620): p. 872-4.

219. Ringo, D.L., *The arrangement of subunits in flagellar fibers.* J Ultrastruct Res, 1967. **17**(3): p. 266-77.

220. Phillips, D.M., *Substructure of flagellar tubules.* J Cell Biol, 1966. **31**(3): p. 635-8.

221. Stephens, R.E., *Reassociation of microtubule protein.* J Mol Biol, 1968. **33**(2): p. 517-9.

222. Stephens, R.E., *Factors influencing the polymerization of outer fibre microtubule protein.* Quarterly Reviews of Biophysics, 1969. **1**(04): p. 377-390.

223. Li, H., et al., *Microtubule structure at 8 A resolution.* Structure, 2002. **10**(10): p. 1317-28.

224. Amos, L.A. and A. Klug, *Arrangement of Subunits in Flagellar Microtubules.* Journal of Cell Science, 1974. **14**(3): p. 523-549.

225. Dentler, W.L., et al., *Directionality of brain microtubule assembly in vitro.* Proc Natl Acad Sci U S A, 1974. **71**(5): p. 1710-4.

226. Binder, L.I., W.L. Dentler, and J.L. Rosenbaum, *Assembly of chick brain tubulin onto flagellar microtubules from Chlamydomonas and sea urchin sperm.* Proc Natl Acad Sci U S A, 1975. **72**(3): p. 1122-6.

227. Allen, C. and G.G. Borisy, *Structural polarity and directional growth of microtubules of Chlamydomonas flagella.* J Mol Biol, 1974. **90**(2): p. 381-402.

228. Bergen, L.G. and G.G. Borisy, *Head-to-tail polymerization of microtubules in vitro. Electron microscope analysis of seeded assembly.* J Cell Biol, 1980. **84**(1): p. 141-50.

229. Shelanski, M.L. and E.W. Taylor, *Properties of the protein subunit of central-pair and outer-doublet microtubules of sea urchin flagella.* J Cell Biol, 1968. **38**(2): p. 304-15.

230. Mitchison, T. and M. Kirschner, *Dynamic instability of microtubule growth.* Nature, 1984. **312**(5991): p. 237-42.

231. Mandelkow, E.M., E. Mandelkow, and R.A. Milligan, *Microtubule dynamics and microtubule caps: a time-resolved cryo-electron microscopy study.* J Cell Biol, 1991. **114**(5): p. 977-91.

232. Hyman, A.A., et al., *Structural changes accompanying GTP hydrolysis in microtubules: information from a slowly hydrolyzable analogue guanylyl-(alpha,beta)-methylene-diphosphonate.* J Cell Biol, 1995. **128**(1-2): p. 117-25.

233. Muller-Reichert, T., et al., *Structural changes at microtubule ends accompanying GTP hydrolysis: information from a slowly hydrolyzable analogue of GTP, guanylyl (alpha,beta)methylenediphosphonate.* Proc Natl Acad Sci U S A, 1998. **95**(7): p. 3661-6.

234. Wang, H.W. and E. Nogales, *Nucleotide-dependent bending flexibility of tubulin regulates microtubule assembly.* Nature, 2005. **435**(7044): p. 911-5.

235. Nogales, E., S.G. Wolf, and K.H. Downing, *Structure of the alpha beta tubulin dimer by electron crystallography.* Nature, 1998. **391**(6663): p. 199-203.

236. Weisenberg, R.C., G.G. Borisy, and E.W. Taylor, *The colchicine-binding protein of mammalian brain and its relation to microtubules.* Biochemistry, 1968. **7**(12): p. 4466-79.

237. Caplow, M., R.L. Ruhlen, and J. Shanks, *The free energy for hydrolysis of a microtubule-bound nucleotide triphosphate is near zero: all of the free energy for hydrolysis is stored in the microtubule lattice.* J Cell Biol, 1994. **127**(3): p. 779-88.

238. Hill, T.L., *Bioenergetic aspects and polymer length distribution in steady-state head-to-tail polymerization of actin or microtubules.* Proc Natl Acad Sci U S A, 1980. **77**(8): p. 4803-7.

239. Hill, T.L., *Microfilament or microtubule assembly or disassembly against a force.* Proc Natl Acad Sci U S A, 1981. **78**(9): p. 5613-7.

240. Coue, M., V.A. Lombillo, and J.R. McIntosh, *Microtubule depolymerization promotes particle and chromosome movement in vitro.* J Cell Biol, 1991. **112**(6): p. 1165-75.

241. Bajer, A.S., et al., *Taxol-induced anaphase reversal: evidence that elongating microtubules can exert a pushing force in living cells.* Proc Natl Acad Sci U S A, 1982. **79**(21): p. 6569-73.

242. Grishchuk, E.L., et al., *Force production by disassembling microtubules.* Nature, 2005. **438**(7066): p. 384-8.

243. Drechsel, D.N. and M.W. Kirschner, *The minimum GTP cap required to stabilize microtubules.* Curr Biol, 1994. **4**(12): p. 1053-61.

244. Caplow, M. and J. Shanks, *Evidence that a single monolayer tubulin-GTP cap is both necessary and sufficient to stabilize microtubules.* Mol Biol Cell, 1996. **7**(4): p. 663-75.

245. Dimitrov, A., et al., *Detection of GTP-tubulin conformation in vivo reveals a role for GTP remnants in microtubule rescues.* Science, 2008. **322**(5906): p. 1353-6.

246. Chretien, D., et al., *Microtubule's conformational cap.* Cell Struct Funct, 1999. **24**(5): p. 299-303.

247. Arnal, I., et al., *CLIP-170/tubulin-curved oligomers coassemble at microtubule ends and promote rescues.* Curr Biol, 2004. **14**(23): p. 2086-95.

248. Gardner, M.K., et al., *Depolymerizing kinesins Kip3 and MCAK shape cellular microtubule architecture by differential control of catastrophe.* Cell. **147**(5): p. 1092-103.

249. Belmont, L.D., et al., *Real-time visualization of cell cycle-dependent changes in microtubule dynamics in cytoplasmic extracts.* Cell, 1990. **62**(3): p. 579-89.

250. Verde, F., et al., *Control of microtubule dynamics and length by cyclin A- and cyclin B-dependent kinases in Xenopus egg extracts.* J Cell Biol, 1992. **118**(5): p. 1097-108.

251. Sammak, P.J. and G.G. Borisy, *Direct observation of microtubule dynamics in living cells.* Nature, 1988. **332**(6166): p. 724-6.

252. Schulze, E. and M. Kirschner, *New features of microtubule behaviour observed in vivo.* Nature, 1988. **334**(6180): p. 356-9.

253. Komarova, Y.A., I.A. Vorobjev, and G.G. Borisy, *Life cycle of MTs: persistent growth in the cell interior, asymmetric transition frequencies and effects of the cell boundary.* J Cell Sci, 2002. **115**(Pt 17): p. 3527-39.

254. Kinoshita, K., et al., *Reconstitution of physiological microtubule dynamics using purified components.* Science, 2001. **294**(5545): p. 1340-3.

255. Kusch, J., et al., *Microtubule capture by the cleavage apparatus is required for proper spindle positioning in yeast.* Genes Dev, 2002. **16**(13): p. 1627-39.

256. Kollman, J.M., et al., *Microtubule nucleation by gamma-tubulin complexes.* Nat Rev Mol Cell Biol, 2011. **12**(11): p. 709-21.

257. Joshi, H.C., et al., *Gamma-tubulin is a centrosomal protein required for cell cycle-dependent microtubule nucleation.* Nature, 1992. **356**(6364): p. 80-3.

258. Wiese, C. and Y. Zheng, *A new function for the gamma-tubulin ring complex as a microtubule minus-end cap.* Nat Cell Biol, 2000. **2**(6): p. 358-64.

259. Keating, T.J. and G.G. Borisy, *Immunostructural evidence for the template mechanism of microtubule nucleation.* Nat Cell Biol, 2000. **2**(6): p. 352-7.

260. Moritz, M., et al., *Structure of the gamma-tubulin ring complex: a template for microtubule nucleation.* Nat Cell Biol, 2000. **2**(6): p. 365-70.

261. Kollman, J.M., et al., *Microtubule nucleating gamma-TuSC assembles structures with 13-fold microtubule-like symmetry.* Nature, 2011. **466**(7308): p. 879-82.

262. Akhmanova, A. and C.C. Hoogenraad, *Microtubule plus-end-tracking proteins: mechanisms and functions.* Curr Opin Cell Biol, 2005. **17**(1): p. 47-54.

263. Lansbergen, G. and A. Akhmanova, *Microtubule plus end: a hub of cellular activities.* Traffic, 2006. **7**(5): p. 499-507.

264. Akhmanova, A. and M.O. Steinmetz, *Tracking the ends: a dynamic protein network controls the fate of microtubule tips.* Nat Rev Mol Cell Biol, 2008. **9**(4): p. 309-22.

265. Su, L.K., et al., *APC binds to the novel protein EB1.* Cancer Res, 1995. **55**(14): p. 2972-7.

266. Mimori-Kiyosue, Y., N. Shiina, and S. Tsukita, *The dynamic behavior of the APC-binding protein EB1 on the distal ends of microtubules.* Curr Biol, 2000. **10**(14): p. 865-8.

267. Dixit, R., et al., *Microtubule plus-end tracking by CLIP-170 requires EB1.* Proc Natl Acad Sci U S A, 2009. **106**(2): p. 492-7.

268. Vitre, B., et al., *EB1 regulates microtubule dynamics and tubulin sheet closure in vitro.* Nat Cell Biol, 2008. **10**(4): p. 415-21.

269. Tirnauer, J.S., et al., *Yeast Bim1p promotes the G1-specific dynamics of microtubules.* J Cell Biol, 1999. **145**(5): p. 993-1007.

270. Rogers, S.L., et al., *Drosophila EB1 is important for proper assembly, dynamics, and positioning of the mitotic spindle.* J Cell Biol, 2002. **158**(5): p. 873-84.

271. Komarova, Y., et al., *EB1 and EB3 control CLIP dissociation from the ends of growing microtubules.* Mol Biol Cell, 2005. **16**(11): p. 5334-45.

272. Peris, L., et al., *Tubulin tyrosination is a major factor affecting the recruitment of CAP-Gly proteins at microtubule plus ends.* J Cell Biol, 2006. **174**(6): p. 839-49.

273. Rickard, J.E. and T.E. Kreis, *Identification of a novel nucleotide-sensitive microtubule-binding protein in HeLa cells.* J Cell Biol, 1990. **110**(5): p. 1623-33.

274. Perez, F., et al., *CLIP-170 highlights growing microtubule ends in vivo.* Cell, 1999. **96**(4): p. 517-27.

275. Ligon, L.A., et al., *Microtubule binding proteins CLIP-170, EB1, and p150Glued form distinct plus-end complexes.* FEBS Lett, 2006. **580**(5): p. 1327-32.

276. Lee, H.S., et al., *Phosphorylation controls autoinhibition of cytoplasmic linker protein-170.* Mol Biol Cell, 2010. **21**(15): p. 2661-73.

277. Vaughan, K.T., et al., *Colocalization of cytoplasmic dynein with dynactin and CLIP-170 at microtubule distal ends.* J Cell Sci, 1999. **112 (Pt 10)**: p. 1437-47.

278. Ligon, L.A., et al., *The microtubule plus-end proteins EB1 and dynactin have differential effects on microtubule polymerization.* Mol Biol Cell, 2003. **14**(4): p. 1405-17.

279. Lansbergen, G., et al., *Conformational changes in CLIP-170 regulate its binding to microtubules and dynactin localization.* J Cell Biol, 2004. **166**(7): p. 1003-14.

280. Hoogenraad, C.C., et al., *Targeted mutation of Cyln2 in the Williams syndrome critical region links CLIP-115 haploinsufficiency to neurodevelopmental abnormalities in mice.* Nat Genet, 2002. **32**(1): p. 116-27.

281. Inoue, Y.H., et al., *Orbit, a novel microtubule-associated protein essential for mitosis in Drosophila melanogaster.* J Cell Biol, 2000. **149**(1): p. 153-66.

282. Lemos, C.L., et al., *Mast, a conserved microtubule-associated protein required for bipolar mitotic spindle organization.* EMBO J, 2000. **19**(14): p. 3668-82.

283. Akhmanova, A., et al., *Clasps are CLIP-115 and -170 associating proteins involved in the regional regulation of microtubule dynamics in motile fibroblasts.* Cell, 2001. **104**(6): p. 923-35.

284. Al-Bassam, J. and F. Chang, *Regulation of microtubule dynamics by TOG-domain proteins XMAP215/Dis1 and CLASP.* Trends Cell Biol. **21**(10): p. 604-14.

285. Wolyniak, M.J., et al., *The regulation of microtubule dynamics in Saccharomyces cerevisiae by three interacting plus-end tracking proteins.* Mol Biol Cell, 2006. **17**(6): p. 2789-98.

286. Al-Bassam, J., et al., *Stu2p binds tubulin and undergoes an open-to-closed conformational change.* J Cell Biol, 2006. **172**(7): p. 1009-22.

287. Kosco, K.A., et al., *Control of microtubule dynamics by Stu2p is essential for spindle orientation and metaphase chromosome alignment in yeast.* Mol Biol Cell, 2001. **12**(9): p. 2870-80.

288. Vasquez, R.J., D.L. Gard, and L. Cassimeris, *XMAP from Xenopus eggs promotes rapid plus end assembly of microtubules and rapid microtubule polymer turnover.* J Cell Biol, 1994. **127**(4): p. 985-93.

289. van Breugel, M., D. Drechsel, and A. Hyman, *Stu2p, the budding yeast member of the conserved Dis1/XMAP215 family of microtubule-associated proteins is a plus end-binding microtubule destabilizer.* J Cell Biol, 2003. **161**(2): p. 359-69.

290. Cheeseman, I.M., et al., *The CENP-F-like proteins HCP-1 and HCP-2 target CLASP to kinetochores to mediate chromosome segregation.* Curr Biol, 2005. **15**(8): p. 771-7.

291. Maiato, H., A. Khodjakov, and C.L. Rieder, *Drosophila CLASP is required for the incorporation of microtubule subunits into fluxing kinetochore fibres.* Nat Cell Biol, 2005. **7**(1): p. 42-7.

292. Gigant, B., et al., *The 4 A X-ray structure of a tubulin:stathmin-like domain complex.* Cell, 2000. **102**(6): p. 809-16.

293. Steinmetz, M.O., et al., *Op18/stathmin caps a kinked protofilament-like tubulin tetramer.* EMBO J, 2000. **19**(4): p. 572-80.

294. Howell, B., et al., *Dissociation of the tubulin-sequestering and microtubule catastrophe-promoting activities of oncoprotein 18/stathmin.* Mol Biol Cell, 1999. **10**(1): p. 105-18.

295. Curmi, P.A., et al., *The stathmin/tubulin interaction in vitro.* J Biol Chem, 1997. **272**(40): p. 25029-36.

296. Walczak, C.E., T.J. Mitchison, and A. Desai, *XKCM1: a Xenopus kinesin-related protein that regulates microtubule dynamics during mitotic spindle assembly.* Cell, 1996. **84**(1): p. 37-47.

297. Wordeman, L. and T.J. Mitchison, *Identification and partial characterization of mitotic centromere-associated kinesin, a kinesin-related protein that associates with centromeres during mitosis.* J Cell Biol, 1995. **128**(1-2): p. 95-104.

298. Desai, A., et al., *Kin I kinesins are microtubule-destabilizing enzymes.* Cell, 1999. **96**(1): p. 69-78.

299. Kline-Smith, S.L. and C.E. Walczak, *The microtubule-destabilizing kinesin XKCM1 regulates microtubule dynamic instability in cells.* Mol Biol Cell, 2002. **13**(8): p. 2718-31.

300. Varga, V., et al., *Yeast kinesin-8 depolymerizes microtubules in a length-dependent manner.* Nat Cell Biol, 2006. **8**(9): p. 957-62.

301. Varga, V., et al., *Kinesin-8 motors act cooperatively to mediate length-dependent microtubule depolymerization.* Cell, 2009. **138**(6): p. 1174-83.

302. Mayr, M.I., et al., *A non-motor microtubule binding site is essential for the high processivity and mitotic function of kinesin-8 Kif18A.* PLoS One. **6**(11): p. e27471.

303. Yang, C.H., E.J. Lambie, and M. Snyder, *NuMA: an unusually long coiled-coil related protein in the mammalian nucleus.* J Cell Biol, 1992. **116**(6): p. 1303-17.

304. Merdes, A., et al., *A complex of NuMA and cytoplasmic dynein is essential for mitotic spindle assembly.* Cell, 1996. **87**(3): p. 447-58.

305. Merdes, A., et al., *Formation of spindle poles by dynein/dynactin-dependent transport of NuMA.* J Cell Biol, 2000. **149**(4): p. 851-62.

306. Raemaekers, T., et al., *NuSAP, a novel microtubule-associated protein involved in mitotic spindle organization.* J Cell Biol, 2003. **162**(6): p. 1017-29.

307. Ribbeck, K., et al., *NuSAP, a mitotic RanGTP target that stabilizes and cross-links microtubules.* Mol Biol Cell, 2006. **17**(6): p. 2646-60.

308. Ribbeck, K., et al., *A role for NuSAP in linking microtubules to mitotic chromosomes.* Curr Biol, 2007. **17**(3): p. 230-6.

309. Wittmann, T., et al., *TPX2, A novel xenopus MAP involved in spindle pole organization.* J Cell Biol, 2000. **149**(7): p. 1405-18.

310. Gruss, O.J., et al., *Chromosome-induced microtubule assembly mediated by TPX2 is required for spindle formation in HeLa cells.* Nat Cell Biol, 2002. **4**(11): p. 871-9.

311. Koffa, M.D., et al., *HURP is part of a Ran-dependent complex involved in spindle formation.* Curr Biol, 2006. **16**(8): p. 743-54.

312. Sillje, H.H., et al., *HURP is a Ran-importin beta-regulated protein that stabilizes kinetochore microtubules in the vicinity of chromosomes.* Curr Biol, 2006. **16**(8): p. 731-42.

313. Deka, J., J. Kuhlmann, and O. Muller, *A domain within the tumor suppressor protein APC shows very similar biochemical properties as the microtubule-associated protein tau.* Eur J Biochem, 1998. **253**(3): p. 591-7.

314. Santarella, R.A., et al., *HURP wraps microtubule ends with an additional tubulin sheet that has a novel conformation of tubulin.* J Mol Biol, 2007. **365**(5): p. 1587-95.

315. Kashina, A.S., et al., *A bipolar kinesin.* Nature, 1996. **379**(6562): p. 270-2.

316. Weinger, J.S., et al., *A nonmotor microtubule binding site in kinesin-5 is required for filament crosslinking and sliding.* Curr Biol. **21**(2): p. 154-60.

317. Sharp, D.J., et al., *The bipolar kinesin, KLP61F, cross-links microtubules within interpolar microtubule bundles of Drosophila embryonic mitotic spindles.* J Cell Biol, 1999. **144**(1): p. 125-38.

318. Mountain, V., et al., *The kinesin-related protein, HSET, opposes the activity of Eg5 and cross-links microtubules in the mammalian mitotic spindle.* J Cell Biol, 1999. **147**(2): p. 351-66.

319. Chandra, R., S.A. Endow, and E.D. Salmon, *An N-terminal truncation of the ncd motor protein supports diffusional movement of microtubules in motility assays.* J Cell Sci, 1993. **104 (Pt 3)**: p. 899-906.

320. Chandra, R., et al., *Structural and functional domains of the Drosophila ncd microtubule motor protein.* J Biol Chem, 1993. **268**(12): p. 9005-13.

321. McDonald, H.B., R.J. Stewart, and L.S. Goldstein, *The kinesin-like ncd protein of Drosophila is a minus end-directed microtubule motor.* Cell, 1990. **63**(6): p. 1159-65.

322. Endow, S.A., et al., *Yeast Kar3 is a minus-end microtubule motor protein that destabilizes microtubules preferentially at the minus ends.* EMBO J, 1994. **13**(11): p. 2708-13.

323. Matuliene, J., et al., *Function of a minus-end-directed kinesin-like motor protein in mammalian cells.* J Cell Sci, 1999. **112 (Pt 22)**: p. 4041-50.

324. Kuriyama, R., et al., *Characterization of a minus end-directed kinesin-like motor protein from cultured mammalian cells.* J Cell Biol, 1995. **129**(4): p. 1049-59.

325. Boleti, H., E. Karsenti, and I. Vernos, *Xklp2, a novel Xenopus centrosomal kinesin-like protein required for centrosome separation during mitosis.* Cell, 1996. **84**(1): p. 49-59.

326. Wittmann, T., et al., *Localization of the kinesin-like protein Xklp2 to spindle poles requires a leucine zipper, a microtubule-associated protein, and dynein.* J Cell Biol, 1998. **143**(3): p. 673-85.

327. Vaughan, K.T. and R.B. Vallee, *Cytoplasmic dynein binds dynactin through a direct interaction between the intermediate chains and p150Glued.* J Cell Biol, 1995. **131**(6 Pt 1): p. 1507-16.

328. King, S.J. and T.A. Schroer, *Dynactin increases the processivity of the cytoplasmic dynein motor.* Nat Cell Biol, 2000. **2**(1): p. 20-4.

329. McKenney, R.J., et al., *LIS1 and NudE induce a persistent dynein force-producing state.* Cell, 2010. **141**(2): p. 304-14.

330. Smith, D.S., et al., *Regulation of cytoplasmic dynein behaviour and microtubule organization by mammalian Lis1.* Nat Cell Biol, 2000. **2**(11): p. 767-75.

331. Faulkner, N.E., et al., *A role for the lissencephaly gene LIS1 in mitosis and cytoplasmic dynein function.* Nat Cell Biol, 2000. **2**(11): p. 784-91.

332. Holzbaur, E.L., et al., *Homology of a 150K cytoplasmic dynein-associated polypeptide with the Drosophila gene Glued.* Nature, 1991. **351**(6327): p. 579-83.

333. Waterman-Storer, C.M., S. Karki, and E.L. Holzbaur, *The p150Glued component of the dynactin complex binds to both microtubules and the actin-related protein centractin (Arp-1).* Proc Natl Acad Sci U S A, 1995. **92**(5): p. 1634-8.

334. Borisy, G.G., *Polarity of microtubules of the mitotic spindle.* J Mol Biol, 1978. **124**(3): p. 565-70.

335. Heidemann, S.R. and J.R. McIntosh, *Visualization of the structural polarity of microtubules.* Nature, 1980. **286**(5772): p. 517-9.

336. Euteneuer, U. and J.R. McIntosh, *Structural polarity of kinetochore microtubules in PtK1 cells.* J Cell Biol, 1981. **89**(2): p. 338-45.

337. Wilson, E.B., *The Cell in Development and Heredity.* 1925.

338. Winey, M., et al., *Three-dimensional ultrastructural analysis of the Saccharomyces cerevisiae mitotic spindle.* J Cell Biol, 1995. **129**(6): p. 1601-15.

339. McDonald, K.L., et al., *Kinetochore microtubules in PTK cells.* J Cell Biol, 1992. **118**(2): p. 369-83.

340. Mastronarde, D.N., et al., *Interpolar spindle microtubules in PTK cells.* J Cell Biol, 1993. **123**(6 Pt 1): p. 1475-89.

341. Sawin, K.E. and T.J. Mitchison, *Mitotic spindle assembly by two different pathways in vitro.* J Cell Biol, 1991. **112**(5): p. 925-40.

342. McGill, M. and B.R. Brinkley, *Human chromosomes and centrioles as nucleating sites for the in vitro assembly of microtubules from bovine brain tubulin.* J Cell Biol, 1975. **67**(1): p. 189-99.

343. Heald, R., et al., *Spindle assembly in Xenopus egg extracts: respective roles of centrosomes and microtubule self-organization.* J Cell Biol, 1997. **138**(3): p. 615-28.

344. Knop, M. and E. Schiebel, *Receptors determine the cellular localization of a gamma-tubulin complex and thereby the site of microtubule formation.* EMBO J, 1998. **17**(14): p. 3952-67.

345. Gardner, M.K., et al., *The microtubule-based motor Kar3 and plus end-binding protein Bim1 provide structural support for the anaphase spindle.* J Cell Biol, 2008. **180**(1): p. 91-100.

346. Chee, M.K. and S.B. Haase, *B-cyclin/CDKs regulate mitotic spindle assembly by phosphorylating kinesins-5 in budding yeast.* PLoS Genet, 2010. **6**(5): p. e1000935.

347. Saunders, W.S., et al., *Saccharomyces cerevisiae kinesin- and dynein-related proteins required for anaphase chromosome segregation.* J Cell Biol, 1995. **128**(4): p. 617-24.

348. Saunders, W., V. Lengyel, and M.A. Hoyt, *Mitotic spindle function in Saccharomyces cerevisiae requires a balance between different types of kinesin-related motors.* Mol Biol Cell, 1997. **8**(6): p. 1025-33.

349. Saunders, W., et al., *The Saccharomyces cerevisiae kinesin-related motor Kar3p acts at preanaphase spindle poles to limit the number and length of cytoplasmic microtubules.* J Cell Biol, 1997. **137**(2): p. 417-31.

350. Cheeseman, I.M., et al., *Mitotic spindle integrity and kinetochore function linked by the Duo1p/Dam1p complex.* J Cell Biol, 2001. **152**(1): p. 197-212.

351. Rosenblatt, J., *Spindle assembly: asters part their separate ways.* Nat Cell Biol, 2005. **7**(3): p. 219-22.

352. Schnackenberg, B.J., et al., *The disassembly and reassembly of functional centrosomes in vitro.* Proc Natl Acad Sci U S A, 1998. **95**(16): p. 9295-300.

353. Moritz, M., et al., *Microtubule nucleation by gamma-tubulin-containing rings in the centrosome.* Nature, 1995. **378**(6557): p. 638-40.

354. Blangy, A., et al., *Phosphorylation by p34cdc2 regulates spindle association of human Eg5, a kinesin-related motor essential for bipolar spindle formation in vivo.* Cell, 1995. **83**(7): p. 1159-69.

355. Sawin, K.E. and T.J. Mitchison, *Mutations in the kinesin-like protein Eg5 disrupting localization to the mitotic spindle.* Proc Natl Acad Sci U S A, 1995. **92**(10): p. 4289-93.

356. Kapoor, T.M., et al., *Probing spindle assembly mechanisms with monastrol, a small molecule inhibitor of the mitotic kinesin, Eg5.* J Cell Biol, 2000. **150**(5): p. 975-88.

357. Kapoor, T.M. and T.J. Mitchison, *Eg5 is static in bipolar spindles relative to tubulin: evidence for a static spindle matrix.* J Cell Biol, 2001. **154**(6): p. 1125-33.

358. Kapitein, L.C., et al., *The bipolar mitotic kinesin Eg5 moves on both microtubules that it crosslinks.* Nature, 2005. **435**(7038): p. 114-8.

359. Oladipo, A., A. Cowan, and V. Rodionov, *Microtubule motor Ncd induces sliding of microtubules in vivo.* Mol Biol Cell, 2007. **18**(9): p. 3601-6.

360. Sharp, D.J., et al., *Functional coordination of three mitotic motors in Drosophila embryos.* Mol Biol Cell, 2000. **11**(1): p. 241-53.

361. Tanenbaum, M.E., et al., *Dynein, Lis1 and CLIP-170 counteract Eg5-dependent centrosome separation during bipolar spindle assembly.* EMBO J, 2008. **27**(24): p. 3235-45.

362. Sawin, K.E., et al., *Mitotic spindle organization by a plus-end-directed microtubule motor.* Nature, 1992. **359**(6395): p. 540-3.

363. Sharp, D.J., et al., *Antagonistic microtubule-sliding motors position mitotic centrosomes in Drosophila early embryos.* Nat Cell Biol, 1999. **1**(1): p. 51-4.

364. Walczak, C.E., S. Verma, and T.J. Mitchison, *XCTK2: a kinesin-related protein that promotes mitotic spindle assembly in Xenopus laevis egg extracts.* J Cell Biol, 1997. **136**(4): p. 859-70.

365. Tao, L., et al., *A homotetrameric kinesin-5, KLP61F, bundles microtubules and antagonizes Ncd in motility assays.* Curr Biol, 2006. **16**(23): p. 2293-302.

366. Goshima, G. and R.D. Vale, *Cell cycle-dependent dynamics and regulation of mitotic kinesins in Drosophila S2 cells.* Mol Biol Cell, 2005. **16**(8): p. 3896-907.

367. Ferenz, N.P., et al., *Dynein antagonizes eg5 by crosslinking and sliding antiparallel microtubules.* Curr Biol, 2009. **19**(21): p. 1833-8.

368. Tanenbaum, M.E., et al., *Kif15 cooperates with eg5 to promote bipolar spindle assembly.* Curr Biol, 2009. **19**(20): p. 1703-11.

369. Toso, A., et al., *Kinetochore-generated pushing forces separate centrosomes during bipolar spindle assembly.* J Cell Biol, 2009. **184**(3): p. 365-72.

370. Rieder, C.L. and E.D. Salmon, *Motile kinetochores and polar ejection forces dictate chromosome position on the vertebrate mitotic spindle.* J Cell Biol, 1994. **124**(3): p. 223-33.

371. Levesque, A.A. and D.A. Compton, *The chromokinesin Kid is necessary for chromosome arm orientation and oscillation, but not congression, on mitotic spindles.* J Cell Biol, 2001. **154**(6): p. 1135-46.

372. Funabiki, H. and A.W. Murray, *The Xenopus chromokinesin Xkid is essential for metaphase chromosome alignment and must be degraded to allow anaphase chromosome movement.* Cell, 2000. **102**(4): p. 411-24.

373. Antonio, C., et al., *Xkid, a chromokinesin required for chromosome alignment on the metaphase plate.* Cell, 2000. **102**(4): p. 425-35.

374. Bullitt, E., et al., *The yeast spindle pole body is assembled around a central crystal of Spc42p.* Cell, 1997. **89**(7): p. 1077-86.

375. Logarinho, E., et al., *CLASPs prevent irreversible multipolarity by ensuring spindle-pole resistance to traction forces during chromosome alignment.* Nat Cell Biol. **14**(3): p. 295-303.

376. Manning, A.L. and D.A. Compton, *Mechanisms of spindle-pole organization are influenced by kinetochore activity in mammalian cells.* Curr Biol, 2007. **17**(3): p. 260-5.

377. O'Connell, C.B., et al., *Relative contributions of chromatin and kinetochores to mitotic spindle assembly.* J Cell Biol, 2009. **187**(1): p. 43-51.

378. Holy, T.E. and S. Leibler, *Dynamic instability of microtubules as an efficient way to search in space.* Proc Natl Acad Sci U S A, 1994. **91**(12): p. 5682-5.

379. Rieder, C.L. and S.P. Alexander, *Kinetochores are transported poleward along a single astral microtubule during chromosome attachment to the spindle in newt lung cells.* J Cell Biol, 1990. **110**(1): p. 81-95.

380. Tanaka, K., et al., *Molecular mechanisms of kinetochore capture by spindle microtubules.* Nature, 2005. **434**(7036): p. 987-94.

381. Gandhi, S.R., et al., *Kinetochore-dependent microtubule rescue ensures their efficient and sustained interactions in early mitosis.* Dev Cell, 2011. **21**(5): p. 920-33.

382. Tanaka, K., et al., *Molecular mechanisms of microtubule-dependent kinetochore transport toward spindle poles.* J Cell Biol, 2007. **178**(2): p. 269-81.

383. Yang, Z., et al., *Kinetochore dynein is required for chromosome motion and congression independent of the spindle checkpoint.* Curr Biol, 2007. **17**(11): p. 973-80.

384. Savoian, M.S., M.L. Goldberg, and C.L. Rieder, *The rate of poleward chromosome motion is attenuated in Drosophila zw10 and rod mutants.* Nat Cell Biol, 2000. **2**(12): p. 948-52.

385. Kapoor, T.M., et al., *Chromosomes can congress to the metaphase plate before biorientation.* Science, 2006. **311**(5759): p. 388-91.

386. Kim, Y., et al., *Aurora kinases and protein phosphatase 1 mediate chromosome congression through regulation of CENP-E.* Cell, 2010. **142**(3): p. 444-55.

387. Kitamura, E., et al., *Kinetochores generate microtubules with distal plus ends: their roles and limited lifetime in mitosis.* Dev Cell, 2010. **18**(2): p. 248-59.

388. Khodjakov, A., et al., *Centrosome-independent mitotic spindle formation in vertebrates.* Curr Biol, 2000. **10**(2): p. 59-67.

389. Heald, R., et al., *Self-organization of microtubules into bipolar spindles around artificial chromosomes in Xenopus egg extracts.* Nature, 1996. **382**(6590): p. 420-5.

390. Wilde, A. and Y. Zheng, *Stimulation of microtubule aster formation and spindle assembly by the small GTPase Ran.* Science, 1999. **284**(5418): p. 1359-62.

391. Kalab, P., R.T. Pu, and M. Dasso, *The ran GTPase regulates mitotic spindle assembly.* Curr Biol, 1999. **9**(9): p. 481-4.

392. Wilde, A., et al., *Ran stimulates spindle assembly by altering microtubule dynamics and the balance of motor activities.* Nat Cell Biol, 2001. **3**(3): p. 221-7.

393. Carazo-Salas, R.E., et al., *Generation of GTP-bound Ran by RCC1 is required for chromatin-induced mitotic spindle formation.* Nature, 1999. **400**(6740): p. 178-81.

394. Tanenbaum, M.E. and R.H. Medema, *Localized Aurora B activity spatially controls non-kinetochore microtubules during spindle assembly.* Chromosoma. **120**(6): p. 599-607.

395. Maresca, T.J., et al., *Spindle assembly in the absence of a RanGTP gradient requires localized CPC activity.* Curr Biol, 2009. **19**(14): p. 1210-5.

396. Niethammer, P., P. Bastiaens, and E. Karsenti, *Stathmin-tubulin interaction gradients in motile and mitotic cells.* Science, 2004. **303**(5665): p. 1862-6.

397. Kalab, P., et al., *Analysis of a RanGTP-regulated gradient in mitotic somatic cells.* Nature, 2006. **440**(7084): p. 697-701.

398. Trieselmann, N., et al., *Ran modulates spindle assembly by regulating a subset of TPX2 and Kid activities including Aurora A activation.* J Cell Sci, 2003. **116**(Pt 23): p. 4791-8.

399. Cai, S., et al., *Kinesin-14 family proteins HSET/XCTK2 control spindle length by cross-linking and sliding microtubules.* Mol Biol Cell, 2009. **20**(5): p. 1348-59.

400. Wiese, C., et al., *Role of importin-beta in coupling Ran to downstream targets in microtubule assembly.* Science, 2001. **291**(5504): p. 653-6.

401. Nachury, M.V., et al., *Importin beta is a mitotic target of the small GTPase Ran in spindle assembly.* Cell, 2001. **104**(1): p. 95-106.

402. Ems-McClung, S.C., Y. Zheng, and C.E. Walczak, *Importin alpha/beta and Ran-GTP regulate XCTK2 microtubule binding through a bipartite nuclear localization signal.* Mol Biol Cell, 2004. **15**(1): p. 46-57.

403. Torosantucci, L., et al., *Localized RanGTP accumulation promotes microtubule nucleation at kinetochores in somatic mammalian cells.* Mol Biol Cell, 2008. **19**(5): p. 1873-82.

404. Mishra, R.K., et al., *The Nup107-160 complex and gamma-TuRC regulate microtubule polymerization at kinetochores.* Nat Cell Biol. **12**(2): p. 164-9.

405. Goshima, G., et al., *Augmin: a protein complex required for centrosome-independent microtubule generation within the spindle.* J Cell Biol, 2008. **181**(3): p. 421-9.

406. Brinkley, B.R. and J. Cartwright, Jr., *Cold-labile and cold-stable microtubules in the mitotic spindle of mammalian cells.* Ann N Y Acad Sci, 1975. **253**: p. 428-39.

407. Rieder, C.L., *The structure of the cold-stable kinetochore fiber in metaphase PtK1 cells.* Chromosoma, 1981. **84**(1): p. 145-158.

408. Witt, P.L., H. Ris, and G.G. Borisy, *Structure of kinetochore fibers: Microtubule continuity and inter-microtubule bridges.* Chromosoma, 1981. **83**(4): p. 523-540.

409. Fodde, R., et al., *Mutations in the APC tumour suppressor gene cause chromosomal instability.* Nat Cell Biol, 2001. **3**(4): p. 433-8.

410. Banks, J.D. and R. Heald, *Adenomatous polyposis coli associates with the microtubule-destabilizing protein XMCAK.* Curr Biol, 2004. **14**(22): p. 2033-8.

411. Hentrich, C. and T. Surrey, *Microtubule organization by the antagonistic mitotic motors kinesin-5 and kinesin-14.* J Cell Biol. **189**(3): p. 465-80.

412. Matthies, H.J., et al., *Anastral meiotic spindle morphogenesis: role of the non-claret disjunctional kinesin-like protein.* J Cell Biol, 1996. **134**(2): p. 455-64.

413. Walczak, C.E., et al., *A model for the proposed roles of different microtubule-based motor proteins in establishing spindle bipolarity.* Curr Biol, 1998. **8**(16): p. 903-13.

414. Verde, F., et al., *Taxol-induced microtubule asters in mitotic extracts of Xenopus eggs: requirement for phosphorylated factors and cytoplasmic dynein.* J Cell Biol, 1991. **112**(6): p. 1177-87.

415. Gaglio, T., A. Saredi, and D.A. Compton, *NuMA is required for the organization of microtubules into aster-like mitotic arrays.* J Cell Biol, 1995. **131**(3): p. 693-708.

416. Gaglio, T., et al., *Opposing motor activities are required for the organization of the mammalian mitotic spindle pole.* J Cell Biol, 1996. **135**(2): p. 399-414.

417. Yang, C.H. and M. Snyder, *The nuclear-mitotic apparatus protein is important in the establishment and maintenance of the bipolar mitotic spindle apparatus.* Mol Biol Cell, 1992. **3**(11): p. 1259-67.

418. Ma, N., et al., *Poleward transport of TPX2 in the mammalian mitotic spindle requires dynein, Eg5, and microtubule flux.* Mol Biol Cell. **21**(6): p. 979-88.

419. Maiato, H., C.L. Rieder, and A. Khodjakov, *Kinetochore-driven formation of kinetochore fibers contributes to spindle assembly during animal mitosis.* J Cell Biol, 2004. **167**(5): p. 831-40.

420. Khodjakov, A., et al., *Minus-end capture of preformed kinetochore fibers contributes to spindle morphogenesis.* J Cell Biol, 2003. **160**(5): p. 671-83.

421. Dogterom, M., et al., *Influence of M-phase chromatin on the anisotropy of microtubule asters.* J Cell Biol, 1996. **133**(1): p. 125-40.

422. Carazo-Salas, R.E. and E. Karsenti, *Long-range communication between chromatin and microtubules in Xenopus egg extracts.* Curr Biol, 2003. **13**(19): p. 1728-33.

423. Sardon, T., et al., *Dissecting the role of Aurora A during spindle assembly.* EMBO J, 2008. **27**(19): p. 2567-79.

424. Maddox, P.S., K.S. Bloom, and E.D. Salmon, *The polarity and dynamics of microtubule assembly in the budding yeast Saccharomyces cerevisiae.* Nat Cell Biol, 2000. **2**(1): p. 36-41.

425. Waters, J.C., et al., *The kinetochore microtubule minus-end disassembly associated with poleward flux produces a force that can do work.* Mol Biol Cell, 1996. **7**(10): p. 1547-58.

426. Mitchison, T.J. and E.D. Salmon, *Poleward kinetochore fiber movement occurs during both metaphase and anaphase-A in newt lung cell mitosis.* J Cell Biol, 1992. **119**(3): p. 569-82.

427. Manning, A.L., et al., *The kinesin-13 proteins Kif2a, Kif2b, and Kif2c/MCAK have distinct roles during mitosis in human cells.* Mol Biol Cell, 2007. **18**(8): p. 2970-9.

428. Ganem, N.J. and D.A. Compton, *The KinI kinesin Kif2a is required for bipolar spindle assembly through a functional relationship with MCAK.* J Cell Biol, 2004. **166**(4): p. 473-8.

429. Yang, G., et al., *Regional variation of microtubule flux reveals microtubule organization in the metaphase meiotic spindle.* J Cell Biol, 2008. **182**(4): p. 631-9.

430. Gaetz, J. and T.M. Kapoor, *Dynein/dynactin regulate metaphase spindle length by targeting depolymerizing activities to spindle poles.* J Cell Biol, 2004. **166**(4): p. 465-71.

431. Miyamoto, D.T., et al., *The kinesin Eg5 drives poleward microtubule flux in Xenopus laevis egg extract spindles.* J Cell Biol, 2004. **167**(5): p. 813-8.

432. Ferenz, N.P. and P. Wadsworth, *Prophase microtubule arrays undergo flux-like behavior in mammalian cells.* Mol Biol Cell, 2007. **18**(10): p. 3993-4002.

433. Burbank, K.S., et al., *A new method reveals microtubule minus ends throughout the meiotic spindle.* J Cell Biol, 2006. **175**(3): p. 369-75.

434. Mitchison, T.J., *Mechanism and function of poleward flux in Xenopus extract meiotic spindles.* Philos Trans R Soc Lond B Biol Sci, 2005. **360**(1455): p. 623-9.

435. Dumont, S. and T.J. Mitchison, *Compression regulates mitotic spindle length by a mechanochemical switch at the poles.* Curr Biol, 2009. **19**(13): p. 1086-95.

436. Maddox, P., et al., *Direct observation of microtubule dynamics at kinetochores in Xenopus extract spindles: implications for spindle mechanics.* J Cell Biol, 2003. **162**(3): p. 377-82.

437. Chen, W. and D. Zhang, *Kinetochore fibre dynamics outside the context of the spindle during anaphase.* Nat Cell Biol, 2004. **6**(3): p. 227-31.

438. LaFountain, J.R., Jr., et al., *Direct visualization of microtubule flux during metaphase and anaphase in crane-fly spermatocytes.* Mol Biol Cell, 2004. **15**(12): p. 5724-32.

439. Ganem, N.J., K. Upton, and D.A. Compton, *Efficient mitosis in human cells lacking poleward microtubule flux.* Curr Biol, 2005. **15**(20): p. 1827-32.

440. Grishchuk, E.L., et al., *The Dam1 ring binds microtubules strongly enough to be a processive as well as energy-efficient coupler for chromosome motion.* Proc Natl Acad Sci U S A, 2008. **105**(40): p. 15423-8.

441. Hill, T.L., *Theoretical problems related to the attachment of microtubules to kinetochores.* Proc Natl Acad Sci U S A, 1985. **82**(13): p. 4404-8.

442. Efremov, A., et al., *In search of an optimal ring to couple microtubule depolymerization to processive chromosome motions.* Proc Natl Acad Sci U S A, 2007. **104**(48): p. 19017-22.

443. Gardner, M.K., et al., *Tension-dependent regulation of microtubule dynamics at kinetochores can explain metaphase congression in yeast.* Mol Biol Cell, 2005. **16**(8): p. 3764-75.

444. Gardner, M.K., et al., *Chromosome congression by Kinesin-5 motor-mediated disassembly of longer kinetochore microtubules.* Cell, 2008. **135**(5): p. 894-906.

445. Wargacki, M.M., et al., *Kip3, the yeast kinesin-8, is required for clustering of kinetochores at metaphase.* Cell Cycle. **9**(13): p. 2581-8.

446. Tytell, J.D. and P.K. Sorger, *Analysis of kinesin motor function at budding yeast kinetochores.* J Cell Biol, 2006. **172**(6): p. 861-74.

447. Maddox, P., et al., *Poleward microtubule flux is a major component of spindle dynamics and anaphase a in mitotic Drosophila embryos.* Curr Biol, 2002. **12**(19): p. 1670-4.

448. Skibbens, R.V., V.P. Skeen, and E.D. Salmon, *Directional instability of kinetochore motility during chromosome congression and segregation in mitotic newt lung cells: a push-pull mechanism.* J Cell Biol, 1993. **122**(4): p. 859-75.

449. Waters, J.C., R.V. Skibbens, and E.D. Salmon, *Oscillating mitotic newt lung cell kinetochores are, on average, under tension and rarely push.* J Cell Sci, 1996. **109 (Pt 12)**: p. 2823-31.

450. Wan, X., et al., *The coupling between sister kinetochore directional instability and oscillations in centromere stretch in metaphase PtK1 cells.* Mol Biol Cell. **23**(6): p. 1035-46.

451. Amaro, A.C., et al., *Molecular control of kinetochore-microtubule dynamics and chromosome oscillations.* Nat Cell Biol, 2011. **12**(4): p. 319-29.

452. Huang, H., et al., *Tripin/hSgo2 recruits MCAK to the inner centromere to correct defective kinetochore attachments.* J Cell Biol, 2007. **177**(3): p. 413-24.

453. Jaqaman, K., et al., *Kinetochore alignment within the metaphase plate is regulated by centromere stiffness and microtubule depolymerases.* J Cell Biol. **188**(5): p. 665-79.

454. Stumpff, J., et al., *The kinesin-8 motor Kif18A suppresses kinetochore movements to control mitotic chromosome alignment.* Dev Cell, 2008. **14**(2): p. 252-62.

455. Du, Y., C.A. English, and R. Ohi, *The kinesin-8 Kif18A dampens microtubule plus-end dynamics.* Curr Biol. **20**(4): p. 374-80.

456. Kline-Smith, S.L., et al., *Depletion of centromeric MCAK leads to chromosome congression and segregation defects due to improper kinetochore attachments.* Mol Biol Cell, 2004. **15**(3): p. 1146-59.

457. Wordeman, L., M. Wagenbach, and G. von Dassow, *MCAK facilitates chromosome movement by promoting kinetochore microtubule turnover.* J Cell Biol, 2007. **179**(5): p. 869-79.

458. Manning, A.L., et al., *CLASP1, astrin and Kif2b form a molecular switch that regulates kinetochore-microtubule dynamics to promote mitotic progression and fidelity.* EMBO J. **29**(20): p. 3531-43.

459. Bakhoum, S.F., et al., *Genome stability is ensured by temporal control of kinetochore-microtubule dynamics.* Nat Cell Biol, 2009. **11**(1): p. 27-35.

460. Schmidt, J.C., et al., *Aurora B kinase controls the targeting of the Astrin-SKAP complex to bioriented kinetochores.* J Cell Biol. **191**(2): p. 269-80.

461. Andrews, P.D., et al., *Aurora B regulates MCAK at the mitotic centromere.* Dev Cell, 2004. **6**(2): p. 253-68.

462. Rivera, T., et al., *Xenopus Shugoshin 2 regulates the spindle assembly pathway mediated by the chromosomal passenger complex.* EMBO J. **31**(6): p. 1467-79.

463. De Wulf, P., A.D. McAinsh, and P.K. Sorger, *Hierarchical assembly of the budding yeast kinetochore from multiple subcomplexes.* Genes Dev, 2003. **17**(23): p. 2902-21.

464. McAinsh, A.D., J.D. Tytell, and P.K. Sorger, *Structure, function, and regulation of budding yeast kinetochores.* Annu Rev Cell Dev Biol, 2003. **19**: p. 519-39.

465. Westermann, S., D.G. Drubin, and G. Barnes, *Structures and functions of yeast kinetochore complexes.* Annu Rev Biochem, 2007. **76**: p. 563-91.

466. Santaguida, S. and A. Musacchio, *The life and miracles of kinetochores.* EMBO J, 2009. **28**(17): p. 2511-31.

467. Zinkowski, R.P., J. Meyne, and B.R. Brinkley, *The centromere-kinetochore complex: a repeat subunit model.* J Cell Biol, 1991. **113**(5): p. 1091-110.

468. Joglekar, A.P., et al., *Molecular architecture of the kinetochore-microtubule attachment site is conserved between point and regional centromeres.* J Cell Biol, 2008. **181**(4): p. 587-94.

469. Joglekar, A.P., K. Bloom, and E.D. Salmon, *In vivo protein architecture of the eukaryotic kinetochore with nanometer scale accuracy.* Curr Biol, 2009. **19**(8): p. 694-9.

470. Wan, X., et al., *Protein architecture of the human kinetochore microtubule attachment site.* Cell, 2009. **137**(4): p. 672-84.

471. Joglekar, A.P., et al., *Molecular architecture of a kinetochore-microtubule attachment site.* Nat Cell Biol, 2006. **8**(6): p. 581-5.

472. Rieder, C.L., *The formation, structure, and composition of the mammalian kinetochore and kinetochore fiber.* Int Rev Cytol, 1982. **79**: p. 1-58.

473. McEwen, B.F., et al., *A new look at kinetochore structure in vertebrate somatic cells using high-pressure freezing and freeze substitution.* Chromosoma, 1998. **107**(6-7): p. 366-75.

474. Dong, Y., et al., *The outer plate in vertebrate kinetochores is a flexible network with multiple microtubule interactions.* Nat Cell Biol, 2007. **9**(5): p. 516-22.

475. Lampert, F. and S. Westermann, *A blueprint for kinetochores - new insights into the molecular mechanics of cell division.* Nat Rev Mol Cell Biol, 2011. **12**(7): p. 407-12.

476. Cheng, L., et al., *Aurora B regulates formin mDia3 in achieving metaphase chromosome alignment.* Dev Cell. **20**(3): p. 342-52.

477. Yasuda, S., et al., *Cdc42 and mDia3 regulate microtubule attachment to kinetochores.* Nature, 2004. **428**(6984): p. 767-71.

478. Cheeseman, I.M., et al., *The conserved KMN network constitutes the core microtubule-binding site of the kinetochore.* Cell, 2006. **127**(5): p. 983-97.

479. Wigge, P.A. and J.V. Kilmartin, *The Ndc80p complex from Saccharomyces cerevisiae contains conserved centromere components and has a function in chromosome segregation.* J Cell Biol, 2001. **152**(2): p. 349-60.

480. Janke, C., et al., *The budding yeast proteins Spc24p and Spc25p interact with Ndc80p and Nuf2p at the kinetochore and are important for kinetochore clustering and checkpoint control.* EMBO J, 2001. **20**(4): p. 777-91.

481. Wei, R.R., P.K. Sorger, and S.C. Harrison, *Molecular organization of the Ndc80 complex, an essential kinetochore component.* Proc Natl Acad Sci U S A, 2005. **102**(15): p. 5363-7.

482. Wei, R.R., et al., *Structure of a central component of the yeast kinetochore: the Spc24p/Spc25p globular domain.* Structure, 2006. **14**(6): p. 1003-9.

483. Wei, R.R., J. Al-Bassam, and S.C. Harrison, *The Ndc80/HEC1 complex is a contact point for kinetochore-microtubule attachment.* Nat Struct Mol Biol, 2007. **14**(1): p. 54-9.

484. Ciferri, C., et al., *Architecture of the human ndc80-hec1 complex, a critical constituent of the outer kinetochore.* J Biol Chem, 2005. **280**(32): p. 29088-95.

485. Zhang, G., et al., *The Ndc80 internal loop is required for recruitment of the Ska complex to establish end-on microtubule attachment to kinetochores.* J Cell Sci.

486. Wilson-Kubalek, E.M., et al., *Orientation and structure of the Ndc80 complex on the microtubule lattice.* J Cell Biol, 2008. **182**(6): p. 1055-61.

487. DeLuca, J.G., et al., *Kinetochore microtubule dynamics and attachment stability are regulated by Hec1.* Cell, 2006. **127**(5): p. 969-82.

488. Hornung, P., et al., *Molecular architecture and connectivity of the budding yeast Mtw1 kinetochore complex.* J Mol Biol, 2011. **405**(2): p. 548-59.

489. Tooley, J.G., S.A. Miller, and P.T. Stukenberg, *The Ndc80 complex uses a tripartite attachment point to couple microtubule depolymerization to chromosome movement.* Mol Biol Cell. **22**(8): p. 1217-26.

490. Miller, S.A., M.L. Johnson, and P.T. Stukenberg, *Kinetochore attachments require an interaction between unstructured tails on microtubules and Ndc80(Hec1).* Curr Biol, 2008. **18**(22): p. 1785-91.

491. Alushin, G.M., et al., *The Ndc80 kinetochore complex forms oligomeric arrays along microtubules.* Nature, 2010. **467**(7317): p. 805-10.

492. Powers, A.F., et al., *The Ndc80 kinetochore complex forms load-bearing attachments to dynamic microtubule tips via biased diffusion.* Cell, 2009. **136**(5): p. 865-75.

493. Pagliuca, C., et al., *Roles for the conserved spc105p/kre28p complex in kinetochore-microtubule binding and the spindle assembly checkpoint.* PLoS One, 2009. **4**(10): p. e7640.

494. Schittenhelm, R.B., R. Chaleckis, and C.F. Lehner, *Intrakinetochore localization and essential functional domains of Drosophila Spc105.* EMBO J, 2009. **28**(16): p. 2374-86.

495. Desai, A., et al., *KNL-1 directs assembly of the microtubule-binding interface of the kinetochore in C. elegans.* Genes Dev, 2003. **17**(19): p. 2421-35.

496. Kiyomitsu, T., C. Obuse, and M. Yanagida, *Human Blinkin/AF15q14 is required for chromosome alignment and the mitotic checkpoint through direct interaction with Bub1 and BubR1.* Dev Cell, 2007. **13**(5): p. 663-76.

497. Maskell, D.P., X.W. Hu, and M.R. Singleton, *Molecular architecture and assembly of the yeast kinetochore MIND complex.* J Cell Biol. **190**(5): p. 823-34.

498. Akiyoshi, B., et al., *Tension directly stabilizes reconstituted kinetochore-microtubule attachments.* Nature, 2010. **468**(7323): p. 576-9.

499. Emanuele, M.J., et al., *Measuring the stoichiometry and physical interactions between components elucidates the architecture of the vertebrate kinetochore.* Mol Biol Cell, 2005. **16**(10): p. 4882-92.

500. DeLuca, J.G., et al., *Hec1 and nuf2 are core components of the kinetochore outer plate essential for organizing microtubule attachment sites.* Mol Biol Cell, 2005. **16**(2): p. 519-31.

501. Suzuki, A., et al., *Spindle microtubules generate tension-dependent changes in the distribution of inner kinetochore proteins.* J Cell Biol, 2011. **193**(1): p. 125-40.

502. Williams, B.C. and M.L. Goldberg, *Determinants of Drosophila zw10 protein localization and function.* J Cell Sci, 1994. **107 (Pt 4)**: p. 785-98.

503. Chan, G.K., et al., *Human Zw10 and ROD are mitotic checkpoint proteins that bind to kinetochores.* Nat Cell Biol, 2000. **2**(12): p. 944-7.

504. Starr, D.A., et al., *HZwint-1, a novel human kinetochore component that interacts with HZW10.* J Cell Sci, 2000. **113 (Pt 11)**: p. 1939-50.

505. Karess, R.E. and D.M. Glover, *rough deal: a gene required for proper mitotic segregation in Drosophila.* J Cell Biol, 1989. **109**(6 Pt 1): p. 2951-61.

506. Kops, G.J., et al., *ZW10 links mitotic checkpoint signaling to the structural kinetochore.* J Cell Biol, 2005. **169**(1): p. 49-60.

507. Starr, D.A., et al., *ZW10 helps recruit dynactin and dynein to the kinetochore.* J Cell Biol, 1998. **142**(3): p. 763-74.

508. Chan, Y.W., et al., *Mitotic control of kinetochore-associated dynein and spindle orientation by human Spindly.* J Cell Biol, 2009. **185**(5): p. 859-74.

509. Griffis, E.R., N. Stuurman, and R.D. Vale, *Spindly, a novel protein essential for silencing the spindle assembly checkpoint, recruits dynein to the kinetochore.* J Cell Biol, 2007. **177**(6): p. 1005-15.

510. Vos, L.J., J.K. Famulski, and G.K. Chan, *hZwint-1 bridges the inner and outer kinetochore: identification of the kinetochore localization domain and the hZw10-interaction domain.* Biochem J. **436**(1): p. 157-68.

511. Lin, Y.T., et al., *Hec1 sequentially recruits Zwint-1 and ZW10 to kinetochores for faithful chromosome segregation and spindle checkpoint control.* Oncogene, 2006. **25**(52): p. 6901-14.

512. Obuse, C., et al., *A conserved Mis12 centromere complex is linked to heterochromatic HP1 and outer kinetochore protein Zwint-1.* Nat Cell Biol, 2004. **6**(11): p. 1135-41.

513. Kiyomitsu, T., et al., *Inner centromere formation requires hMis14, a trident kinetochore protein that specifically recruits HP1 to human chromosomes.* J Cell Biol. **188**(6): p. 791-807.

514. Whyte, J., et al., *Phosphorylation regulates targeting of cytoplasmic dynein to kinetochores during mitosis.* J Cell Biol, 2008. **183**(5): p. 819-34.

515. Gassmann, R., et al., *A new mechanism controlling kinetochore-microtubule interactions revealed by comparison of two dynein-targeting components: SPDL-1 and the Rod/Zwilch/Zw10 complex.* Genes Dev, 2008. **22**(17): p. 2385-99.

516. Howell, B.J., et al., *Cytoplasmic dynein/dynactin drives kinetochore protein transport to the spindle poles and has a role in mitotic spindle checkpoint inactivation.* J Cell Biol, 2001. **155**(7): p. 1159-72.

517. Scaerou, F., et al., *The ZW10 and Rough Deal checkpoint proteins function together in a large, evolutionarily conserved complex targeted to the kinetochore*. J Cell Sci, 2001. **114**(Pt 17): p. 3103-14.

518. Williams, B.C., M. Gatti, and M.L. Goldberg, *Bipolar spindle attachments affect redistributions of ZW10, a Drosophila centromere/kinetochore component required for accurate chromosome segregation.* J Cell Biol, 1996. **134**(5): p. 1127-40.

519. Famulski, J.K. and G.K. Chan, *Aurora B kinase-dependent recruitment of hZW10 and hROD to tensionless kinetochores.* Curr Biol, 2007. **17**(24): p. 2143-9.

520. Bader, J.R., et al., *Polo-like kinase1 is required for recruitment of dynein to kinetochores during mitosis.* J Biol Chem. **286**(23): p. 20769-77.

521. Liu, S.T., et al., *Human CENP-I specifies localization of CENP-F, MAD1 and MAD2 to kinetochores and is essential for mitosis.* Nat Cell Biol, 2003. **5**(4): p. 341-5.

522. Klebig, C., D. Korinth, and P. Meraldi, *Bub1 regulates chromosome segregation in a kinetochore-independent manner.* J Cell Biol, 2009. **185**(5): p. 841-58.

523. Martin-Lluesma, S., V.M. Stucke, and E.A. Nigg, *Role of Hec1 in spindle checkpoint signaling and kinetochore recruitment of Mad1/Mad2.* Science, 2002. **297**(5590): p. 2267-70.

524. Cheeseman, I.M., et al., *KNL1 and the CENP-H/I/K complex coordinately direct kinetochore assembly in vertebrates.* Mol Biol Cell, 2008. **19**(2): p. 587-94.

525. Vergnolle, M.A. and S.S. Taylor, *Cenp-F links kinetochores to Ndel1/Nde1/Lis1/dynein microtubule motor complexes.* Curr Biol, 2007. **17**(13): p. 1173-9.

526. Feng, J., H. Huang, and T.J. Yen, *CENP-F is a novel microtubule-binding protein that is essential for kinetochore attachments and affects the duration of the mitotic checkpoint delay.* Chromosoma, 2006. **115**(4): p. 320-9.

527. Yang, Z.Y., et al., *Mitosin/CENP-F is a conserved kinetochore protein subjected to cytoplasmic dynein-mediated poleward transport.* Cell Res, 2003. **13**(4): p. 275-83.

528. Zhang, X.D., et al., *SUMO-2/3 modification and binding regulate the association of CENP-E with kinetochores and progression through mitosis.* Mol Cell, 2008. **29**(6): p. 729-41.

529. Zhu, M., et al., *Septin 7 interacts with centromere-associated protein E and is required for its kinetochore localization.* J Biol Chem, 2008. **283**(27): p. 18916-25.

530. Sharp-Baker, H. and R.H. Chen, *Spindle checkpoint protein Bub1 is required for kinetochore localization of Mad1, Mad2, Bub3, and CENP-E, independently of its kinase activity.* J Cell Biol, 2001. **153**(6): p. 1239-50.

531. Johnson, V.L., et al., *Bub1 is required for kinetochore localization of BubR1, Cenp-E, Cenp-F and Mad2, and chromosome congression.* J Cell Sci, 2004. **117**(Pt 8): p. 1577-89.

532. Meraldi, P., et al., *Phylogenetic and structural analysis of centromeric DNA and kinetochore proteins.* Genome Biol, 2006. **7**(3): p. R23.

533. Jin, F., et al., *Loss of function of the cik1/kar3 motor complex results in chromosomes with syntelic attachment that are sensed by the tension checkpoint.* PLoS Genet, 2012. **8**(2): p. e1002492.

534. Welburn, J.P., et al., *The human kinetochore Ska1 complex facilitates microtubule depolymerization-coupled motility.* Dev Cell, 2009. **16**(3): p. 374-85.

535. Gaitanos, T.N., et al., *Stable kinetochore-microtubule interactions depend on the Ska complex and its new component Ska3/C13Orf3.* EMBO J, 2009. **28**(10): p. 1442-52.

536. Daum, J.R., et al., *Ska3 is required for spindle checkpoint silencing and the maintenance of chromosome cohesion in mitosis.* Curr Biol, 2009. **19**(17): p. 1467-72.

537. Theis, M., et al., *Comparative profiling identifies C13orf3 as a component of the Ska complex required for mammalian cell division.* EMBO J, 2009. **28**(10): p. 1453-65.

538. Hanisch, A., H.H. Sillje, and E.A. Nigg, *Timely anaphase onset requires a novel spindle and kinetochore complex comprising Ska1 and Ska2.* EMBO J, 2006. **25**(23): p. 5504-15.

539. Enquist-Newman, M., et al., *Dad1p, third component of the Duo1p/Dam1p complex involved in kinetochore function and mitotic spindle integrity.* Mol Biol Cell, 2001. **12**(9): p. 2601-13.

540. Hofmann, C., et al., *Saccharomyces cerevisiae Duo1p and Dam1p, novel proteins involved in mitotic spindle function.* J Cell Biol, 1998. **143**(4): p. 1029-40.

541. Janke, C., et al., *Four new subunits of the Dam1-Duo1 complex reveal novel functions in sister kinetochore biorientation.* EMBO J, 2002. **21**(1-2): p. 181-93.

542. Cheeseman, I.M., et al., *Implication of a novel multiprotein Dam1p complex in outer kinetochore function.* J Cell Biol, 2001. **155**(7): p. 1137-45.

543. Li, Y., et al., *The mitotic spindle is required for loading of the DASH complex onto the kinetochore.* Genes Dev, 2002. **16**(2): p. 183-97.

544. Li, J.M., Y. Li, and S.J. Elledge, *Genetic analysis of the kinetochore DASH complex reveals an antagonistic relationship with the ras/protein kinase A pathway and a novel subunit required for Ask1 association.* Mol Cell Biol, 2005. **25**(2): p. 767-78.

545. Maure, J.F., et al., *The Ndc80 loop region facilitates formation of kinetochore attachment to the dynamic microtubule plus end.* Curr Biol, 2011. **21**(3): p. 207-13.

546. Westermann, S., et al., *The Dam1 kinetochore ring complex moves processively on depolymerizing microtubule ends.* Nature, 2006. **440**(7083): p. 565-9.

547. Asbury, C.L., et al., *The Dam1 kinetochore complex harnesses microtubule dynamics to produce force and movement.* Proc Natl Acad Sci U S A, 2006. **103**(26): p. 9873-8.

548. Miranda, J.J., et al., *The yeast DASH complex forms closed rings on microtubules.* Nat Struct Mol Biol, 2005. **12**(2): p. 138-43.

549. Westermann, S., et al., *Formation of a dynamic kinetochore- microtubule interface through assembly of the Dam1 ring complex.* Mol Cell, 2005. **17**(2): p. 277-90.

550. Ramey, V.H., et al., *The Dam1 ring binds to the E-hook of tubulin and diffuses along the microtubule.* Mol Biol Cell, 2010. **22**(4): p. 457-66.

551. Molodtsov, M.I., et al., *Force production by depolymerizing microtubules: a theoretical study.* Proc Natl Acad Sci U S A, 2005. **102**(12): p. 4353-8.

552. Tien, J.F., et al., *Cooperation of the Dam1 and Ndc80 kinetochore complexes enhances microtubule coupling and is regulated by aurora B.* J Cell Biol, 2010. **189**(4): p. 713-23.

553. Lampert, F., P. Hornung, and S. Westermann, *The Dam1 complex confers microtubule plus end-tracking activity to the Ndc80 kinetochore complex.* J Cell Biol, 2010. **189**(4): p. 641-9.

554. Nishihashi, A., et al., *CENP-I is essential for centromere function in vertebrate cells.* Dev Cell, 2002. **2**(4): p. 463-76.

555. Foltz, D.R., et al., *The human CENP-A centromeric nucleosome-associated complex.* Nat Cell Biol, 2006. **8**(5): p. 458-69.

556. Okada, M., et al., *The CENP-H-I complex is required for the efficient incorporation of newly synthesized CENP-A into centromeres.* Nat Cell Biol, 2006. **8**(5): p. 446-57.

557. Sugata, N., E. Munekata, and K. Todokoro, *Characterization of a novel kinetochore protein, CENP-H.* J Biol Chem, 1999. **274**(39): p. 27343-6.

558. Minoshima, Y., et al., *The constitutive centromere component CENP-50 is required for recovery from spindle damage.* Mol Cell Biol, 2005. **25**(23): p. 10315-28.

559. Saitoh, H., et al., *CENP-C, an autoantigen in scleroderma, is a component of the human inner kinetochore plate.* Cell, 1992. **70**(1): p. 115-25.

560. Maine, G.T., P. Sinha, and B.K. Tye, *Mutants of S. cerevisiae defective in the maintenance of minichromosomes.* Genetics, 1984. **106**(3): p. 365-85.

561. Roy, N., et al., *The mcm17 mutation of yeast shows a size-dependent segregational defect of a mini-chromosome.* Curr Genet, 1997. **32**(3): p. 182-9.

562. Sanyal, K., S.K. Ghosh, and P. Sinha, *The MCM16 gene of the yeast Saccharomyces cerevisiae is required for chromosome segregation.* Mol Gen Genet, 1998. **260**(2-3): p. 242-50.

563. Poddar, A., N. Roy, and P. Sinha, *MCM21 and MCM22, two novel genes of the yeast Saccharomyces cerevisiae are required for chromosome transmission.* Mol Microbiol, 1999. **31**(1): p. 349-60.

564. Ghosh, S.K., et al., *The IML3/MCM19 gene of Saccharomyces cerevisiae is required for a kinetochore-related process during chromosome segregation.* Mol Genet Genomics, 2001. **265**(2): p. 249-57.

565. Spencer, F., et al., *Mitotic chromosome transmission fidelity mutants in Saccharomyces cerevisiae.* Genetics, 1990. **124**(2): p. 237-49.

566. Measday, V., et al., *Ctf3p, the Mis6 budding yeast homolog, interacts with Mcm22p and Mcm16p at the yeast outer kinetochore.* Genes Dev, 2002. **16**(1): p. 101-13.

567. Pot, I., et al., *Chl4p and iml3p are two new members of the budding yeast outer kinetochore.* Mol Biol Cell, 2003. **14**(2): p. 460-76.

568. Ortiz, J., et al., *A putative protein complex consisting of Ctf19, Mcm21, and Okp1 represents a missing link in the budding yeast kinetochore.* Genes Dev, 1999. **13**(9): p. 1140-55.

569. Cheeseman, I.M., et al., *Phospho-regulation of kinetochore-microtubule attachments by the Aurora kinase Ipl1p.* Cell, 2002. **111**(2): p. 163-72.

570. McClelland, S.E., et al., *The CENP-A NAC/CAD kinetochore complex controls chromosome congression and spindle bipolarity.* EMBO J, 2007. **26**(24): p. 5033-47.

571. Liu, X., et al., *Molecular analysis of kinetochore architecture in fission yeast.* EMBO J, 2005. **24**(16): p. 2919-30.

572. Heeger, S., et al., *Genetic interactions of separase regulatory subunits reveal the diverged Drosophila Cenp-C homolog.* Genes Dev, 2005. **19**(17): p. 2041-53.

573. Kwon, M.S., et al., *CENP-C is involved in chromosome segregation, mitotic checkpoint function, and kinetochore assembly.* Mol Biol Cell, 2007. **18**(6): p. 2155-68.

574. Oegema, K., et al., *Functional analysis of kinetochore assembly in Caenorhabditis elegans.* J Cell Biol, 2001. **153**(6): p. 1209-26.

575. Howman, E.V., et al., *Early disruption of centromeric chromatin organization in centromere protein A (Cenpa) null mice.* Proc Natl Acad Sci U S A, 2000. **97**(3): p. 1148-53.

576. Hori, T., et al., *CCAN makes multiple contacts with centromeric DNA to provide distinct pathways to the outer kinetochore.* Cell, 2008. **135**(6): p. 1039-52.

577. Gascoigne, K.E., et al., *Induced ectopic kinetochore assembly bypasses the requirement for CENP-A nucleosomes.* Cell, 2011. **145**(3): p. 410-22.

578. Fukagawa, T., et al., *CENP-H, a constitutive centromere component, is required for centromere targeting of CENP-C in vertebrate cells.* EMBO J, 2001. **20**(16): p. 4603-17.

579. Milks, K.J., B. Moree, and A.F. Straight, *Dissection of CENP-C-directed centromere and kinetochore assembly.* Mol Biol Cell, 2009. **20**(19): p. 4246-55.

580. Tanaka, K., et al., *CENP-C functions as a scaffold for effectors with essential kinetochore functions in mitosis and meiosis.* Dev Cell, 2009. **17**(3): p. 334-43.

581. Amano, M., et al., *The CENP-S complex is essential for the stable assembly of outer kinetochore structure.* J Cell Biol, 2009. **186**(2): p. 173-82.

582. Hori, T., et al., *CENP-O class proteins form a stable complex and are required for proper kinetochore function.* Mol Biol Cell, 2008. **19**(3): p. 843-54.

583. Sugimoto, K., et al., *Human centromere protein C (CENP-C) is a DNA-binding protein which possesses a novel DNA-binding motif.* J Biochem, 1994. **116**(4): p. 877-81.

584. Sugimoto, K., et al., *Characterization of internal DNA-binding and C-terminal dimerization domains of human centromere/kinetochore autoantigen CENP-C in vitro: role of DNA-binding and self-associating activities in kinetochore organization.* Chromosome Res, 1997. **5**(2): p. 132-41.

585. Brown, M.T., *Sequence similarities between the yeast chromosome segregation protein Mif2 and the mammalian centromere protein CENP-C.* Gene, 1995. **160**(1): p. 111-6.

586. Ross-Macdonald, P., et al., *A multipurpose transposon system for analyzing protein production, localization, and function in Saccharomyces cerevisiae.* Proc Natl Acad Sci U S A, 1997. **94**(1): p. 190-5.

587. Carroll, C.W., et al., *Centromere assembly requires the direct recognition of CENP-A nucleosomes by CENP-N.* Nat Cell Biol, 2009. **11**(7): p. 896-902.

588. Carroll, C.W., K.J. Milks, and A.F. Straight, *Dual recognition of CENP-A nucleosomes is required for centromere assembly.* J Cell Biol, 2010. **189**(7): p. 1143-55.

589. Rodriguez-Navarro, S., F. Estruch, and J.E. Perez-Ortin, *Functional analysis of 12 ORFs from Saccharomyces cerevisiae chromosome II.* Yeast, 1999. **15**(10B): p. 913-9.

590. Fernius, J. and A.L. Marston, *Establishment of cohesion at the pericentromere by the Ctf19 kinetochore subcomplex and the replication fork-associated factor, Csm3.* PLoS Genet, 2009. **5**(9): p. e1000629.

591. Pot, I., et al., *Spindle checkpoint maintenance requires Ame1 and Okp1.* Cell Cycle, 2005. **4**(10): p. 1448-56.

592. Westermann, S., et al., *Architecture of the budding yeast kinetochore reveals a conserved molecular core.* J Cell Biol, 2003. **163**(2): p. 215-22.

593. Uetz, P., et al., *A comprehensive analysis of protein-protein interactions in Saccharomyces cerevisiae.* Nature, 2000. **403**(6770): p. 623-7.

594. Nekrasov, V.S., et al., *Interactions between centromere complexes in Saccharomyces cerevisiae.* Mol Biol Cell, 2003. **14**(12): p. 4931-46.

595. Ranjitkar, P., et al., *An E3 ubiquitin ligase prevents ectopic localization of the centromeric histone H3 variant via the centromere targeting domain.* Mol Cell, 2010. **40**(3): p. 455-64.

596. Liu, S.T., et al., *Mapping the assembly pathways that specify formation of the trilaminar kinetochore plates in human cells.* J Cell Biol, 2006. **175**(1): p. 41-53.

597. Goshima, G., et al., *Human centromere chromatin protein hMis12, essential for equal segregation, is independent of CENP-A loading pathway.* J Cell Biol, 2003. **160**(1): p. 25-39.

598. Screpanti, E., et al., *Direct binding of Cenp-C to the Mis12 complex joins the inner and outer kinetochore.* Curr Biol, 2011. **21**(5): p. 391-8.

599. Przewloka, M.R., et al., *CENP-C is a structural platform for kinetochore assembly.* Curr Biol, 2011. **21**(5): p. 399-405.

600. Scharfenberger, M., et al., *Nsl1p is essential for the establishment of bipolarity and the localization of the Dam-Duo complex.* EMBO J, 2003. **22**(24): p. 6584-97.

601. Kemmler, S., et al., *Mimicking Ndc80 phosphorylation triggers spindle assembly checkpoint signalling.* EMBO J, 2009. **28**(8): p. 1099-110.

602. Gillett, E.S., C.W. Espelin, and P.K. Sorger, *Spindle checkpoint proteins and chromosome-microtubule attachment in budding yeast.* J Cell Biol, 2004. **164**(4): p. 535-46.

603. Saurin, A.T., et al., *Aurora B potentiates Mps1 activation to ensure rapid checkpoint establishment at the onset of mitosis.* Nat Commun, 2011. **2**: p. 316.

604. London, N., et al., *Phosphoregulation of Spc105 by Mps1 and PP1 regulates Bub1 localization to kinetochores.* Curr Biol. **22**(10): p. 900-6.

605. Shepperd, L.A., et al., *Phosphodependent recruitment of Bub1 and Bub3 to Spc7/KNL1 by Mph1 kinase maintains the spindle checkpoint.* Curr Biol. **22**(10): p. 891-9.

606. Maciejowski, J., et al., *Mps1 directs the assembly of Cdc20 inhibitory complexes during interphase and mitosis to control M phase timing and spindle checkpoint signaling.* J Cell Biol, 2010. **190**(1): p. 89-100.

607. Santaguida, S., et al., *Dissecting the role of MPS1 in chromosome biorientation and the spindle checkpoint through the small molecule inhibitor reversine.* J Cell Biol, 2010. **190**(1): p. 73-87.

608. Wong, O.K. and G. Fang, *Loading of the 3F3/2 antigen onto kinetochores is dependent on the ordered assembly of the spindle checkpoint proteins.* Mol Biol Cell, 2006. **17**(10): p. 4390-9.

609. Vigneron, S., et al., *Kinetochore localization of spindle checkpoint proteins: who controls whom?* Mol Biol Cell, 2004. **15**(10): p. 4584-96.

610. Jelluma, N., et al., *Mps1 phosphorylates Borealin to control Aurora B activity and chromosome alignment.* Cell, 2008. **132**(2): p. 233-46.

611. Jelluma, N., et al., *Release of Mps1 from kinetochores is crucial for timely anaphase onset.* J Cell Biol, 2010. **191**(2): p. 281-90.

612. Jablonski, S.A., et al., *The hBUB1 and hBUBR1 kinases sequentially assemble onto kinetochores during prophase with hBUBR1 concentrating at the kinetochore plates in mitosis.* Chromosoma, 1998. **107**(6-7): p. 386-96.

613. Ruchaud, S., M. Carmena, and W.C. Earnshaw, *Chromosomal passengers: conducting cell division.* Nat Rev Mol Cell Biol, 2007. **8**(10): p. 798-812.

614. Kelly, A.E., et al., *Survivin reads phosphorylated histone H3 threonine 3 to activate the mitotic kinase Aurora B.* Science, 2010. **330**(6001): p. 235-9.

615. Wang, F., et al., *Histone H3 Thr-3 phosphorylation by Haspin positions Aurora B at centromeres in mitosis.* Science, 2010. **330**(6001): p. 231-5.

616. Kawashima, S.A., et al., *Shugoshin enables tension-generating attachment of kinetochores by loading Aurora to centromeres.* Genes Dev, 2007. **21**(4): p. 420-35.

617. Tsukahara, T., Y. Tanno, and Y. Watanabe, *Phosphorylation of the CPC by Cdk1 promotes chromosome bi-orientation.* Nature, 2010. **467**(7316): p. 719-23.

618. Yamagishi, Y., et al., *Two histone marks establish the inner centromere and chromosome bi-orientation.* Science, 2010. **330**(6001): p. 239-43.

619. Jeyaprakash, A.A., et al., *Structural basis for the recognition of phosphorylated histone h3 by the survivin subunit of the chromosomal passenger complex.* Structure, 2011. **19**(11): p. 1625-34.

620. Wang, F., et al., *A positive feedback loop involving Haspin and Aurora B promotes CPC accumulation at centromeres in mitosis.* Curr Biol, 2011. **21**(12): p. 1061-9.

621. van der Waal, M.S., et al., *Mps1 promotes rapid centromere accumulation of Aurora B.* EMBO Rep.

622. Salimian, K.J., et al., *Feedback control in sensing chromosome biorientation by the Aurora B kinase.* Curr Biol. **21**(13): p. 1158-65.

623. Carmena, M., et al., *The chromosomal passenger complex activates polo kinase at centromeres.* PLoS Biol, 2012. **10**(1): p. e1001250.

624. Jeyaprakash, A.A., et al., *Structure of a Survivin-Borealin-INCENP core complex reveals how chromosomal passengers travel together.* Cell, 2007. **131**(2): p. 271-85.

625. DeLuca, K.F., S.M. Lens, and J.G. DeLuca, *Temporal changes in Hec1 phosphorylation control kinetochore-microtubule attachment stability during mitosis.* J Cell Sci. **124**(Pt 4): p. 622-34.

626. Sandall, S., et al., *A Bir1-Sli15 complex connects centromeres to microtubules and is required to sense kinetochore tension.* Cell, 2006. **127**(6): p. 1179-91.

627. Knockleby, J. and J. Vogel, *The COMA complex is required for Sli15/INCENP-mediated correction of defective kinetochore attachments.* Cell Cycle, 2009. **8**(16): p. 2570-7.

628. Park, J.E., R.L. Erikson, and K.S. Lee, *Feed-forward mechanism of converting biochemical cooperativity to mitotic processes at the kinetochore plate.* Proc Natl Acad Sci U S A. **108**(20): p. 8200-5.

629. Park, J.E., et al., *Polo-box domain: a versatile mediator of polo-like kinase function.* Cell Mol Life Sci. **67**(12): p. 1957-70.

630. Nishino, M., et al., *NudC is required for Plk1 targeting to the kinetochore and chromosome congression.* Curr Biol, 2006. **16**(14): p. 1414-21.

631. Zhou, T., et al., *A mammalian NudC-like protein essential for dynein stability and cell viability.* Proc Natl Acad Sci U S A, 2006. **103**(24): p. 9039-44.

632. Kang, Y.H., et al., *Self-regulated Plk1 recruitment to kinetochores by the Plk1-PBIP1 interaction is critical for proper chromosome segregation.* Mol Cell, 2006. **24**(3): p. 409-22.

633. Wong, O.K. and G. Fang, *Cdk1 phosphorylation of BubR1 controls spindle checkpoint arrest and Plk1-mediated formation of the 3F3/2 epitope.* J Cell Biol, 2007. **179**(4): p. 611-7.

634. Goto, H., et al., *Complex formation of Plk1 and INCENP required for metaphase-anaphase transition.* Nat Cell Biol, 2006. **8**(2): p. 180-7.

635. Qi, W., Z. Tang, and H. Yu, *Phosphorylation- and polo-box-dependent binding of Plk1 to Bub1 is required for the kinetochore localization of Plk1.* Mol Biol Cell, 2006. **17**(8): p. 3705-16.

636. Boyarchuk, Y., et al., *Bub1 is essential for assembly of the functional inner centromere.* J Cell Biol, 2007. **176**(7): p. 919-28.

637. Morrow, C.J., et al., *Bub1 and aurora B cooperate to maintain BubR1-mediated inhibition of APC/CCdc20.* J Cell Sci, 2005. **118**(Pt 16): p. 3639-52.

638. Ditchfield, C., et al., *Aurora B couples chromosome alignment with anaphase by targeting BubR1, Mad2, and Cenp-E to kinetochores.* J Cell Biol, 2003. **161**(2): p. 267-80.

639. Carvalho, A., et al., *Survivin is required for stable checkpoint activation in taxol-treated HeLa cells.* J Cell Sci, 2003. **116**(Pt 14): p. 2987-98.

640. Bentley, A.M., et al., *Distinct sequence elements of cyclin B1 promote localization to chromatin, centrosomes, and kinetochores during mitosis.* Mol Biol Cell, 2007. **18**(12): p. 4847-58.

641. Chen, Q., et al., *Cyclin B1 is localized to unattached kinetochores and contributes to efficient microtubule attachment and proper chromosome alignment during mitosis.* Cell Res, 2008. **18**(2): p. 268-80.

642. Liu, D., et al., *Sensing chromosome bi-orientation by spatial separation of aurora B kinase from kinetochore substrates.* Science, 2009. **323**(5919): p. 1350-3.

643. Welburn, J.P., et al., *Aurora B phosphorylates spatially distinct targets to differentially regulate the kinetochore-microtubule interface.* Mol Cell. **38**(3): p. 383-92.

644. Nicklas, R.B., S.C. Ward, and G.J. Gorbsky, *Kinetochore chemistry is sensitive to tension and may link mitotic forces to a cell cycle checkpoint.* J Cell Biol, 1995. **130**(4): p. 929-39.

645. Ahonen, L.J., et al., *Polo-like kinase 1 creates the tension-sensing 3F3/2 phosphoepitope and modulates the association of spindle-checkpoint proteins at kinetochores.* Curr Biol, 2005. **15**(12): p. 1078-89.

646. Wong, O.K. and G. Fang, *Plx1 is the 3F3/2 kinase responsible for targeting spindle checkpoint proteins to kinetochores.* J Cell Biol, 2005. **170**(5): p. 709-19.

647. Huang, H., et al., *Phosphorylation sites in BubR1 that regulate kinetochore attachment, tension, and mitotic exit.* J Cell Biol, 2008. **183**(4): p. 667-80.

648. Adams, R.R., et al., *INCENP binds the Aurora-related kinase AIRK2 and is required to target it to chromosomes, the central spindle and cleavage furrow.* Curr Biol, 2000. **10**(17): p. 1075-8.

649. Ainsztein, A.M., et al., *INCENP centromere and spindle targeting: identification of essential conserved motifs and involvement of heterochromatin protein HP1.* J Cell Biol, 1998. **143**(7): p. 1763-74.

650. Mackay, A.M., et al., *A dominant mutant of inner centromere protein (INCENP), a chromosomal protein, disrupts prometaphase congression and cytokinesis.* J Cell Biol, 1998. **140**(5): p. 991-1002.

651. Kaitna, S., et al., *Incenp and an aurora-like kinase form a complex essential for chromosome segregation and efficient completion of cytokinesis.* Curr Biol, 2000. **10**(19): p. 1172-81.

652. Kang, J., et al., *Functional cooperation of Dam1, Ipl1, and the inner centromere protein (INCENP)-related protein Sli15 during chromosome segregation.* J Cell Biol, 2001. **155**(5): p. 763-74.

653. Francisco, L., W. Wang, and C.S. Chan, *Type 1 protein phosphatase acts in opposition to IpL1 protein kinase in regulating yeast chromosome segregation.* Mol Cell Biol, 1994. **14**(7): p. 4731-40.

654. Tanaka, T.U., et al., *Evidence that the Ipl1-Sli15 (Aurora kinase-INCENP) complex promotes chromosome bi-orientation by altering kinetochore-spindle pole connections.* Cell, 2002. **108**(3): p. 317-29.

655. Hauf, S., et al., *The small molecule Hesperadin reveals a role for Aurora B in correcting kinetochore-microtubule attachment and in maintaining the spindle assembly checkpoint.* J Cell Biol, 2003. **161**(2): p. 281-94.

656. Biggins, S., et al., *The conserved protein kinase Ipl1 regulates microtubule binding to kinetochores in budding yeast.* Genes Dev, 1999. **13**(5): p. 532-44.

657. Cimini, D., et al., *Aurora kinase promotes turnover of kinetochore microtubules to reduce chromosome segregation errors.* Curr Biol, 2006. **16**(17): p. 1711-8.

658. Nicklas, R.B. and C.A. Koch, *Chromosome micromanipulation. 3. Spindle fiber tension and the reorientation of mal-oriented chromosomes.* J Cell Biol, 1969. **43**(1): p. 40-50.

659. Henderson, S.A. and C.A. Koch, *Co-orientation stability by physical tension: a demonstration with experimentally interlocked bivalents.* Chromosoma, 1970. **29**(2): p. 207-216.

660. Dewar, H., et al., *Tension between two kinetochores suffices for their bi-orientation on the mitotic spindle.* Nature, 2004. **428**(6978): p. 93-7.

661. Inamdar, N.B., *A note on the reorientation within the spindle of the sex trivalent in a mantid.* Biol Bull, 1949. **97**(3): p. 300-301.

662. Hughes-Schrader, S., *Polarization, kinetochore movements and bivalent structure in the meiosis of the male mantids.* Biol Bull, 1943. **85**(3): p. 265-300.

663. Pinsky, B.A., et al., *The Ipl1-Aurora protein kinase activates the spindle checkpoint by creating unattached kinetochores.* Nat Cell Biol, 2006. **8**(1): p. 78-83.

664. Gestaut, D.R., et al., *Phosphoregulation and depolymerization-driven movement of the Dam1 complex do not require ring formation.* Nat Cell Biol, 2008. **10**(4): p. 407-14.

665. Shang, C., et al., *Kinetochore protein interactions and their regulation by the Aurora kinase Ipl1p.* Mol Biol Cell, 2003. **14**(8): p. 3342-55.

666. Chan, Y.W., et al., *Aurora B controls kinetochore-microtubule attachments by inhibiting Ska complex-KMN network interaction.* J Cell Biol. **196**(5): p. 563-71.

667. Cimini, D., et al., *Merotelic kinetochore orientation is a major mechanism of aneuploidy in mitotic mammalian tissue cells.* J Cell Biol, 2001. **153**(3): p. 517-27.

668. Lampson, M.A., et al., *Correcting improper chromosome-spindle attachments during cell division.* Nat Cell Biol, 2004. **6**(3): p. 232-7.

669. Bakhoum, S.F., G. Genovese, and D.A. Compton, *Deviant kinetochore microtubule dynamics underlie chromosomal instability.* Curr Biol, 2009. **19**(22): p. 1937-42.

670. Zhai, Y., P.J. Kronebusch, and G.G. Borisy, *Kinetochore microtubule dynamics and the metaphase-anaphase transition.* J Cell Biol, 1995. **131**(3): p. 721-34.

671. Maney, T., et al., *Mitotic centromere-associated kinesin is important for anaphase chromosome segregation.* J Cell Biol, 1998. **142**(3): p. 787-801.

672. Knowlton, A.L., W. Lan, and P.T. Stukenberg, *Aurora B is enriched at merotelic attachment sites, where it regulates MCAK.* Curr Biol, 2006. **16**(17): p. 1705-10.

673. Lan, W., et al., *Aurora B phosphorylates centromeric MCAK and regulates its localization and microtubule depolymerization activity.* Curr Biol, 2004. **14**(4): p. 273-86.

674. Salic, A., J.C. Waters, and T.J. Mitchison, *Vertebrate shugoshin links sister centromere cohesion and kinetochore microtubule stability in mitosis.* Cell, 2004. **118**(5): p. 567-78.

675. McCleland, M.L., et al., *The highly conserved Ndc80 complex is required for kinetochore assembly, chromosome congression, and spindle checkpoint activity.* Genes Dev, 2003. **17**(1): p. 101-14.

676. Kline, S.L., et al., *The human Mis12 complex is required for kinetochore assembly and proper chromosome segregation.* J Cell Biol, 2006. **173**(1): p. 9-17.

677. Hua, S., et al., *CENP-U cooperates with Hec1 to orchestrate kinetochore-microtubule attachment.* J Biol Chem. **286**(2): p. 1627-38.

678. Sugata, N., et al., *Human CENP-H multimers colocalize with CENP-A and CENP-C at active centromere--kinetochore complexes.* Hum Mol Genet, 2000. **9**(19): p. 2919-26.

679. Mikami, Y., et al., *The functional region of CENP-H interacts with the Nuf2 complex that localizes to centromere during mitosis.* Mol Cell Biol, 2005. **25**(5): p. 1958-70.

680. Sardar, H.S., et al., *Mitotic kinesin CENP-E promotes microtubule plus-end elongation.* Curr Biol, 2010. **20**(18): p. 1648-53.

681. Franck, A.D., et al., *Tension applied through the Dam1 complex promotes microtubule elongation providing a direct mechanism for length control in mitosis.* Nat Cell Biol, 2007. **9**(7): p. 832-7.

682. Du, J., et al., *The mitotic checkpoint kinase NEK2A regulates kinetochore microtubule attachment stability.* Oncogene, 2008. **27**(29): p. 4107-14.

683. Lampson, M.A. and T.M. Kapoor, *The human mitotic checkpoint protein BubR1 regulates chromosome-spindle attachments.* Nat Cell Biol, 2005. **7**(1): p. 93-8.

684. Harris, L., et al., *The mitotic checkpoint gene BubR1 has two distinct functions in mitosis.* Exp Cell Res, 2005. **308**(1): p. 85-100.

685. Logarinho, E., et al., *The human spindle assembly checkpoint protein Bub3 is required for the establishment of efficient kinetochore-microtubule attachments.* Mol Biol Cell, 2008. **19**(4): p. 1798-813.

686. Meraldi, P. and P.K. Sorger, *A dual role for Bub1 in the spindle checkpoint and chromosome congression.* EMBO J, 2005. **24**(8): p. 1621-33.

687. Warren, C.D., et al., *Distinct chromosome segregation roles for spindle checkpoint proteins.* Mol Biol Cell, 2002. **13**(9): p. 3029-41.

688. Mao, Y., A. Abrieu, and D.W. Cleveland, *Activating and silencing the mitotic checkpoint through CENP-E-dependent activation/inactivation of BubR1.* Cell, 2003. **114**(1): p. 87-98.

689. Larsen, N.A., et al., *Structural analysis of Bub3 interactions in the mitotic spindle checkpoint.* Proc Natl Acad Sci U S A, 2007. **104**(4): p. 1201-6.

690. Lenart, P., et al., *The small-molecule inhibitor BI 2536 reveals novel insights into mitotic roles of polo-like kinase 1.* Curr Biol, 2007. **17**(4): p. 304-15.

691. Matsumura, S., F. Toyoshima, and E. Nishida, *Polo-like kinase 1 facilitates chromosome alignment during prometaphase through BubR1.* J Biol Chem, 2007. **282**(20): p. 15217-27.

692. Elowe, S., et al., *Tension-sensitive Plk1 phosphorylation on BubR1 regulates the stability of kinetochore microtubule interactions.* Genes Dev, 2007. **21**(17): p. 2205-19.

693. Foley, E.A., M. Maldonado, and T.M. Kapoor, *Formation of stable attachments between kinetochores and microtubules depends on the B56-PP2A phosphatase.* Nat Cell Biol. **13**(10): p. 1265-71.

694. Suijkerbuijk, S.J., et al., *Integration of kinase and phosphatase activities by BUBR1 ensures formation of stable kinetochore-microtubule attachments.* Dev Cell. **23**(4): p. 745-55.

695. Huang, Y., et al., *Defects in chromosome congression and mitotic progression in KIF18A-deficient cells are partly mediated through impaired functions of CENP-E.* Cell Cycle, 2009. **8**(16): p. 2643-9.

696. Zhang, J., S. Ahmad, and Y. Mao, *BubR1 and APC/EB1 cooperate to maintain metaphase chromosome alignment.* J Cell Biol, 2007. **178**(5): p. 773-84.

697. Kaplan, K.B., et al., *A role for the Adenomatous Polyposis Coli protein in chromosome segregation.* Nat Cell Biol, 2001. **3**(4): p. 429-32.

698. Ishizaki, T., et al., *Coordination of microtubules and the actin cytoskeleton by the Rho effector mDia1.* Nat Cell Biol, 2001. **3**(1): p. 8-14.

699. Green, R.A., R. Wollman, and K.B. Kaplan, *APC and EB1 function together in mitosis to regulate spindle dynamics and chromosome alignment.* Mol Biol Cell, 2005. **16**(10): p. 4609-22.

700. Draviam, V.M., et al., *Misorientation and reduced stretching of aligned sister kinetochores promote chromosome missegregation in EB1- or APC-depleted cells.* EMBO J, 2006. **25**(12): p. 2814-27.

701. Zumbrunn, J., et al., *Binding of the adenomatous polyposis coli protein to microtubules increases microtubule stability and is regulated by GSK3 beta phosphorylation.* Curr Biol, 2001. **11**(1): p. 44-9.

702. Hewitt, L., et al., *Sustained Mps1 activity is required in mitosis to recruit O-Mad2 to the Mad1-C-Mad2 core complex.* J Cell Biol, 2010. **190**(1): p. 25-34.

703. Basu, J., et al., *Mutations in the essential spindle checkpoint gene bub1 cause chromosome missegregation and fail to block apoptosis in Drosophila.* J Cell Biol, 1999. **146**(1): p. 13-28.

704. Lan, W. and D.W. Cleveland, *A chemical tool box defines mitotic and interphase roles for Mps1 kinase.* J Cell Biol, 2010. **190**(1): p. 21-4.

705. Rahmani, Z., et al., *Separating the spindle, checkpoint, and timer functions of BubR1.* J Cell Biol, 2009. **187**(5): p. 597-605.

706. Kops, G.J., D.R. Foltz, and D.W. Cleveland, *Lethality to human cancer cells through massive chromosome loss by inhibition of the mitotic checkpoint.* Proc Natl Acad Sci U S A, 2004. **101**(23): p. 8699-704.

707. Kasuboski, J.M., et al., *Zwint-1 is a novel Aurora B substrate required for the assembly of a dynein-binding platform on kinetochores.* Mol Biol Cell. **22**(18): p. 3318-30.

708. Hood, E.A., et al., *Plk1 regulates the kinesin-13 protein Kif2b to promote faithful chromosome segregation.* Mol Biol Cell. **23**(12): p. 2264-74.

709. Tanno, Y., et al., *Phosphorylation of mammalian Sgo2 by Aurora B recruits PP2A and MCAK to centromeres.* Genes Dev. **24**(19): p. 2169-79.

710. VandenBeldt, K.J., et al., *Kinetochores use a novel mechanism for coordinating the dynamics of individual microtubules.* Curr Biol, 2006. **16**(12): p. 1217-23.

711. Vizeacoumar, F.J., et al., *Integrating high-throughput genetic interaction mapping and high-content screening to explore yeast spindle morphogenesis.* J Cell Biol, 2010. **188**(1): p. 69-81.

712. Mirchenko, L. and F. Uhlmann, *Sli15(INCENP) dephosphorylation prevents mitotic checkpoint reengagement due to loss of tension at anaphase onset.* Curr Biol, 2010. **20**(15): p. 1396-401.

713. Montpetit, B., et al., *Sumoylation of the budding yeast kinetochore protein Ndc10 is required for Ndc10 spindle localization and regulation of anaphase spindle elongation.* J Cell Biol, 2006. **174**(5): p. 653-63.

714. Klein, U.R., et al., *RanBP2 and SENP3 function in a mitotic SUMO2/3 conjugation-deconjugation cycle on Borealin.* Mol Biol Cell, 2009. **20**(1): p. 410-8.

715. Mukhopadhyay, D. and M. Dasso, *The fate of metaphase kinetochores is weighed in the balance of SUMOylation during S phase.* Cell Cycle. **9**(16): p. 3194-201.

716. Goshima, G. and R.D. Vale, *The roles of microtubule-based motor proteins in mitosis: comprehensive RNAi analysis in the Drosophila S2 cell line.* J Cell Biol, 2003. **162**(6): p. 1003-16.

717. McAinsh, A.D., et al., *The human kinetochore proteins Nnf1R and Mcm21R are required for accurate chromosome segregation.* EMBO J, 2006. **25**(17): p. 4033-49.

718. Maure, J.F., E. Kitamura, and T.U. Tanaka, *Mps1 kinase promotes sister-kinetochore bi-orientation by a tension-dependent mechanism.* Curr Biol, 2007. **17**(24): p. 2175-82.

719. Fernius, J. and K.G. Hardwick, *Bub1 kinase targets Sgo1 to ensure efficient chromosome biorientation in budding yeast mitosis.* PLoS Genet, 2007. **3**(11): p. e213.

720. Storchova, Z., et al., *Bub1, Sgo1, and Mps1 mediate a distinct pathway for chromosome biorientation in budding yeast.* Mol Biol Cell, 2011. **22**(9): p. 1473-85.

721. Shimogawa, M.M., et al., *Mps1 phosphorylation of Dam1 couples kinetochores to microtubule plus ends at metaphase.* Curr Biol, 2006. **16**(15): p. 1489-501.

722. Ng, T.M., et al., *Pericentromeric sister chromatid cohesion promotes kinetochore biorientation.* Mol Biol Cell, 2009. **20**(17): p. 3818-27.

723. Waters, J.C., et al., *Localization of Mad2 to kinetochores depends on microtubule attachment, not tension.* J Cell Biol, 1998. **141**(5): p. 1181-91.

724. Amon, A., *The spindle checkpoint.* Curr Opin Genet Dev, 1999. **9**(1): p. 69-75.

725. Li, X. and R.B. Nicklas, *Mitotic forces control a cell-cycle checkpoint.* Nature, 1995. **373**(6515): p. 630-2.

726. Uchida, K.S., et al., *Kinetochore stretching inactivates the spindle assembly checkpoint.* J Cell Biol, 2009. **184**(3): p. 383-90.

727. O'Connell, C.B., et al., *The spindle assembly checkpoint is satisfied in the absence of interkinetochore tension during mitosis with unreplicated genomes.* J Cell Biol, 2008. **183**(1): p. 29-36.

728. Taylor, S.S., et al., *Kinetochore localisation and phosphorylation of the mitotic checkpoint components Bub1 and BubR1 are differentially regulated by spindle events in human cells.* J Cell Sci, 2001. **114**(Pt 24): p. 4385-95.

729. Skoufias, D.A., et al., *Mammalian mad2 and bub1/bubR1 recognize distinct spindle-attachment and kinetochore-tension checkpoints.* Proc Natl Acad Sci U S A, 2001. **98**(8): p. 4492-7.

730. Martinez-Exposito, M.J., et al., *Retention of the BUB3 checkpoint protein on lagging chromosomes.* Proc Natl Acad Sci U S A, 1999. **96**(15): p. 8493-8.

731. Basu, J., et al., *Localization of the Drosophila checkpoint control protein Bub3 to the kinetochore requires Bub1 but not Zw10 or Rod.* Chromosoma, 1998. **107**(6-7): p. 376-85.

732. Lens, S.M., et al., *Survivin is required for a sustained spindle checkpoint arrest in response to lack of tension.* EMBO J, 2003. **22**(12): p. 2934-47.

733. King, E.M., et al., *Ipl1p-dependent phosphorylation of Mad3p is required for the spindle checkpoint response to lack of tension at kinetochores.* Genes Dev, 2007. **21**(10): p. 1163-8.

734. Lo, K.W., J.M. Kogoy, and K.K. Pfister, *The DYNLT3 light chain directly links cytoplasmic dynein to a spindle checkpoint protein, Bub3.* J Biol Chem, 2007. **282**(15): p. 11205-12.

735. Vanoosthuyse, V., et al., *Bub3p facilitates spindle checkpoint silencing in fission yeast.* Mol Biol Cell, 2009. **20**(24): p. 5096-105.

736. Maresca, T.J. and E.D. Salmon, *Welcome to a new kind of tension: translating kinetochore mechanics into a wait-anaphase signal.* J Cell Sci. **123**(Pt 6): p. 825-35.

737. DeLuca, J.G., et al., *Nuf2 and Hec1 are required for retention of the checkpoint proteins Mad1 and Mad2 to kinetochores.* Curr Biol, 2003. **13**(23): p. 2103-9.

738. Buffin, E., et al., *Recruitment of Mad2 to the kinetochore requires the Rod/Zw10 complex.* Curr Biol, 2005. **15**(9): p. 856-61.

739. Scott, R.J., et al., *Interactions between Mad1p and the nuclear transport machinery in the yeast Saccharomyces cerevisiae.* Mol Biol Cell, 2005. **16**(9): p. 4362-74.

740. Scott, R.J., et al., *The nuclear export factor Xpo1p targets Mad1p to kinetochores in yeast.* J Cell Biol, 2009. **184**(1): p. 21-9.

741. Campbell, M.S., G.K. Chan, and T.J. Yen, *Mitotic checkpoint proteins HsMAD1 and HsMAD2 are associated with nuclear pore complexes in interphase.* J Cell Sci, 2001. **114**(Pt 5): p. 953-63.

742. Hoelz, A., E.W. Debler, and G. Blobel, *The structure of the nuclear pore complex.* Annu Rev Biochem. **80**: p. 613-43.

743. Iouk, T., et al., *The yeast nuclear pore complex functionally interacts with components of the spindle assembly checkpoint.* J Cell Biol, 2002. **159**(5): p. 807-19.

744. Kang, J., et al., *Autophosphorylation-dependent activation of human Mps1 is required for the spindle checkpoint.* Proc Natl Acad Sci U S A, 2007. **104**(51): p. 20232-7.

745. Fraschini, R., et al., *Role of the kinetochore protein Ndc10 in mitotic checkpoint activation in Saccharomyces cerevisiae.* Mol Genet Genomics, 2001. **266**(1): p. 115-25.

746. Hardwick, K.G., et al., *Activation of the budding yeast spindle assembly checkpoint without mitotic spindle disruption.* Science, 1996. **273**(5277): p. 953-6.

747. Euskirchen, G.M., *Nnf1p, Dsn1p, Mtw1p, and Nsl1p: a new group of proteins important for chromosome segregation in Saccharomyces cerevisiae.* Eukaryot Cell, 2002. **1**(2): p. 229-40.

748. Gardner, R.D., et al., *The spindle checkpoint of the yeast Saccharomyces cerevisiae requires kinetochore function and maps to the CBF3 domain.* Genetics, 2001. **157**(4): p. 1493-502.

749. Cottarel, G., et al., *A 125-base-pair CEN6 DNA fragment is sufficient for complete meiotic and mitotic centromere functions in Saccharomyces cerevisiae.* Mol Cell Biol, 1989. **9**(8): p. 3342-9.

750. Ikeno, M., et al., *Construction of YAC-based mammalian artificial chromosomes.* Nat Biotechnol, 1998. **16**(5): p. 431-9.

751. Ohzeki, J., et al., *CENP-B box is required for de novo centromere chromatin assembly on human alphoid DNA.* J Cell Biol, 2002. **159**(5): p. 765-75.

752. Okada, T., et al., *CENP-B controls centromere formation depending on the chromatin context.* Cell, 2007. **131**(7): p. 1287-300.

753. Tyler-Smith, C. and G. Floridia, *Many paths to the top of the mountain: diverse evolutionary solutions to centromere structure.* Cell, 2000. **102**(1): p. 5-8.

754. du Sart, D., et al., *A functional neo-centromere formed through activation of a latent human centromere and consisting of non-alpha-satellite DNA.* Nat Genet, 1997. **16**(2): p. 144-53.

755. Barry, A.E., et al., *Sequence analysis of an 80 kb human neocentromere.* Hum Mol Genet, 1999. **8**(2): p. 217-27.

756. Saffery, R., et al., *Human centromeres and neocentromeres show identical distribution patterns of >20 functionally important kinetochore-associated proteins.* Hum Mol Genet, 2000. **9**(2): p. 175-85.

757. Lo, A.W., et al., *A 330 kb CENP-A binding domain and altered replication timing at a human neocentromere.* EMBO J, 2001. **20**(8): p. 2087-96.

758. Cancilla, M.R., et al., *Direct cloning of human 10q25 neocentromere DNA using transformation-associated recombination (TAR) in yeast.* Genomics, 1998. **47**(3): p. 399-404.

759. Tyler-Smith, C., et al., *Transmission of a fully functional human neocentromere through three generations.* Am J Hum Genet, 1999. **64**(5): p. 1440-4.

760. Steiner, N.C. and L. Clarke, *A novel epigenetic effect can alter centromere function in fission yeast.* Cell, 1994. **79**(5): p. 865-74.

761. Fitzgerald-Hayes, M., L. Clarke, and J. Carbon, *Nucleotide sequence comparisons and functional analysis of yeast centromere DNAs.* Cell, 1982. **29**(1): p. 235-44.

762. Lechner, J. and J. Carbon, *A 240 kd multisubunit protein complex, CBF3, is a major component of the budding yeast centromere.* Cell, 1991. **64**(4): p. 717-25.

763. Jiang, W., J. Lechner, and J. Carbon, *Isolation and characterization of a gene (CBF2) specifying a protein component of the budding yeast kinetochore.* J Cell Biol, 1993. **121**(3): p. 513-9.

764. Sorger, P.K., et al., *Two genes required for the binding of an essential Saccharomyces cerevisiae kinetochore complex to DNA.* Proc Natl Acad Sci U S A, 1995. **92**(26): p. 12026-30.

765. Espelin, C.W., K.B. Kaplan, and P.K. Sorger, *Probing the architecture of a simple kinetochore using DNA-protein crosslinking.* J Cell Biol, 1997. **139**(6): p. 1383-96.

766. Russell, I.D., A.S. Grancell, and P.K. Sorger, *The unstable F-box protein p58-Ctf13 forms the structural core of the CBF3 kinetochore complex.* J Cell Biol, 1999. **145**(5): p. 933-50.

767. He, X., et al., *Molecular analysis of kinetochore-microtubule attachment in budding yeast.* Cell, 2001. **106**(2): p. 195-206.

768. Saunders, M., M. Fitzgerald-Hayes, and K. Bloom, *Chromatin structure of altered yeast centromeres.* Proc Natl Acad Sci U S A, 1988. **85**(1): p. 175-9.

769. Cole, H.A., B.H. Howard, and D.J. Clark, *The centromeric nucleosome of budding yeast is perfectly positioned and covers the entire centromere.* Proc Natl Acad Sci U S A, 2011. **108**(31): p. 12687-92.

770. Furuyama, S. and S. Biggins, *Centromere identity is specified by a single centromeric nucleosome in budding yeast.* Proc Natl Acad Sci U S A, 2007. **104**(37): p. 14706-11.

771. Camahort, R., et al., *Cse4 is part of an octameric nucleosome in budding yeast.* Mol Cell, 2009. **35**(6): p. 794-805.

772. Saunders, M.J., et al., *Nucleosome depletion alters the chromatin structure of Saccharomyces cerevisiae centromeres.* Mol Cell Biol, 1990. **10**(11): p. 5721-7.

773. Niedenthal, R.K., et al., *Cpf1 protein induced bending of yeast centromere DNA element I.* Nucleic Acids Res, 1993. **21**(20): p. 4726-33.

774. Baker, R.E., M. Fitzgerald-Hayes, and T.C. O'Brien, *Purification of the yeast centromere binding protein CP1 and a mutational analysis of its binding site.* J Biol Chem, 1989. **264**(18): p. 10843-50.

775. Baker, R.E. and D.C. Masison, *Isolation of the gene encoding the Saccharomyces cerevisiae centromere-binding protein CP1.* Mol Cell Biol, 1990. **10**(6): p. 2458-67.

776. Cai, M. and R.W. Davis, *Yeast centromere binding protein CBF1, of the helix-loop-helix protein family, is required for chromosome stability and methionine prototrophy.* Cell, 1990. **61**(3): p. 437-46.

777. Foreman, P.K. and R.W. Davis, *Point mutations that separate the role of Saccharomyces cerevisiae centromere binding factor 1 in chromosome segregation from its role in transcriptional activation.* Genetics, 1993. **135**(2): p. 287-96.

778. Hemmerich, P., et al., *Interaction of yeast kinetochore proteins with centromere-protein/transcription factor Cbf1.* Proc Natl Acad Sci U S A, 2000. **97**(23): p. 12583-8.

779. Kent, N.A., et al., *Chromatin structure modulation in Saccharomyces cerevisiae by centromere and promoter factor 1.* Mol Cell Biol, 1994. **14**(8): p. 5229-41.

780. Mellor, J., et al., *CPF1, a yeast protein which functions in centromeres and promoters.* EMBO J, 1990. **9**(12): p. 4017-26.

781. Mellor, J., et al., *DNA binding of CPF1 is required for optimal centromere function but not for maintaining methionine prototrophy in yeast.* Nucleic Acids Res, 1991. **19**(11): p. 2961-9.

782. Bram, R.J. and R.D. Kornberg, *Isolation of a Saccharomyces cerevisiae centromere DNA-binding protein, its human homolog, and its possible role as a transcription factor.* Mol Cell Biol, 1987. **7**(1): p. 403-9.

783. Sanchez-Pulido, L., et al., *Common ancestry of the CENP-A chaperones Scm3 and HJURP.* Cell, 2009. **137**(7): p. 1173-4.

784. Dunleavy, E.M., et al., *HJURP is a cell-cycle-dependent maintenance and deposition factor of CENP-A at centromeres.* Cell, 2009. **137**(3): p. 485-97.

785. Foltz, D.R., et al., *Centromere-specific assembly of CENP-A nucleosomes is mediated by HJURP.* Cell, 2009. **137**(3): p. 472-84.

786. Pidoux, A.L., et al., *Fission yeast Scm3: A CENP-A receptor required for integrity of subkinetochore chromatin.* Mol Cell, 2009. **33**(3): p. 299-311.

787. Williams, J.S., et al., *Fission yeast Scm3 mediates stable assembly of Cnp1/CENP-A into centromeric chromatin.* Mol Cell, 2009. **33**(3): p. 287-98.

788. Camahort, R., et al., *Scm3 is essential to recruit the histone h3 variant cse4 to centromeres and to maintain a functional kinetochore.* Mol Cell, 2007. **26**(6): p. 853-65.

789. Palmer, D.K., et al., *A 17-kD centromere protein (CENP-A) copurifies with nucleosome core particles and with histones.* J Cell Biol, 1987. **104**(4): p. 805-15.

790. Palmer, D.K., et al., *Purification of the centromere-specific protein CENP-A and demonstration that it is a distinctive histone.* Proc Natl Acad Sci U S A, 1991. **88**(9): p. 3734-8.

791. Sullivan, K.F., M. Hechenberger, and K. Masri, *Human CENP-A contains a histone H3 related histone fold domain that is required for targeting to the centromere.* J Cell Biol, 1994. **127**(3): p. 581-92.

792. Stoler, S., et al., *A mutation in CSE4, an essential gene encoding a novel chromatin-associated protein in yeast, causes chromosome nondisjunction and cell cycle arrest at mitosis.* Genes Dev, 1995. **9**(5): p. 573-86.

793. Palmer, D.K., K. O'Day, and R.L. Margolis, *The centromere specific histone CENP-A is selectively retained in discrete foci in mammalian sperm nuclei.* Chromosoma, 1990. **100**(1): p. 32-6.

794. Shelby, R.D., K. Monier, and K.F. Sullivan, *Chromatin assembly at kinetochores is uncoupled from DNA replication.* J Cell Biol, 2000. **151**(5): p. 1113-8.

795. Hemmerich, P., et al., *Dynamics of inner kinetochore assembly and maintenance in living cells.* J Cell Biol, 2008. **180**(6): p. 1101-14.

796. Jansen, L.E., et al., *Propagation of centromeric chromatin requires exit from mitosis.* J Cell Biol, 2007. **176**(6): p. 795-805.

797. Fujita, Y., et al., *Priming of centromere for CENP-A recruitment by human hMis18alpha, hMis18beta, and M18BP1.* Dev Cell, 2007. **12**(1): p. 17-30.

798. Maddox, P.S., et al., *Functional genomics identifies a Myb domain-containing protein family required for assembly of CENP-A chromatin.* J Cell Biol, 2007. **176**(6): p. 757-63.

799. Hayashi, T., et al., *Mis16 and Mis18 are required for CENP-A loading and histone deacetylation at centromeres.* Cell, 2004. **118**(6): p. 715-29.

800. Barnhart, M.C., et al., *HJURP is a CENP-A chromatin assembly factor sufficient to form a functional de novo kinetochore.* J Cell Biol, 2011. **194**(2): p. 229-43.

801. Ohzeki, J., et al., *Breaking the HAC Barrier: histone H3K9 acetyl/methyl balance regulates CENP-A assembly.* EMBO J. **31**(10): p. 2391-402.

802. Furuyama, T., Y. Dalal, and S. Henikoff, *Chaperone-mediated assembly of centromeric chromatin in vitro.* Proc Natl Acad Sci U S A, 2006. **103**(16): p. 6172-7.

803. Lagana, A., et al., *A small GTPase molecular switch regulates epigenetic centromere maintenance by stabilizing newly incorporated CENP-A.* Nat Cell Biol. **12**(12): p. 1186-93.

804. Perpelescu, M., et al., *Active establishment of centromeric CENP-A chromatin by RSF complex.* J Cell Biol, 2009. **185**(3): p. 397-407.

805. Takahashi, K., E.S. Chen, and M. Yanagida, *Requirement of Mis6 centromere connector for localizing a CENP-A-like protein in fission yeast.* Science, 2000. **288**(5474): p. 2215-9.

806. Saitoh, S., K. Takahashi, and M. Yanagida, *Mis6, a fission yeast inner centromere protein, acts during G1/S and forms specialized chromatin required for equal segregation.* Cell, 1997. **90**(1): p. 131-43.

807. Partridge, J.F., B. Borgstrom, and R.C. Allshire, *Distinct protein interaction domains and protein spreading in a complex centromere.* Genes Dev, 2000. **14**(7): p. 783-91.

808. Pearson, C.G., et al., *Stable kinetochore-microtubule attachment constrains centromere positioning in metaphase.* Curr Biol, 2004. **14**(21): p. 1962-7.

809. Mythreye, K. and K.S. Bloom, *Differential kinetochore protein requirements for establishment versus propagation of centromere activity in Saccharomyces cerevisiae.* J Cell Biol, 2003. **160**(6): p. 833-43.

810. Vermaak, D., H.S. Hayden, and S. Henikoff, *Centromere targeting element within the histone fold domain of Cid.* Mol Cell Biol, 2002. **22**(21): p. 7553-61.

811. Shelby, R.D., O. Vafa, and K.F. Sullivan, *Assembly of CENP-A into centromeric chromatin requires a cooperative array of nucleosomal DNA contact sites.* J Cell Biol, 1997. **136**(3): p. 501-13.

812. Black, B.E., et al., *Structural determinants for generating centromeric chromatin.* Nature, 2004. **430**(6999): p. 578-82.

813. Black, B.E., et al., *Centromere identity maintained by nucleosomes assembled with histone H3 containing the CENP-A targeting domain.* Mol Cell, 2007. **25**(2): p. 309-22.

814. Moreno-Moreno, O., M. Torras-Llort, and F. Azorin, *Proteolysis restricts localization of CID, the centromere-specific histone H3 variant of Drosophila, to centromeres.* Nucleic Acids Res, 2006. **34**(21): p. 6247-55.

815. Hewawasam, G., et al., *Psh1 is an E3 ubiquitin ligase that targets the centromeric histone variant Cse4.* Mol Cell, 2010. **40**(3): p. 444-54.

816. Collins, K.A., S. Furuyama, and S. Biggins, *Proteolysis contributes to the exclusive centromere localization of the yeast Cse4/CENP-A histone H3 variant.* Curr Biol, 2004. **14**(21): p. 1968-72.

817. Zhou, Z., et al., *Structural basis for recognition of centromere histone variant CenH3 by the chaperone Scm3.* Nature, 2011. **472**(7342): p. 234-7.

818. Shuaib, M., et al., *HJURP binds CENP-A via a highly conserved N-terminal domain and mediates its deposition at centromeres.* Proceedings of the National Academy of Sciences, 2010. **107**(4): p. 1349-1354.

819. Thakur, J. and K. Sanyal, *A coordinated interdependent protein circuitry stabilizes the kinetochore ensemble to protect CENP-A in the human pathogenic yeast Candida albicans.* PLoS Genet. **8**(4): p. e1002661.

820. Moree, B., et al., *CENP-C recruits M18BP1 to centromeres to promote CENP-A chromatin assembly.* J Cell Biol. **194**(6): p. 855-71.

821. Dernburg, A.F., *Here, there, and everywhere: kinetochore function on holocentric chromosomes.* J Cell Biol, 2001. **153**(6): p. F33-8.

822. Mellone, B.G., et al., *Assembly of Drosophila centromeric chromatin proteins during mitosis.* PLoS Genet, 2011. **7**(5): p. e1002068.

823. Weber, S.A., et al., *The kinetochore is an enhancer of pericentric cohesin binding.* PLoS Biol, 2004. **2**(9): p. E260.

824. Kogut, I., et al., *The Scc2/Scc4 cohesin loader determines the distribution of cohesin on budding yeast chromosomes.* Genes Dev, 2009. **23**(19): p. 2345-57.

825. Scheller, J., et al., *MPH1, a yeast gene encoding a DEAH protein, plays a role in protection of the genome from spontaneous and chemically induced damage.* Genetics, 2000. **155**(3): p. 1069-81.

826. Prakash, R., et al., *Saccharomyces cerevisiae MPH1 gene, required for homologous recombination-mediated mutation avoidance, encodes a 3' to 5' DNA helicase.* J Biol Chem, 2005. **280**(9): p. 7854-60.

827. Schurer, K.A., et al., *Yeast MPH1 gene functions in an error-free DNA damage bypass pathway that requires genes from Homologous recombination, but not from postreplicative repair.* Genetics, 2004. **166**(4): p. 1673-86.

828. Sun, W., et al., *The FANCM ortholog Fml1 promotes recombination at stalled replication forks and limits crossing over during DNA double-strand break repair.* Mol Cell, 2008. **32**(1): p. 118-28.

829. Panico, E.R., et al., *Genetic evidence for a role of Saccharomyces cerevisiae Mph1 in recombinational DNA repair under replicative stress.* Yeast. **27**(1): p. 11-27.

830. Choi, K., et al., *The Smc5/6 complex and Esc2 influence multiple replication-associated recombination processes in Saccharomyces cerevisiae.* Mol Biol Cell. **21**(13): p. 2306-14.

831. Ward, T.A., et al., *Components of a fanconi-like pathway control pso2-independent DNA interstrand crosslink repair in yeast.* PLoS Genet. **8**(8): p. e1002884.

832. Whitby, M.C., *The FANCM family of DNA helicases/translocases.* DNA Repair (Amst). **9**(3): p. 224-36.

833. Putnam, C.D., E.J. Jaehnig, and R.D. Kolodner, *Perspectives on the DNA damage and replication checkpoint responses in Saccharomyces cerevisiae.* DNA Repair (Amst), 2009. **8**(9): p. 974-82.

834. Yan, Z., et al., *A histone-fold complex and FANCM form a conserved DNA-remodeling complex to maintain genome stability.* Mol Cell. **37**(6): p. 865-78.

835. Zhu, W., J.W. Smith, and C.M. Huang, *Mass spectrometry-based label-free quantitative proteomics.* J Biomed Biotechnol. **2010**: p. 840518.

836. Bock, L.J., et al., *Cnn1 inhibits the interactions between the KMN complexes of the yeast kinetochore.* Nat Cell Biol. **14**(6): p. 614-24.

837. Tan, S., *A modular polycistronic expression system for overexpressing protein complexes in Escherichia coli.* Protein Expr Purif, 2001. **21**(1): p. 224-34.

838. Tolia, N.H. and L. Joshua-Tor, *Strategies for protein coexpression in Escherichia coli.* Nat Methods, 2006. **3**(1): p. 55-64.

839. Rieder, C.L., *Ribonucleoprotein staining of centrioles and kinetochores in newt lung cell spindles.* J Cell Biol, 1979. **80**(1): p. 1-9.

840. Rieder, C.L., *Localization of ribonucleoprotein in the trilaminar kinetochore of PtK1.* J Ultrastruct Res, 1979. **66**(2): p. 109-19.

841. Parra, M.T., et al., *A perikinetochoric ring defined by MCAK and Aurora-B as a novel centromere domain.* PLoS Genet, 2006. **2**(6): p. e84.

842. Du, Y., C.N. Topp, and R.K. Dawe, *DNA binding of centromere protein C (CENPC) is stabilized by single-stranded RNA.* PLoS Genet. **6**(2): p. e1000835.

843. Wong, L.H., et al., *Centromere RNA is a key component for the assembly of nucleoproteins at the nucleolus and centromere.* Genome Res, 2007. **17**(8): p. 1146-60.

844. Stelkić, A., *Characterization of the protein-protein interaction network within the central domain of the S. cerevisiae kinetochore.* Doctoral Thesis, 2012.

845. Moses, A.M., J.K. Heriche, and R. Durbin, *Clustering of phosphorylation site recognition motifs can be exploited to predict the targets of cyclin-dependent kinase.* Genome Biol, 2007. **8**(2): p. R23.

846. Vazquez-Novelle, M.D., et al., *The 'anaphase problem': how to disable the mitotic checkpoint when sisters split.* Biochem Soc Trans. **38**(6): p. 1660-6.

847. Sorger, P.K., F.F. Severin, and A.A. Hyman, *Factors required for the binding of reassembled yeast kinetochores to microtubules in vitro.* J Cell Biol, 1994. **127**(4): p. 995-1008.

848. Haruki, H., J. Nishikawa, and U.K. Laemmli, *The anchor-away technique: rapid, conditional establishment of yeast mutant phenotypes.* Mol Cell, 2008. **31**(6): p. 925-32.

849. Zhang, G., et al., *The Ndc80 internal loop is required for recruitment of the Ska complex to establish end-on microtubule attachment to kinetochores.* J Cell Sci. **125**(Pt 13): p. 3243-53.

850. Cheeseman, I.M., et al., *A conserved protein network controls assembly of the outer kinetochore and its ability to sustain tension.* Genes Dev, 2004. **18**(18): p. 2255-68.

851. Lawrimore, J., K.S. Bloom, and E.D. Salmon, *Point centromeres contain more than a single centromere-specific Cse4 (CENP-A) nucleosome.* J Cell Biol. **195**(4): p. 573-82.

852. Vaziri, C. and H. Masai, *Integrating DNA replication with trans-lesion synthesis via Cdc7.* Cell Cycle. **9**(24): p. 4818-23.

853. Schild, D. and B. Byers, *Meiotic effects of DNA-defective cell division cycle mutations of Saccharomyces cerevisiae.* Chromosoma, 1978. **70**(1): p. 109-30.

854. Njagi, G.D. and B.J. Kilbey, *cdc7-1 a temperature sensitive cell-cycle mutant which interferes with induced mutagenesis in Saccharomyces cerevisiae.* Mol Gen Genet, 1982. **186**(4): p. 478-81.

855. Buck, V., A. White, and J. Rosamond, *CDC7 protein kinase activity is required for mitosis and meiosis in Saccharomyces cerevisiae.* Mol Gen Genet, 1991. **227**(3): p. 452-7.

856. Raghuraman, M.K., et al., *Replication dynamics of the yeast genome.* Science, 2001. **294**(5540): p. 115-21.

857. Gammie, A.E. and M.D. Rose, *Identification and characterization of CEN12 in the budding yeast Saccharomyces cerevisiae.* Curr Genet, 1995. **28**(6): p. 512-6.

858. Takahashi, T.S., et al., *Cdc7-Drf1 kinase links chromosome cohesion to the initiation of DNA replication in Xenopus egg extracts.* Genes Dev, 2008. **22**(14): p. 1894-905.

859. Samel, A., et al., *Methylation of CenH3 arginine 37 regulates kinetochore integrity and chromosome segregation.* Proc Natl Acad Sci U S A. **109**(23): p. 9029-34.

860. Keith, K.C., et al., *Analysis of primary structural determinants that distinguish the centromere-specific function of histone variant Cse4p from histone H3.* Mol Cell Biol, 1999. **19**(9): p. 6130-9.

861. Chen, Y., et al., *The N terminus of the centromere H3-like protein Cse4p performs an essential function distinct from that of the histone fold domain.* Mol Cell Biol, 2000. **20**(18): p. 7037-48.

862. Morey, L., et al., *The histone fold domain of Cse4 is sufficient for CEN targeting and propagation of active centromeres in budding yeast.* Eukaryot Cell, 2004. **3**(6): p. 1533-43.

863. Pereira, G. and E. Schiebel, *Separase regulates INCENP-Aurora B anaphase spindle function through Cdc14.* Science, 2003. **302**(5653): p. 2120-4.

864. Zimniak, T., et al., *Spatiotemporal regulation of Ipl1/Aurora activity by direct Cdk1 phosphorylation.* Curr Biol. **22**(9): p. 787-93.

865. Pinsky, B.A., et al., *An Mtw1 complex promotes kinetochore biorientation that is monitored by the Ipl1/Aurora protein kinase.* Dev Cell, 2003. **5**(5): p. 735-45.

866. Ribeiro, S.A., et al., *A super-resolution map of the vertebrate kinetochore.* Proc Natl Acad Sci U S A. **107**(23): p. 10484-9.

867. Liu, D., et al., *Human NUF2 interacts with centromere-associated protein E and is essential for a stable spindle microtubule-kinetochore attachment.* J Biol Chem, 2007. **282**(29): p. 21415-24.

7. Supplementary Information

7.1 Oligo sequences

Name	Description	Sequence
oMM1	5' Mcm22 - NdeI	GGAATTC CATATG GATGTTGAAAAGGATGTCCTGGATGTC
oMM2	3' Mcm22 - BamHI	CGC GGATCC TTAAGTTAGACTGGTCTCATTGAAATCTAT
oMM3	5' Ctf3 - BamHI	CGC GGATCC ATGAGTCTTATACTAGATGATATCATCCTC
oMM5	5' Mcm16 - NdeI	GGAATTC CATATG ACAAACAGTAGTGAAAAACAATGGG
oMM6	3' Mcm16 - internal, overlapPCR,-SacI	CCTAACGATTGCAACAGCTCATAGTCC
oMM7	5' Mcm16 - internal, overlapPCR,-SacI	GAAAGCAATTCTCTGGACTATGAGCTgTT
oMM8	3' Mcm16 - KpnI	CGG GGTACC TCAAATTGTGTAGGATATGTTTGTATATCCTGAGTG
oMM9	3' Mcm16 - 6xHN - KpnI	CGG GGTACC TCA GTTGTGATTATGATTATGATTATGATTATGATTATG AATTGTGTAGGATATGTTTGTATATCCTGAGTG
oMM10	3' Mcm16 - StrepII - KpnI	CGG GGTACC TCA TTTTTCAAACTGCGGATGGCTCCA AATTGTGTAGGATATGTTTGTATATCCTGAGTG
oMM12	3' Iml3 - BamHI	CGC GGATCC TTACTCGCTGGTAAACTGAATCGATTGGAG
oMM13	5' Chl4 Longtine TAP C-Term	AACGATAATGAATGGAGATTTTCAGCGAGAGCAGGTTGCTAAAGGTGGTTTACTG cggatccccgggttaattaa
oMM15	5' Ctf19 Longtine TAP C-Term	AACCGGGTTAAAGGAGATCTGCAACGTTTGCCTATTCCCGGACATGTACGCCAGG cggatccccgggttaattaa
oMM17	5' Mcm16 Longtine TAP C-Term	ATTGATGATTGCTTTACAGATACACTCCGGATATACAAACATATCCTACACAATT cggatccccgggttaattaa
oMM19	5' Chl4 - NdeI	GGAATTC CATATG TCTAACGAATTACGGCTTGAAGATAAC
oMM20	3' Chl4 - KpnI	CGG GGTACC CTACAGTAAACCACCTTTAGCAACCTGCTC
oMM21	3' Chl4 - 6xHN - KpnI	CGG GGTACC CTA GTTGTGATTATGATTATGATTATGATTATGATTATG CAGTAAACCACCTTTAGCAACCTGCTC
oMM22	3' Chl4 - FLAG - KpnI	CGG GGTACC CTA CTTGTCGTCATCGTCTTTGTAGTC CAGTAAACCACCTTTAGCAACCTGCTC
oMM23	3' Mcm16 - 6xHis - KpnI	CGG GGTACC TCA ATGATGATGATGATGATG AATTGTGTAGGATATGTTTGTATATCCTGAGTG
oMM24	3' Chl4 Longtine TAP C-Term	CTATGCAAAAATTTCAGTCAAAGCATAACAAAACGAACCTTTTTTGTACTGCTCA gaattcgagctcgtttaaac
oMM25	3' Ctf19 Longtine TAP C-Term	TCGCTTGGCCTTACCGCCCATGATGTCTGTAAAGTACCGTTCCCTCATCCGAGCT gaattcgagctcgtttaaac
oMM26	3' Mcm16 Longtine TAP C-Term	CTTTTTTTTTTCTCGAAGATTCAAACCTTAATTAAGTAACTATTATTATTAGCGT gaattcgagctcgtttaaac
oMM27	5' Iml3 - NcoI/Gly	CATG CCATGG GG CCTTATACTTGGAAGTTTTTAGGAATCAGC
oMM28	pCOLADuett UP1 Sequencing Primer	GGATCTCGACGCTCTCCCT
oMM29	pCOLADuett UP2 Sequencing Primer	TTGTACACGGCCGCATAATC
oMM30	pCOLADuett Down1 Sequencing Primer	GATTATGCGGCCGTGTACAA
oMM31	3' Ctf3 - BamH1	CGC GGATCC CTAAGAATTTTGAACGCTATACTTTGAG
oMM32	3' Mcm21 6x His BamHI	CGC GGATCC TCA ATGATGATGATGATGATG CTTGAATATTGTCGCGAAAGAATGG
oMM33	3' Mcm21 6xHN BamHI	CGC GGATCC TCA GTTGTGATTATGATTATGATTATGATTATGATTATG CTTGAATATTGTCGCGAAAGAATGG
oMM34	3' Chl4 - Xho	CCG CTCGAG CTA CAGTAAACCACCTTTAGCAACCTGCTC
oMM35	3' Chl4 - 6xHN - Xho	CCG CTCGAG CTA GTTGTGATTATGATTATGATTATGATTATGATTATG CAGTAAACCACCTTTAGCAACCTGCTC
oMM36	3' Chl4 - FLAG - Xho	CCG CTCGAG CTA CTTGTCGTCATCGTCTTTGTAGTC CAGTAAACCACCTTTAGCAACCTGCTC
oMM40	Ctf3 seq from Mcm22 in pst39	CAGTAATTGAGGGCTCTACAAATCCAGGG
oMM41	internal Ctf3 seq 700	TTGAAAAGAATATTATCCAGAGCACATCCCG
oMM42	internal Ctf3 seq 1415	GGGTTTTAGATGATAAATTGATAGCACTCGGG
oMM43	internal Ctf3 seq 1881	CGCTAAATTTTTCACGATAACTGGTATACC
oMM44	5' AmeI Longtine TAP C-Term	CTTCTGAAAAAGATAAATAAAATTAATGAAAATCTTTCTAACGAATTACAACCAAGTCTA cggatccccgggttaattaa
oMM45	3' AmeI Longtine TAP C-Term	CCTTATAACACAACTTCCTTAGTATGGAAGTAATACATATATACATATATACATATATAC gaattcgagctcgtttaaac
oMM46	Quikchange mutated KpnI site in pET-OKP	gatccagatctaagcttgataccatggcagctgatag
oMM47	3' Mcm21 FLAG BamHI	CGC GGATCC TCA CTTGTCGTCATCGTCTTTGTAGTC CTTGAATATTGTCGCGAAAGAATGG
oMM48	AmeI-TAP 3' UTR c-PCR Primer	GGTCTTATACTGAATTGTTTGAATTCC
oMM49	Mcm16-TAP 3' UTR c-PCR Primer	GTGGAACTTTAAGGGTTGAATATAAGCGAT
oMM50	CHL4-TAP 3' UTR c-PCR Primer	CGTTATTTATAAAAGAATATTGTGCTG
oMM51	YOL086W-A (CENP-S) Longtine C-Term TAP/GFP/Myc	GAGCGACCTCATGCTATACCTGAGAAAGCAACCTGACCTACAGGAAAGAGTTACTCAAGAA cggatccccgggttaattaa
oMM52	YOL086W-A (CENP-S) Longtine C-Term TAP/GFP/Myc	GAATTTCTTATGATTTATGATTTTTATTATTAAATAAGTTATAAAAAAAA gaattcgagctcgtttaaac
oMM53	YOL086W-A (CENP-S) 3´UTR c-PCR Primer	CTTCTTCGCCAGAGGTTTGGTCAAGTCTC
oMM54	3' Okp-His-KpnI	GCGCG GGTACC CTA ATGATGATGATGATGATG GTGTATATCTTCTTCGGTCTTATCTTGG
oMM55	YDL160C-A (CENP-X/MHF2) Longtine C-Term 5'	CCCTTAGAGTTATCGCATCAAGATTTAGAGCGTATCGTAGGGCTTCTTCTGATGGATATG cggatccccgggttaattaa

oMM56	YDL160C-A (CENP-X/MHF2) Longtine C-Term 3'	GTAAACTAACGTAGTTCAGGACGACTGAAAGAAAATATAGTGCTTTAAATTTATCAGACA gaattcgagctcgtttaaac
oMM57	YDL160C-A (CENP-X/MHF2) 3´UTR c-PCR Primer	GAACTGTATATTTGTATATGTGAGCGCACG
oMM58	5' Ame1End of Gene for Tag verification	CTTTCTAACGAATTACAACCAAGTCTA
oMM59	5' Mcm16 End of Gene for Tag verification	CCGGATATACAAACATATCCTACACAATT
oMM60	5' CHL4 End of Gene for Tag verification	GCGAGAGCAGGTTGCTAAAGGTGGTTTACTG
oMM61	5' YOL086W-A End of Gene for Tag verification	CCTGACCTACAGGAAAGAGTTACTCAAGAA
oMM62	5' YDL160C-A End of Gene for Tag verification	GCGTATCGTAGGGCTTCTTCTGATGGATATG
oMM63	Mcm21 5' Sequencing Primer	ATGAGTAGAATCGATGATTTACAGCAGGAC
oMM64	3' Mcm22-His-BamHI	CGC GGATCC TTA ATGATGATGATGATGATG AGTTAGACTGGTCTCATTGAAATCTAT
oMM65	3' Ctf3-His-BamHI	CGC GGATCC CTA ATGATGATGATGATGATG AGAATTTTGAACGCTATACTTTGAGAG
oMM66	3' Iml3-His-BamHI	CGC GGATCC TTA ATGATGATGATGATGATG CTCGCTGGTAAACTGAATCGATTGGAG
oMM67	COMA-Sequencing Ctf19 700bp fwd	CTGAAGGCCAAGCAATTACTGGCAACACG
oMM68	COMA-Seqencing Ctf19 300bp rev	GATATCGTTTTGGAGGATATCACCATTTTT
oMM69	COMA-Seqencing Ctf19 1bp fwd	ATGGATTTTACGTCTGATACGACGAATTCGC
oMM70	COMA-Seqencing Ame1 800bp fwd	GACTTCTACTTTGCTAGGCAAATACGAGGG
oMM71	CICMM-Seqencing Mcm22 1bp fwd	ATGGATGTTGAAAAGGATGTCCTGGATGTC
oMM72	CICMM-Seqencing Mcm16 500bp fwd	GGAAAATGAAACGATACAAGAATTGATGATTG
oMM73	CICMM-Seqencing Mcm22 300bp rev	GGCCTTTTGATCAACTGATTGATCATTCATAAGCG
oMM74	CICMM-Seqencing Mcm16 1bp fwd	ATGACAAACAGTAGTGAAAAACAATGGG
oMM75	CICMM-Seqencing Iml3 100 bp fwd	GACATTCAAACCATTCGAGTACCCAGTGATCC
oMM76	CICMM-Seqencing Iml3 200bp rev	CCCCAAGAAAATGAACTTAGAGTAAGTGCCC
oMM77	CICMM-Seqencing Chl4 1bp fwd	ATGTCTAACGAATTACGGCTTGAAGATAAC
oMM78	CICMM-Seqencing Chl4 700bp fwd	CGATATCAGAAAGAGAAACAATCATCTTC
oMM79	CICMM-Seqencing Chl4 1250bp fwd	GTTCCTGGGTGGTTGGCTGGAGAAAATGG
oMM82	Ame1 pRS306 3' XhoI	CG CCG CTCGAG CTTCTACAGAATGGTCACAGCGTTACTTG
oMM83	Ame1 pRS306 5' XbaI	CG CTAG TCTAGA GAATACAAGTTTGGGGAACGCTTTTTGGAACGGC
oMM86	Mcm21 cterm Tagging 3' verification	CATATACCACATTCTACCCAAAATTGGG
oMM87	Okp cterm Tagging 3' verification	CCAAGGTTTTCTGAGGCTCGTTGGCGG
oMM88	Ctf19 cterm Tagging 3' verification	GCTGTCGCAAGCATCGATGGCGGTGTCGC
oMM89	CENP-S in gene verification 2, bit upstream	GCATATCTACAATTGGGTGAAATGGGG
oMM90	Ame Site multi-phosphosite mutagenesis 91 A->G	ATGTTATTGTATTTAAGGCGCCAAATGCTGTTTAT
oMM91	Ame Site multi-phosphosite mutagenesis 121 T->G	TTTATAGAGAGGAGAACGCACCTATTCAAGCTCCT
oMM92	Ame Site multi-phosphosite mutagenesis 133 T->G	AGAACGCACCTATTCAAGCTCCTGTTCAACCCATT
oMM93	Ame Site multi-phosphosite mutagenesis 157 T->G	TCAACCCATTTTGTCTGCACCAAAACTTGCGAATT
oMM94	Ame Site multi-phosphosite mutagenesis 301 T->G	AAAGTCTTATAAGCGAAGCGCCGCAAAATGTTAGA
oMM95	internal Ctf3 seq 1000	GCCATCTTTAAACAGCAATGTTTTACTGCCGCG

7.2 Strains and Plasmids

Yeast strains based on S288C

Strain	Genotype	Source
MMY1	MAT a; leu2, *ura3-52*, trp1, prb1-1122, pep4-3, pre1-451,YOL086W-A-STag-TEV-ZZ::KanMX	This study
MMY2	MAT a; leu2, *ura3-52*, trp1, prb1-1122, pep4-3, pre1-451,YDL160C-A-STag-TEV-ZZ::KanMX	This study
MMY3	MAT a, leu2, ura3-52, trp1, prb1-1122, pep4-3, pre1-451, Ame1-STag-TEV-ZZ::KanMX	This study
MMY4	MAT a; leu2, *ura3-52*, trp1, prb1-1122, pep4-3, pre1-451,Chl4-STag-TEV-ZZ::KanMX	This study
MMY5	MAT a; leu2, *ura3-52*, trp1, prb1-1122, pep4-3, pre1-451,Mcm16-STag-TEV-ZZ::KanMX	This study
SWY102	MAT a; leu2, *ura3-52*, trp1, prb1-1122, pep4-3, pre1-451,Cnn1-TAP::KanMX	This study
SWY550	Wip1-GFP::KanMX Nuf2-mCherry::KanMX cnn1Δ::HIS3	This study
SWY551	Wip1-GFP::KanMX Nuf2-mCherry::KanMX	This study

Plasmids:

Plasmid number	gene	plasmid
1	Ctf19	pET3aTr
2	Ctf19His	pET3aTr
3	Mcm21	pET3aTr
4	Mcm21His	pET3aTr
5	Mcm21FLAG	pET3aTr
6	Okp1	pET3aTr
7	Okp1 Kpn mut	pET3aTr
8	Ame	pET3aTr
9	AmeH	pET3aTr
10	AmeF	pET3aTr
11	Mcm21HN	pET3aTr
12	Mcm22	pET3aTr
13	Ctf3	pET3aTr
14	Mcm16	pET3aTr
15	Mcm16H	pET3aTr
16	Mcm16Strep	pET3aTr
17	Ctf3 His	pET3aTr
18	Mcm22 His	pET3aTr
19	Iml3	pCOLADuett
20	Iml3+Chl4 (CI)	pCOLADuett
21	Iml3+Chl4-Flag (CI)	pCOLADuett
22	Ctf19 (mutated)	pST39
23	Ctf19 + Mcm21	pST39
24	Ctf19 + Mcm21 +Okp1	pST39
25	COMA-His (Tag on Ame1)	pST39
26	COMA-Flag (Tag on Ame1)	pST39

27	COMA-Flag (Tag on Ame1)	pST39
28	Ctf19 + Mcm21 - His	pST39
29	Ctf19 + Mcm21 - Flag	pST39
30	Ctf19 + Mcm21 - HN	pST39
31	COMA-His (Tag on Mcm21)	pST39
32	COMA-Flag (Tag on Mcm21)	pST39
33	COMA-HN (Tag on Mcm21)	pST39
34	Okp1 (mut)	pST39
35	Mcm22	pST39
36	Mcm22 Ctf3	pST39
37	Mcm22 + Ctf3 + Mcm16	pST39
38	Mcm22 + Ctf3 + Mcm16-HN	pST39
39	Mcm22 + Ctf3 + Mcm16-His	pST39
40	Mcm22 + Ctf3 + Mcm16-Strep2	pST39
41	clean pst39 plasmid	pST39
42	Ame1 pRS306	pRS306
43	Mcm22 + Ctf3 + Mcm16-Strep2	pST39
44	Iml3+Chl4-Flag (CI)	pCOLADuett
45	COMA-Flag (Tag on Ame1)	pST39
46	COMA-Flag (Tag on Ame1)	pST39
47	COMA-His (Tag on Mcm21)	pST39

7.3 Mass spectrometry data

Susanne Opravil, Richard Imre, Otto Hudecz

Information and figures supplied by IMP/IMBA protein chemistry core facility

Summary:

instrument	stringency	bait / sample	enzyme			identified proteins	bait seq cov [%]
			trypsin	chymotrypsin	subtilisin		
LTQ Orbitrap Velos	high	Chl4_pool	x	x	x	122	98
LTQ Orbitrap Velos	low	Chl4	x	x	x	398	99
LTQ Orbitrap Velos	high	CNN1_pool	x	x	x	50	84
LTQ Orbitrap Velos	low	CNN1	x	x	x	295	97
LTQ Orbitrap Velos	high	Mcm16_pool	x	x	x	140	97
LTQ Orbitrap Velos	low	Mcm16	x	x	x	390	95
LTQ Orbitrap Velos	high	Ame1 (sample A)	x			90	72
LTQ Orbitrap Velos	low	Ame1 (sample B)	x			93	70
LTQ Orbitrap Velos	high	YDL160C-A (sample C)	x			34	100
LTQ Orbitrap Velos	low	YDL160C-A (X)	x	x	x	305	98
LTQ Orbitrap Velos	high	YOL06W-A (sample D)	x			66	89
LTQ Orbitrap Velos	low	YOL06W-A (sample E)	x			98	93

Search Engines

Mascot & Sequest via Thermo Proteome Discoverer 1.3.0.339

Protein Sequence Database

yeast SGD (6717 sequences; 3020761 residues)

Peptide Filters	**filter options**
Peptide Rank	1
Peptide Confidence	High (1% FDR)
Protein Filters	
Minimum Peptides Per Protein	2

# identified proteins

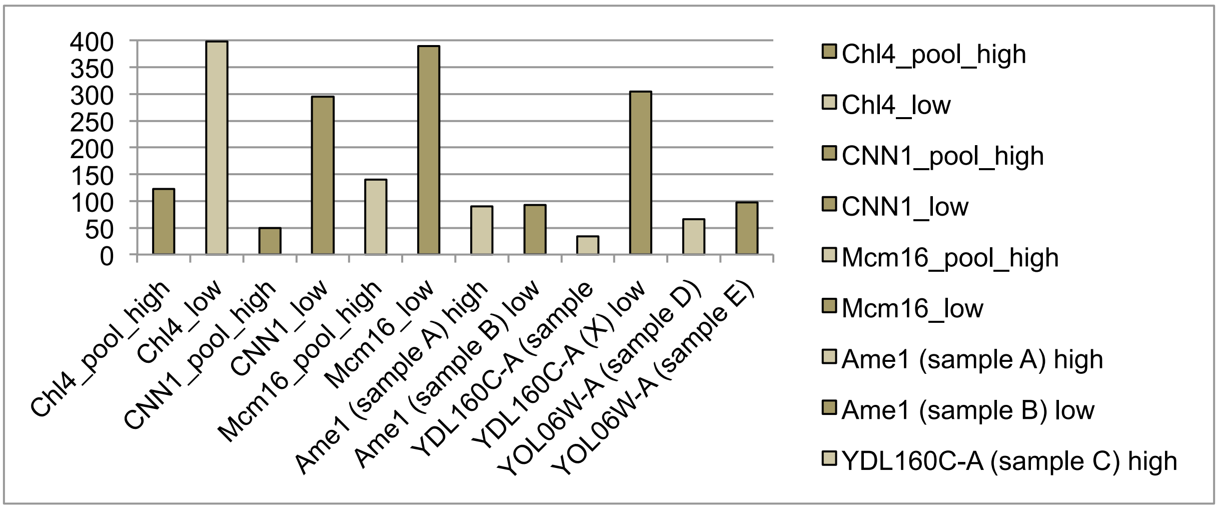

sequence coverage of the bait [%]

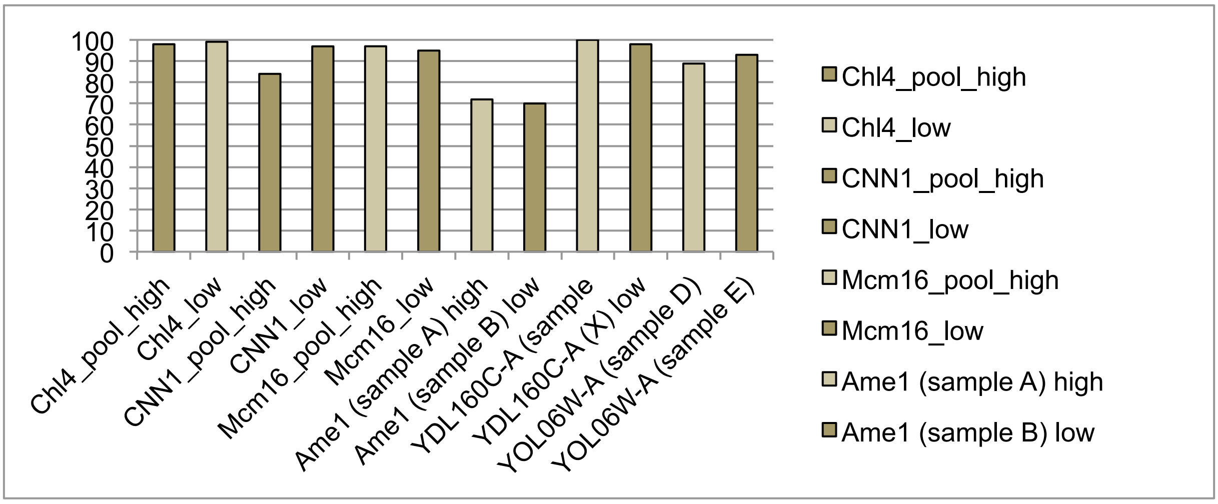

# Unique Peptides

Displays the number of peptide sequences unique to a protein group

# Peptides

Displays the number of distinct peptide sequences in the protein group

# PSMs

Displays the total number of identified peptide sequences (peptide spectrum matches) for the protein, including those redundantly identified

# Proteins

Displays the number of identified proteins in the protein group of a master protein

Coverage

Displays the percentage of the protein sequence covered by identified peptides

bait highlighted

ScCENP-U^{Ame1}, High stringency

#	Accession	ΣCoverage	Σ# Proteins	Σ# Unique Peptides	Σ# Peptides	Σ# PSMs
1	YGR179C	62,6%	1	32	32	123
2	YLR381W	44,6%	1	29	29	84
3	YBR211C	72,2%	1	29	29	276
4	YDR254W	57,4%	1	27	27	93
5	YIR010W	36,6%	1	24	24	62
6	YDL229W	32,6%	1	21	21	40
7	YDR318W	44,3%	1	21	21	56
8	YDR383C	75,6%	1	20	20	58
9	YJR135C	75,7%	1	19	19	71
10	YPL018W	43,9%	1	17	17	60
11	YBR107C	66,1%	1	17	17	50
12	YJR112W	66,2%	1	16	16	49
13	YAL034W-A	33,9%	1	15	15	32
14	YPL233W	56,0%	1	15	15	37
15	YJR045C	23,2%	1	15	15	31
16	YOR063W	29,5%	1	13	13	26
17	YPR046W	66,9%	1	13	13	47
18	YOL054W	23,2%	1	10	10	23
19	YNL178W	37,5%	1	8	8	14
20	YHR203C	28,4%	1	8	8	14
21	YDR450W	53,4%	1	8	8	17
22	YKL049C	30,1%	1	7	7	15

23	YBR118W	15,1%	1	7	7	14
24	YJL034W	12,8%	1	7	9	13
25	YCL018W	23,6%	1	7	7	14
26	YFR031C-A	30,3%	1	7	7	15
27	YKL089W	13,3%	1	6	6	11
28	YBR009C	51,5%	1	6	6	14
29	YLR315W	31,4%	1	6	6	23
30	YLL024C	39,9%	1	6	22	76
31	YDR012W	22,1%	1	6	6	12
32	YPL249C-A	41,0%	1	6	6	12
33	YPL106C	8,4%	1	6	6	10
34	YBL072C	34,5%	1	6	6	12
35	YGL234W	9,4%	1	6	6	11
36	YLL045C	24,2%	2	6	6	6
37	YHR174W	14,9%	1	5	5	14
38	YGL123W	23,2%	1	5	5	9
39	YHL015W	35,5%	1	5	5	12
40	YJR123W	22,7%	1	5	5	8
41	YGR192C	15,7%	2	5	5	8
42	YDL082W	22,6%	2	5	5	11
43	YNL301C	26,9%	1	5	5	8
44	YGR085C	23,0%	2	5	5	8
45	YBR181C	25,4%	1	5	5	12
46	YGL008C	5,6%	2	5	5	10
47	YAL005C	38,9%	1	5	21	56
48	YER074W	32,6%	1	5	5	11
49	YOL086C	16,1%	1	5	5	9
50	YDL182W	10,1%	1	4	4	7
51	YBR048W	20,5%	1	4	4	8
52	YBL002W	22,9%	2	4	4	7
53	YLR075W	20,4%	1	4	4	7
54	YDR447C	37,5%	2	4	4	8
55	YLR029C	17,2%	1	4	4	6
56	YBR189W	23,6%	1	4	4	7
57	YGR034W	29,9%	2	4	4	7
58	YDR471W	38,2%	2	4	4	14
59	YML063W	16,5%	1	4	4	7
60	YMR242C	29,1%	1	4	4	8
61	YGR159C	8,9%	1	3	3	6
62	YGL147C	12,0%	2	3	3	8
63	YBR191W	16,9%	2	3	3	6
64	YHR021C	37,8%	2	3	3	6
65	YCR031C	24,1%	2	3	3	7
66	YOL127W	23,2%	1	3	3	6
67	YKL180W	21,2%	1	3	3	8
68	YDR418W	21,8%	1	3	3	5
69	YBL087C	22,6%	1	3	3	8

70	YGR118W	18,6%	1	3	3	5
71	YOR369C	14,0%	1	2	2	4
72	YGR027C	19,4%	2	2	2	4
73	YLR448W	22,7%	1	2	4	4
74	YGL076C	6,2%	1	2	2	2
75	YER056C-A	12,4%	2	2	2	2
76	YKL054C	3,1%	1	2	2	4
77	YDL136W	11,7%	1	2	2	4
78	YDL083C	14,7%	1	2	2	6
79	YLR167W	15,8%	1	2	2	5
80	YML123C	4,6%	1	2	2	8
81	YGL031C	13,6%	2	2	2	4
82	YJL136C	27,6%	2	2	2	4
83	YPL131W	8,1%	1	2	2	4
84	YGL135W	10,1%	1	2	2	2
85	YBL092W	14,6%	1	2	2	2
86	YML073C	21,0%	1	2	4	4
87	YJL008C	2,8%	1	2	2	2
88	YOL040C	16,9%	1	2	2	3
89	YDR064W	12,6%	1	2	2	2
90	YLR325C	33,3%	1	2	2	2

ScCENP-U^{Ame1}, Low stringency

#	Accession	ΣCoverage	Σ# Proteins	Σ# Unique Peptides	Σ# Peptides	Σ# PSMs
1	YGR179C	72,2%	1	36	36	205
2	YLR381W	45,3%	1	27	27	86
3	YDR318W	68,8%	1	27	27	97
4	YBR211C	70,1%	1	26	26	252
5	YDR254W	46,1%	1	25	25	88
6	YIR010W	38,0%	1	25	25	63
7	YDR383C	77,7%	1	22	22	104
8	YJR135C	79,9%	1	20	20	77
9	YPL018W	47,7%	1	19	19	102
10	YDL229W	30,7%	1	19	19	49
11	YAL034W-A	36,7%	1	17	17	43
12	YKL089W	31,0%	1	17	17	34
13	YJR045C	27,1%	1	17	17	33
14	YOL054W	33,0%	1	17	17	41
15	YBR107C	64,9%	1	16	16	43
16	YJR112W	59,2%	1	14	14	47
17	YPL233W	56,0%	1	13	13	39
18	YHR203C	36,8%	1	11	11	23
19	YPR046W	66,9%	1	11	11	52
20	YKL049C	33,2%	1	10	10	27
21	YNL178W	42,9%	1	9	9	18

22	YOR063W	24,6%	1	9	9	24
23	YGL008C	9,5%	2	9	9	20
24	YBR009C	52,4%	1	8	8	20
25	YDL082W	34,7%	2	8	8	14
26	YLR315W	63,4%	1	8	8	57
27	YDR450W	53,4%	1	8	8	20
28	YHR174W	21,1%	1	7	7	14
29	YLR448W	38,1%	1	7	7	12
30	YDR012W	23,8%	1	7	7	13
31	YBR118W	15,1%	1	7	7	12
32	YJL008C	14,1%	1	7	7	12
33	YJL034W	16,0%	1	7	10	16
34	YFR031C-A	30,3%	1	7	7	16
35	YMR242C	36,6%	1	7	7	16
36	YPL249C-A	43,0%	1	6	6	14
37	YBR181C	30,5%	1	6	6	12
38	YGR148C	27,7%	1	6	6	9
39	YBL072C	28,5%	1	6	6	11
40	YML063W	23,5%	1	6	6	12
41	YGL123W	23,2%	1	5	5	9
42	YDL182W	11,7%	1	5	5	8
43	YJR123W	19,6%	1	5	5	11
44	YBR191W	28,8%	1	5	5	10
45	YBL002W	32,8%	2	5	5	8
46	YLL024C	36,6%	1	5	20	69
47	YLR029C	27,5%	1	5	5	10
48	YLR344W	39,4%	1	5	5	12
49	YCL018W	20,9%	1	5	5	10
50	YDR471W	38,2%	2	5	5	18
51	YLL045C	41,4%	1	5	12	23
52	YOL086C	17,5%	1	5	5	10
53	YHL015W	35,5%	1	4	4	8
54	YOR369C	33,6%	1	4	4	8
55	YGR192C	15,4%	2	4	4	6
56	YBR048W	20,5%	1	4	4	10
57	YNL301C	23,1%	1	4	4	9
58	YHR021C	46,3%	2	4	4	8
59	YDL136W	24,2%	1	4	4	7
60	YDR447C	27,2%	2	4	4	6
61	YER074W	27,4%	1	4	4	12
62	YKR092C	7,6%	1	3	3	6
63	YBL092W	22,3%	1	3	3	7
64	YLR185W	42,1%	1	3	5	11
65	YCR031C	24,1%	2	3	3	8
66	YDR064W	19,9%	1	3	3	5
67	YML123C	6,1%	1	3	3	5
68	YAL005C	32,7%	1	3	18	51

69	YOL127W	23,2%	1	3	3	6
70	YBL003C	34,1%	2	3	3	10
71	YDR418W	21,8%	1	3	3	8
72	YBL087C	22,6%	1	3	3	6
73	YGR118W	18,6%	1	3	3	6
74	YPL131W	10,8%	1	3	3	6
75	YGL135W	6,5%	1	2	2	5
76	YBR010W	11,0%	1	2	2	4
77	YJR094W-A	18,5%	1	2	2	4
78	YJL130C	0,9%	1	2	2	4
79	YGL147C	12,0%	2	2	2	4
80	YDR500C	36,4%	1	2	4	7
81	YGL076C	8,6%	1	2	2	4
82	YER056C-A	12,4%	2	2	2	2
83	YLR075W	10,9%	1	2	2	4
84	YDL083C	14,7%	1	2	2	6
85	YIL148W	14,8%	1	2	2	2
86	YJL177W	15,8%	2	2	2	6
87	YNL069C	9,1%	1	2	2	4
88	YNL302C	12,5%	2	2	2	2
89	YHR216W	6,3%	3	2	2	8
90	YIL035C	4,6%	1	2	2	2
91	YMR186W	2,8%	1	2	2	2
92	YAR010C	5,2%	44	2	2	2
93	YHL033C	29,3%	1	1	8	8

ScCENP-N^{Chl4}, High stringency

#	**Accession**	**ΣCoverage**	**Σ# Proteins**	**Σ# Unique Peptides**	**Σ# Peptides**	**Σ# PSMs**
1	YDR254W	98,3%	1	248	248	986
2	YGR179C	94,3%	1	122	122	377
3	YBR107C	99,6%	1	107	107	410
4	YLR381W	74,1%	1	105	105	266
5	YPL018W	91,3%	1	79	79	224
6	YBR211C	75,6%	1	67	67	189
7	YDR318W	85,9%	1	67	67	189
8	YJR135C	87,9%	1	61	61	205
9	YDR383C	92,0%	1	59	59	178
10	YLR259C	65,4%	1	49	49	124
11	YPR046W	90,6%	1	31	31	114
12	YBR031W	68,8%	2	27	27	70
13	YJR045C	40,1%	2	27	27	67
14	YDL229W	37,2%	2	23	24	56
15	YHR203C	67,4%	1	23	23	54
16	YBR181C	67,0%	1	22	22	50
17	YIR010W	34,7%	1	21	21	45

18	YLL024C	58,7%	1	20	51	139
19	YOR063W	39,5%	1	18	18	49
20	YBL027W	48,2%	1	18	18	50
21	YLR315W	69,9%	1	17	17	48
22	YCL018W	48,6%	1	17	17	36
23	YBR048W	69,2%	1	16	16	42
24	YFR031C-A	50,4%	1	16	16	45
25	YNL178W	58,8%	1	16	16	32
26	YBR118W	40,8%	1	15	15	33
27	YGR192C	41,6%	3	15	15	31
28	YJR123W	58,7%	1	14	14	34
29	YLR075W	53,4%	1	13	13	31
30	YBL087C	55,5%	1	13	13	70
31	YDR450W	56,9%	1	13	13	37
32	YBL072C	48,5%	1	13	13	40
33	YER074W	60,7%	1	13	13	30
34	YGL123W	39,8%	1	11	11	23
35	YAL034W-A	37,4%	1	11	11	20
36	YDL082W	35,7%	2	11	11	23
37	YCR031C	67,9%	2	11	11	41
38	YGL076C	34,4%	1	10	10	17
39	YPL131W	28,3%	1	10	10	17
40	YGL031C	39,4%	2	10	10	24
41	YGL103W	54,4%	1	10	10	34
42	YPL233W	48,2%	1	10	10	23
43	YHL015W	55,4%	1	10	10	27
44	YDL083C	55,9%	1	10	10	24
45	YGL234W	15,6%	1	10	10	22
46	YJR112W	55,2%	1	10	10	25
47	YGR027C	43,5%	2	9	9	25
48	YLR029C	32,8%	2	9	9	23
49	YNL301C	40,3%	1	9	9	19
50	YDR471W	57,4%	2	9	9	28
51	YDR447C	60,3%	2	9	9	35
52	YGL008C	11,2%	1	9	9	17
53	YMR242C	44,2%	1	9	9	22
54	YGR118W	43,5%	1	8	8	18
55	YLR441C	68,2%	1	8	22	44
56	YDL182W	21,7%	1	8	8	16
57	YJL130C	4,1%	1	8	8	17
58	YNL064C	28,6%	1	8	8	23
59	YNL302C	47,2%	2	8	8	20
60	YOL040C	40,9%	1	7	7	43
61	YPL079W	38,1%	1	7	7	16
62	YNL096C	63,7%	1	7	11	23
63	YPL249C-A	49,0%	1	7	7	24
64	YDL136W	41,7%	1	7	7	20

65	YDR261C-D	5,4%	22	7	7	15
66	YOL127W	47,9%	1	7	7	22
67	YAL005C	49,5%	1	6	37	99
68	YLL045C	59,8%	1	6	24	54
69	YLR344W	66,1%	1	6	15	29
70	YDL075W	57,5%	1	6	6	12
71	YER056C-A	42,2%	2	5	5	11
72	YBL092W	35,4%	1	5	5	12
73	YIL133C	26,6%	1	5	8	14
74	YLR167W	34,2%	1	5	5	9
75	YDR064W	30,5%	1	5	5	11
76	YPL143W	45,8%	1	5	5	8
77	YNL055C	23,0%	1	5	5	7
78	YNL069C	25,3%	1	5	8	14
79	YML063W	64,3%	1	5	19	41
80	YOR369C	30,1%	1	4	4	7
81	YDL061C	69,6%	1	4	5	9
82	YML073C	22,7%	1	4	4	11
83	YHR021C	46,3%	2	4	4	8
84	YMR230W	43,8%	2	4	4	11
85	YGR254W	10,5%	2	4	4	7
86	YJL034W	8,1%	1	4	5	9
87	YLR325C	42,3%	1	4	4	11
88	YML123C	6,0%	1	4	4	8
89	YLR044C	8,7%	1	4	4	8
90	YKL006W	21,7%	1	4	4	8
91	YOR096W	44,2%	1	4	8	19
92	YMR241W	15,0%	1	4	4	6
93	YDR418W	30,9%	1	4	4	8
94	YHR064C	9,1%	1	4	4	7
95	YKL152C	12,6%	1	3	3	7
96	YBL002W	14,5%	2	3	3	5
97	YLR388W	55,4%	1	3	4	8
98	YCL030C	5,1%	1	3	3	8
99	YAR002W	7,6%	1	3	3	5
100	YJL008C	5,8%	1	3	3	6
101	YMR246W	4,5%	1	3	3	6
102	YPR163C	7,1%	1	3	3	5
103	YMR186W	4,3%	2	3	3	8
104	YGR214W	13,1%	2	3	3	7
105	YLR287C-A	31,8%	1	3	3	5
106	YLR340W	10,6%	1	3	3	10
107	YPL081W	43,7%	1	3	9	13
108	YKL180W	54,4%	1	2	13	36
109	YDR233C	9,5%	1	2	2	2
110	YJR094W-A	29,4%	1	2	2	8
111	YGL147C	9,4%	2	2	2	6

112	YBR085W	6,2%	1	2	2	5
113	YBR189W	38,5%	1	2	8	13
114	YOR232W	7,9%	1	2	2	6
115	YFL022C	3,6%	1	2	2	4
116	YHR020W	3,3%	1	2	2	2
117	YBL003C	12,1%	2	2	2	4
118	YOL086C	6,0%	1	2	2	4
119	YDL137W	12,2%	2	2	2	2
120	YIL043C	7,0%	1	2	2	2
121	YHL033C	48,1%	1	1	19	26
122	YJL177W	54,4%	1	1	12	21

ScCENP-N^{Chl4}, Low stringency

#	Accession	ΣCoverage	Σ# Proteins	Σ# Unique Peptides	Σ# Peptides	Σ# PSMs
1	YDR254W	98,9%	1	398	398	1554
2	YBR107C	100,0%	1	147	147	575
3	YGR179C	95,1%	1	134	134	459
4	YFR031C-A	85,4%	1	91	91	253
5	YBR211C	93,5%	1	82	82	243
6	YLR381W	78,2%	1	80	80	276
7	YDR318W	94,8%	1	77	77	232
8	YJR135C	97,1%	1	75	75	277
9	YOR063W	81,1%	1	74	74	215
10	YDR383C	88,2%	1	68	68	215
11	YPL018W	84,6%	1	67	67	217
12	YGL008C	40,7%	1	65	65	172
13	YHR203C	90,4%	1	62	62	169
14	YBR118W	77,7%	1	57	57	163
15	YLR259C	73,4%	1	56	56	137
16	YLR075W	85,5%	1	54	54	141
17	YGL123W	92,1%	1	51	51	133
18	YLR029C	87,3%	1	50	50	124
19	YBR181C	96,6%	1	49	49	139
20	YBL072C	90,5%	1	49	49	136
21	YPR046W	98,3%	1	48	48	156
22	YJR045C	59,9%	1	47	47	104
23	YNL301C	87,6%	1	45	45	129
24	YGL076C	95,1%	1	44	60	163
25	YGL103W	96,6%	1	44	44	128
26	YPL131W	78,5%	1	44	44	125
27	YBR048W	96,8%	1	42	42	115
28	YOL127W	96,5%	1	41	41	116
29	YBL027W	84,7%	1	41	41	105
30	YHR010W	93,4%	2	38	38	111
31	YLR150W	78,4%	1	38	38	99

32	YPL231W	20,0%	1	38	38	87
33	YIR010W	55,2%	1	36	36	81
34	YMR242C	89,5%	1	36	36	98
35	YDL136W	81,7%	1	36	36	91
36	YBL092W	93,1%	1	34	34	92
37	YDL083C	81,8%	1	34	34	83
38	YER074W	83,7%	1	33	33	91
39	YGL135W	70,1%	1	33	34	96
40	YGR192C	68,4%	1	32	32	80
41	YDR450W	81,5%	1	32	32	96
42	YJR123W	79,6%	1	31	31	84
43	YDR064W	92,1%	1	30	30	74
44	YNL178W	80,4%	1	29	29	89
45	YKL180W	90,2%	1	29	45	110
46	YLL024C	85,6%	1	28	101	284
47	YJL130C	13,6%	1	28	28	60
48	YDR447C	86,8%	2	27	27	66
49	YDR381W	70,4%	1	27	27	59
50	YGR027C	86,1%	2	26	26	90
51	YHR174W	70,3%	1	26	50	135
52	YNL064C	57,5%	1	26	26	80
53	YAL035W	26,0%	1	26	27	61
54	YKL182W	14,3%	1	26	26	56
55	YLR044C	43,9%	1	25	25	56
56	YJL034W	38,6%	1	25	28	50
57	YMR142C	97,5%	1	24	54	127
58	YLL045C	96,9%	1	24	94	304
59	YLR340W	49,7%	1	24	24	62
60	YAL034W-A	58,5%	1	23	24	52
61	YPL233W	94,0%	1	23	23	62
62	YHL015W	74,4%	1	23	23	73
63	YHL034C	67,4%	1	23	23	53
64	YGR085C	58,1%	2	23	23	61
65	YJL190C	89,2%	2	23	23	61
66	YLR432W	65,4%	3	22	39	95
67	YLR448W	87,5%	1	22	52	123
68	YGL147C	87,4%	2	21	21	56
69	YJL191W	89,1%	2	21	21	55
70	YLR249W	20,3%	1	21	21	44
71	YDR418W	76,4%	1	21	21	65
72	YER165W	49,1%	1	21	21	53
73	YML056C	66,4%	1	21	38	95
74	YPR137C-B	23,4%	9	21	35	80
75	YPL106C	38,7%	1	21	21	47
76	YPL093W	32,6%	1	21	21	42
77	YBR079C	24,8%	1	21	21	42
78	YOL086C	47,7%	1	20	20	57

79	YOR204W	35,4%	1	20	20	42
80	YCL018W	48,9%	1	20	20	54
81	YDL229W	79,3%	1	19	77	199
82	YBL087C	65,7%	1	19	19	60
83	YDR385W	23,4%	1	19	19	38
84	YGR118W	71,7%	1	19	19	47
85	YOL040C	68,3%	1	18	18	63
86	YHL033C	93,0%	1	18	88	263
87	YBR189W	80,5%	1	18	31	65
88	YML073C	89,8%	1	18	48	116
89	YLR197W	36,7%	1	18	18	36
90	YOR341W	11,3%	1	18	18	44
91	YLR315W	77,8%	1	17	17	57
92	YBR191W	75,0%	1	17	28	56
93	YNL069C	86,9%	1	17	39	90
94	YJR094W-A	80,4%	1	17	17	44
95	YOR096W	88,4%	1	17	27	67
96	YAL038W	42,8%	1	17	17	37
97	YIL133C	89,5%	1	16	38	90
98	YGR159C	35,3%	1	16	16	39
99	YLR167W	59,2%	1	16	19	34
100	YDR224C	83,2%	2	16	16	54
101	YDR496C	25,8%	1	16	16	35
102	YPL143W	99,1%	1	15	31	68
103	YLR175W	26,1%	1	15	15	31
104	YNL112W	30,8%	1	15	15	28
105	YJR112W	63,7%	1	15	15	38
106	YDL014W	39,5%	1	14	14	33
107	YGL031C	85,8%	1	14	23	48
108	YHL001W	99,3%	1	14	33	59
109	YML063W	82,0%	1	14	39	96
110	YML123C	26,6%	1	14	14	36
111	YDL182W	37,2%	1	14	14	29
112	YMR229C	8,3%	1	14	14	29
113	YLR344W	84,3%	1	13	30	86
114	YCR012W	36,3%	1	13	13	32
115	YDL075W	81,4%	2	13	13	30
116	YOL041C	33,6%	1	13	13	33
117	YPL081W	76,1%	1	13	26	56
118	YMR012W	10,8%	1	13	13	31
119	YLR441C	80,4%	1	12	37	94
120	YGL030W	93,3%	1	12	12	38
121	YKL172W	30,9%	1	12	12	25
122	YNL175C	28,8%	1	12	12	21
123	YBR127C	25,0%	1	12	12	29
124	YHR021C	74,4%	2	11	11	23
125	YLR287C-A	96,8%	1	11	11	30

126	YDR120C	19,5%	1	11	11	23
127	YMR246W	16,9%	1	11	11	21
128	YOR310C	29,4%	1	11	11	26
129	YER025W	26,9%	1	11	11	28
130	YPL249C-A	99,0%	1	10	35	96
131	YNL302C	50,7%	2	10	10	29
132	YJL189W	58,8%	1	10	10	29
133	YNL096C	87,9%	1	10	20	53
134	YDL208W	63,5%	1	10	10	25
135	YHR020W	18,6%	1	10	10	19
136	YML061C	13,4%	1	10	10	18
137	YPL012W	8,4%	1	10	10	20
138	YAL005C	74,5%	1	9	82	216
139	YLR325C	80,8%	1	9	9	21
140	YKL054C	13,0%	1	9	9	22
141	YFR032C-A	89,8%	1	9	9	21
142	YHR089C	28,3%	1	9	9	16
143	YER006W	20,8%	1	9	9	16
144	YPL237W	41,4%	1	9	9	25
145	YDL061C	73,2%	1	8	9	21
146	YLR061W	72,7%	1	8	9	21
147	YML074C	21,4%	1	8	10	20
148	YEL026W	54,8%	1	8	8	18
149	YDR052C	12,8%	1	8	8	14
150	YCL037C	25,4%	1	8	8	19
151	YGR103W	14,7%	1	8	9	19
152	YDR365C	15,6%	1	8	8	20
153	YNL248C	19,8%	1	8	8	18
154	YGR240C	10,1%	1	8	8	19
155	YGL195W	3,0%	1	8	8	15
156	YBR084W	8,7%	1	8	8	15
157	YHR027C	9,5%	1	8	8	15
158	YJL012C	10,7%	1	7	7	16
159	YJL148W	33,5%	1	7	7	12
160	YLR264W	67,2%	2	7	7	14
161	YBR009C	62,1%	1	7	7	13
162	YLR185W	88,6%	1	7	20	52
163	YHR052W	15,2%	1	7	7	15
164	YOL077C	24,7%	1	7	7	16
165	YBR196C	10,7%	1	7	7	17
166	YDL031W	7,0%	1	7	7	11
167	YHR146W	21,7%	1	7	7	12
168	YMR290C	14,3%	1	7	7	14
169	YLR196W	12,9%	1	7	7	16
170	YKL152C	25,5%	1	7	7	16
171	YOR361C	8,5%	1	7	7	12
172	YGL206C	4,6%	1	7	7	15

173	YDL126C	9,6%	1	7	7	12
174	YFL039C	24,5%	1	7	7	16
175	YNL132W	6,3%	1	7	7	16
176	YBL003C	62,9%	2	6	6	16
177	YDR233C	22,0%	1	6	6	12
178	YLL008W	9,0%	1	6	6	15
179	YBR010W	46,3%	1	6	6	8
180	YGL173C	4,1%	1	6	6	10
181	YDR382W	55,5%	1	6	6	16
182	YDR500C	87,5%	1	6	19	50
183	YLR449W	23,5%	1	6	9	23
184	YOR294W	45,8%	1	6	6	16
185	YNR053C	11,5%	1	6	6	11
186	YML028W	30,6%	1	6	6	10
187	YMR146C	15,9%	1	6	6	12
188	YKL060C	29,0%	1	6	6	14
189	YNL007C	22,4%	1	6	6	14
190	YPR010C	4,7%	1	6	6	11
191	YJL008C	12,0%	1	6	6	14
192	YBL030C	18,9%	1	6	6	14
193	YPL217C	5,3%	1	6	6	12
194	YNR016C	3,5%	1	6	6	12
195	YDL195W	6,4%	1	6	7	13
196	YHR064C	17,3%	1	6	6	14
197	YIL052C	85,1%	1	5	24	56
198	YMR194W	99,0%	1	5	30	85
199	YOR293W	76,2%	1	5	12	37
200	YHR066W	14,6%	1	5	5	8
201	YIL148W	30,5%	1	5	8	12
202	YOR369C	43,4%	1	5	5	12
203	YBR221C	14,5%	1	5	5	9
204	YKR001C	7,4%	1	5	5	8
205	YDR429C	20,4%	1	5	5	9
206	YNL002C	13,4%	1	5	5	13
207	YGR233C	4,3%	1	5	5	12
208	YFL037W	12,7%	1	5	5	11
209	YOL054W	14,0%	1	5	5	14
210	YJR121W	13,1%	1	5	5	12
211	YHR190W	11,3%	1	5	5	12
212	YGR090W	3,7%	1	5	5	10
213	YGL234W	6,5%	1	5	5	9
214	YBL099W	8,8%	1	5	5	14
215	YMR186W	37,7%	1	4	30	64
216	YNL209W	77,5%	1	4	60	159
217	YHR141C	42,5%	1	4	4	8
218	YNL110C	24,1%	1	4	4	11
219	YDL081C	50,0%	1	4	4	6

220	YDL130W	32,1%	1	4	4	9
221	YBR078W	12,0%	1	4	4	8
222	YNL113W	30,3%	1	4	4	12
223	YDL082W	88,4%	1	4	34	57
224	YAL003W	22,3%	1	4	4	6
225	YHR072W-A	67,2%	1	4	4	9
226	YFR001W	27,0%	1	4	4	12
227	YCL059C	12,0%	1	4	4	8
228	YER126C	12,3%	1	4	4	7
229	YNR051C	12,8%	1	4	4	9
230	YNL308C	9,1%	1	4	4	12
231	YHR127W	17,7%	1	4	4	6
232	YLR388W	67,9%	1	4	5	10
233	YGR185C	10,9%	1	4	4	7
234	YKL082C	8,3%	1	4	4	9
235	YJL014W	7,7%	1	4	4	8
236	YHR007C	10,2%	1	4	4	8
237	YOL139C	23,0%	1	4	4	8
238	YLR276C	7,4%	1	4	4	7
239	YLR303W	10,1%	1	4	4	7
240	YKL081W	8,5%	1	4	4	7
241	YGL078C	10,9%	1	4	4	8
242	YNL255C	26,1%	1	4	4	6
243	YGR214W	23,0%	2	4	4	8
244	YPL127C	17,8%	1	4	4	8
245	YOR217W	4,4%	1	4	4	7
246	YBR086C	4,6%	1	4	4	7
247	YBR031W	91,4%	1	3	84	234
248	YOR234C	85,1%	1	3	19	36
249	YMR230W	73,3%	1	3	10	30
250	YOL039W	49,1%	1	3	3	11
251	YGL189C	63,9%	1	3	15	56
252	YDR098C-A	24,6%	2	3	13	14
253	YGR148C	48,4%	1	3	12	22
254	YNL088W	2,2%	1	3	3	6
255	YML072C	2,0%	1	3	3	6
256	YOR206W	4,4%	1	3	3	6
257	YPL019C	4,2%	1	3	3	5
258	YMR309C	4,6%	1	3	3	8
259	YDR033W	10,3%	1	3	3	6
260	YOR117W	7,6%	1	3	3	3
261	YHR183W	5,9%	1	3	3	8
262	YDR238C	3,3%	1	3	3	5
263	YHR047C	3,5%	1	3	3	6
264	YMR108W	6,7%	1	3	3	6
265	YBR142W	2,5%	1	3	3	7
266	YHR088W	8,1%	1	3	3	8

267	YIL078W	3,8%	1	3	3	6
268	YNL071W	6,2%	1	3	3	6
269	YIL035C	8,9%	1	3	3	6
270	YGR162W	3,3%	1	3	3	7
271	YPL061W	6,8%	1	3	3	6
272	YER120W	15,2%	1	3	3	6
273	YGL099W	4,1%	1	3	3	7
274	YCL030C	4,1%	1	3	3	6
275	YGR264C	3,6%	1	3	3	6
276	YOR260W	6,1%	1	3	3	7
277	YHR143W-A	51,4%	1	3	3	6
278	YPL043W	5,6%	1	3	3	8
279	YHR019C	6,7%	1	3	3	5
280	YMR116C	11,9%	1	3	3	6
281	YNL287W	3,0%	1	3	3	6
282	YFR037C	7,4%	1	3	3	6
283	YFR051C	5,5%	1	3	3	5
284	YDR170C	1,6%	1	3	3	6
285	YER110C	3,1%	1	3	3	8
286	YDR050C	15,3%	1	3	3	7
287	YDR190C	8,0%	1	3	3	5
288	YER177W	10,5%	2	3	3	5
289	YHR039C	5,6%	1	3	3	3
290	YGR083C	5,4%	1	3	3	6
291	YGL019W	14,0%	1	3	3	6
292	YLR398C	2,7%	1	3	3	5
293	YDR194C	6,0%	1	3	3	7
294	YGL137W	4,2%	1	3	3	8
295	YDL213C	17,8%	1	3	3	6
296	YER056C-A	85,1%	1	2	21	43
297	YDR012W	90,9%	1	2	83	228
298	YGL171W	5,1%	1	2	2	4
299	YDR174W	11,8%	1	2	2	4
300	YGR054W	7,0%	1	2	2	2
301	YER082C	5,1%	1	2	2	4
302	YGR027W-A	48,6%	1	2	28	37
303	YER131W	63,9%	1	2	14	36
304	YKL006W	65,2%	1	2	21	36
305	YJL177W	69,6%	1	2	18	33
306	YGR178C	3,6%	1	2	2	6
307	YMR024W	5,6%	1	2	2	4
308	YKR081C	4,9%	1	2	2	4
309	YKR046C	7,8%	1	2	2	2
310	YKL173W	2,7%	1	2	2	4
311	YHL007C	2,3%	1	2	2	6
312	YPR041W	5,9%	1	2	2	4
313	YPR028W	8,9%	1	2	2	6

314	YKR008W	5,4%	1	2	2	2
315	YGL105W	5,3%	1	2	2	2
316	YOR001W	2,1%	1	2	2	2
317	YLL018C	2,7%	1	2	2	5
318	YNL138W	3,4%	1	2	2	4
319	YPR110C	6,3%	1	2	2	4
320	YPL266W	6,6%	1	2	2	4
321	YDL007W	5,5%	1	2	2	4
322	YBR039W	7,7%	1	2	2	4
323	YOR004W	8,3%	1	2	2	6
324	YDR298C	10,4%	1	2	2	4
325	YBL076C	1,7%	1	2	2	2
326	YHR193C	20,7%	1	2	2	3
327	YJR104C	13,0%	1	2	2	4
328	YFL045C	6,3%	1	2	2	2
329	YNL189W	3,9%	1	2	2	6
330	YDL137W	12,2%	2	2	2	4
331	YHR068W	4,1%	1	2	2	2
332	YJR077C	8,4%	1	2	2	4
333	YIL038C	2,3%	1	2	2	4
334	YJL041W	5,2%	1	2	2	4
335	YPL235W	4,9%	1	2	2	4
336	YDR510W	17,8%	1	2	2	4
337	YOR259C	3,7%	1	2	2	4
338	YPL226W	1,8%	1	2	2	4
339	YMR128W	1,7%	1	2	2	4
340	YBR154C	7,9%	1	2	2	4
341	YDR101C	4,2%	1	2	2	4
342	YDR377W	19,8%	1	2	2	2
343	YJR070C	10,8%	1	2	2	4
344	YGL014W	2,6%	1	2	2	4
345	YPL146C	3,1%	1	2	2	2
346	YPR183W	6,4%	1	2	2	5
347	YLR430W	0,8%	1	2	2	2
348	YNL005C	6,7%	1	2	2	4
349	YNL137C	3,5%	1	2	2	5
350	YGR165W	8,1%	1	2	2	4
351	YGR220C	8,6%	1	2	2	5
352	YDL053C	12,4%	1	2	2	4
353	YOR272W	4,4%	1	2	2	6
354	YMR105C	3,5%	2	2	2	4
355	YJL080C	1,8%	1	2	2	2
356	YCR016W	11,4%	1	2	2	4
357	YLR384C	1,6%	1	2	2	2
358	YMR072W	10,4%	1	2	2	2
359	YPR163C	8,3%	1	2	2	2
360	YOR375C	7,3%	1	2	2	4

361	YER029C	11,2%	1	2	2	4
362	YMR307W	4,1%	1	2	2	6
363	YNL055C	6,4%	1	2	2	2
364	YLR342W	1,4%	2	2	2	4
365	YGL129C	3,7%	1	2	2	4
366	YDR342C	4,9%	1	2	2	2
367	YLR355C	5,3%	1	2	2	4
368	YMR205C	2,3%	1	2	2	3
369	YKL145W	4,1%	1	2	2	5
370	YIL075C	2,2%	1	2	2	4
371	YER178W	5,0%	1	2	2	4
372	YDR155C	14,8%	1	2	2	2
373	YLR056W	4,7%	1	2	2	6
374	YOR056C	4,6%	1	2	2	6
375	YMR241W	5,4%	1	2	2	2
376	YJL136C	27,6%	2	2	2	8
377	YML008C	7,1%	1	2	2	4
378	YJL122W	9,1%	1	2	2	4
379	YPL110C	1,6%	1	2	2	2
380	YER151C	3,2%	1	2	2	2
381	YGR175C	3,6%	1	2	2	2
382	YMR145C	3,6%	1	2	2	2
383	YIL093C	8,3%	1	2	2	2
384	YFL022C	4,0%	1	2	2	2
385	YLR180W	8,6%	1	2	2	2
386	YOR340C	6,8%	1	2	2	2
387	YCL031C	6,7%	1	2	2	3
388	YOR086C	1,9%	1	2	2	2
389	YGR034W	72,4%	1	1	18	51
390	YPL240C	36,5%	1	1	28	58
391	YMR185W	2,2%	1	1	2	2
392	YGR254W	46,0%	1	1	25	35
393	YJR028W	47,3%	1	1	16	23
394	YPL079W	45,6%	1	1	12	26
395	YPL198W	44,3%	1	1	17	19
396	YGR027W-B	6,5%	1	1	16	18
397	YFL034C-A	23,0%	1	1	2	2
398	YKR048C	7,7%	1	1	2	2

ScCENP-H^{Mcm16}, High stringency

#	Accession	ΣCoverage	Σ# Proteins	Σ# Unique Peptides	Σ# Peptides	Σ# PSMs
1	YLR381W	80,6%	1	143	143	409
2	YJR135C	100,0%	1	122	122	556
3	YGR179C	92,9%	1	112	112	361
4	YDR254W	81,4%	1	93	93	256

5	YDR318W	87,0%	1	75	75	204
6	YPL018W	89,4%	1	70	70	196
7	YPR046W	96,7%	1	70	70	361
8	YBR211C	79,3%	1	65	65	197
9	YDR383C	90,8%	1	49	49	145
10	YBR107C	88,2%	1	42	42	101
11	YIR010W	59,6%	1	40	40	108
12	YNL178W	74,6%	1	24	24	55
13	YCL018W	61,5%	1	24	24	57
14	YGR192C	49,7%	1	23	23	59
15	YBR181C	66,1%	1	23	23	58
16	YAL034W-A	52,9%	1	23	23	59
17	YPL233W	83,3%	1	21	21	68
18	YBR031W	52,8%	2	20	20	49
19	YBR118W	40,4%	1	19	19	49
20	YDR450W	64,4%	1	18	18	48
21	YHR203C	50,2%	1	17	17	44
22	YDL229W	31,7%	2	17	17	39
23	YJL008C	29,6%	1	16	16	31
24	YGL245W	23,2%	1	16	16	31
25	YLR075W	57,5%	1	15	15	32
26	YGL123W	52,8%	1	15	15	31
27	YDL182W	40,9%	1	15	15	31
28	YKL180W	66,3%	2	14	14	38
29	YOR063W	34,4%	1	14	14	34
30	YJR045C	21,4%	1	13	13	28
31	YJR112W	57,2%	1	13	13	38
32	YJL191W	71,7%	2	11	11	27
33	YBL087C	51,1%	1	11	11	29
34	YLR315W	55,6%	1	11	11	31
35	YJR123W	51,6%	1	11	11	28
36	YBL027W	37,6%	1	11	11	32
37	YLR180W	33,3%	1	10	10	19
38	YER074W	48,9%	1	10	10	31
39	YGL234W	16,2%	1	10	10	24
40	YOR293W	82,9%	2	9	9	26
41	YLL024C	43,8%	1	9	27	69
42	YLR167W	50,0%	3	9	9	22
43	YGL031C	39,4%	2	9	9	23
44	YFR031C-A	30,3%	1	9	9	23
45	YBL072C	40,5%	1	9	9	24
46	YHL015W	55,4%	1	9	9	30
47	YGL105W	31,4%	1	9	9	21
48	YBR048W	42,3%	1	9	9	24
49	YLR344W	47,2%	2	9	9	22
50	YHR064C	20,1%	1	9	9	21
51	YMR242C	47,7%	1	9	9	21

52	YHR010W	47,1%	2	8	8	26
53	YBR191W	36,3%	1	8	8	16
54	YDL082W	32,7%	2	8	8	16
55	YGL103W	39,6%	1	8	8	24
56	YDR447C	53,7%	2	8	8	22
57	YMR186W	12,2%	2	8	8	15
58	YHR174W	19,0%	1	7	7	14
59	YJL130C	3,6%	1	7	7	14
60	YNL064C	23,5%	1	7	7	18
61	YCL030C	8,6%	1	7	7	15
62	YPL249C-A	50,0%	1	7	7	15
63	YMR246W	13,7%	1	7	7	13
64	YFL022C	14,5%	1	7	7	14
65	YML123C	11,4%	1	7	7	15
66	YLR044C	15,6%	1	7	7	20
67	YPL131W	18,9%	1	6	6	11
68	YKL152C	25,5%	1	6	6	13
69	YHR047C	6,4%	1	6	6	11
70	YGL076C	29,9%	1	6	6	13
71	YNL301C	31,7%	1	6	6	13
72	YHR021C	50,0%	2	6	6	11
73	YBL030C	16,0%	1	6	6	16
74	YDR064W	35,1%	1	6	6	14
75	YFL037W	15,3%	1	6	6	11
76	YMR241W	21,7%	1	6	6	12
77	YLR340W	21,8%	1	6	6	12
78	YOR369C	33,6%	1	5	5	11
79	YLR388W	69,6%	1	5	6	14
80	YDR385W	7,0%	1	5	5	11
81	YIL133C	35,7%	1	5	8	17
82	YDL083C	43,4%	1	5	5	17
83	YLR029C	25,5%	1	5	5	16
84	YBR127C	11,8%	1	5	5	10
85	YGL008C	8,0%	2	5	5	12
86	YPL143W	33,6%	1	5	5	9
87	YHR020W	6,4%	1	5	5	7
88	YLR441C	66,7%	1	5	19	46
89	YDR418W	42,4%	1	5	5	15
90	YGR118W	25,5%	1	5	5	8
91	YLL045C	19,1%	2	5	5	5
92	YAL005C	36,9%	1	4	22	54
93	YKL120W	12,7%	1	4	4	8
94	YNL096C	35,3%	1	4	6	10
95	YDL136W	22,5%	1	4	4	12
96	YHR019C	10,5%	1	4	4	9
97	YGR240C	3,6%	1	4	4	7
98	YBR189W	23,6%	1	4	4	9

99	YNL069C	25,8%	1	4	7	18
100	YOR096W	35,8%	1	4	6	14
101	YML063W	66,3%	1	4	18	44
102	YOL086C	12,6%	1	4	4	8
103	YMR146C	11,0%	1	3	3	4
104	YGL147C	12,0%	2	3	3	8
105	YGR027C	22,2%	2	3	3	9
106	YDL007W	8,5%	1	3	3	6
107	YBL092W	20,0%	1	3	3	5
108	YOL040C	24,7%	1	3	3	10
109	YLR250W	12,0%	1	3	3	7
110	YLR325C	42,3%	1	3	3	8
111	YGR218W	3,3%	1	3	3	8
112	YLR287C-A	30,2%	1	3	3	8
113	YIL043C	10,9%	1	3	3	8
114	YAR010C	8,6%	44	3	3	8
115	YDL075W	23,9%	2	3	3	3
116	YGR234W	6,8%	1	2	2	4
117	YGL135W	6,5%	1	2	2	4
118	YJR094W-A	29,4%	1	2	2	8
119	YER131W	20,2%	2	2	2	4
120	YDL061C	51,8%	1	2	3	6
121	YER056C-A	20,7%	2	2	2	6
122	YAL042W	4,3%	1	2	2	4
123	YJR070C	8,0%	1	2	2	4
124	YML124C	7,4%	1	2	2	4
125	YGR085C	13,8%	2	2	2	4
126	YJL014W	4,1%	1	2	2	2
127	YGL068W	12,4%	1	2	2	4
128	YER110C	2,1%	1	2	2	4
129	YBR014C	10,3%	1	2	2	4
130	YNL055C	8,8%	1	2	2	4
131	YOL127W	15,5%	1	2	2	4
132	YJL189W	21,6%	1	2	2	2
133	YDR190C	5,0%	1	2	2	4
134	YBL003C	12,1%	2	2	2	4
135	YBR106W	14,9%	1	2	2	6
136	YFL039C	7,5%	1	2	2	4
137	YFR046C	5,5%	1	2	2	4
138	YBR291C	6,4%	1	2	2	4
139	YNL302C	13,2%	2	2	2	4
140	YGR214W	8,3%	2	2	2	4

ScCENP-H^{Mcm16}, Low stringency

#	Accession	ΣCoverage	Σ# Proteins	Σ# Unique Peptides	Σ# Peptides	Σ# PSMs

1	YGR179C	97,5%	1	192	192	657
2	YJR135C	97,9%	1	177	178	772
3	YDR254W	98,3%	1	171	171	529
4	YLR381W	92,8%	1	155	155	570
5	YDR318W	96,7%	1	123	123	386
6	YPR046W	95,0%	1	103	104	459
7	YBR211C	92,0%	1	102	102	328
8	YDR383C	94,5%	1	96	96	303
9	YPL018W	86,5%	1	94	94	283
10	YBR118W	79,5%	1	73	73	216
11	YIR010W	73,6%	1	64	64	158
12	YGL008C	43,6%	1	64	64	159
13	YBR107C	94,3%	1	60	60	161
14	YJR045C	68,8%	1	58	58	136
15	YAL034W-A	70,9%	1	47	47	117
16	YHR174W	87,0%	1	46	73	189
17	YPL233W	97,7%	1	44	44	123
18	YFR031C-A	81,9%	1	44	44	115
19	YOR063W	68,0%	1	43	43	118
20	YDR385W	42,0%	1	41	41	90
21	YPL231W	22,2%	1	40	40	79
22	YNL178W	85,4%	1	37	37	102
23	YLR044C	61,5%	1	36	36	102
24	YGL076C	82,4%	1	36	36	84
25	YLR249W	30,7%	1	36	36	80
26	YHR203C	78,9%	1	34	34	97
27	YJL130C	16,4%	1	33	34	72
28	YBR181C	79,2%	1	32	32	84
29	YGR192C	72,3%	1	32	42	110
30	YAL038W	62,4%	1	32	32	69
31	YMR142C	87,9%	2	31	31	80
32	YPL131W	63,3%	1	31	31	73
33	YJL008C	50,2%	1	31	31	71
34	YCL018W	70,3%	1	31	31	74
35	YJR112W	83,6%	1	31	31	82
36	YHL015W	74,4%	1	29	29	92
37	YDR450W	73,3%	1	29	29	88
38	YLR259C	46,7%	1	29	29	63
39	YLL045C	91,8%	1	28	63	162
40	YLR315W	86,9%	1	27	27	76
41	YJR123W	82,2%	1	27	27	77
42	YLR075W	74,2%	1	26	26	65
43	YOL086C	65,2%	1	26	29	77
44	YNL064C	54,5%	1	25	25	81
45	YPL106C	36,7%	1	25	25	54
46	YHR010W	84,6%	2	24	24	74
47	YLL024C	89,1%	1	24	103	303

48	YGL103W	85,9%	1	24	24	69
49	YGL123W	78,0%	1	24	24	56
50	YHR064C	43,1%	1	24	24	52
51	YGL105W	52,1%	1	24	24	62
52	YLR029C	65,2%	1	23	23	63
53	YGL245W	33,1%	1	23	23	54
54	YHR020W	36,3%	1	23	23	41
55	YOL127W	83,1%	1	22	22	56
56	YFR046C	46,5%	1	21	21	41
57	YNL301C	70,4%	1	21	21	45
58	YLR340W	45,2%	1	21	21	54
59	YBL072C	80,0%	1	21	21	56
60	YDL083C	78,3%	1	21	21	52
61	YBR079C	22,5%	1	21	21	44
62	YMR246W	30,1%	1	21	21	42
63	YCR012W	51,7%	1	21	21	44
64	YLR150W	65,2%	1	21	21	50
65	YKL180W	85,3%	1	21	21	62
66	YGR027C	75,9%	2	20	20	54
67	YBL027W	66,1%	1	20	20	56
68	YGR085C	55,2%	2	20	20	51
69	YDR447C	81,6%	2	20	20	45
70	YBR127C	40,2%	1	20	20	46
71	YJL034W	32,7%	1	20	22	47
72	YKL182W	8,9%	1	20	20	41
73	YMR186W	48,8%	1	19	45	97
74	YBL087C	62,0%	1	19	19	62
75	YJL191W	91,3%	2	19	19	49
76	YER074W	80,0%	1	19	19	47
77	YDL136W	62,5%	1	19	19	38
78	YML061C	26,3%	1	19	19	37
79	YGL135W	54,8%	1	19	19	44
80	YNR016C	8,8%	1	19	19	39
81	YDR261C-D	15,2%	9	19	19	49
82	YDR418W	61,8%	1	18	18	48
83	YGR159C	38,7%	1	17	17	40
84	YBR048W	72,4%	1	17	17	42
85	YHL034C	58,5%	1	17	17	45
86	YDR224C	83,2%	2	16	16	41
87	YKL054C	26,2%	1	16	16	32
88	YJL190C	86,2%	2	16	16	37
89	YOL054W	31,3%	1	16	16	41
90	YAL005C	82,6%	1	16	95	242
91	YML123C	27,6%	1	16	16	37
92	YDR064W	78,8%	1	16	16	27
93	YMR242C	71,5%	1	15	15	37
94	YPL143W	76,6%	2	15	15	28

95	YOL040C	70,4%	1	15	15	41
96	YAL035W	16,1%	1	15	15	39
97	YOR096W	81,1%	1	15	23	53
98	YDR052C	21,2%	1	15	15	32
99	YHR027C	17,1%	1	15	15	31
100	YML073C	74,4%	1	14	25	59
101	YBL092W	79,2%	1	14	14	29
102	YLR180W	49,2%	2	14	14	29
103	YGR038C-B	11,5%	1	14	16	46
104	YHR021C	63,4%	2	13	13	32
105	YML063W	75,7%	1	13	31	74
106	YOR204W	20,2%	1	13	13	28
107	YER165W	28,8%	1	13	13	29
108	YPL079W	50,0%	2	12	12	22
109	YNL302C	58,3%	2	12	12	32
110	YLR287C-A	87,3%	1	11	11	25
111	YFL037W	28,0%	1	11	11	24
112	YBR189W	70,3%	1	11	21	43
113	YKL060C	44,3%	1	11	11	21
114	YGL147C	54,5%	2	11	11	23
115	YDL014W	32,1%	1	11	11	24
116	YKL152C	40,1%	1	11	11	26
117	YBR196C	23,7%	1	11	11	23
118	YIL078W	13,6%	1	11	11	21
119	YJL041W	26,3%	1	11	11	21
120	YGR240C	12,7%	1	11	11	24
121	YFL022C	21,7%	1	11	11	20
122	YHR107C	28,0%	1	11	11	21
123	YGR118W	57,2%	1	11	11	23
124	YDL075W	62,8%	2	10	10	22
125	YLR061W	72,7%	1	10	10	28
126	YHR047C	11,3%	1	10	10	19
127	YEL034W	52,2%	1	10	10	20
128	YLR448W	76,1%	1	10	21	44
129	YNL069C	52,5%	1	10	14	31
130	YDR050C	43,2%	1	10	10	26
131	YGR214W	33,7%	2	10	10	24
132	YGL189C	54,6%	2	9	9	28
133	YDR381W	32,3%	1	9	9	21
134	YJL136C	66,7%	2	9	9	24
135	YBR072W	50,5%	1	9	9	18
136	YDL182W	59,1%	1	9	23	48
137	YOR361C	12,8%	1	9	9	15
138	YOR341W	6,9%	1	9	9	24
139	YPL249C-A	83,0%	1	9	15	48
140	YHR019C	17,9%	1	9	9	21
141	YHR007C	23,0%	1	9	9	15

142	YER025W	23,3%	1	9	9	22
143	YKL081W	21,8%	1	9	9	19
144	YMR205C	9,6%	1	9	9	16
145	YDL185W	9,4%	1	9	9	16
146	YGL234W	13,2%	1	9	9	20
147	YOR293W	77,1%	1	8	15	43
148	YOR369C	46,9%	1	8	8	22
149	YDL126C	11,3%	1	8	8	12
150	YDR233C	23,4%	1	8	8	20
151	YJR094W-A	64,1%	1	8	8	20
152	YMR229C	5,2%	1	8	8	18
153	YNL096C	74,7%	1	8	16	39
154	YJR070C	30,2%	1	8	8	16
155	YJL014W	15,4%	1	8	8	17
156	YBL030C	28,0%	1	8	8	15
157	YLR197W	17,5%	1	8	8	17
158	YML028W	44,9%	1	8	8	18
159	YNL209W	81,6%	1	7	70	175
160	YDL061C	73,2%	1	7	9	22
161	YDR382W	63,6%	1	7	7	16
162	YGR234W	20,6%	1	7	7	14
163	YBR009C	52,4%	1	7	7	16
164	YIL148W	43,0%	1	7	11	20
165	YLR264W	79,1%	2	7	7	12
166	YDR037W	11,0%	1	7	7	19
167	YLR355C	19,0%	1	7	7	18
168	YMR072W	31,2%	1	6	6	6
169	YDR238C	6,6%	1	6	6	11
170	YGL030W	61,9%	1	6	6	15
171	YLR175W	13,3%	1	6	6	10
172	YHR193C	42,5%	1	6	6	17
173	YMR012W	4,0%	1	6	6	12
174	YLR388W	71,4%	1	6	8	13
175	YHL030W	3,9%	1	6	6	12
176	YHL033C	81,3%	1	6	41	105
177	YCL030C	9,4%	1	6	6	16
178	YLR167W	57,9%	1	6	10	20
179	YGL195W	2,1%	1	6	6	10
180	YPR163C	20,4%	1	6	6	16
181	YLR303W	18,5%	1	6	6	11
182	YHR190W	14,9%	1	6	6	16
183	YNL085W	7,6%	1	6	6	12
184	YLR441C	67,8%	1	6	24	47
185	YNL132W	4,8%	1	6	6	13
186	YJL012C	9,3%	1	6	6	12
187	YCL037C	23,3%	1	6	6	14
188	YGR034W	87,4%	1	5	25	47

189	YLR185W	69,3%	1	5	13	31
190	YDL229W	83,0%	1	5	68	125
191	YFR032C-A	57,6%	1	5	5	13
192	YMR146C	13,5%	1	5	5	12
193	YGL206C	3,1%	1	5	5	9
194	YML056C	22,5%	1	5	9	26
195	YNL248C	12,3%	1	5	5	10
196	YPL235W	12,1%	1	5	5	10
197	YPL061W	10,4%	1	5	5	9
198	YGR282C	18,2%	1	5	5	10
199	YDR496C	6,4%	1	5	5	12
200	YOL139C	27,7%	1	5	5	12
201	YDR170C	2,5%	1	5	5	8
202	YJR121W	12,5%	1	5	5	10
203	YJL189W	43,1%	1	5	5	10
204	YFL039C	15,5%	1	5	5	16
205	YML008C	14,6%	1	5	5	13
206	YBL099W	8,3%	1	5	5	12
207	YDR374W-A	62,9%	1	5	5	11
208	YAL003W	19,9%	1	4	4	8
209	YOL039W	34,9%	1	4	4	10
210	YDR500C	67,1%	1	4	12	26
211	YKR046C	17,0%	1	4	4	8
212	YPL019C	5,2%	1	4	4	8
213	YNL007C	13,9%	1	4	4	9
214	YMR108W	7,7%	1	4	4	7
215	YNL071W	9,3%	1	4	4	8
216	YKR001C	6,5%	1	4	4	8
217	YER120W	21,3%	1	4	4	10
218	YML111W	4,0%	1	4	4	7
219	YML124C	10,6%	2	4	4	7
220	YIL142W	9,9%	1	4	4	10
221	YMR116C	14,7%	1	4	4	8
222	YDR023W	11,9%	1	4	4	6
223	YKL145W	8,8%	1	4	4	9
224	YOL004W	3,0%	1	4	4	8
225	YOR317W	6,7%	1	4	4	7
226	YMR241W	12,7%	1	4	4	6
227	YNR050C	8,7%	1	4	4	7
228	YHR146W	12,0%	1	4	4	8
229	YDL195W	3,9%	1	4	4	7
230	YLR325C	42,3%	1	4	4	7
231	YEL026W	27,0%	1	4	4	6
232	YBR010W	26,5%	1	4	4	11
233	YBR031W	75,1%	1	3	38	90
234	YDL208W	26,3%	1	3	3	5
235	YDR365W-A	35,0%	5	3	17	19

236	YDR188W	5,1%	1	3	3	6
237	YML072C	2,7%	1	3	3	6
238	YHL007C	3,8%	1	3	3	8
239	YMR309C	3,9%	1	3	3	6
240	YPR041W	8,9%	1	3	3	8
241	YDR033W	10,3%	1	3	3	6
242	YLR432W	18,0%	1	3	7	20
243	YHR183W	7,2%	1	3	3	6
244	YOL109W	31,0%	1	3	3	6
245	YLL018C	4,3%	1	3	3	8
246	YBR221C	10,1%	1	3	3	7
247	YDL052C	13,9%	1	3	3	5
248	YNL112W	5,9%	1	3	3	7
249	YDL137W	16,6%	2	3	3	8
250	YJR077C	10,6%	1	3	3	6
251	YGR175C	7,1%	1	3	3	6
252	YOR259C	5,7%	1	3	3	6
253	YOR151C	2,9%	1	3	3	6
254	YPR010C	2,4%	1	3	3	5
255	YMR128W	2,5%	1	3	3	5
256	YGR185C	8,9%	1	3	3	5
257	YOR310C	5,5%	1	3	3	5
258	YGL173C	2,1%	1	3	3	5
259	YIL133C	28,1%	1	3	7	13
260	YGR135W	12,4%	1	3	3	5
261	YGL148W	8,2%	1	3	3	5
262	YPL237W	11,6%	1	3	3	6
263	YCR087C-A	20,3%	1	3	3	5
264	YER110C	2,3%	1	3	3	6
265	YDR158W	7,7%	1	3	3	5
266	YLR449W	8,2%	1	3	3	7
267	YDR190C	8,2%	1	3	3	6
268	YGR285C	7,6%	1	3	3	5
269	YER178W	8,1%	1	3	3	6
270	YLR056W	7,1%	1	3	3	5
271	YKL172W	6,6%	1	3	3	6
272	YPR108W	6,1%	1	3	3	8
273	YJR109C	3,9%	1	3	4	7
274	YGL026C	5,5%	1	3	3	3
275	YER151C	4,5%	1	3	3	6
276	YBR086C	3,7%	1	3	3	7
277	YBR078W	5,6%	1	3	3	6
278	YHR141C	32,1%	1	3	3	5
279	YDL130W	28,3%	1	3	3	8
280	YGR148C	51,6%	1	2	12	22
281	YGL031C	51,6%	1	2	12	23
282	YGR253C	9,6%	1	2	2	2

283	YDR261C-C	33,2%	1	2	16	17
284	YDR174W	9,8%	1	2	2	2
285	YPL240C	36,7%	1	2	28	52
286	YIL115C	1,4%	1	2	2	3
287	YOR206W	2,8%	1	2	2	4
288	YKL120W	7,4%	1	2	2	4
289	YOR117W	7,1%	1	2	2	4
290	YPR028W	8,9%	1	2	2	4
291	YOR153W	1,5%	1	2	2	4
292	YJR072C	5,7%	1	2	2	4
293	YLR293C	9,6%	2	2	2	4
294	YLR196W	5,4%	1	2	2	2
295	YJR009C	33,4%	1	2	12	32
296	YNR051C	5,8%	1	2	2	4
297	YDL131W	41,8%	1	2	16	34
298	YLR304C	3,3%	1	2	2	2
299	YJL138C	6,3%	1	2	2	4
300	YDL007W	5,7%	1	2	2	4
301	YBL076C	2,2%	1	2	2	3
302	YJR104C	13,0%	1	2	2	6
303	YFL045C	6,3%	1	2	2	6
304	YEL022W	1,5%	1	2	2	4
305	YPL160W	2,0%	1	2	2	4
306	YOL041C	6,5%	1	2	2	4
307	YDR510W	17,8%	1	2	2	4
308	YPL226W	1,8%	1	2	2	2
309	YMR145C	3,4%	1	2	2	4
310	YGR264C	2,4%	1	2	2	2
311	YDR377W	19,8%	1	2	2	4
312	YJL020C	2,0%	1	2	2	4
313	YDR429C	12,0%	1	2	2	4
314	YPR072W	4,3%	1	2	2	2
315	YNL002C	7,1%	1	2	2	4
316	YHR179W	5,3%	1	2	2	6
317	YPR145W	3,9%	1	2	2	4
318	YPL146C	5,7%	1	2	2	2
319	YPR183W	6,4%	1	2	2	4
320	YKL029C	3,3%	1	2	2	4
321	YMR230W	72,4%	1	2	9	22
322	YLR153C	2,9%	1	2	2	6
323	YAL019W	2,0%	1	2	2	4
324	YNL287W	1,9%	1	2	2	4
325	YJL080C	1,8%	1	2	2	4
326	YHR052W	4,8%	1	2	2	4
327	YFR051C	4,0%	1	2	2	4
328	YPL217C	2,0%	1	2	2	2
329	YMR303C	18,1%	1	2	5	14

330	YBR084W	2,1%	1	2	2	4
331	YDR312W	4,2%	1	2	2	2
332	YFL038C	9,7%	1	2	2	4
333	YPL048W	6,8%	1	2	2	4
334	YGL253W	4,3%	1	2	2	4
335	YOR375C	7,3%	1	2	2	4
336	YMR307W	4,1%	1	2	2	5
337	YNL055C	6,4%	1	2	2	4
338	YDL055C	8,0%	1	2	2	6
339	YDL017W	4,5%	1	2	2	4
340	YKL191W	3,9%	1	2	2	4
341	YMR194W	50,0%	1	2	8	23
342	YOR157C	8,4%	1	2	2	4
343	YCL064C	5,3%	1	2	2	2
344	YJL111W	4,6%	1	2	2	4
345	YGL055W	4,3%	1	2	2	4
346	YNL113W	19,0%	1	2	2	4
347	YIL075C	2,2%	1	2	2	4
348	YPL115C	2,0%	1	2	2	2
349	YDR155C	14,8%	1	2	2	8
350	YBR291C	6,4%	1	2	2	4
351	YGR086C	6,2%	1	2	2	4
352	YDL081C	28,3%	1	2	2	8
353	YER177W	7,1%	2	2	2	4
354	YDR150W	8,0%	1	2	2	4
355	YLR208W	7,7%	1	2	2	4
356	YJL122W	9,1%	1	2	2	2
357	YJL123C	5,0%	1	2	2	4
358	YPL127C	8,5%	1	2	2	4
359	YOR217W	2,6%	1	2	2	4
360	YGL137W	3,2%	1	2	2	4
361	YBR263W	4,7%	1	2	2	4
362	YBR172C	3,0%	1	2	2	2
363	YMR214W	6,9%	1	2	2	4
364	YLL012W	3,7%	1	2	2	2
365	YKL127W	3,2%	1	2	2	2
366	YFR037C	1,8%	1	2	2	2
367	YGL048C	6,4%	1	2	2	2
368	YLR276C	3,2%	1	2	2	2
369	YHR089C	9,3%	1	2	2	3
370	YMR015C	3,7%	1	2	2	2
371	YGR167W	8,2%	1	2	2	2
372	YEL051W	6,6%	1	2	2	2
373	YML048W	7,2%	1	2	2	4
374	YNL255C	17,7%	1	2	2	6
375	YMR185W	2,2%	1	2	2	2
376	YKR092C	8,1%	1	2	2	2

377	YMR058W	3,0%	1	2	2	2
378	YDR012W	73,8%	1	1	36	70
379	YDR225W	60,6%	1	1	7	13
380	YBL003C	61,4%	1	1	7	13
381	YHL001W	79,7%	1	1	12	17
382	YKL006W	79,7%	1	1	12	17
383	YPL081W	55,8%	1	1	11	17
384	YIL052C	56,2%	1	1	11	23
385	YER056C-A	57,9%	1	1	11	23
386	YLR344W	86,6%	1	1	21	38
387	YNL087W	1,8%	1	1	2	3
388	YGL228W	1,2%	1	1	2	2
389	YGR254W	49,4%	1	1	28	58
390	YOR086C	2,0%	1	1	2	2

ScCENP-T$^{\text{Cnn1}}$, High stringency

#	Accession	ΣCoverage	Σ# Proteins	Σ# Unique Peptides	Σ# Peptides	Σ# PSMs
1	YFR046C	83,9%	1	57	57	168
2	YBR181C	58,5%	1	19	19	42
3	YJL177W	62,0%	2	11	11	26
4	YBR048W	52,6%	1	11	11	21
5	YDR450W	54,8%	1	10	10	19
6	YBR031W	31,2%	2	9	9	25
7	YPL143W	62,6%	2	8	8	13
8	YBL027W	26,5%	1	8	8	14
9	YJR045C	11,8%	1	7	7	14
10	YBL087C	41,6%	1	6	6	7
11	YHL015W	37,2%	1	6	6	11
12	YGL123W	17,3%	1	5	5	8
13	YNL178W	20,8%	1	5	5	9
14	YGR192C	18,7%	2	5	5	9
15	YLR075W	19,5%	1	5	5	9
16	YDR471W	38,2%	2	5	5	14
17	YGL031C	27,7%	1	5	5	11
18	YFR031C-A	26,4%	1	5	5	10
19	YMR242C	21,5%	1	5	5	8
20	YGR118W	33,1%	1	4	4	4
21	YDL061C	69,6%	1	4	5	8
22	YDL082W	20,6%	2	4	4	7
23	YLL024C	27,7%	1	4	14	26
24	YOR063W	11,4%	1	4	4	11
25	YCR031C	18,3%	2	4	4	6
26	YBR191W	23,8%	1	4	4	5
27	YGR027C	21,3%	2	3	3	7
28	YNL301C	16,1%	1	3	3	7
29	YOL040C	24,7%	1	3	3	9

30	YDR447C	27,2%	2	3	3	8
31	YLR167W	18,4%	1	3	3	4
32	YHR203C	13,4%	1	3	3	6
33	YCL018W	11,5%	1	3	3	4
34	YML063W	22,4%	1	3	7	10
35	YER074W	24,4%	1	3	3	3
36	YPR046W	22,7%	1	2	2	2
37	YJR123W	9,3%	1	2	2	3
38	YBL092W	17,7%	1	2	2	4
39	YLR388W	55,4%	1	2	3	6
40	YBR118W	5,0%	1	2	2	5
41	YHR021C	18,3%	2	2	2	2
42	YDL083C	18,2%	1	2	2	8
43	YAL005C	22,4%	1	2	12	21
44	YGR214W	8,3%	2	2	2	4
45	YPL018W	5,4%	1	2	2	2
46	YPL249C-A	10,0%	1	2	2	2
47	YGR034W	15,0%	2	2	2	2
48	YNL069C	12,1%	1	2	2	2
49	YFL039C	5,6%	1	2	2	2
50	YLR441C	22,4%	1	2	6	6

ScCENP-T^{Cnn1}, Low stringency

#	Accession	ΣCoverage	Σ# Proteins	Σ# Unique Peptides	Σ# Peptides	Σ# PSMs
1	YFR046C	96,7%	1	187	187	663
2	YHR174W	84,4%	1	71	71	176
3	YIL144W	71,8%	1	67	67	152
4	YBR118W	75,3%	1	57	57	161
5	YJR045C	68,2%	1	56	56	120
6	YGL008C	39,7%	1	47	47	105
7	YDL229W	75,9%	1	45	71	156
8	YOR063W	63,8%	1	39	39	87
9	YLR259C	57,0%	1	38	38	75
10	YFR031C-A	81,1%	1	38	38	99
11	YPL106C	46,6%	1	37	37	79
12	YLR044C	55,4%	1	37	37	87
13	YPL231W	18,0%	1	34	34	61
14	YMR117C	81,2%	1	34	34	69
15	YGR192C	76,5%	1	33	52	120
16	YAL038W	57,0%	1	33	33	68
17	YDR012W	72,4%	2	33	33	82
18	YHR203C	64,8%	1	32	32	82
19	YOL069W	55,9%	1	31	31	59
20	YJL130C	13,6%	1	30	30	56
21	YKL182W	12,8%	1	29	29	55

22	YCL018W	61,3%	1	29	29	59
23	YOL086C	64,1%	1	28	28	71
24	YGL103W	83,2%	1	27	27	75
25	YGL076C	69,3%	2	27	27	58
26	YLL024C	88,1%	1	27	125	356
27	YBR181C	79,2%	1	27	27	72
28	YLR075W	75,6%	1	26	26	62
29	YJR123W	76,4%	1	25	25	57
30	YPL131W	53,9%	1	25	25	56
31	YCR012W	53,6%	1	23	23	53
32	YOL127W	78,2%	1	23	23	49
33	YDR450W	69,9%	1	23	23	59
34	YBL072C	79,0%	1	23	23	56
35	YLR340W	47,1%	1	23	23	54
36	YHL015W	74,4%	1	22	22	60
37	YDL083C	77,6%	1	22	22	50
38	YGL123W	60,2%	1	21	21	49
39	YMR142C	74,4%	2	21	21	50
40	YBR048W	84,0%	1	21	21	41
41	YDR385W	27,1%	1	21	21	50
42	YNL301C	67,2%	1	21	21	45
43	YER018C	76,5%	1	21	21	47
44	YKL152C	62,4%	1	20	20	39
45	YJL034W	36,5%	1	20	23	49
46	YDR064W	92,7%	1	20	20	48
47	YNL178W	70,0%	1	19	19	47
48	YDL182W	44,2%	2	19	19	38
49	YHR010W	77,9%	2	19	19	56
50	YLR249W	20,5%	1	19	19	40
51	YGR179C	29,1%	1	18	18	39
52	YLR150W	60,4%	1	18	18	41
53	YAL005C	85,5%	1	18	116	322
54	YMR242C	77,3%	1	18	18	37
55	YGL135W	56,7%	1	17	17	47
56	YKL060C	50,4%	1	17	17	49
57	YBL092W	82,3%	1	17	17	33
58	YGR085C	50,6%	2	17	17	46
59	YHR020W	23,3%	1	17	17	38
60	YNL064C	40,1%	1	16	16	38
61	YDR447C	71,3%	2	16	16	45
62	YGL147C	67,5%	2	15	15	33
63	YBL027W	61,4%	1	15	15	46
64	YBL087C	61,3%	1	15	15	27
65	YOR293W	74,3%	2	14	14	36
66	YDL136W	70,0%	1	14	14	30
67	YPL143W	73,8%	2	14	14	26
68	YER074W	65,9%	1	14	14	40

69	YGR118W	52,4%	1	14	14	28
70	YBR189W	53,9%	1	14	14	29
71	YHL034C	44,6%	1	13	13	26
72	YKL054C	24,9%	1	13	13	24
73	YJR121W	27,4%	1	13	13	26
74	YLR367W	76,2%	2	13	13	26
75	YLR432W	32,9%	1	12	16	29
76	YBR196C	24,7%	1	12	12	27
77	YGR027C	73,2%	2	12	12	22
78	YOL040C	60,6%	1	12	12	40
79	YER165W	25,5%	1	12	12	28
80	YAL035W	12,9%	1	12	12	23
81	YDL126C	14,4%	1	12	12	22
82	YDR050C	43,2%	1	12	12	28
83	YKL180W	75,5%	1	12	20	44
84	YJL191W	75,4%	2	11	11	28
85	YLR029C	46,6%	2	11	11	34
86	YHL001W	72,5%	2	11	11	18
87	YBR211C	33,0%	1	11	11	26
88	YDR365W-A	42,7%	17	11	19	33
89	YGL234W	14,6%	1	11	11	22
90	YDR418W	66,1%	1	11	11	29
91	YLL045C	81,6%	1	11	40	92
92	YBL099W	18,4%	1	11	11	22
93	YER120W	39,8%	1	10	10	21
94	YFL037W	18,6%	1	10	10	19
95	YHR117W	14,9%	1	10	10	22
96	YJL012C	12,9%	1	10	10	20
97	YNL054W-A	50,7%	9	10	18	34
98	YDR254W	19,4%	1	9	9	18
99	YDL014W	25,1%	1	9	9	20
100	YJR094W-A	64,1%	1	9	9	24
101	YML073C	61,9%	1	9	17	35
102	YHR021C	62,2%	2	9	9	23
103	YLR061W	62,0%	1	9	9	17
104	YPR163C	29,4%	1	9	9	21
105	YBR106W	43,6%	1	9	9	20
106	YNL302C	45,8%	2	9	9	18
107	YGR214W	25,0%	2	9	9	22
108	YHR064C	20,3%	1	9	9	17
109	YGL189C	41,2%	2	9	9	24
110	YDR233C	27,1%	1	8	8	14
111	YNL096C	73,7%	1	8	16	37
112	YPL081W	36,6%	1	8	8	15
113	YML123C	17,4%	1	8	8	16
114	YOR096W	75,3%	1	8	16	37
115	YLR287C-A	95,2%	1	8	8	14

116	YML063W	71,0%	1	8	25	56
117	YBR078W	15,0%	1	8	8	17
118	YPL018W	17,1%	1	7	7	14
119	YPL019C	8,3%	1	7	7	14
120	YOR369C	48,3%	1	7	7	23
121	YDR382W	63,6%	1	7	7	16
122	YBR039W	24,8%	1	7	7	16
123	YLR448W	56,8%	1	7	15	31
124	YIL133C	47,7%	1	7	15	23
125	YLR167W	37,5%	1	7	8	15
126	YPR120C	20,2%	1	7	7	11
127	YBR127C	15,7%	1	7	7	15
128	YLR325C	61,5%	1	7	7	14
129	YLR264W	77,6%	2	7	7	15
130	YLR355C	20,0%	1	7	7	10
131	YFL039C	23,5%	1	7	7	14
132	YLR441C	71,0%	1	7	24	47
133	YEL034W	41,4%	1	7	7	14
134	YML028W	37,8%	1	7	7	13
135	YGR159C	17,9%	1	6	6	14
136	YGL030W	71,4%	1	6	6	15
137	YOR341W	3,9%	1	6	6	11
138	YHL033C	75,0%	1	6	35	88
139	YJR135C	25,1%	1	6	6	11
140	YBL030C	18,6%	1	6	6	11
141	YER025W	17,3%	1	6	6	11
142	YLR342W	4,0%	1	6	6	11
143	YHR190W	14,9%	1	6	6	16
144	YNL069C	49,0%	1	6	14	26
145	YJL136C	64,4%	2	6	6	16
146	YJR009C	58,4%	1	6	25	46
147	YPL079W	49,4%	1	5	12	24
148	YML048W	11,7%	1	5	5	8
149	YNL007C	18,5%	1	5	5	9
150	YGL206C	3,5%	1	5	5	12
151	YBR221C	11,2%	1	5	5	6
152	YHR193C	40,2%	1	5	5	14
153	YNL071W	12,7%	1	5	5	10
154	YLR185W	67,1%	1	5	7	13
155	YPL061W	11,0%	1	5	5	7
156	YCL030C	6,5%	1	5	5	10
157	YJR070C	18,8%	1	5	5	8
158	YPL249C-A	66,0%	1	5	11	28
159	YMR246W	7,9%	1	5	5	11
160	YGR240C	6,3%	1	5	5	9
161	YLR303W	14,9%	1	5	5	11
162	YER178W	12,1%	1	5	5	9

163	YPR046W	28,7%	1	5	5	13
164	YMR241W	15,3%	1	5	5	7
165	YDR383C	24,8%	1	5	5	10
166	YHR007C	7,9%	1	5	5	11
167	YHR183W	9,6%	1	4	4	10
168	YOL109W	41,6%	1	4	4	8
169	YDL061C	69,6%	1	4	5	12
170	YNL112W	7,5%	1	4	4	8
171	YLR388W	67,9%	1	4	5	12
172	YPR010C	3,2%	1	4	4	6
173	YOR310C	8,6%	1	4	4	9
174	YEL031W	3,7%	1	4	4	8
175	YJL014W	7,7%	1	4	4	7
176	YOR204W	8,1%	1	4	4	7
177	YDR381W	20,8%	1	4	4	12
178	YGL031C	45,8%	1	4	9	14
179	YNR050C	9,0%	1	4	4	7
180	YHR146W	11,4%	1	4	4	8
181	YGR167W	16,7%	1	4	4	8
182	YDL075W	33,6%	2	4	4	6
183	YHR072W-A	67,2%	1	4	4	5
184	YKL212W	4,3%	1	3	3	5
185	YDR033W	10,3%	1	3	3	6
186	YDL192W	17,7%	1	3	3	6
187	YAR007C	3,4%	1	3	3	5
188	YJL138C	6,3%	1	3	3	7
189	YMR108W	5,4%	1	3	3	5
190	YBR009C	31,1%	1	3	3	6
191	YJR104C	18,8%	1	3	3	6
192	YBL002W	16,0%	2	3	3	7
193	YKR001C	5,1%	1	3	3	5
194	YLR315W	15,0%	1	3	3	5
195	YHR179W	7,5%	1	3	3	6
196	YPR183W	12,0%	1	3	3	7
197	YDR483W	10,2%	1	3	3	6
198	YLR153C	4,3%	1	3	3	4
199	YMR116C	11,9%	1	3	3	7
200	YBR160W	11,4%	1	3	3	6
201	YPL237W	9,8%	1	3	3	5
202	YIL053W	15,2%	1	3	3	5
203	YLR197W	6,6%	1	3	3	6
204	YJL151C	14,3%	1	3	3	8
205	YDR171W	6,4%	1	3	3	7
206	YNL055C	11,0%	1	3	3	5
207	YBL003C	29,6%	2	3	3	11
208	YNR016C	1,3%	1	3	3	6
209	YMR205C	2,9%	1	3	3	6

210	YKL145W	6,9%	1	3	3	6
211	YDR155C	19,8%	1	3	3	6
212	YER177W	11,6%	1	3	3	5
213	YBR086C	3,7%	1	3	3	6
214	YGR034W	79,5%	1	3	18	33
215	YHR141C	34,9%	1	3	3	5
216	YDL081C	42,5%	1	3	3	6
217	YDL130W	29,3%	1	3	3	5
218	YML056C	15,3%	1	3	7	13
219	YFR032C-A	50,9%	1	3	3	3
220	YPR041W	9,6%	1	2	2	4
221	YDL072C	13,8%	1	2	2	6
222	YBR072W	12,2%	1	2	2	4
223	YOR117W	5,1%	1	2	2	4
224	YLL018C	3,1%	1	2	2	4
225	YBR079C	1,9%	1	2	2	4
226	YMR229C	1,0%	1	2	2	4
227	YNL121C	3,7%	1	2	2	4
228	YLR175W	6,0%	1	2	2	4
229	YNL122C	15,7%	1	2	2	4
230	YDR500C	36,4%	1	2	4	6
231	YHR068W	2,8%	1	2	2	4
232	YJR077C	8,0%	1	2	2	5
233	YGR193C	6,3%	1	2	2	8
234	YMR012W	1,9%	1	2	2	2
235	YGR282C	6,7%	1	2	2	4
236	YOR259C	4,6%	1	2	2	4
237	YAL042W	5,5%	1	2	2	6
238	YDL147W	3,8%	1	2	2	4
239	YDR101C	4,2%	1	2	2	4
240	YDR377W	19,8%	1	2	2	4
241	YJL008C	4,1%	1	2	2	6
242	YDL143W	4,6%	1	2	2	4
243	YGR135W	7,4%	1	2	2	2
244	YDR345C	3,9%	1	2	2	5
245	YOR261C	6,2%	1	2	2	2
246	YGL195W	0,8%	1	2	2	4
247	YBR107C	11,4%	1	2	2	4
248	YMR264W	10,3%	1	2	2	2
249	YJL080C	1,8%	1	2	2	6
250	YDR481C	4,4%	1	2	2	4
251	YFL038C	9,7%	1	2	2	4
252	YFL022C	4,0%	1	2	2	6
253	YOL139C	13,2%	1	2	2	4
254	YIL148W	14,8%	1	2	3	7
255	YDR343C	4,9%	1	2	2	6
256	YOR323C	4,6%	1	2	2	2

257	YDR158W	5,2%	1	2	2	4
258	YMR307W	4,1%	1	2	2	4
259	YKL081W	3,9%	1	2	2	4
260	YGL093W	2,9%	1	2	2	6
261	YJL189W	21,6%	1	2	2	6
262	YJR007W	4,6%	1	2	2	2
263	YMR194W	50,0%	1	2	8	19
264	YFL048C	5,4%	1	2	2	4
265	YMR186W	29,5%	1	2	20	54
266	YCR034W	6,9%	1	2	2	4
267	YOR317W	3,3%	1	2	2	4
268	YNL255C	13,7%	1	2	2	4
269	YDR508C	3,6%	1	2	2	4
270	YLR216C	7,3%	1	2	2	4
271	YGR103W	3,8%	1	2	2	4
272	YNL209W	46,7%	1	2	24	56
273	YOL086W-A	21,1%	1	2	2	4
274	YDL213C	17,8%	1	2	2	4
275	YDL160C-A	30,0%	1	2	2	4
276	YMR295C	12,7%	1	2	2	2
277	YKL120W	7,4%	1	2	2	3
278	YNR051C	4,7%	1	2	2	2
279	YEL013W	4,3%	1	2	2	2
280	YHL031C	6,7%	1	2	2	3
281	YGR204W	2,1%	1	2	2	2
282	YOR375C	5,3%	1	2	2	3
283	YGR285C	4,2%	1	2	2	2
284	YLR429W	3,4%	1	2	2	2
285	YAL003W	13,1%	1	2	2	5
286	YKL056C	10,2%	1	2	2	4
287	YLR056W	6,3%	1	2	2	4
288	YIL052C	56,2%	1	1	8	19
289	YER056C-A	57,9%	1	1	8	18
290	YLR344W	78,7%	1	1	16	31
291	YPL240C	27,5%	1	1	19	43
292	YBR191W	45,6%	1	1	8	13
293	YJL177W	54,4%	1	1	9	13
294	YGR148C	34,2%	1	1	6	6
295	YDR374W-A	22,5%	1	2	2	5

ScCENP-S$^{YOL086W-A}$, High stringency

#	**Accession**	**ΣCoverage**	**Σ# Proteins**	**Σ# Unique Peptides**	**Σ# Peptides**	**Σ# PSMs**
1	YIR002C	39,2%	1	43	43	144
2	YGR042W	38,8%	1	14	14	45
3	YDL229W	21,4%	1	13	13	27
4	YJR045C	19,7%	1	11	11	22

5	YOR063W	23,8%	1	10	10	21
6	YOL086W-A	88,9%	1	10	10	102
7	YDL160C-A	100,0%	1	10	10	194
8	YNL178W	42,1%	1	9	9	19
9	YHL015W	37,2%	1	6	6	15
10	YBL072C	32,0%	1	6	6	13
11	YER074W	29,6%	1	6	6	15
12	YFR031C-A	29,9%	1	6	6	12
13	YBR048W	26,3%	1	5	5	11
14	YNL301C	24,7%	1	5	5	7
15	YBR181C	25,4%	1	5	5	12
16	YGL008C	6,0%	1	5	5	12
17	YGR148C	27,1%	2	5	5	5
18	YDL182W	11,9%	1	4	4	8
19	YLL024C	27,7%	1	4	15	46
20	YER120W	20,9%	1	4	4	10
21	YBR118W	10,0%	1	4	4	8
22	YHR021C	46,3%	2	4	4	8
23	YPL249C-A	24,0%	1	4	4	10
24	YDR447C	36,0%	2	4	4	10
25	YHR203C	12,6%	1	4	4	8
26	YBR211C	14,5%	1	4	4	8
27	YNL055C	16,6%	1	4	4	7
28	YDR450W	23,3%	1	4	4	7
29	YDR471W	35,3%	2	4	4	10
30	YML063W	16,5%	1	4	4	8
31	YGR118W	23,5%	1	4	4	5
32	YGL123W	13,8%	1	3	3	5
33	YGR027C	27,8%	2	3	3	6
34	YNL096C	15,8%	1	3	3	6
35	YBR009C	31,1%	1	3	3	6
36	YDL082W	12,6%	2	3	3	5
37	YBL002W	22,9%	2	3	3	8
38	YLR029C	15,2%	2	3	3	6
39	YCR031C	24,8%	2	3	3	6
40	YBR031W	11,6%	1	3	3	8
41	YCR028C-A	28,2%	1	3	3	8
42	YLR344W	15,0%	2	3	3	5
43	YJL034W	7,8%	1	3	5	9
44	YBL027W	14,8%	1	3	3	6
45	YER148W	12,9%	1	3	3	7
46	YPL131W	8,4%	1	3	3	5
47	YGR159C	4,6%	1	2	2	4
48	YJR123W	9,8%	1	2	2	4
49	YAR007C	3,2%	1	2	2	4
50	YBR191W	11,3%	2	2	2	4
51	YDR064W	15,2%	1	2	2	4

52	YML123C	5,1%	1	2	2	4
53	YAL005C	23,7%	1	2	13	36
54	YCL018W	5,8%	1	2	2	4
55	YLR044C	3,6%	1	2	2	2
56	YGL234W	2,6%	1	2	2	4
57	YAR010C	5,9%	44	2	2	4
58	YDL192W	9,4%	1	2	2	2
59	YER131W	13,5%	2	2	2	2
60	YOR234C	10,3%	2	2	2	3
61	YML073C	11,9%	1	2	2	2
62	YLR167W	11,2%	1	2	2	2
63	YNL312W	5,9%	1	2	2	3
64	YBL087C	11,7%	1	2	2	2
65	YKL180W	21,2%	1	1	3	4
66	YJL177W	21,2%	1	1	3	4

ScCENP-S$^{\text{YOL086W-A}}$, Low stringency

#	Accession	ΣCoverage	Σ# Proteins	Σ# Unique Peptides	Σ# Peptides	Σ# PSMs
1	YIR002C	38,4%	1	40	40	133
2	YAR007C	30,0%	1	18	18	44
3	YGR042W	47,2%	1	16	16	43
4	YJR045C	29,2%	1	16	16	40
5	YCR092C	15,8%	1	15	15	28
6	YOL090W	14,3%	1	13	13	22
7	YOL086W-A	93,3%	1	11	11	117
8	YDL160C-A	100,0%	1	11	11	246
9	YER148W	35,4%	1	10	10	22
10	YNL178W	42,9%	1	9	9	23
11	YIL131C	21,1%	1	9	9	20
12	YNL301C	40,3%	1	9	9	18
13	YFR031C-A	36,2%	1	9	9	19
14	YOR063W	19,6%	1	8	8	22
15	YLR344W	42,5%	1	8	8	16
16	YBL072C	42,5%	1	8	8	18
17	YMR242C	42,4%	1	8	8	19
18	YHR174W	17,9%	1	7	7	16
19	YNL312W	27,8%	1	7	7	17
20	YHL015W	37,2%	1	6	6	13
21	YKR025W	25,9%	1	6	6	14
22	YBR009C	51,5%	1	6	6	17
23	YOR116C	4,3%	1	6	6	12
24	YBR048W	26,9%	1	5	5	10
25	YBL002W	28,2%	2	5	5	11
26	YLL024C	31,6%	1	5	18	52
27	YDR447C	43,4%	2	5	5	13

28	YHR203C	16,9%	1	5	5	8
29	YDL150W	14,0%	1	5	5	11
30	YBR181C	25,4%	1	5	5	14
31	YDR450W	31,5%	1	5	5	10
32	YER074W	23,0%	1	5	5	11
33	YBR010W	22,1%	1	4	4	7
34	YPR110C	12,8%	1	4	4	8
35	YNL064C	12,5%	1	4	4	7
36	YGR027C	30,6%	2	4	4	9
37	YBL092W	29,2%	1	4	4	9
38	YJL011C	25,5%	1	4	4	8
39	YDL082W	17,1%	2	4	4	8
40	YKL058W	36,1%	1	4	4	8
41	YDR012W	13,8%	1	4	4	9
42	YJL173C	43,4%	1	4	4	11
43	YHR021C	46,3%	2	4	4	7
44	YPL249C-A	24,0%	1	4	4	17
45	YDL136W	23,3%	1	4	4	6
46	YCR031C	32,1%	2	4	4	8
47	YCR028C-A	34,8%	1	4	4	9
48	YGL008C	4,6%	1	4	4	8
49	YAL005C	31,5%	1	4	17	46
50	YOL127W	32,4%	1	4	4	12
51	YDR471W	35,3%	2	4	4	12
52	YBL027W	15,3%	1	4	4	9
53	YGL123W	13,8%	1	3	3	5
54	YJR123W	14,7%	1	3	3	5
55	YOR234C	17,8%	2	3	3	5
56	YGR192C	7,8%	2	3	3	3
57	YNL096C	15,8%	1	3	3	5
58	YLR185W	29,6%	1	3	3	5
59	YKL144C	15,1%	1	3	3	5
60	YER120W	17,2%	1	3	3	6
61	YML073C	15,3%	1	3	3	4
62	YBR118W	6,8%	1	3	3	6
63	YLR075W	14,0%	1	3	3	6
64	YLR029C	17,2%	2	3	3	6
65	YCL018W	12,1%	1	3	3	7
66	YLR441C	23,9%	1	3	6	12
67	YNL113W	19,0%	1	3	3	5
68	YML063W	23,5%	1	3	6	12
69	YBL087C	22,6%	1	3	3	8
70	YGR118W	17,2%	1	3	3	5
71	YOR207C	2,5%	1	3	3	6
72	YGR148C	27,1%	1	3	5	6
73	YNR003C	7,6%	1	2	2	6
74	YIL133C	15,1%	1	2	3	3

75	YLR167W	11,2%	1	2	2	2
76	YHL001W	13,8%	2	2	2	2
77	YJL034W	6,3%	1	2	4	10
78	YDR064W	15,2%	1	2	2	4
79	YMR072W	12,0%	1	2	2	4
80	YNL151C	7,6%	1	2	2	4
81	YDR381W	10,2%	1	2	2	2
82	YOL012C	12,7%	1	2	2	4
83	YPR190C	2,9%	1	2	2	4
84	YGL234W	3,0%	1	2	2	4
85	YDR418W	14,6%	1	2	2	4
86	YNL209W	23,2%	1	2	15	16
87	YAR010C	4,1%	42	2	2	4
88	YDL229W	23,0%	1	2	15	16
89	YOR369C	14,7%	1	2	2	3
90	YBR189W	11,8%	1	2	2	2
91	YLL045C	25,8%	1	2	8	8
92	YPL079W	27,5%	1	1	5	5
93	YHL033C	26,2%	1	1	7	8
94	YJL177W	12,5%	1	1	2	3
95	YNL069C	12,1%	1	1	2	4
96	YGL031C	21,3%	1	1	3	4
97	YBR191W	27,5%	1	1	5	5
98	YKL180W	12,5%	1	1	2	3

ScCENP-X$^{\text{YDL160C-A}}$, High stringency

#	Accession	ΣCoverage	Σ# Proteins	Σ# Unique Peptides	Σ# Peptides	Σ# PSMs
1	YJR045C	30,6%	1	18	18	36
2	YOL086W-A	93,3%	1	11	11	107
3	YDL160C-A	100,0%	1	10	10	249
4	YBR211C	21,9%	1	8	8	16
5	YDR447C	43,4%	2	5	5	10
6	YLR344W	37,8%	1	5	5	9
7	YDL082W	17,1%	2	4	4	7
8	YOR063W	12,1%	1	4	4	9
9	YNL301C	19,9%	1	4	4	8
10	YPL249C-A	24,0%	1	4	4	7
11	YGL008C	4,9%	1	4	4	7
12	YAL005C	28,4%	1	4	16	39
13	YFR031C-A	22,1%	1	4	4	7
14	YGR159C	7,3%	1	3	3	8
15	YGR179C	9,9%	1	3	3	6
16	YLL024C	26,6%	1	3	15	40
17	YHL033C	12,1%	2	3	3	5
18	YDL083C	21,7%	1	3	3	6

19	YBR181C	18,2%	1	3	3	6
20	YKL180W	21,2%	1	3	3	6
21	YDR471W	23,5%	2	3	3	5
22	YBL027W	15,3%	1	3	3	6
23	YMR242C	13,4%	1	3	3	5
24	YDL229W	3,1%	2	2	2	4
25	YHL015W	21,5%	1	2	2	4
26	YBR118W	4,4%	1	2	2	6
27	YBR031W	7,7%	2	2	2	4
28	YOL127W	16,9%	1	2	2	4
29	YFL039C	5,6%	1	2	2	4
30	YGL031C	14,8%	2	2	2	4
31	YLR075W	10,0%	1	2	2	2
32	YHR021C	29,3%	2	2	2	2
33	YBL072C	8,0%	1	2	2	2
34	YGR118W	12,4%	1	2	2	2

ScCENP-X$^{YDL160C-A}$, Low stringency

#	Accession	ΣCoverage	Σ# Proteins	Σ# Unique Peptides	Σ# Peptides	Σ# PSMs
1	YDL160C-A	97,5%	1	124	124	983
2	YOL086W-A	100,0%	1	87	87	622
3	YBR118W	73,6%	1	50	50	140
4	YJR045C	58,0%	1	44	44	98
5	YGL008C	35,5%	1	43	43	106
6	YHR203C	70,1%	1	34	34	72
7	YHR174W	58,1%	1	31	31	80
8	YGL076C	82,4%	1	31	31	68
9	YOL086C	75,0%	1	30	30	66
10	YLR075W	81,0%	1	29	29	65
11	YJR123W	71,6%	1	27	27	65
12	YBR181C	70,3%	1	27	27	68
13	YAL035W	26,8%	1	27	27	68
14	YMR186W	51,6%	1	27	47	105
15	YFR031C-A	70,9%	1	27	27	69
16	YLR340W	60,9%	1	27	27	63
17	YDL082W	77,9%	2	26	26	53
18	YGR192C	69,9%	1	25	36	82
19	YAL038W	49,4%	1	25	25	54
20	YGL103W	76,5%	1	23	23	58
21	YHR020W	36,8%	1	23	23	51
22	YGL123W	58,7%	1	22	22	47
23	YLL024C	73,9%	1	22	66	162

24	YHR007C	38,9%	1	22	22	43
25	YOR063W	46,0%	1	21	21	47
26	YNL301C	79,6%	1	21	21	57
27	YDL083C	78,3%	1	21	21	40
28	YER165W	42,1%	1	21	21	44
29	YKL081W	40,1%	1	20	20	40
30	YCL018W	52,8%	1	20	20	44
31	YLR044C	30,7%	1	19	19	38
32	YPL131W	52,9%	1	19	19	42
33	YNL209W	42,3%	1	18	25	58
34	YBR189W	65,6%	1	18	27	49
35	YDL229W	43,4%	1	18	28	58
36	YHL015W	76,9%	1	17	17	42
37	YBL027W	57,7%	1	17	17	49
38	YML008C	38,4%	1	17	17	34
39	YDL182W	50,9%	1	16	26	51
40	YNL064C	44,0%	1	16	16	43
41	YDR447C	73,5%	2	16	16	51
42	YJL190C	77,7%	2	16	16	45
43	YBL072C	63,5%	1	16	16	35
44	YKL180W	77,2%	1	16	16	39
45	YMR242C	66,3%	1	16	16	37
46	YDR233C	43,4%	1	15	15	32
47	YNL178W	67,5%	1	15	15	36
48	YBL092W	68,5%	1	15	15	31
49	YDR064W	73,5%	1	15	15	39
50	YDR471W	66,2%	2	15	15	39
51	YLL045C	72,3%	1	15	37	93
52	YDL136W	70,8%	1	14	14	38
53	YGR085C	56,9%	2	14	14	30
54	YJR121W	28,0%	1	14	14	32
55	YDR418W	68,5%	1	14	14	42
56	YOR293W	73,3%	2	13	13	34
57	YPL143W	83,2%	2	13	13	19
58	YOR204W	24,2%	1	13	14	26
59	YBL099W	26,4%	1	13	13	28
60	YHR042W	17,2%	1	12	12	21
61	YGL147C	61,3%	2	12	12	30
62	YLR259C	27,6%	1	12	12	26
63	YNL069C	59,1%	1	12	18	34
64	YBR106W	57,5%	1	12	12	28
65	YLR029C	52,5%	1	11	11	32
66	YBR107C	47,4%	1	11	11	57
67	YNL055C	41,7%	1	11	11	22
68	YNL302C	69,4%	2	11	11	28
69	YDR254W	34,7%	1	10	10	41
70	YJL130C	5,1%	1	10	10	22

71	YGR185C	23,4%	1	10	10	22
72	YOL127W	66,2%	1	10	10	30
73	YDR450W	52,7%	1	10	10	20
74	YOR096W	72,1%	1	10	15	33
75	YJL012C	13,5%	1	10	10	19
76	YKL152C	39,3%	1	9	9	20
77	YGL105W	25,8%	1	9	9	17
78	YPL079W	40,6%	2	9	9	19
79	YBR048W	59,6%	1	9	9	21
80	YPR183W	31,5%	1	9	9	18
81	YPR163C	28,9%	1	9	9	17
82	YGL234W	12,5%	1	9	9	23
83	YHR146W	24,1%	1	9	9	20
84	YOL039W	55,7%	1	8	8	19
85	YJL191W	54,4%	2	8	8	17
86	YOR332W	38,2%	1	8	8	17
87	YDL192W	42,0%	2	8	8	17
88	YJL041W	17,0%	1	8	8	20
89	YGR175C	13,1%	1	8	8	15
90	YER056C-A	51,2%	2	8	8	17
91	YGR264C	10,9%	1	8	8	14
92	YML073C	65,9%	1	8	16	34
93	YOL040C	40,9%	1	8	8	27
94	YHR021C	59,8%	2	8	8	19
95	YBL030C	32,4%	1	8	10	21
96	YAL005C	67,8%	1	8	52	125
97	YGL031C	32,3%	1	8	8	19
98	YBL087C	54,7%	1	8	8	20
99	YGL135W	21,7%	1	7	7	13
100	YML048W	14,9%	1	7	7	16
101	YBR039W	26,7%	1	7	7	12
102	YNL112W	15,8%	1	7	8	15
103	YDR500C	63,6%	1	7	7	15
104	YER120W	26,2%	1	7	7	13
105	YEL031W	6,5%	1	7	7	13
106	YMR246W	11,1%	1	7	7	14
107	YLR150W	35,2%	1	7	7	19
108	YMR072W	33,9%	1	7	7	13
109	YDR381W	29,7%	1	7	7	13
110	YDL075W	46,0%	2	7	7	16
111	YGR118W	37,2%	1	7	7	17
112	YLR249W	8,0%	1	7	7	13
113	YBR078W	16,9%	1	7	7	12
114	YPL019C	7,3%	1	6	6	14
115	YAR007C	11,4%	1	6	6	13
116	YGR027C	38,0%	2	6	6	16
117	YNL096C	62,6%	1	6	11	25

118	YCR012W	13,7%	1	6	6	11
119	YHL001W	50,0%	1	6	11	23
120	YPL237W	22,8%	1	6	6	14
121	YJL034W	14,2%	1	6	9	17
122	YER074W	34,1%	1	6	6	18
123	YGL245W	9,0%	1	6	6	15
124	YGR179C	16,0%	1	6	6	16
125	YIL041W	19,0%	1	5	5	10
126	YDR174W	20,3%	1	5	5	11
127	YOR369C	33,6%	1	5	5	16
128	YDR385W	6,8%	1	5	5	10
129	YDR429C	21,2%	1	5	5	10
130	YGR082W	25,1%	1	5	5	7
131	YLR061W	65,3%	2	5	5	15
132	YDR483W	14,9%	1	5	5	10
133	YNL312W	23,8%	1	5	5	8
134	YLR325C	47,4%	1	5	5	12
135	YFL037W	11,8%	1	5	5	9
136	YLR342W	2,8%	1	5	5	12
137	YHR190W	11,9%	1	5	5	8
138	YMR079W	16,1%	1	5	5	10
139	YGR214W	23,0%	2	5	5	10
140	YPL127C	22,9%	1	5	5	13
141	YMR183C	10,5%	1	4	4	9
142	YFR001W	20,6%	1	4	4	8
143	YJR094W-A	43,5%	1	4	4	12
144	YGL030W	39,1%	1	4	4	8
145	YDR529C	34,7%	1	4	4	11
146	YDR298C	21,7%	1	4	4	8
147	YMR108W	8,4%	1	4	4	8
148	YBL002W	22,9%	2	4	4	9
149	YCL030C	7,0%	1	4	4	8
150	YAR002W	8,5%	1	4	4	6
151	YOR271C	12,2%	1	4	4	9
152	YHL031C	15,3%	1	4	4	9
153	YIL133C	39,7%	1	4	10	19
154	YGR135W	15,5%	1	4	4	8
155	YPL106C	9,4%	1	4	4	8
156	YPL218W	24,7%	1	4	4	8
157	YML123C	8,5%	1	4	4	7
158	YMR307W	8,1%	1	4	4	8
159	YDL055C	13,6%	1	4	4	7
160	YFL048C	9,9%	1	4	4	8
161	YLR441C	58,4%	1	4	15	26
162	YML063W	54,5%	1	4	15	32
163	YJL136C	42,5%	2	4	4	7
164	YBR015C	5,7%	1	4	4	6

165	YDL130W	28,3%	1	4	4	12
166	YGR234W	11,0%	1	3	3	6
167	YKL060C	10,3%	1	3	3	5
168	YDL226C	12,2%	1	3	3	6
169	YKL127W	6,3%	1	3	3	6
170	YBR079C	3,0%	1	3	3	3
171	YDL131W	33,2%	1	3	13	28
172	YDR382W	33,6%	1	3	3	8
173	YDL061C	64,3%	1	3	4	9
174	YKL016C	21,8%	1	3	3	6
175	YLR448W	54,6%	1	3	11	26
176	YLR388W	64,3%	1	3	4	8
177	YGR282C	11,8%	1	3	3	6
178	YBR120C	15,4%	1	3	3	6
179	YHL033C	66,4%	1	3	25	56
180	YJL104W	20,1%	1	3	3	6
181	YPL199C	17,9%	1	3	3	6
182	YOR254C	4,2%	1	3	3	5
183	YAL023C	5,0%	1	3	3	6
184	YNL287W	2,9%	1	3	3	5
185	YFL022C	7,0%	1	3	3	5
186	YDL126C	4,3%	1	3	3	6
187	YJL189W	21,6%	1	3	3	4
188	YOR099W	6,6%	1	3	3	6
189	YNR021W	9,2%	1	3	3	6
190	YFL039C	8,3%	1	3	3	6
191	YNL255C	21,6%	1	3	3	5
192	YMR241W	9,9%	1	3	3	4
193	YNR050C	6,7%	1	3	3	4
194	YLR287C-A	30,2%	1	3	3	6
195	YHR027C	3,1%	1	3	3	6
196	YHR064C	5,8%	1	3	3	7
197	YOR091W	7,8%	1	3	3	5
198	YGR027W-A	63,6%	2	3	39	56
199	YDR365W-A	52,7%	5	3	28	52
200	YDL081C	42,5%	1	3	3	8
201	YDR086C	47,5%	1	3	3	5
202	YMR146C	4,0%	1	2	2	4
203	YDR032C	11,6%	1	2	2	4
204	YDR212W	3,2%	1	2	2	2
205	YKL120W	7,7%	1	2	2	2
206	YKL212W	3,1%	1	2	2	4
207	YDL014W	5,2%	1	2	2	2
208	YPR028W	8,9%	1	2	2	4
209	YNL138W	3,6%	1	2	2	2
210	YPL231W	1,2%	1	2	2	2
211	YPR110C	7,2%	1	2	2	2

212	YER131W	20,2%	2	2	2	4
213	YLR068W	15,9%	1	2	2	2
214	YOR361C	3,2%	1	2	2	4
215	YPR159W	3,9%	1	2	2	4
216	YEL042W	4,3%	1	2	2	6
217	YHR121W	14,4%	1	2	2	2
218	YPR165W	10,1%	1	2	2	5
219	YBR009C	19,4%	1	2	2	4
220	YDL100C	4,0%	1	2	2	4
221	YNL071W	3,5%	1	2	2	6
222	YLR185W	21,6%	1	2	2	2
223	YNL131W	16,5%	1	2	2	6
224	YHR127W	8,6%	1	2	2	2
225	YGR162W	2,2%	1	2	2	4
226	YNL248C	4,6%	1	2	2	2
227	YGR119C	3,7%	1	2	2	4
228	YMR012W	1,3%	1	2	2	4
229	YPL081W	50,8%	1	2	11	14
230	YDR012W	76,5%	1	2	48	117
231	YHR143W-A	41,4%	1	2	2	2
232	YJR070C	5,2%	1	2	2	4
233	YPL249C-A	57,0%	1	2	9	27
234	YDL143W	3,0%	1	2	2	2
235	YNL002C	7,5%	1	2	2	2
236	YER044C	15,5%	1	2	2	4
237	YBR031W	76,5%	1	2	48	121
238	YBR283C	4,7%	1	2	2	6
239	YLR167W	22,4%	1	2	3	6
240	YDL051W	5,1%	1	2	2	4
241	YOR270C	2,5%	1	2	2	2
242	YLR344W	64,6%	1	2	14	32
243	YDL208W	14,1%	1	2	2	4
244	YJL080C	1,8%	1	2	2	6
245	YCL009C	7,1%	1	2	2	6
246	YGR034W	64,6%	1	2	14	30
247	YML086C	4,8%	1	2	2	2
248	YFL038C	12,1%	1	2	2	2
249	YGL068W	9,8%	1	2	2	3
250	YIL148W	14,8%	1	2	3	3
251	YCL043C	3,6%	1	2	2	2
252	YJL151C	13,5%	1	2	2	4
253	YGR207C	7,7%	1	2	2	2
254	YPL010W	12,2%	1	2	2	4
255	YGL200C	11,3%	1	2	2	4
256	YDL095W	3,1%	1	2	2	4
257	YLR008C	14,3%	1	2	2	4
258	YER004W	7,8%	1	2	2	4

259	YML129C	40,0%	1	2	2	4
260	YDR050C	12,1%	1	2	2	4
261	YLR355C	4,1%	1	2	2	2
262	YHR196W	2,6%	1	2	2	2
263	YMR194W	57,0%	1	2	9	24
264	YOR340C	6,4%	1	2	2	2
265	YBL003C	29,6%	2	2	3	6
266	YLR100W	4,6%	1	2	2	4
267	YKL006W	31,9%	1	2	7	7
268	YKL007W	6,7%	1	2	2	2
269	YBR291C	6,4%	1	2	2	4
270	YPR046W	9,9%	1	2	2	4
271	YHR216W	6,3%	3	2	2	6
272	YPR018W	3,1%	1	2	2	2
273	YEL026W	13,5%	1	2	2	4
274	YHR081W	12,0%	1	2	2	4
275	YOR007C	8,1%	1	2	2	2
276	YHR039C	3,4%	1	2	2	2
277	YOL061W	4,6%	1	2	2	4
278	YML028W	9,2%	1	2	2	2
279	YPR036W	3,4%	1	2	2	2
280	YER112W	15,0%	1	2	2	2
281	YOL111C	10,4%	1	2	2	6
282	YJL122W	9,1%	1	2	2	4
283	YOR176W	5,1%	1	2	2	2
284	YJL123C	4,6%	1	2	2	4
285	YGR231C	6,5%	1	2	2	4
286	YIL043C	8,1%	1	2	2	2
287	YDR188W	3,5%	1	2	2	2
288	YOR153W	0,9%	1	2	2	2
289	YDL202W	7,2%	1	2	2	2
290	YGL020C	8,5%	1	2	2	2
291	YDR071C	8,9%	1	2	2	2
292	YDR383C	9,2%	1	2	2	4
293	YGR148C	13,6%	1	2	2	4
294	YJR009C	44,6%	1	2	13	31
295	YNL054W-A	47,5%	1	2	17	46
296	YOR327C	27,0%	1	2	2	5
297	YFR032C-A	39,0%	1	2	2	5
298	YLR056W	4,9%	1	2	2	2
299	YMR203W	7,2%	1	2	2	2
300	YBR085W	7,8%	1	2	4	4
301	YHR192W	6,1%	1	2	2	2
302	YOL012C	12,7%	1	1	2	6
303	YPL240C	29,2%	1	1	21	44
304	YHR214C-C	31,4%	8	1	11	17
305	YGR038C-A	62,5%	2	1	28	65

8.Appendix: Published results

8.1 Molecular architecture and connectivity of the budding yeast Mtw1 kinetochore complex

NIH Public Access
Author Manuscript
J Mol Biol. Author manuscript; available in PMC 2012 January 14.

Published in final edited form as:
J Mol Biol. 2011 January 14; 405(2): 548–559. doi:10.1016/j.jmb.2010.11.012.

NIH-PA Author Manuscript NIH-PA Author Manuscript NIH-PA Author Manuscript

Molecular architecture and connectivity of the budding yeast Mtw1 kinetochore complex

Peter Hornung[1], **Michael Maier**[1], **Gregory M Alushin**[2], **Gabriel C Lander**[3], **Eva Nogales**[3,4,5], and **Stefan Westermann**[1,*]

[1] Research Institute of Molecular Pathology, Dr. Bohr Gasse 7, 1030 Vienna, Austria

[2] Biophysics Graduate Group, University of California, Berkeley, Berkeley CA 94720. Department of Molecular and Cell Biology, University of California, Berkeley, Berkeley, CA 94720 USA

[3] Life Science Division, Lawrence Berkeley National Lab, 1 Cyclotron Road, Berkeley, 94720, USA

[4] Life Science Division, Lawrence Berkeley National Lab, 1 Cyclotron Road, Berkeley, CA 94720, USA

[5] Howard Hughes Medical Institute, Chevy Chase, MD, USA

Abstract

Kinetochores are large multi-protein complexes that connect centromeres to spindle microtubules in all eukaryotes. Among the biochemically distinct kinetochore complexes, the conserved four-protein Mtw1 complex is a central part of the kinetochore in all organisms. Here we present the biochemical reconstitution and characterization of the budding yeast Mtw1 complex. Direct visualization by EM revealed an elongated, bi-lobed structure with a 25 nm long axis. The complex can be assembled from two stable heterodimers consisting of Mtw1p-Nnf1p and Dsn1p-Nsl1p and it interacts directly with the microtubule-binding Ndc80 kinetochore complex via the centromere-proximal Spc24/25 head domain. In addition we have reconstituted a partial Ctf19 complex and show that it directly associates with the Mtw1 complex in vitro. Ndc80 and Ctf19 complexes do not compete for binding to the Mtw1 complex, suggesting that Mtw1 can bridge the microtubule-binding components of the kinetochore to the inner centromere.

Keywords

Kinetochore; KMN network; chromosome segregation; force generation; microtubule; centromere

Introduction

The interaction between chromosomes and spindle microtubules requires the action of a complex multi-protein machine termed the kinetochore[1; 2]. Kinetochores are responsible for microtubule-based force generation that drives sister chromatid separation in anaphase. They additionally contain an error-correction mechanism that ensures the bipolar attachments of sister chromatids to opposite spindle poles 3 and they relay signals to the mitotic checkpoint

---

[*] to whom correspondence should be addressed: Tel. +43 (1) 79730-3450; westermann@imp.ac.at.

Publisher's Disclaimer: This is a PDF file of an unedited manuscript that has been accepted for publication. As a service to our customers we are providing this early version of the manuscript. The manuscript will undergo copyediting, typesetting, and review of the resulting proof before it is published in its final citable form. Please note that during the production process errors may be discovered which could affect the content, and all legal disclaimers that apply to the journal pertain.

NIH-PA Author Manuscript NIH-PA Author Manuscript NIH-PA Author Manuscript

that prevents the cell from entering anaphase in the presence of unattached kinetochores 4. In budding yeast, the structural core of the kinetochore consists of at least seven biochemically distinct subcomplexes that are present in fixed copy numbers in mature budding yeast kinetochores 5 and assemble on centromeric DNA in a hierarchical manner 6. A current challenge in the field is to elucidate the architecture of the kinetochore by defining the binding interfaces between kinetochore complexes. Previous biochemical studies have focused on the reconstitution and functional analysis of two important parts of the budding yeast outer kinetochore: the Dam1 complex and the Ndc80 complex. Both of these complexes directly interact with microtubules and are required for force generation at yeast kinetochores 7; 8. The Dam1 complex has the ability to oligomerize into rings *in vitro* 9; 10, opening up the possibility that a Dam1 ring is a physiologically relevant coupling device for kinetochores on microtubule plus-ends in yeast. Recent experiments have demonstrated that Dam1 is a specialized plus-end tracking complex required for a persistent attachment of the Ndc80 complex to dynamic microtubule ends *in vitro* 11; 12.

The four-protein 180kDa Ndc80 complex is a conserved component of all kinetochores. Biochemical isolations from extracts and *in vitro* reconstitution experiments using *C. elegans* Ndc80 subunits have demonstrated that the complex functions together with the conserved four-protein complex Mtw1 (also called Mis12 or MIND) and the protein KNL-1/Blinkin (Spc105p in budding yeast) as part of a larger network termed KMN (KNL-1 Mis12 Ndc80) 13. Analysis of temperature-sensitive mutants of MTW1 complex subunits in fission yeast and budding yeast, as well as depletion experiments in worms and human cells, have demonstrated that the complex is essential for kinetochore bi-orientation and chromosome segregation 14; 15; 16. Since biochemical reconstitution experiments have so far only been performed with *C. elegans* kinetochore proteins, it is an open question whether the architecture, topology and biochemical activities of the KMN network are conserved among evolutionary distinct eukaryotes. Furthermore, it is unknown how the KMN network is anchored to the inner kinetochore, a critical step in creating a microtubule attachment site specifically at the centromere. Here, we report the reconstitution and biochemical characterization of the budding yeast Mtw1 complex. Our analysis defines the architecture of this central kinetochore complex and is an important step towards a reconstitution of the full yeast kinetochore.

Results and Discussion

Reconstitution of the four-protein Mtw1 complex

To reconstitute the budding yeast Mtw1 complex, we employed a poly-cistronic expression strategy. Genes encoding all four subunits (DSN1, MTW1, NNF1 and NSL1) of the complex were placed under the control of a T7 promoter and expressed in BL21 DE3 cells. The purification strategy used a 6xhistidine tag on the Nnf1p subunit allowing initial purification with a Ni-NTA resin. After elution, the complex was further purified by size exclusion chromatography (Figure 1A). Analysis of the complex on Coomassie stained gels revealed that all four subunits of the complex were present in 1:1:1:1 stoichiometry. The complex eluted earlier than expected from a size exclusion chromatography with a Stokes radius of 74.3 Å. The sedimentation coefficient of the Mtw1 complex was determined by glycerol gradient centrifugation and estimated to be 6S (data not shown). Thus, the native molecular weight of the recombinant complex is 183 kDa, compared to the calculated molecular weight of 148 kDa, and the frictional coefficient f/f_0 is 2.0, predicting a complex that is moderately to highly elongated. These values are in close agreement to those obtained for the Mtw1 complex in yeast extracts 17 suggesting that the recombinant complex closely resembles its native counterpart. We noticed that the Dsn1p subunit of the complex was particularly prone to proteolytic degradation during purification (Figure 1A). Sequencing of the major proteolysis products revealed that the N-terminus of Dsn1p is easily cleaved. We

NIH-PA Author Manuscript NIH-PA Author Manuscript NIH-PA Author Manuscript

subsequently cloned an N-terminally shortened version of the Dsn1 subunit corresponding to the major proteolysis product, which lacks amino acids 1–171. Expression of Dsn1$^{172-567}$ in combination with full-length MTW1, NNF1-6xHIS and NSL1 allowed the purification of the entire four-protein Mtw1 complex (Figure 1B). We conclude that the N-terminal extension of Dsn1, which is unusually long in budding yeast compared to other eukaryotes and predicted to be unstructured, is dispensable for complex formation *in vitro*. To determine whether this N-terminal extension has an essential function *in vivo*, we expressed wild-type or N-terminally truncated DSN1$^{172-576}$ on centromeric plasmids in a haploid DSN1 deletion strain that was kept viable by containing a wild-type copy of DSN1 on a CEN-based URA plasmid. Selection against the URA plasmid on 5-FOA plates demonstrated that Dsn1$^{172-576}$ supported wild-type growth (Supplementary Figure 1). Thus, the N-terminal 172 amino acids of Dsn1 are not required for complex formation *in vitro* and do not have an essential function *in vivo*.

The Mtw1 complex can be assembled from two stable heterodimers

SEC analysis of epitope-tagged kinetochore proteins in yeast extracts has suggests that Dam1 and Ndc80 complexes are present only in their fully assembled state, although Mtw1 complexes of different compositions can be detected 17. To identify such stable subcomplexes we expressed various combinations of Mtw1 complex subunits. We were able to express and purify two stable complexes: A heterodimer consisting of Mtw1p and Nnf1p (MN complex) (Figure 1D), and a heterodimer consisting of Dsn1p and Nsl1p (DN complex) (Figure 1C). We next asked whether the Mtw1 heterotetramer can be reconstituted by combining the two stable dimers. After mixing of MN and DN subcomplexes followed by size exclusion chromatography, we observed reconstitution of the full Mtw1 complex, which eluted at a position identical to the native complex (Figure 1E). Thus, the four-protein Mtw1 complex is composed of two stable heterodimers consisting of Mtw1p-Nnf1p and Dsn1p-Nsl1p, a result that is in agreement with binary two-hybrid interactions between these subunits 18.

EM analysis of the reconstituted Mtw1 complex

Negative stain single-particle electron microscopy was used to characterize the structural architecture of the Mtw1 complex. Despite our efforts to cross-link and purify the complex, the imaged fields of particles contained a heterogeneous mixture of aggregates and small fragments, as well as the monomeric, full size complex (Figure 2A). We manually picked the particle images that appeared to correspond to the monomeric, full-length complex based on their consistent size (indicated by white circles in Fig. 2A). After reference-free classification, we observed a distinct bi-lobed rod-like structure approximately 250Å in length, with one of the lobes consistently appearing slightly larger than the other (Figure 2B and D). The larger lobe varied in size, likely reflecting the presence of degrons of the Dsn1p subunit and/or different views around the long axis of the complex.

The larger globular lobe has an approximate diameter of 71 Å, and the smaller lobe 47 Å. Assuming a spherical shape for each, this would correspond to an approximate mass of 150 kDa and 45 kDa, respectively, the sum of which (195 kDa) very closely matches the experimentally determined mass. The calculated mass of the smaller lobe matches well with the combined predicted masses of Mtw1p and Nnf1p (57kDa) assuming that their coiled-coil domains project outwards from the lobe. The calculated mass of the larger lobe exceeds the combined masses of Dsn1p and Nsl1p (91kDa), suggesting that this lobe deviates from spherical geometry (the smaller lobe is too small to accommodate the mass of this subcomplex). The thin density connecting the two globular lobes is approximately 90Å long (Figure 2B), which matches the length of a predicted dimeric coiled-coil between the Mtw1p and Nnf1p subunits (Figure 2C). We also experimentally demonstrated that these two

NIH-PA Author Manuscript

NIH-PA Author Manuscript

NIH-PA Author Manuscript

proteins form a stable subcomplex, supporting the proposal that the coiled-coil regions of these two proteins probably dimerize in the context of the full complex. While this is the most parsimonious explanation for complex topology, we can't exclude the possibility that each globular head is occupied by more than two subunits.

In vivo the Mtw1 complex acts as a bridge between the microtubule-binding Ndc80 complex and the inner kinetochore 6. The Ndc80 complex is 57 nm in length 19, and the Mtw1 complex 25nm. Taken together, these dimensions suggest that the KMN network is long enough to span the full length of the outer kinetochore, consistent with high-resolution fluorescence microscopy studies 20.

Reconstitution of the interaction between Ndc80 and Mtw1 complexes

We next asked whether the recombinant Mtw1 complex can directly interact with the Ndc80 complex. To this end we purified the four-protein Ndc80 complex by expressing the Nuf2-Ndc80 and Spc24-Spc25 heterodimers individually and then reconstituted the entire complex using SEC (Figure 3A). When Mtw1 and Ndc80 complexes were mixed and subjected to gelfiltration, the elution profile of the assembly was shifted with respect to the individual complexes. Coomassie stained gels revealed that the complexes co-eluted, and densitometry of the Coomassie-stained bands indicated a 1:1 stoichiometry of the Mtw1-Ndc80 binary complex (Figure 3B and C). The elution position indicated that the Ndc80-Mtw1 assembly is a dimer containing one copy of each complex. The Ndc80-Mtw1 stoichiometry obtained from this biochemical experiment is in agreement with quantitative fluorescence microscopy data indicating the presence of nearly identical numbers of Ndc80 (8 copies) and Mtw1 (6–7 copies) complexes per each budding yeast kinetochore 5. Another important implication is that budding yeast Ndc80 and Mtw1 complexes form a stable association that does not depend on the presence of the KNL-1 protein Spc105p. This is in contrast to the *in vitro* reconstituted *C. elegans* KMN network, where only a Mis12-Knl1 association is competent to interact with the Ndc80 complex 13. Thus, while the overall association of Ndc80 and Mtw1 complexes is critical for the function of all kinetochores, the molecular details of this association can vary significantly in different organisms. Despite extensive efforts we were unable to express sufficient amounts of full-length or partial Spc105p/KNL-1 fragments, leaving open the possibility that the affinity of the Mtw1 complex for the Ndc80 complex may be increased by the presence of Spc105p.

The two globular domains of the Ndc80 complex have different functions: The Ndc80-Nuf2 head displays microtubule-binding activity through the presence of two Calponin-Homology (CH) domains and a basic N-terminal tail 8; 21. The Spc24/25 head, on the other hand, is thought to reside centromere-proximal and connect the Ndc80 complex to the rest of the kinetochore. We tested which of the Ndc80 subcomplexes provides the binding site for the Mtw1 complex. Therefore we subjected the purified Spc24/25 head of the Ndc80 complex and the Mtw1 complex to size exclusion chromatography first individually and then in combination. Upon pre-incubation with Mtw1 complex, part of the isolated Spc24/25 head was found co-eluting with the Mtw1 complex (Figure 3D and E). The interaction with the head domain seemed to be less efficient when compared to the full Ndc80 complex, suggesting that high-affinity may require the full Ndc80 complex. We conclude that the Ndc80 complex directly binds to the Mtw1 complex via its centromere-proximal Spc24/25 head domain, a result that is in agreement with high resolution microscopy data that place Spc24/25 in the immediate vicinity of Mtw1 complex subunits 20.

Consistent with the results obtained for the *C. elegans* KMN network, the reconstituted Mtw1 complex did not bind directly to taxol-stabilized microtubules in co-sedimentation experiments (Supplementary Figure 2). Only upon inclusion of the purified Ndc80 complex, the Ndc80-Mtw1 assembly was found co-pelleting with microtubules. Furthermore, binding

NIH-PA Author Manuscript

NIH-PA Author Manuscript

NIH-PA Author Manuscript

of the Mtw1 complex did not significantly alter the microtubule-binding properties of the Ndc80 complex (Supplementary Figure 2).

A Ctf19 core complex directly associates with the Mtw1 complex

High-resolution co-localization data place the Mtw1 complex close to the centromere-kinetochore interface 20, but the inner centromere receptor for the complex has not been identified. Human Mis12 complex has been reported to co-purify and directly interact with the inner centromere protein HP1 via the hNSL1 subunit 22; 23. The importance of this interaction for mitotic kinetochore function, however, is unclear and an HP1 homolog is absent from the *Saccharomyces cerevisiae* genome. Biochemical purifications of epitope-tagged Mtw1 subunits from yeast extracts 17; 24 have suggested two candidate interaction partners at the inner centromere interface - the budding yeast CENP-C homolog Mif2p and the Ctf19 complex. Initial experiments failed to detect a direct interaction between recombinant Mif2p fragments and the Mtw1 complex (data not shown), prompting us to focus on the Ctf19 complex as a potential binding partner. The yeast Ctf19 complex is the functional homolog of the constitutive-centromere associated network (CCAN) of higher eukaryotes. The CCAN was originally indentified as a set of polypeptides that co-purify with CENP-A containing nucleosomes 25; 26. The budding yeast Ctf19 complex consists of at least 11 subunits, some of which are organized into more stable subcomplexes. We reconstituted a core Ctf19 complex consisting of the proteins Ctf19p, Okp1p, Mcm21p and Ame1p (also termed COMA 17) by co-expression in *E. coli.* A purification procedure utilizing the 6xHis-tagged Ame1p subunit allowed isolation of the four-protein complex to near homogeneity (Figure 4A). Mcm21, Ame1-6xHis and Ctf19 polypeptides could be resolved on a 20 cm long SDS-PAGE gel (Figure 4A, right panel), and individual bands were excised and analyzed by mass spectrometry. This allowed assignment of the subunits to the corresponding bands on the SDS-PAGE. The intensity of the Coomassie stained bands suggest the presence of all four subunits of the COMA complex in a 1:1:1:1 stoichiometry.

To analyze potential associations with other kinetochore complexes, different concentrations of FLAG-tagged COMA complex were immobilized on beads, incubated with recombinant Mtw1, Ndc80 and Dam1 kinetochore complexes, washed and subsequently eluted with FLAG peptide (Figure 4B). While we failed to detect a direct association of the purified COMA complex with recombinant Ndc80 and Dam1 complexes, the Mtw1 complex consistently co-eluted together with COMA in a concentration-dependent manner (Figure 4C).

To verify the direct interaction between Mtw1 and COMA complexes we performed a reciprocal experiment in which 6xHis-tagged Mtw1, Ndc80 and Dam1 complexes were each immobilized on Ni-NTA agarose, incubated with recombinant Ctf19-Flag core complex, washed and eluted with imidazole. Only in the presence of Mtw1 complex is co-elution of the COMA complex observed (Figure 4C). To more stringently test the physical interaction, we analyzed Mtw1 and COMA complexes by size exclusion chromatography and found that the complexes co-eluted (Figure 5). This result raises the possibility that COMA is involved in recruiting the Mtw1 complex to the inner centromere in budding yeast. A strong prediction from this hypothesis is that Ndc80 and COMA complexes should not compete for binding to the Mtw1 complex. We tested this by pre-incubating Mtw1- and Ndc80 complexes, allowing formation of the binary Mtw1-Ndc80 assembly, followed by incubation with COMA-Flag beads. Incubation with Ndc80 did not prevent the interaction between COMA and Mtw1 complexes and both complexes co-eluted from the beads (Figure 6A). This result indicates that Ndc80 and COMA complexes occupy different binding sites on the Mtw1 complex. When testing the Mtw1-Nnf1 (MN) and Dsn1-Nsl1 (DN) subcomplexes separately in pull-down experiments we found that the MN subcomplex interacted more efficiently with COMA (Figure 6, B and C). Interestingly, of all Mtw1

NIH-PA Author Manuscript NIH-PA Author Manuscript NIH-PA Author Manuscript

subunits, high-resolution co-localization data place Nnf1p closest to the inner centromere in both humans and *S. cerevisiae* 27. Since the size of the smaller lobe of the Mtw1 complex roughly fits the combined masses of Mtw1-Nnf1, we tentatively speculate that the larger lobe, predominantly consisting of Dsn1p and Nsl1p, interacts with Spc24/Spc25, while the smaller lobe makes contact to the inner centromere complex COMA. Further antibody decoration experiments and direct visualization by electron microscopy will have to test this hypothesis.

In summary we have characterized the basic architecture of the budding yeast Mtw1 complex. Very recently, two manuscripts have described the reconstitution of the yeast28 and human Mis12 complex29. Our independent results regarding the overall shape of the yeast Mtw1 complex as judged by electron microscopy, its assembly from two stable heterodimers and the high affinity interaction with the Ndc80 complex are in close agreement with the experiments by Maskell et al. A comparison to the human Mis12 complex reveals interesting similarities and differences: The overall architecture of the complex, its topology based on stable Mtw1-Nnf1 and Dsn1-Nsl1 heterodimers is conserved between yeast and human. However, the molecular mechanism by which a high-affinity interaction with the Ndc80 complex is achieved differs considerably between the two organisms. In particular, a yeast Dsn1-Nsl1 heterodimer alone is not competent to bind the Ndc80 complex (our unpublished observations). Yeast Nsl1 lacks a critical binding motif (PVIHL) and a c-terminal tail which is necessary for the interaction between human Nsl1 and the Ndc80 complex 29. Instead, the binding interface between Mtw1 and Ndc80 complexes seems to receive significant contributions from Mtw1 and/or Nnf1. These findings highlight the necessity to analyze kinetochores biochemically in evolutionary distinct organisms in order to reveal common architectural principles and local binding interfaces.

Our results extend the studies by Maskell et al., and Petrovic et al., to provide a potential inner centromere receptor for the Mtw1 complex. The precise molecular basis for the interaction with the yeast Ctf19/COMA complex remains to be investigated. A puzzling aspect is that there is a considerably lower copy number of Ctf19 complex subunits (1–2) versus Mtw1 complexes (6–7) per each budding yeast kinetochore as judged by fluorescence microscopy 5. Furthermore, only OKP1 and AME1 are essential genes in budding yeast 30. It will be important to dissect the molecular binding interface between Ctf19/COMA and Mtw1 complexes in detail and evaluate the disruption of this binding interface *in vivo*. There may be considerable flexibility in the way the KMN network is anchored to the inner centromere. Some organisms like *C. elegans* or *Drosophila melanogaster* for example, seem to lack proteins related to the CCAN network entirely 2. In these kinetochores, the Mtw1 complex may rely on direct interactions with CENP-C for recruitment to the inner centromere.

Materials and Methods

Cloning of polycistronic expression vectors for MTW1 and CTF19

Open reading frames corresponding to Mtw1 complex subunits were amplified from yeast genomic DNA, cloned and expressed using the polycistronic expression system pET3aTr/pST39 that has been described previously 31. Genes were subcloned from the monocistronic pET3aTr vector into the polycistronic cassettes (1–4) of pST39 in the following order for the Mtw1-complex: (1) MTW1, (2) NSL1, (3) NNF1-6xHis, (4) DSN1. The truncated version DSN$^{172-576}$ was cloned into pET28a(+) and expressed in combination with pST39 (MTW1-NSL1-NNF1-6xHis).

NIH-PA Author Manuscript NIH-PA Author Manuscript NIH-PA Author Manuscript

The Ctf19 COMA subcomplex was cloned in the following order into the pST39 plasmid: (1) CTF19, (2) MCM21, (3) OKP1 and (4) AME1-6xHis/FLAG. Because of the presence of an intron, MCM21 was amplified from yeast cDNA.

Protein Expression and Purification

The Mtw1 complex was expressed in BL21 DE3 (Novagen) for 4h at 37°C after induction at $OD_{600} = 0.6$ with 0.4 mM isopropyl-β-D-thiogalactopyranosid (IPTG). The coexpression with $DSN^{172-576}$ was performed overnight (o/n) in the presence of 0.2 mM IPTG. The Mtw1 subcomplexes MN and DN were cloned into cassette 1 and 2 of the pST39 vector and the expression conditions were 37°C for 4h (MN) and 18°C overnight (DN). The COMA subcomplex was expressed at 18°C overnight after induction with 0.2 mM IPTG.

Bacteria were lysed by sonication in the presence of protease inhibitors (Roche) and the fusion proteins were isolated using Ni-NTA agarose beads (Qiagen). Binding and subsequent washing was performed in 20 mM HEPES pH 7.0, 300 mM NaCl, 30 mM imidazole. The Mtw1 complex or its two subcomplexes was eluted from Ni-NTA beads with 20 mM Tris pH 8.5, 80 mM NaCl and 250 mM imidazole, subsequently, it was subjected to anion exchange chromatography using a MonoQ 5/50 GL column (GE Healthcare) The column was developed with 10 bed volumes of a linear gradient from 80 mM to 1M NaCl in 20 mM Tris pH 8.5 containing 5% glycerol. The DN-subcomplex was further purified using size exclusion chromatography on a Superose 6 10/30 column.

The COMA-6xHis subcomplex was either purified with Ni-NTA agarose beads or by Anti-FLAG M2 affinity gel (Sigma Aldrich). COMA-6xHis was eluted with 20 mM HEPES pH 7, 150 mM NaCl, 5% Glycerol, 250 mM Imidazol, and loaded onto a size exclusion chromatography (SEC) Superdex 200 HiLoad 16/60 column equilibrated in 20 mM HEPES pH 7, 150 mM NaCl, 5% Glycerol. COMA-FLAG was eluted from M2 affinity gel with 3x FLAG peptide in TBS and the complex was concentrated using ultrafiltration (Vivaspins, cut off 10000 MW) followed by buffer exchange into 20 mM HEPES, pH 7.0, 150 mM NaCl, 5% Glycerol using PD-10 columns (GE Healthcare). Protein concentration was determined with DC Protein Assay kit (Bio-Rad Laboratories).

The Ndc80 and Dam1 kinetochore complexes were expressed and purified as described previously 9; 11; 24.

Interaction studies

0.1 –1 uM kinetochore protein complex in 500 µl binding buffer was immobilized on 20 µl Anti-Flag M2 Affinity gel or 20 µl Ni-NTA agarose beads. The interaction partner to be tested was used at 1 µM in binding buffer (TBS or PBS containing 30 mM imidazole). After incubation for 1h at 4°C, beads were washed three times in either TBS with 0.1% (v/v) NP-40 or in PBS with 30 mM imidazole and complexes were specifically eluted with 3x FLAG peptide or 250 mM imidazole.

Electron Microscopy

Mtw1 complex was thawed and prepared for EM analysis by the GraFix method 32. 150 µg of the complex was layered on to a 5–40% glycerol gradient in 20mM HEPES pH 7.6, 100mM NaCl, 1mM EDTA, 1mM DTT, which also contained a 0.02 – 0.15% gluteraldehyde gradient, and ultracentrifuged at 55,000 rpm for 13 hours in a TLS55 rotor at 4°C. Fractions were analyzed by SDS-PAGE, and the fraction containing the monomeric cross-linked complex was applied to a glow-discharged C-flat grid (Protochips) augmented with a layer of thin carbon and stained with 2% uranyl formate.

Images were collected on a Gatan 4kx4k CCD camera using a Tecnai F20 electron microscope operating at 120kV and 30,000x magnification. Despite purification by glycerol gradient, the images contained a mixture of aggregates and fragments, as well as the monodispersed full complex. Approximately 5,000 particles that appeared to correspond to the full monomeric complex were picked manually with the BOXER program 33 and subjected to reference-free classification as described 34.

Coiled-coil predictions were performed with the MARCOIL program 35. The regions indicated with grey boxes in Figure 2C correspond to areas of greater than 50% coiled-coil probability, all of which contain regions of greater than 80% coiled-coil probability.

Supplementary Material

Refer to Web version on PubMed Central for supplementary material.

Acknowledgments

The authors wish to thank all members of the Westermann lab for discussions, and Fabienne Lampert for the gift of purified Dam1 complex. The research leading to these results has received funding from the European Research Council under the European Community's Seventh Framework Programme (S.W., FP7/2007-2013)/ERC grant agreement n° [203499], by the Austrian Science Fund FWF (S.W., SFB F34-B03), and by the National Institutes of Health (E.N. PO1GM51487) and the Damon Ranyon Foundation (G.C.L.).

Abbreviations

SEC	size exclusion chromatography
MT	microtubule
5-FOA	5-Fluoroorotic Acid

References

1. Cheeseman IM, Desai A. Molecular architecture of the kinetochore-microtubule interface. Nat Rev Mol Cell Biol. 2008; 9:33–46. [PubMed: 18097444]
2. Santaguida S, Musacchio A. The life and miracles of kinetochores. Embo J. 2009; 28:2511–31. [PubMed: 19629042]
3. Tanaka TU, Rachidi N, Janke C, Pereira G, Galova M, Schiebel E, Stark MJ, Nasmyth K. Evidence that the Ipl1-Sli15 (Aurora kinase-INCENP) complex promotes chromosome bi-orientation by altering kinetochore-spindle pole connections. Cell. 2002; 108:317–29. [PubMed: 11853667]
4. Musacchio A, Salmon ED. The spindle-assembly checkpoint in space and time. Nat Rev Mol Cell Biol. 2007; 8:379–93. [PubMed: 17426725]
5. Joglekar AP, Bouck DC, Molk JN, Bloom KS, Salmon ED. Molecular architecture of a kinetochore-microtubule attachment site. Nat Cell Biol. 2006; 8:581–5. [PubMed: 16715078]
6. Westermann S, Drubin DG, Barnes G. Structures and functions of yeast kinetochore complexes. Annu Rev Biochem. 2007; 76:563–91. [PubMed: 17362199]
7. Westermann S, Wang HW, Avila-Sakar A, Drubin DG, Nogales E, Barnes G. The Dam1 kinetochore ring complex moves processively on depolymerizing microtubule ends. Nature. 2006; 440:565–9. [PubMed: 16415853]
8. Ciferri C, Pasqualato S, Screpanti E, Varetti G, Santaguida S, Dos Reis G, Maiolica A, Polka J, De Luca JG, De Wulf P, Salek M, Rappsilber J, Moores CA, Salmon ED, Musacchio A. Implications for kinetochore-microtubule attachment from the structure of an engineered Ndc80 complex. Cell. 2008; 133:427–39. [PubMed: 18455984]
9. Westermann S, Avila-Sakar A, Wang HW, Niederstrasser H, Wong J, Drubin DG, Nogales E, Barnes G. Formation of a dynamic kinetochore- microtubule interface through assembly of the Dam1 ring complex. Mol Cell. 2005; 17:277–90. [PubMed: 15664196]

NIH-PA Author Manuscript

NIH-PA Author Manuscript

NIH-PA Author Manuscript

10. Miranda JJ, De Wulf P, Sorger PK, Harrison SC. The yeast DASH complex forms closed rings on microtubules. Nat Struct Mol Biol. 2005; 12:138–43. [PubMed: 15640796]
11. Lampert F, Hornung P, Westermann S. The Dam1 complex confers microtubule plus end-tracking activity to the Ndc80 kinetochore complex. J Cell Biol. 189:641–9. [PubMed: 20479465]
12. Tien JF, Umbreit NT, Gestaut DR, Franck AD, Cooper J, Wordeman L, Gonen T, Asbury CL, Davis TN. Cooperation of the Dam1 and Ndc80 kinetochore complexes enhances microtubule coupling and is regulated by aurora B. J Cell Biol. 189:713–23. [PubMed: 20479468]
13. Cheeseman IM, Chappie JS, Wilson-Kubalek EM, Desai A. The conserved KMN network constitutes the core microtubule-binding site of the kinetochore. Cell. 2006; 127:983–97. [PubMed: 17129783]
14. Goshima G, Kiyomitsu T, Yoda K, Yanagida M. Human centromere chromatin protein hMis12, essential for equal segregation, is independent of CENP-A loading pathway. J Cell Biol. 2003; 160:25–39. [PubMed: 12515822]
15. Cheeseman IM, Niessen S, Anderson S, Hyndman F, Yates JR 3rd, Oegema K, Desai A. A conserved protein network controls assembly of the outer kinetochore and its ability to sustain tension. Genes Dev. 2004; 18:2255–68. [PubMed: 15371340]
16. Kline SL, Cheeseman IM, Hori T, Fukagawa T, Desai A. The human Mis12 complex is required for kinetochore assembly and proper chromosome segregation. J Cell Biol. 2006; 173:9–17. [PubMed: 16585270]
17. De Wulf P, McAinsh AD, Sorger PK. Hierarchical assembly of the budding yeast kinetochore from multiple subcomplexes. Genes Dev. 2003; 17:2902–21. [PubMed: 14633972]
18. Kiyomitsu T, Obuse C, Yanagida M. Human Blinkin/AF15q14 is required for chromosome alignment and the mitotic checkpoint through direct interaction with Bub1 and BubR1. Dev Cell. 2007; 13:663–76. [PubMed: 17981135]
19. Wang HW, Long S, Ciferri C, Westermann S, Drubin D, Barnes G, Nogales E. Architecture and flexibility of the yeast Ndc80 kinetochore complex. J Mol Biol. 2008; 383:894–903. [PubMed: 18793650]
20. Joglekar AP, Bloom K, Salmon ED. In vivo protein architecture of the eukaryotic kinetochore with nanometer scale accuracy. Curr Biol. 2009; 19:694–9. [PubMed: 19345105]
21. Wei RR, Al-Bassam J, Harrison SC. The Ndc80/HEC1 complex is a contact point for kinetochore-microtubule attachment. Nat Struct Mol Biol. 2006
22. Obuse C, Iwasaki O, Kiyomitsu T, Goshima G, Toyoda Y, Yanagida M. A conserved Mis12 centromere complex is linked to heterochromatic HP1 and outer kinetochore protein Zwint-1. Nat Cell Biol. 2004; 6:1135–41. [PubMed: 15502821]
23. Kiyomitsu T, Iwasaki O, Obuse C, Yanagida M. Inner centromere formation requires hMis14, a trident kinetochore protein that specifically recruits HP1 to human chromosomes. J Cell Biol. 188:791–807. [PubMed: 20231385]
24. Westermann S, Cheeseman IM, Anderson S, Yates JR 3rd, Drubin DG, Barnes G. Architecture of the budding yeast kinetochore reveals a conserved molecular core. J Cell Biol. 2003; 163:215–22. [PubMed: 14581449]
25. Foltz DR, Jansen LE, Black BE, Bailey AO, Yates JR 3rd, Cleveland DW. The human CENP-A centromeric nucleosome-associated complex. Nat Cell Biol. 2006; 8:458–69. [PubMed: 16622419]
26. Okada M, Cheeseman IM, Hori T, Okawa K, McLeod IX, Yates JR 3rd, Desai A, Fukagawa T. The CENP-H-I complex is required for the efficient incorporation of newly synthesized CENP-A into centromeres. Nat Cell Biol. 2006; 8:446–57. [PubMed: 16622420]
27. Wan X, O'Quinn RP, Pierce HL, Joglekar AP, Gall WE, DeLuca JG, Carroll CW, Liu ST, Yen TJ, McEwen BF, Stukenberg PT, Desai A, Salmon ED. Protein architecture of the human kinetochore microtubule attachment site. Cell. 2009; 137:672–84. [PubMed: 19450515]
28. Maskell DP, Hu XW, Singleton MR. Molecular architecture and assembly of the yeast kinetochore MIND complex. J Cell Biol. 190:823–34. [PubMed: 20819936]
29. Petrovic A, Pasqualato S, Dube P, Krenn V, Santaguida S, Cittaro D, Monzani S, Massimiliano L, Keller J, Tarricone A, Maiolica A, Stark H, Musacchio A. The MIS12 complex is a protein interaction hub for outer kinetochore assembly. J Cell Biol. 190:835–52. [PubMed: 20819937]

NIH-PA Author Manuscript

NIH-PA Author Manuscript

NIH-PA Author Manuscript

30. Ortiz J, Stemmann O, Rank S, Lechner J. A putative protein complex consisting of Ctf19, Mcm21, and Okp1 represents a missing link in the budding yeast kinetochore. Genes Dev. 1999; 13:1140–55. [PubMed: 10323865]

31. Tan S. A modular polycistronic expression system for overexpressing protein complexes in Escherichia coli. Protein Expr Purif. 2001; 21:224–34. [PubMed: 11162410]

32. Kastner B, Fischer N, Golas MM, Sander B, Dube P, Boehringer D, Hartmuth K, Deckert J, Hauer F, Wolf E, Uchtenhagen H, Urlaub H, Herzog F, Peters JM, Poerschke D, Luhrmann R, Stark H. GraFix: sample preparation for single-particle electron cryomicroscopy. Nat Methods. 2008; 5:53–5. [PubMed: 18157137]

33. Ludtke SJ, Baldwin PR, Chiu W. EMAN: semiautomated software for high-resolution single-particle reconstructions. J Struct Biol. 1999; 128:82–97. [PubMed: 10600563]

34. Ramey VH, Wang HW, Nogales E. Ab initio reconstruction of helical samples with heterogeneity, disorder and coexisting symmetries. J Struct Biol. 2009; 167:97–105. [PubMed: 19447181]

35. Delorenzi M, Speed T. An HMM model for coiled-coil domains and a comparison with PSSM-based predictions. Bioinformatics. 2002; 18:617–25. [PubMed: 12016059]

NIH-PA Author Manuscript

NIH-PA Author Manuscript

NIH-PA Author Manuscript

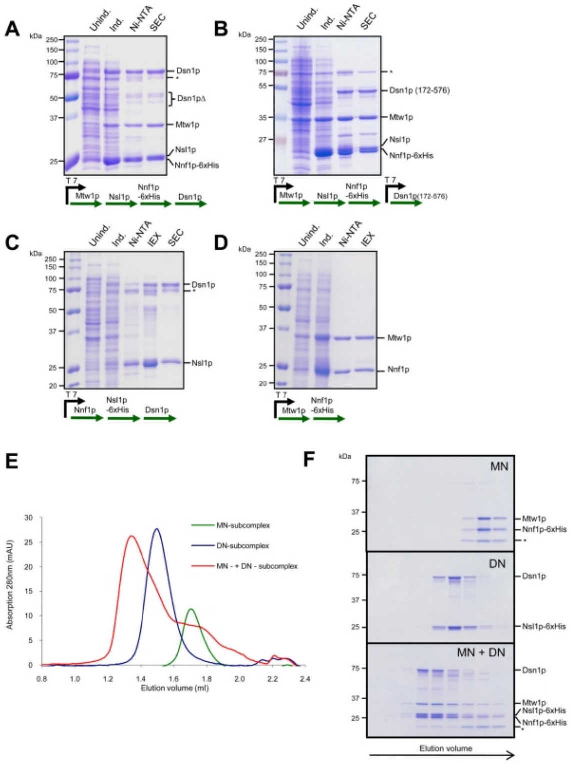

Figure 1. Reconstitution of the Mtw1 complex

A. Expression and purification of the Mtw1 complex. The coomassie-stained gel shows different steps of the purification scheme: control extract and extract after induction with IPTG, eluate from Ni-NTA beads and purified fraction after SEC. Note the presence of degradation products of the Dsn1p subunit. **B**. Expression and purification of a complex with an N-terminally truncated Dsn1p subunit. **C**. Expression and purification of a stable Dsn1-Nsl1 heterodimer. IEX denotes anion exchange chromatorgraphy. Asterisks in A, B and C indicate a contamination with the *E. coli* Hsp70 chaperone **D**. Expression and purification of Mtw1-Nnf1 heterodimer. **E**. SEC runs of Dsn1p-Nsl1p and Mtw1p-Nnf1p subcomplexes (8 μM each) and of the full complex after reconstitution. **F**. Coomassie-stained SDS-PAGE of fractions from E. Asterisks indicate an Nnf1 truncation product.

NIH-PA Author Manuscript NIH-PA Author Manuscript NIH-PA Author Manuscript

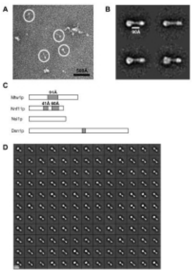

Figure 2. EM analysis of the Mtw1 complex

A. Negative stain EM image of the Mtw1 complex. Note the heterogeneous composition of the sample. White circles correspond to particles chosen for further analysis. **B**. Selected class averages showing the architecture and dimensions of the complex. The complex is a bi-lobed rod, with one large and one small globular domain. **C**. Coiled-coil predictions for the protein subunits of the complex. Grey regions correspond to greater than 50% coiled-coil probability. **D**. Entire complement of class averages obtained for the complex. They all display the bi-lobed architecture, with most heterogeneity occurring in the size of the larger globular domain.

NIH-PA Author Manuscript

NIH-PA Author Manuscript

NIH-PA Author Manuscript

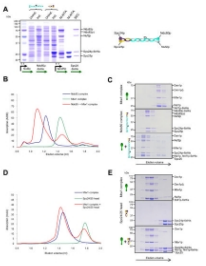

Figure 3. The Mtw1 complex interacts with Ndc80 via the Spc24/25 head

A. Expression and purification of the Ndc80 kinetochore complex. The Ndc80-Nuf2 and Spc24-Spc25 heterodimers are expressed individually and after combination the reconstituted full complex is purified by SEC. **B**. Coomassie-stained gels of gelfiltration runs of Mtw1 complex and Ndc80 complex alone, or after combination (9 μM each). **C**. Gelfiltration profile corresponding to B. **D**. Coomassie-stained gels of Mtw1 complex and purified Spc24/25 head domain alone, or after combination (6 μM each). **E**. Gelfiltration profile corresponding to D.

NIH-PA Author Manuscript NIH-PA Author Manuscript NIH-PA Author Manuscript

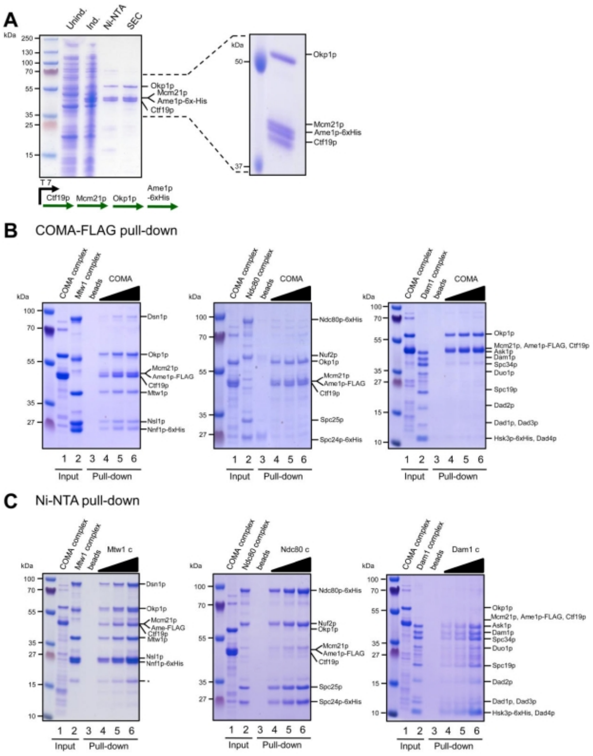
A
Unind.
Ind.
Ni-NTA
SEC
kDa
Okp1p
Mcm21p
Ame1p-6x-His
Ctf19p
Ame1p-6xHis
T 7
Ctf19p
Mcm21p
Okp1p
Ame1p -6xHis
B COMA-FLAG pull-down
COMA complex
Mtw1 complex
Ndc80 complex
Dam1 complex
beads
COMA
Dsn1p
Mcm21p
Ame1p-FLAG
Mtw1p
Nsl1p
Nnf1p-6xHis
Ndc80p-6xHis
Nuf2p
Spc25p
Spc24p-6xHis
Mcm21p, Ame1p-FLAG, Ctf19p
Ask1p
Dam1p
Spc34p
Duo1p
Spc19p
Dad2p
Dad1p, Dad3p
Hsk3p-6xHis, Dad4p
1 2 3 4 5 6
Input
Pull-down
C Ni-NTA pull-down
Mtw1 c
Ndc80 c
Dam1 c

Figure 4. Reconstitution of a Ctf19 core complex (COMA) and interaction with Mtw1

A. Reconstitution of the Ctf19-Okp1-Mcm21-Ame1 complex (COMA). Coomassie stained gel of different stages of the purification. Right panel: The four polypeptides of the complex are resolved on large SDS-PAGE gels. **B.** Pull-down experiment with immobilized COMA complex. Different amounts of recombinant COMA complex (lane 1) were immobilized on Anti-FLAG M2 affinity gel and incubated with Mtw1, Ndc80 or Dam1 complex (lane 2). Control pull-downs contained only M2 beads (lane 3). After washing, bound complexes were eluted with FLAG-peptide (lane 4–6). Note that the Mtw1 complex co-elutes with COMA from the beads. C. COMA-Flag complex (lane 1) was incubated with His-tagged Mtw1-, Ndc80 or Dam1 complex which were immobilized on Ni-NTA beads (lane 2, lane 3 denotes Ni-NTA beads as a negative control). After washing, bound complexes were eluted with imidazole (lanes 4–6). Note that the COMA complex is co-eluted with the Mtw1 complex from Ni-NTA beads.

NIH-PA Author Manuscript

NIH-PA Author Manuscript

NIH-PA Author Manuscript

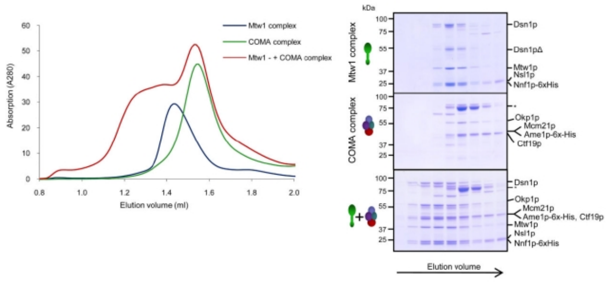

Figure 5. Size-exclusion chromatography of Mtw1 and COMA complexes

Coomassie-stained gels and gelfiltration profiles of Mtw1 complex and Ndc80 complex individually, or after combination (5 µM each). Asterisk indicates Hsp70 contamination in the COMA complex sample.

NIH-PA Author Manuscript

NIH-PA Author Manuscript

NIH-PA Author Manuscript

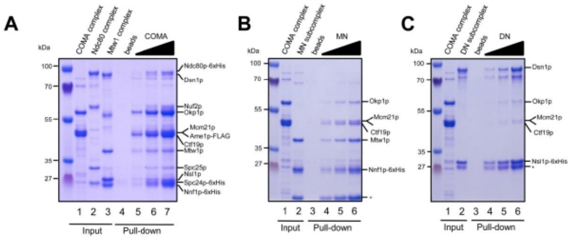
A
kDa
100
70
55
35
27
COMA complex
Ndc80 complex
Mtw1 complex
beads
COMA
Ndc80p-6xHis
Dsn1p
Nuf2p
Okp1p
Mcm21p
Ame1p-FLAG
Ctf19p
Mtw1p
Spc25p
Nsl1p
Spc24p-6xHis
Nnf1p-6xHis
1 2 3 4 5 6 7
Input
Pull-down
B
kDa
100
70
55
35
27
COMA complex
MN subcomplex
beads
MN
Okp1p
Mcm21p
Ctf19p
Mtw1p
Nnf1p-6xHis
*
1 2 3 4 5 6
Input
Pull-down
C
kDa
100
70
55
35
27
COMA complex
DN subcomplex
beads
DN
Dsn1p
Okp1p
Mcm21p
Ctf19p
Nsl1p-6xHis
*
1 2 3 4 5 6
Input
Pull-down

Figure 6. Ndc80 and the COMA complex bind non-competitively to the Mtw1 complex

A. COMA-flag complex (lane1) was immobilized on M2 beads. Mtw1 (lane2) and Ndc80 complexes (lane 3) were pre-mixed and incubated with control-beads (lane 4) or COMA-flag beads. After washing, bound complexes were eluted with Flag peptide (lanes 5–7). **B.** Pull-down experiment using 6xHis tagged MN-subcomplex on Ni-NTA agarose and and FLAG-tagged COMA complex. Note co-elution of the complexes from the Ni-NTA beads. Asterisk indicates Nnf1 truncation product **C**. Pull-down experiment using 6xHis tagged DN-subcomplex on Ni-NTA agarose and FLAG-tagged COMA complex. The COMA complex fails to interact with the DN subcomplex. Asterisk denotes Nsl1 truncation product.

8.2 CENP-T proteins are conserved centromere receptors of the Ndc80 complex

nature cell biology

CENP-T proteins are conserved centromere receptors of the Ndc80 complex

Alexander Schleiffer[1], Michael Maier[2], Gabriele Litos[2], Fabienne Lampert[2], Peter Hornung[2], Karl Mechtler[2] and Stefan Westermann[2,3]

Centromeres direct the assembly of kinetochores, microtubule-attachment sites that allow chromosome segregation on the mitotic spindle. Fundamental differences in size and organization between evolutionarily distant eukaryotic centromeres have in many cases obscured general principles of their function. Here we demonstrate that centromere-binding proteins are highly conserved between budding yeast and humans. We identify the histone-fold protein Cnn1$^{\mathrm{CENP\text{-}T}}$ as a direct centromere receptor of the microtubule-binding Ndc80 complex. The amino terminus of Cnn1 contains a conserved peptide motif that mediates stoichiometric binding to the Spc24–25 domain of the Ndc80 complex. Consistent with the critical role of this interaction, artificial tethering of the Ndc80 complex through Cnn1 allows mini-chromosomes to segregate in the absence of a natural centromere. Our results reveal the molecular function of CENP-T proteins and demonstrate how the Ndc80 complex is anchored to centromeres in a manner that couples chromosome movement to spindle dynamics.

Kinetochores are large assemblies of multiple-protein complexes exceeding 60 proteins in budding yeast and more than 100 components in humans[1–3]. As essential cell-division organelles, kinetochores allow the mitotic spindle to drive chromosome segregation by productively coupling microtubule plus-end dynamics to the separation of sister chromatids. In addition, kinetochores contain error-correction and signalling mechanisms that relay the establishment of correct kinetochore bi-orientation on the spindle to the onset of anaphase[4,5]. Kinetochores have the following general building plan: the KMN network (consisting of the four-protein Mtw1 complex, the four-protein Ndc80 complex and KNL-1 in complex with Zwint) is a supramolecular assembly that forms the architectural core of the kinetochore and contacts spindle microtubules directly[6,7]. By means that are not well understood, the KMN network is anchored to centromeric chromatin that is characterized by the presence of a specialized nucleosome that contains the histone variant CENP-A replacing the canonical histone H3. The conserved DNA-binding protein CENP-C closely associates with and probably directly recognizes CENP-A nucleosomes[8,9] to provide an essential step in kinetochore assembly. In addition, a group of at least 15 polypeptides, in humans termed the centromere constitutive-associated network (CCAN) co-purify specifically with CENP-A nucleosomes[10,11]. Similar proteomic approaches have identified centromere proteins in budding yeast[12,13] (collectively called the Ctf19 complex) and fission yeast[14] (Sim4 complex). Although the evolutionary conservation of the KMN network has been well documented[15], phylogenetic relationships between centromere proteins have remained uncertain. Centromere DNA is highly divergent between species, bearing no resemblance in length or sequence between evolutionarily distant yeasts such as *Saccharomyces cerevisiae* and *Schizosaccharomyces pombe* and between yeast and humans. The simplest centromeres are found in *S. cerevisiae*, comprising only 125 base pairs of DNA (point centromere) with three sequence elements that are conserved between the 16 chromosomes[15,16]. The centromeres of *S. pombe* are regional, built on more complex DNA that contains repeated sequence elements and has the hallmarks of heterochromatin. Centromeric DNA in human cells spans over many megabases and contains α-satellite repeats that are, however, neither necessary nor sufficient to initiate kinetochore assembly[17]. These marked differences in centromere organization have led to the notion that budding yeast may employ many proteins dedicated to the sequence-determined point centromere and thus may have a fundamentally different kinetochore architecture when compared with higher eukaryotes.

Here we reveal a number of previously undetected homology relationships between yeast and human centromere proteins leading to the conclusion that structurally similar kinetochores assemble on small point and large regional centromeres. We show that the histone-fold protein Cnn1$^{\mathrm{CENP\text{-}T}}$ provides an evolutionarily conserved

---

[1] IMP/IMBA Bioinformatics Core Facility, Research Institute of Molecular Pathology (IMP), Dr. Bohr Gasse 7, 1030 Vienna, Austria. [2] Research Institute of Molecular Pathology (IMP), Dr. Bohr Gasse 7, 1030 Vienna, Austria.
[3] Correspondence should be addressed to S.W. (e-mail: westermann@imp.ac.at)

Received 29 September 2011; accepted 30 March 2012; published online 6 May 2012; DOI: 10.1038/ncb2493

© 2012 Macmillan Publishers Limited. All rights reserved.

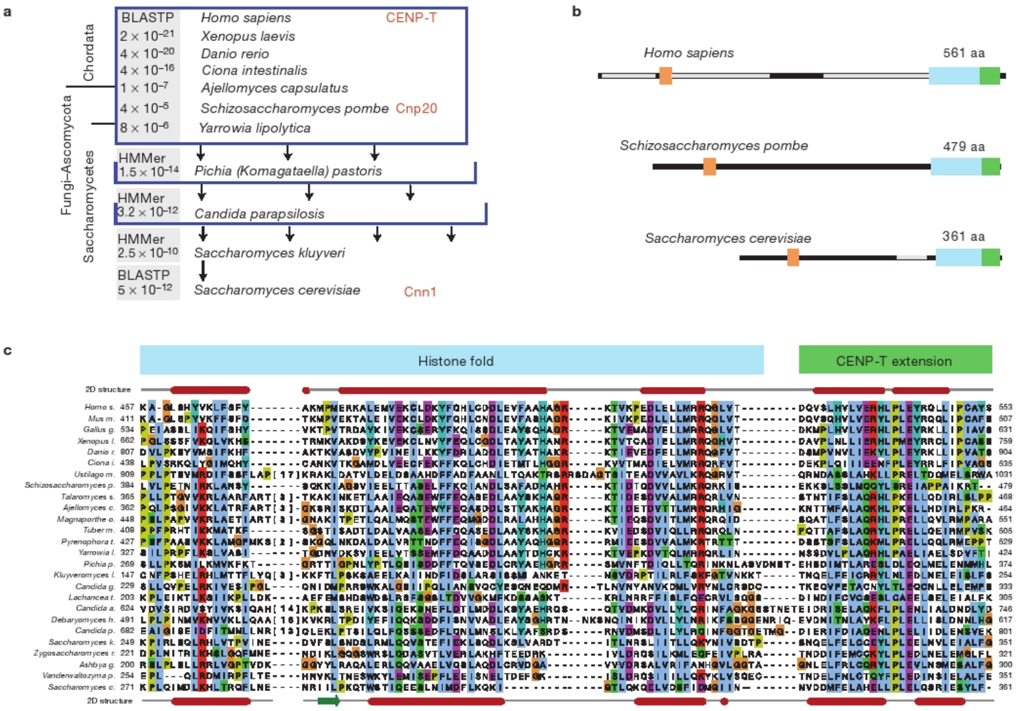
a
Chordata
Fungi–Ascomycota
Saccharomycetes
BLASTP
2 × 10−21
4 × 10−20
4 × 10−16
1 × 10−7
4 × 10−5
8 × 10−6
Homo sapiens
CENP-T
Xenopus laevis
Danio rerio
Ciona intestinalis
Ajellomyces capsulatus
Schizosaccharomyces pombe
Cnp20
Yarrowia lipolytica
HMMer
1.5 × 10−14
Pichia (Komagataella) pastoris
HMMer
3.2 × 10−12
Candida parapsilosis
HMMer
2.5 × 10−10
Saccharomyces kluyveri
BLASTP
5 × 10−12
Saccharomyces cerevisiae
Cnn1
b
Homo sapiens
561 aa
Schizosaccharomyces pombe
479 aa
Saccharomyces cerevisiae
361 aa
c
Histone fold
CENP-T extension
2D structure
2D structure

Figure 1 Identification of Cnn1 as a budding yeast CENP-T homologue. (**a**) Summary of the search strategy to deduce phylogenetic relationships between human CENP-T and *S. cerevisiae* Cnn1. A series of BLASTP and HMM searches using sequences of the conserved domain (see below) were applied. (**b**) Graphical representation of Cnn1/CENP-T sequence features, showing the location of the N-terminal motif (orange), the histone fold (blue) and the C-terminal CENP-T family specific extension (green). Low-complexity regions are indicated in grey. (**c**) Multiple alignment of the histone fold and the C-terminal extension of the Cnn1/CENP-T protein family. *H. sapiens* (above) and *S. cerevisiae* (below) secondary-structure predictions are derived from the Jpred 3 server (α-helical regions are in red; β-strands in green[46]). Species and accession numbers are listed in Supplementary Table S2. Background colouring of the residues is based on the clustalx colouring scheme. Brackets indicate the number of omitted residues.

direct link to the Ndc80 complex, the key microtubule-binding activity of the kinetochore.

RESULTS

Evolutionary conservation of centromere-proximal proteins between yeast and humans

To examine whether centromere-binding proteins of evolutionarily distant organisms share common ancestry, we performed a comprehensive bioinformatic analysis using sensitive remote homology searches in combination with secondary-structure predictions. Our analysis indicates a remarkable conservation of the centromere–kinetochore interface across eukaryotes (Table 1). We detected previously unrecognized homology relationships between the essential budding yeast proteins Ame1 and Okp1 and the human CCAN subunits CENP-U and CENP-Q, respectively (Supplementary Figs S1 and S2 and Methods). Importantly, this indicates that the budding yeast COMA (Ctf19–Okp1–Mcm21–Ame1) complex may have a biochemical counterpart in the human CENP-O/P/Q/U complex, which also forms a stable entity[18,19]. In addition, we find that the yeast Ctf19 complex subunit Mcm22 is orthologous to human CENP-K (Supplementary Fig. S3 and Methods).

Identification of fungal orthologues of the human kinetochore protein CENP-T

Recent studies have demonstrated a critical role for the DNA-binding activity of the human CENP-T/W complex in kinetochore function[20] and together with CENP-C, CENP-T plays an instructive role in kinetochore assembly[21]. Human CENP-T is 561 residues long, but besides a histone domain at the carboxy terminus[20,22], most of the protein consists of regions of compositional bias, rich in polar residues. On the sequence level, generally the histone fold is highly variable—pairwise identities between archaeal and eukaryotic histones range from 15 to 20%, but the structure is highly defined, consisting of three α-helices separated by two β-strand loops[23–26]. A single BLASTP search identified orthologues in chordates and fungi with significant *E* values ($<4 \times 10^{-5}$), among those, the known *S. pombe* CENP-T homologue Cnp20 (SPBC800.13; ref. 27) and the uncharacterized protein YALI0A19162p in the Saccharomycetes *Yarrowia lipolytica*.

© 2012 Macmillan Publishers Limited. All rights reserved.

Table 1 Homology relationships between centromere proteins from human, *S. pombe* and *S. cerevisiae* based on sequence analysis.

H. sapiens	*S. pombe*	*S. cerevisiae*	CCAN module
CENP-C	Cnp3	Mif2	C
CENP-O	Mal2	Mcm21	O/P/Q/U/R
CENP-P	Fta2	Ctf19	
CENP-Q	Fta7	Okp1	
CENP-U	Mis17	Ame1	
CENP-R			
CENP-H	Fta3	Mcm16	H/I/K
CENP-I	Mis6	Ctf3	
CENP-K	Sim4	Mcm22	
CENP-T	SPBC800.13/Cnp20	Cnn1	CCAN-HF
CENP-W	SPAC17G8.15	YDR374W-A/Wip1	
CENP-S	SPBC2D10.16	YOL086W-A/Mhf1	
CENP-X	SPCC576.12c	YDL160C-A/Mhf2	
CENP-M			MNL
CENP-N	Mis15	Chl4	
CENP-L	Fta1	Iml3 (Mcm19)	
	Fta4	Nkp1	
	Cnl2	Nkp2	
	Fta5		
	Fta6		

The grouping reflects biochemically distinct subcomplexes. For a comprehensive overview of the CCAN subunits and their taxonomic distribution, see Supplementary Table S1.

Reciprocal BLASTP searches confirmed the orthologous relationship between fungal and mammalian CENP-T proteins. Iterative PSI-BLAST searches with the conserved C-terminal domain first collected CENP-T proteins, but in further iterations included histone H4 and other histone-fold proteins. To search for a *S. cerevisiae* homologue, we applied a series of sensitive hidden Markov model (HMM) profile searches within specified proteomes, where we first identified a candidate in *Pichia pastoris* (Pipas_chr3_0909, *E* value 1.5×10^{-14}), then in *Candida parapsilosis* (CPAG_01066, *E* value 3.2×10^{-12}) and then in *Saccharomyces kluyveri* (SAKL0F01012g, *E* value 2.5×10^{-10}; Fig. 1a). In all proteomes, the second best hit was to histone H4 with highly significant *E* values as well (7.1×10^{-12}, 7.1×10^{-9} and 1.2×10^{-8} for *P. pastoris* Pipas_c034_0035, *C. parapsilosis* CPAG_04945 and *S. kluyveri* SAKL0C10714g, respectively). The *S. kluyveri* CENP-T candidate SAKL0F01012g was annotated to be weakly similar to *S. cerevisiae* Cnn1, and the homology was confirmed by BLASTP (*E* value 5×10^{-12}).

Although the sequence identity on the primary amino-acid level is low, CENP-T proteins share a conserved architecture. At the C terminus, there is the conserved CENP-T domain, consisting of a histone fold and two extra helices (Fig. 1b,c). The highly conserved central helix of the histone fold spans around 29 residues. In *S. cerevisiae* Cnn1, this helix is considerably shorter (20 residues), and less conserved in comparison with the adjacent non-histone-fold helices. Although no direct phylogenetic relationship between CENP-T and Cnn1 can be deduced, a common sequence architecture and experimental data, such as the biological significance of a conserved N-terminal motif (see below), lead to the conclusion that both proteins are indeed orthologous.

Proteomic analysis of the budding yeast CCAN

To gain insight into the molecular organization of the budding yeast CCAN network, we performed systematic tandem-affinity purifications followed by mass spectrometry to identify associated proteins (Fig. 2a). For Ame1$^{\text{CENP-U}}$, Chl4$^{\text{CENP-N}}$ and Mcm16$^{\text{CENP-H}}$, this approach yielded a similar interaction profile with each protein co-purifying all other members of the Ctf19 complex and all four subunits of the Mtw1 complex, demonstrating that the Mtw1 complex provides an important attachment point between CCAN and KMN components. Remarkably, purification of Cnn1$^{\text{CENP-T}}$ resulted in a different set of co-purifying polypeptides: whereas most members of the Ctf19 complex could be detected, assigning Cnn1 as a CCAN component, Mtw1 complex subunits were absent from this purification and instead all four subunits of the Ndc80 complex were co-purified. This indicated that Cnn1$^{\text{CENP-T}}$ might form a unique point of contact between the inner and outer kinetochore. In Mcm16$^{\text{CENP-H}}$ and Cnn1$^{\text{CENP-T}}$ purifications we additionally detected the product of an uncharacterized open reading frame, YDR374W-A, encoding an 89-amino-acid protein with a predicted high α-helical content. A GFP-fusion to YDR374W-A co-localized with the kinetochore marker Nuf2 and this localization was abolished in a *cnn1*-deletion mutant (Fig. 2b). Recombinant YDR374W-A expressed in bacteria formed a complex with the C terminus of Cnn1, which contains the predicted histone fold (Fig. 2c). Furthermore, chromatin immunoprecipitation (ChIP) in combination with quantitative real-time PCR showed both Cnn1 and YDR374W-A to be enriched at centromeric chromatin (Fig. 2d). Sensitive homology searches could not enlarge the YDR374W-A protein family outside the Saccharomycetes class, with the *Debaryomyces hansenii* protein DEHA2G10538g being the most distant homologue. However, DEHA2G10538g has also been identified in a CENP-W-derived HMM search (Methods). Taken together, these results indicate that YDR374W-A is the budding yeast homologue of human CENP-W and we will refer to this protein as Wip1 (W-like protein 1, Supplementary Fig. S4).

In mammals, two further histone-fold proteins are known to interact with the core CCAN complex: CENP-S and CENP-X (refs 20, 28), forming CENP-S/CENP-X (ref. 29) and CENP-T/CENP-W heterodimeric complexes or SXTW heterotetrameric complexes[22]. The yeast CENP-S and -X homologues Mhf1 and Mhf2 (refs 29,30) co-purified each other, Mhf2 exhibited further associations with a subset of CCAN subunits and Mhf1 interacted with the DEAH box helicase Mph1 and the DNA repair proteins Msh2 and 3, indicating that Mhf1 and Mhf2 might have dual functions at centromeres and in DNA repair (Supplementary Table S3).

To characterize the protein Wip1 further, we examined its localization in deletion mutants of other CCAN subunits. Whereas the typical bi-lobed localization to kinetochore clusters was unchanged in deletion mutants of *mcm16*$^{\textit{CENP-H}}$, *iml3*$^{\textit{CENP-L}}$ and *mcm21*$^{\textit{CENP-O}}$, it was abolished in a *chl4*$^{\textit{CENP-N}}$-deletion mutant, demonstrating that in addition to Cnn1, the protein critically depends on this CCAN subunit for its localization to kinetochores (Fig. 3a). In a reciprocal experiment we investigated whether any other CCAN subunit depended on the presence of Wip1 for kinetochore localization. We found that the localization of Mcm16$^{\text{CENP-H}}$, Ctf19$^{\text{CENP-P}}$ and Chl4$^{\text{CENP-N}}$ was maintained in a *wip1*-deletion mutant (data not shown), but the intensity of the fluorescent signal of Cnn1 was severely reduced by about 80%, consistent with the observed physical interaction between Cnn1 and Wip1 (Fig. 3b). Cnn1 localization was disrupted to a similar extent in a *chl4*-deletion mutant (data not shown), as

© 2012 Macmillan Publishers Limited. All rights reserved.

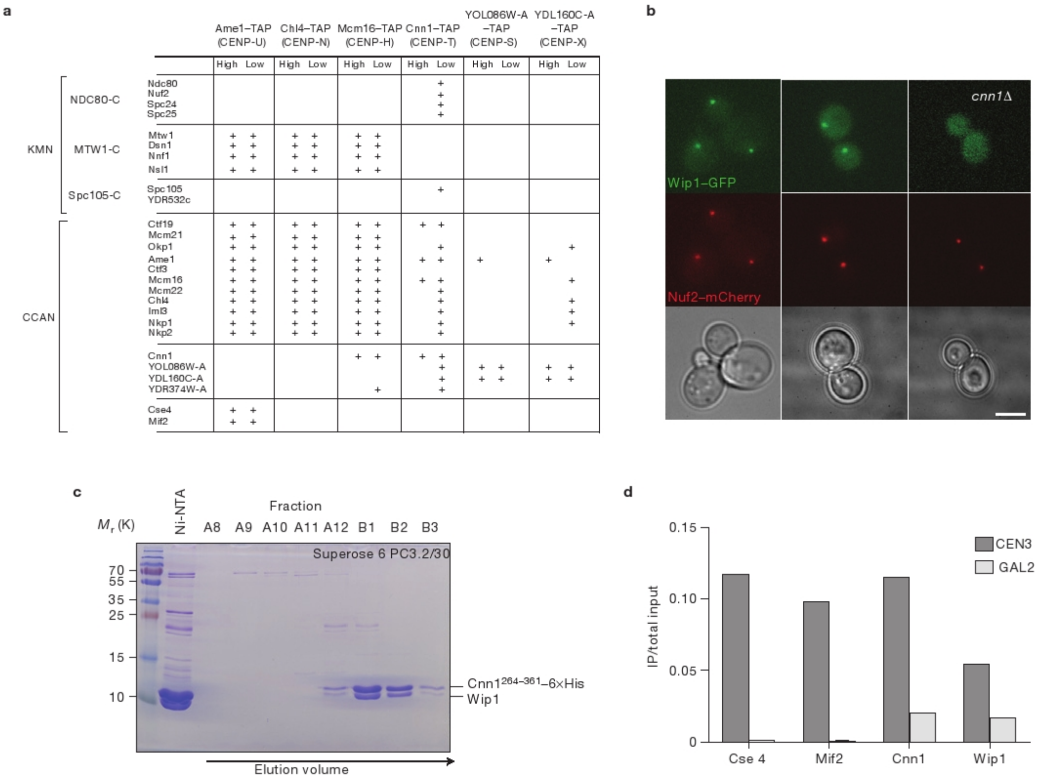

			Ame1–TAP (CENP-U)		Chl4–TAP (CENP-N)		Mcm16–TAP (CENP-H)		Cnn1–TAP (CENP-T)		YOL086W-A –TAP (CENP-S)		YDL160C-A –TAP (CENP-X)	
			High	Low	High	Low	High	Low	High	Low	High	Low	High	Low
KMN	NDC80-C	Ndc80								+				
		Nuf2								+				
		Spc24								+				
		Spc25								+				
	MTW1-C	Mtw1	+	+	+	+	+	+						
		Dsn1	+	+	+	+	+	+						
		Nnf1	+	+	+	+	+	+						
		Nsl1	+	+	+	+	+	+						
	Spc105-C	Spc105								+				
		YDR532c												
CCAN		Ctf19	+	+	+	+	+	+	+	+				
		Mcm21	+	+	+	+	+	+						
		Okp1	+	+	+	+	+	+		+				+
		Ame1	+	+	+	+	+	+	+	+	+		+	
		Ctf3	+	+	+	+	+	+						
		Mcm16	+	+	+	+	+	+	+	+				+
		Mcm22	+	+	+	+	+	+		+				
		Chl4	+	+	+	+	+	+		+				+
		Iml3	+	+	+	+	+	+		+				+
		Nkp1	+	+	+	+	+	+		+				+
		Nkp2	+	+	+	+	+	+		+				
		Cnn1					+	+	+	+				
		YOL086W-A								+	+	+	+	+
		YDL160C-A								+	+	+	+	+
		YDR374W-A						+		+				
		Cse4	+	+										
		Mif2	+	+										

Figure 2 Proteomic analysis of the yeast CCAN and identification of the subunit Wip1. (**a**) Summary of the systematic tandem-affinity purifications (TAPs) of CCAN components. '+' denotes that a protein was co-purified with the respective bait; 'high' and 'low' denote stringency conditions during purification of 300 mM or 100 mM KCl, respectively. (**b**) Live-cell microscopy of Wip–GFP in wild-type cells or in a *cnn1*-deletion background. Scale bar, 5 μm. (**c**) Wip1 forms a complex with the histone fold of Cnn1. Analytical size-exclusion chromatography of Wip1 co-expressed with Cnn1 (residues 264–361) in bacteria after initial purification using Ni-NTA agarose. (**d**) ChIP with quantitative PCR was performed for Cse4–13xMyc, Mif2–13xMyc, Cnn1–13xMyc and Wip1–13xMyc using primers spanning a centromeric (CEN3) and a non-centromeric region (GAL2, chromosome XII). The no-antibody control/total-input control has been subtracted for each experiment. Data represent the mean of ≥ 2 independent experiments.

predicted from the observation that Wip1 depended on Chl4 for kinetochore localization.

Cnn1/CENP-T is a centromere receptor for the Ndc80 complex

Its unique protein interaction profile prompted us to investigate the role of Cnn1$^{\text{CENP-T}}$ more closely. Physical interactions between CENP-T and KMN components have been reported[21], but the specificity and molecular basis of these associations have remained uncharacterized. To rigorously probe potential interactions, we purified full-length Cnn1$^{\text{CENP-T}}$ from yeast extracts and examined its association with reconstituted recombinant budding yeast Ndc80 and Mtw1 kinetochore complexes by size-exclusion chromatography. The appearance of a fast-eluting species indicated complex formation between the Ndc80 complex and Cnn1$^{\text{CENP-T}}$ (Fig. 4a). The complex seemed stoichiometric on Coomassie-stained gels and formed under submicromolar input concentrations, indicating a high-affinity interaction. Under the same conditions, no complex formation was observed between Cnn1–Flag and the Mtw1 complex (Supplementary Fig. S5a) or between Cnn1 and the purified Spc105/YDR532c complex (data not shown). We next examined whether the interaction of Cnn1 with the Ndc80 complex is compatible with simultaneous binding of the Mtw1 complex and thus would allow interaction with the KMN network. In three-component gel filtration experiments with an excess of Mtw1 complex, Ndc80–Mtw1 complex formation was readily observed as reported previously[31–33]. Interestingly, under these conditions, Cnn1 failed to co-elute effectively with the Mtw1–Ndc80 supercomplex, indicating that the Mtw1 complex and Cnn1$^{\text{CENP-T}}$ are competing binding partners of the Ndc80 complex (Supplementary Fig. S5b). Supporting this, Cnn1–Flag immobilized on beads efficiently pulled down the free recombinant Ndc80 complex, but the amount of interacting Ndc80 complex was reduced in a dose-dependent manner with increasing concentration of Mtw1 complex included in the reaction. Cnn1–Flag failed to pull down the Mtw1 complex, either alone or in the presence of the Ndc80

© 2012 Macmillan Publishers Limited. All rights reserved.

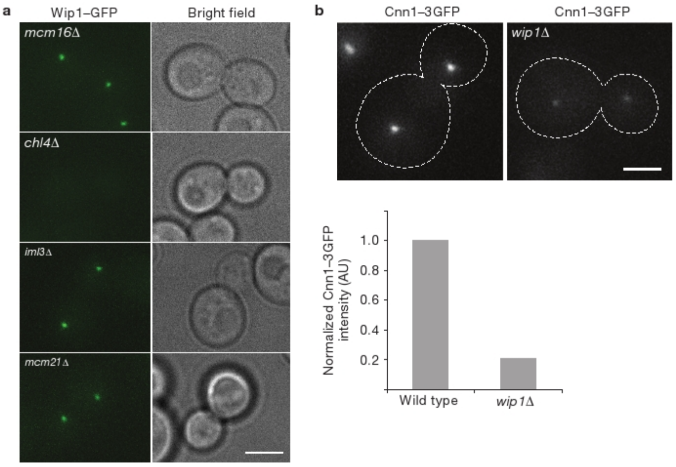

Figure 3 Localization dependencies of yeast CCAN histone-fold proteins. (**a**) Live-cell microscopy of Wip1–GFP in various CCAN-deletion mutants. Note the absence of kinetochore localization in the *chl4*-deletion mutant. (**b**) Live-cell microscopy of yeast strains expressing Cnn1–3GFP in a wild-type or *wip1*-deletion background. Lower panel: Quantification of Cnn1–3GFP fluorescence intensity in a wild-type or *wip1*-deletion strain. The intensity of Cnn1–3GFP in a wild-type strain was normalized to 1; kinetochore clusters in 10 anaphase cells were quantified. Scale bar, 2 μm.

complex (Fig. 4b,c). Taken together, these experiments indicate that Cnn1$^{\text{CENP-T}}$ and the Mtw1 complex are competing binding partners for the Ndc80 complex.

To probe the interaction between the Ndc80 complex and Cnn1 in the cell, we performed co-immunoprecipitation experiments using myc-tagged Nuf2. Cnn1–Flag could be specifically co-immunoprecipitated from log-phase extracts, confirming an association between these proteins *in vivo* (Fig. 5a). Notably, when immunoprecipitations were performed from extracts that had been synchronized by release from an α-factor arrest, the interaction was detectable only in a time window of about 90–105 min after the release. Immunofluorescence microscopy indicated that these time points corresponded to the time of mitotic spindle elongation (Fig. 5b). In contrast, co-immunoprecipitation experiments indicated a relatively constant affinity between the Ndc80 complex and the Mtw1 complex over the cell cycle (Fig. 5c). We conclude that the interaction between Cnn1 and Ndc80 occurs in a cell-cycle-specific manner and is predominantly detectable in anaphase.

Identification of an Ndc80 receptor motif in the N terminus of Cnn1

Using the motif search program MEME, we could identify a short conserved motif in the otherwise unstructured N terminus of CENP-T proteins, predicted to fold into an α-helix with several conserved hydrophobic residues (Fig. 6a). We reasoned that this N-terminal motif might be involved in the interaction with the Ndc80 complex. Consistent with our hypothesis, a mutant Cnn1 protein lacking the 15-amino-acid conserved motif (Cnn1$^{\Delta 65-79}$, Fig. 6b) failed to interact with the recombinant Ndc80 complex (Fig. 6c). We next established the binding site on the Ndc80 complex: the Ndc80 heterotetramer contains two functionally distinct ends, the microtubule-binding Ndc80–Nuf2 dimer and the Spc24–25 dimer, which is required for centromere localization of the complex[34]. Size-exclusion chromatography indicated the formation of a tight complex between the Spc24–25 dimer and Cnn1, which was abolished in the Cnn1 mutant lacking the conserved N-terminal motif (Fig. 6d). We also established that the Ndc80 complex can recruit Cnn1 to taxol-stabilized microtubules in co-sedimentation experiments (Supplementary Fig. S7). To determine whether the conserved motif is also sufficient for Ndc80 binding, we synthesized a 25-amino-acid peptide including the 15-residue binding motif. We characterized the association using isothermal titration calorimetry and found that this peptide binds in a 1:1 stoichiometry to the Spc24–25 heterodimer with an apparent dissociation constant of 3.2 μM (Fig. 6e). This affinity seems to be lower than observed in gel filtration experiments with full-length Cnn1, indicating that additional parts of the N terminus may contribute to the high-affinity interaction with the Ndc80 complex. As the Spc24–25 domain has previously been identified as the binding site for the Mtw1 complex[31–33], this result can explain the observed competition for Ndc80-complex binding and implies that the Spc24–25 domain has at least two distinct, mutually exclusive binding partners within the yeast kinetochore, the N terminus of Cnn1$^{\text{CENP-T}}$ and the Mtw1 complex.

Artificial tethering of the Ndc80 complex through Cnn1 promotes mini-chromosome segregation in the absence of a centromere

Budding yeast strains with a deletion of Cnn1$^{\text{CENP-T}}$ and/or Wip1$^{\text{CENP-W}}$ did not exhibit an obvious growth or chromosome segregation defect (data not shown), indicating that in principle the Mtw1-based Ndc80 recruitment pathway is sufficient to support viability in this organism. In addition, by fluorescence microscopy we could not detect a substantial reduction of Ndc80 signal intensity in a *cnn1*-deletion mutant (Supplementary Fig. S8). In contrast, the putative *S. pombe* CENP-T homologue Cnp20 is an

© 2012 Macmillan Publishers Limited. All rights reserved.

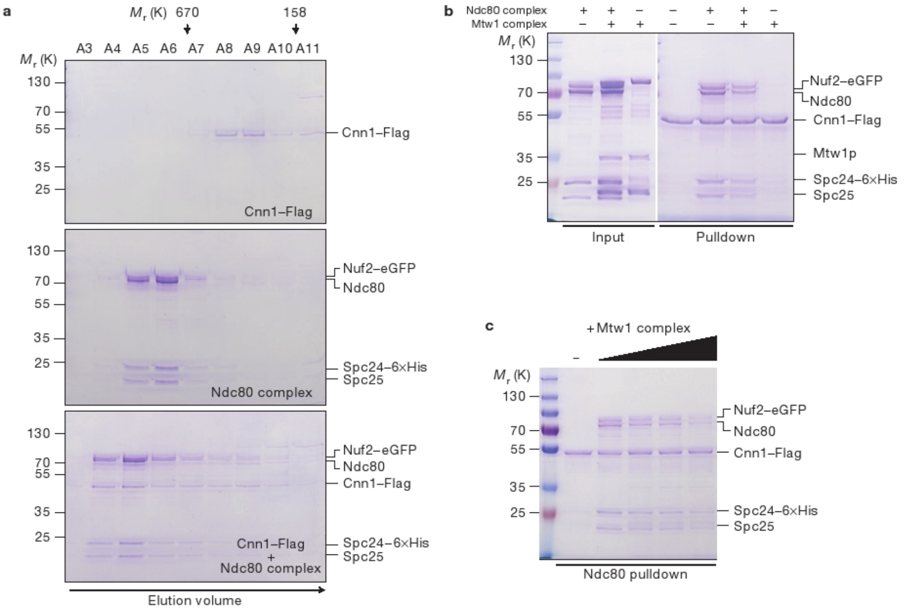

Figure 4 Cnn1$^{\text{CENP-T}}$ is an exclusive and direct interaction partner of the Ndc80 complex. (**a**) Analytical size-exclusion chromatography of recombinant Cnn1–Flag (upper panel), reconstituted yeast Ndc80 complex (middle) or a combination of both (lower panel). Elution positions of standard proteins are indicated at the top. (**b**) Pulldown experiment with recombinant Ndc80 and Mtw1 kinetochore complexes and Cnn1–Flag immobilized on beads. (**c**) Pulldown experiment with Cnn1–Flag, Ndc80 complex and increasing concentrations of the Mtw1 complex.

essential protein and mutants exhibit very severe chromosome segregation phenotypes[27].

To probe the biological function of Ndc80 recruitment by Cnn1$^{\text{CENP-T}}$ in budding yeast we therefore employed a synthetic gain-of function approach (Fig. 7a). As described previously, artificial tethering of proteins to a replication-competent mini-chromosome that lacks an authentic centromere can be used to determine whether candidate proteins are able to provide the function of an artificial kinetochore[35,36]. Direct tethering of the Ndc80 complex through a C-terminal TetR fusion to the Spc24 subunit failed to induce a mitotic stabilization of mini-chromosomes[35]. As a result of our biochemical experiments, we reasoned that it might be essential to recruit the Ndc80 complex through the elongated, flexible Cnn1 N terminus. We constructed a strain in which the histone-fold domain of Cnn1 was replaced with the TetR repressor and compared the stability of an acentric *tetO* mini-chromosome in this strain with that of a number of control strains (Fig. 7b). Notably, the Cnn1$^{\Delta\text{HF}}$–TetR fusion, but not the Spc24–TetR fusion, strongly enhanced mini-chromosome stability over multiple generations. The stabilizing effect exceeded that of Ask1–TetR, a known force-transducing component of the budding yeast Dam1 kinetochore complex[37]. Importantly, the artificial kinetochore function supplied by Cnn1$^{\Delta\text{HF}}$–TetR was abolished in a mutant lacking amino acids 65–79 (Fig. 7c), demonstrating that it strictly depended on the ability of Cnn1 to interact with the Ndc80 complex. On the other hand, recruiting subunits of the Mtw1 complex (Mtw1–TetR and Nnf1–TetR) to the tetO array did not lead to plasmid stabilization. In similar experiments, LacI fusions to CENP-T have been shown to recruit KMN components to ectopic chromosomal lacO arrays in human cells and they can partially replace the activity of an endogenous centromere in chicken DT40 cells[21]. Thus, the ability of Cnn1$^{\text{CENP-T}}$ to anchor Ndc80 complexes to DNA in a manner that allows them to productively interact with the mitotic spindle seems to be a conserved feature of these proteins.

A Wip1-deletion allele exhibits severe synthetic phenotypes in combination with other kinetochore mutants

The experiments so far indicate that different receptors for Ndc80 complexes are present at yeast kinetochores. This could explain why Ndc80 loss-of-function mutants exhibit severe chromosome-detachment phenotypes[38] whereas mutants of Mtw1 complex subunits or Mif2$^{\text{CENP-C}}$ do not[39]. To address this issue, we combined temperature-sensitive *mif2* or *mtw1* mutants with *cnn1* or *wip1* deletions and investigated their phenotypes. *mif2 wip1* double mutants showed a severe growth defect (Fig. 7d) and similar synthetic interactions were detected with *okp1* and *mtw1* alleles (data not shown). Inspection of chromosome segregation by immunofluorescence microscopy showed that the *mif2 wip1* double mutant contained elongated mitotic spindles with a single mass of unsegregated DNA, phenotypically similar to the defects seen in an *ndc80-1* mutant at the restrictive temperature, but distinct from the *mif2-3* and *wip1* single mutants (Fig. 7e). Thus, simultaneously interfering with both Ndc80 recruitment modes leads to severe defects in chromosome segregation.

© 2012 Macmillan Publishers Limited. All rights reserved.

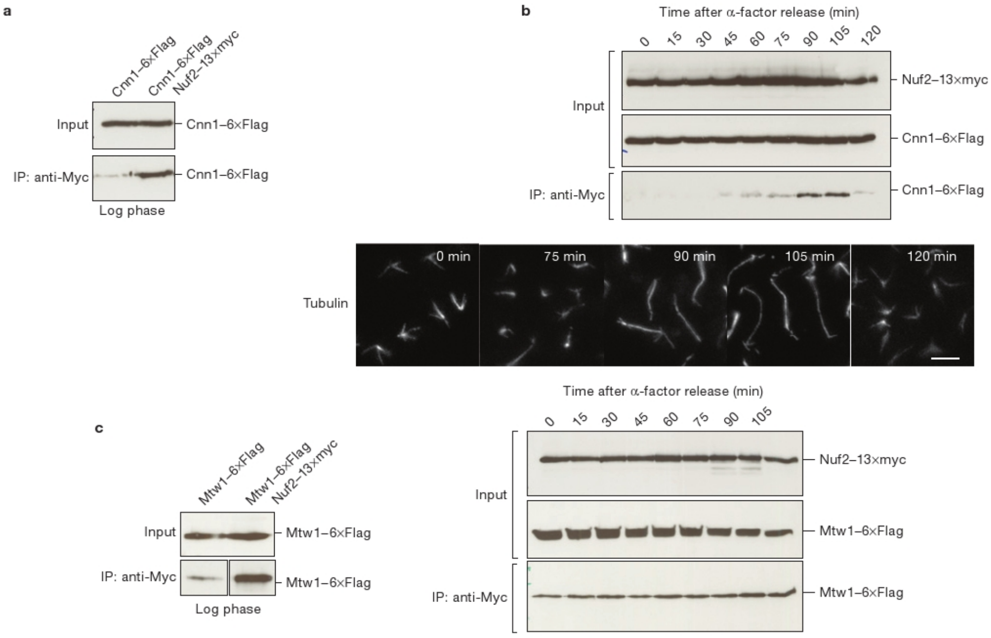

Figure 5 Cell-cycle-dependent interaction between Ndc80 and Cnn1$^{\text{CENP-T}}$. (**a**) Co-immunoprecipitation between Nuf2–13xMyc and Cnn1–6xFlag from yeast log-phase extracts. (**b**) Cell-cycle co-immunoprecipitation experiment (top panel): after release from an α-factor arrest, extracts were prepared at the indicated times and Nuf2 was immunoprecipitated using anti-myc beads. Cnn1 was detected by anti-Flag western blot. Lower panel: anti-tubulin immunofluorescence microscopy of samples taken at the indicated time points from the cell-cycle experiment. Note the presence of long anaphase spindles in the 90 and 105 min time points. Scale bar, 5 μm. (**c**) Corresponding experiment probing the interaction between the Ndc80 and the Mtw1 complex. Nuf2–13xMyc was immunoprecipitated and the association with Mtw1–6xFlag was detected by western blot. Uncropped images of western blots are shown in Supplementary Fig. S6.

DISCUSSION

Our investigations into budding yeast centromere proteins have uncovered general organization principles of kinetochores (Fig. 7f). The conserved role of CENP-T proteins is to act as direct, KMN-independent centromere receptors of the Ndc80 complex. This provides a molecular understanding for the requirement of the CENP-T N terminus for kinetochore assembly in human cells[21] and can explain the observation that it undergoes a tension-dependent conformational change in response to microtubule attachments[40]. The original identification of Cnn1 as an interaction partner of the Mtw1 complex[19] was probably due to the use of a single-step purification protocol, which has been shown to co-purify a large set of kinetochore proteins[41]. Our results raise the question as to why kinetochores contain multiple different Ndc80 recruiters. In budding yeast, the interaction between Ndc80 and Cnn1 is detectable predominantly in anaphase, the mitotic phase in which cells have irreversibly committed to segregate their chromosomes. Consistent with this observation, the levels of Cnn1 at kinetochores seem to be increased in anaphase, as judged by live-cell microsocopy[42]. Recruitment through CENP-T incorporates the Ndc80 complex into a flexible attachment filament that might be especially suited for force transduction to move chromosomes, a property that was reflected in our artificial kinetochore experiment[43]. As part of the KMN network, on the other hand, Ndc80 complexes are linked to signalling molecules of the mitotic checkpoint machinery[44] and thus play important roles in sensing the presence and quality of kinetochore–microtubule attachments. The observation that Cnn1 and the Mtw1 complex compete for Ndc80 binding and that the Cnn1–Ndc80 affinity is increased during anaphase is indicative of significant changes in kinetochore architecture that occur at the metaphase–anaphase transition. Future experiments will have to reveal how these structural rearrangements are established and what their precise functional consequence is. CENP-T proteins and CCAN subunits other than CENP-C seem to be absent from the kinetochores of *Caenorhabditis elegans* and *Drosophila melanogaster*. Consistent with the existence of different Ndc80 recruitment pathways, *mis12* mutants in these organisms exhibit a true kinetochore-null phenotype[45] because here Ndc80 is exclusively recruited as part of the KMN network. ☐

METHODS

Methods and any associated references are available in the online version of the paper at www.nature.com/naturecellbiology

Note: Supplementary Information is available on the Nature Cell Biology website

ACKNOWLEDGEMENTS

The authors thank all members of the Westermann laboratory for discussions and J. M. Peters for critical reading of the manuscript. We thank T. Burkard for suggestions, W. Lugmayr for support with high-performance computing,

© 2012 Macmillan Publishers Limited. All rights reserved.

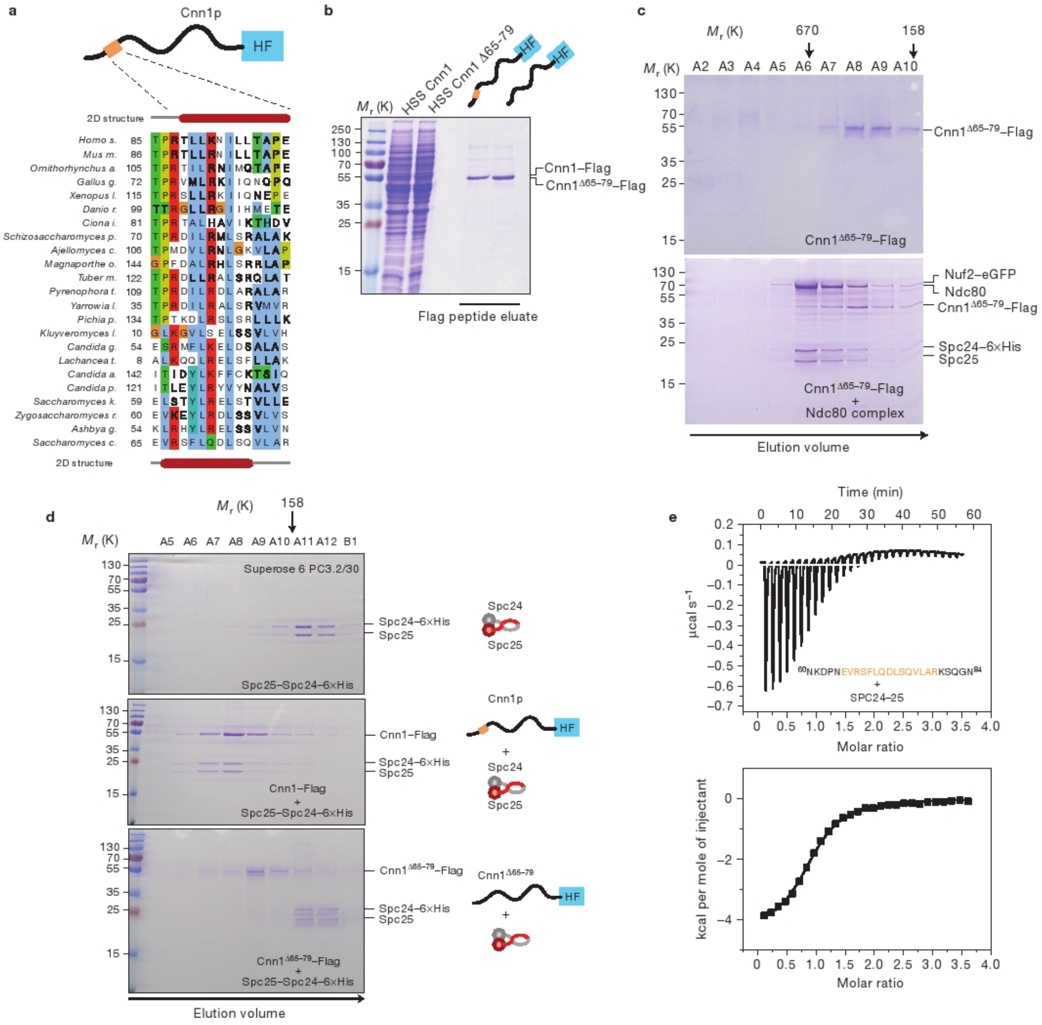

Figure 6 The N terminus of Cnn1$^{CENP\text{-}T}$ contains a conserved binding motif for the Spc24/25 domain of the Ndc80 complex. (**a**) Multiple sequence alignment of a conserved motif present in the N termini of CENP-T proteins. Secondary-structure predictions identify a potential α-helix in human (top) and budding yeast (bottom) CENP-T proteins. (**b**) Purification of overexpressed Cnn1–Flag and Cnn1$^{Δ65–79}$–Flag lacking the conserved N-terminal motif from yeast extracts. HSS: high-speed supernatant. (**c**) Size-exclusion chromatography of Cnn1$^{Δ65–79}$–Flag alone (top panel) or in combination with reconstituted yeast Ndc80 complex (lower panel). (**d**) Analytical size-exclusion chromatography of the recombinant Spc24–25 heterodimer alone (upper panel), or in combination with full-length Cnn1–Flag (middle panel) or Cnn1$^{Δ65–79}$–Flag (lower panel). (**e**) Isothermal titration calorimetry with a Cnn1-derived peptide (residues 60–84) encompassing the conserved N-terminal motif and the Spc24–25 heterodimer. Upper panel shows raw data of heat change on binding; lower panel depicts binding isotherm derived from the data.

O. Hudecz for help with presentation of the mass spectrometry results and M. Madalinski for peptide synthesis. We thank P. De Wulf (European Institute of Oncology, Milan, Italy) for the Cnn1–3GFP strain and communicating results before publication. Research in the Westermann laboratory receives funding from the European Research Council under the European Community's Seventh Framework Programme (S.W. FP7/2007-2013)/ERC grant agreement no. 203499, and from the Austrian Science Fund FWF (S.W., SFB F34-B03).

AUTHOR CONTRIBUTIONS

A.S. performed bioinformatic sequence analysis. M.M. purified CCAN proteins and performed characterization of proteins. P.H. performed interaction studies. F.L. conducted ChIP and biochemical experiments. K.M. guided the mass spectrometry analysis. S.W. guided the study and performed biochemical and genetic experiments supported by G.L. All authors discussed results and analysed data. S.W. and A.S. wrote the manuscript.

© 2012 Macmillan Publishers Limited. All rights reserved.

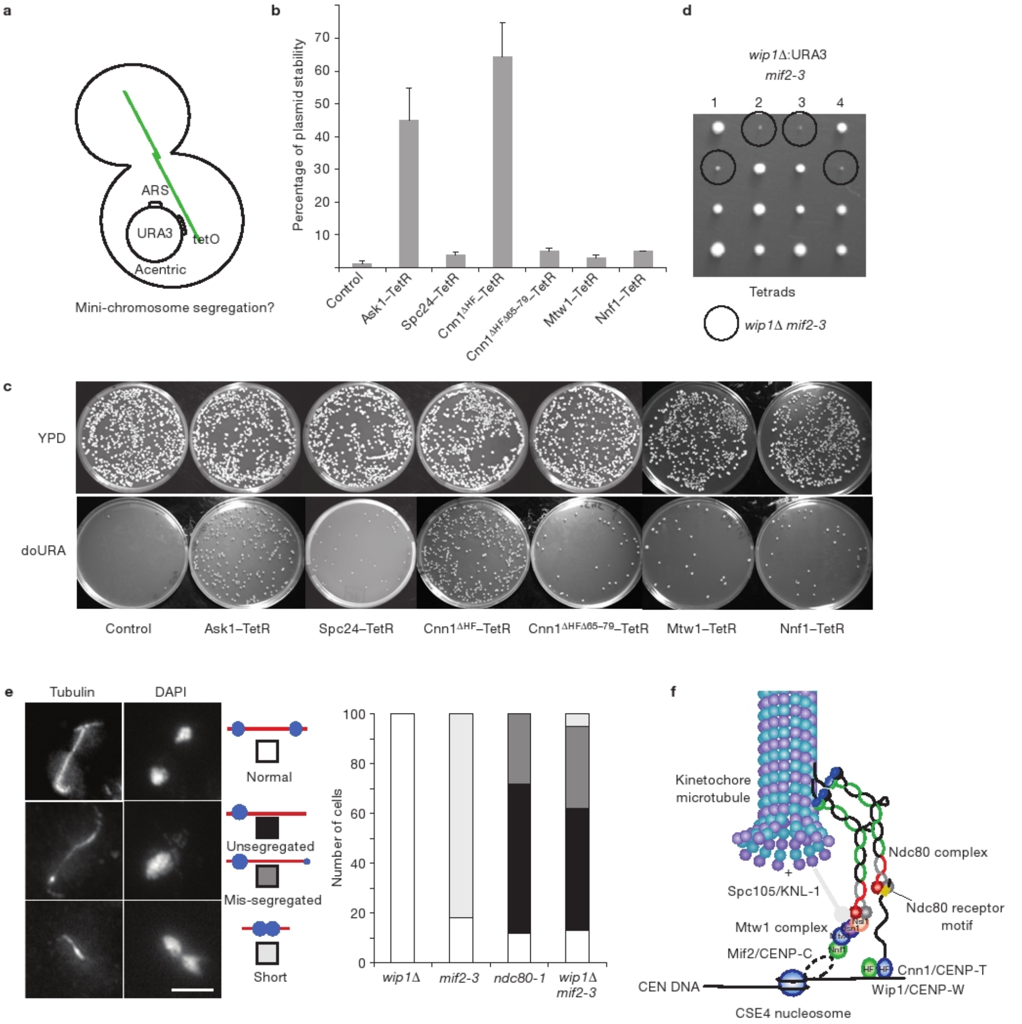

Figure 7 Artificial tethering of the Ndc80 complex through Cnn1$^{\mathrm{CENP\text{-}T}}$ allows mini-chromosomes to segregate in the absence of a centromere. (**a**) Scheme of the mini-chromosome stability assay. The segregation of a URA3-containing mini-chromosome containing a *tetO* array but lacking a centromere is assayed in different strain backgrounds. (**b**) Stability of URA3 mini-chromosomes in different strain backgrounds. Error bars denote s.e.m. $n = 3$. (**c**) Examples of plating assays for fusion strains Ask1–TetR, Spc24–TetR, Cnn1$^{\Delta\mathrm{HF}}$–TetR, Cnn1$^{\Delta\mathrm{HF}\Delta 65-79}$–TetR, Mtw1–TetR and Nnf1–TetR on YPD and doURA. (**d**) Double deficiency of the Ndc80 recruitment pathways: tetrad dissection of *wip1Δ mif2-3* double mutants. (**e**) Chromosome segregation defects in *wip1Δ mif2-3* double mutants. Left panel: Cells were processed for immunofluorescence microscopy two hours after shift to the restrictive temperature of the temperature-sensitive mutants. DNA is stained with DAPI; microtubules are stained with an anti-tubulin antibody. Right panel: Phenotypic categories are indicated and the respective phenotypes were quantified for the individual strains. Scale bar, 5 μm. (**f**) Two distinct receptors for Ndc80 molecules are present at yeast centromeres, one is the Mtw1 complex, which in turn may require the conserved protein Mif2/CENP-C for association with centromeric DNA. In a second pathway, Ndc80 molecules directly interact with the histone-fold complex Cnn1–Wip1 through a conserved receptor motif in the N-terminal extension of Cnn1. In a normal budding yeast cell cycle this linkage is not required for viability, but it becomes essential when Mtw1 subunits or Mif2 are functionally compromised.

COMPETING FINANCIAL INTERESTS

The authors declare no competing financial interests.

Published online at www.nature.com/naturecellbiology
Reprints and permissions information is available online at www.nature.com/reprints

1. Cheeseman, I. M. & Desai, A. Molecular architecture of the kinetochore-microtubule interface. *Nat. Rev. Mol. Cell Biol.* **9**, 33–46 (2008).
2. Lampert, F. & Westermann, S. A blueprint for kinetochores—new insights into the molecular mechanics of cell division. *Nat. Rev. Mol. Cell Biol.* **12**, 407–412 (2011).

© 2012 Macmillan Publishers Limited. All rights reserved.

3. Santaguida, S. & Musacchio, A. The life and miracles of kinetochores. *EMBO J.* **28,** 2511–2531 (2009).
4. Liu, D., Vader, G., Vromans, M. J., Lampson, M. A. & Lens, S. M. Sensing chromosome bi-orientation by spatial separation of aurora B kinase from kinetochore substrates. *Science* **323,** 1350–1353 (2009).
5. Musacchio, A. & Salmon, E. D. The spindle-assembly checkpoint in space and time. *Nat. Rev. Mol. Cell Biol.* **8,** 379–393 (2007).
6. Cheeseman, I. M., Chappie, J. S., Wilson-Kubalek, E. M. & Desai, A. The conserved KMN network constitutes the core microtubule-binding site of the kinetochore. *Cell* **127,** 983–997 (2006).
7. Alushin, G. M. *et al.* The Ndc80 kinetochore complex forms oligomeric arrays along microtubules. *Nature* **467,** 805–810 (2010).
8. Guse, A., Carroll, C. W., Moree, B., Fuller, C. J. & Straight, A. F. *In vitro* centromere and kinetochore assembly on defined chromatin templates. *Nature* **477,** 354–358 (2011).
9. Carroll, C. W., Milks, K. J. & Straight, A. F. Dual recognition of CENP-A nucleosomes is required for centromere assembly. *J. Cell Biol.* **189,** 1143–1155 (2010).
10. Foltz, D. R. *et al.* The human CENP-A centromeric nucleosome-associated complex. *Nat. Cell Biol.* **8,** 458–469 (2006).
11. Okada, M. *et al.* The CENP-H-I complex is required for the efficient incorporation of newly synthesized CENP-A into centromeres. *Nat. Cell Biol.* **8,** 446–457 (2006).
12. Cheeseman, I. M. *et al.* Phospho-regulation of kinetochore-microtubule attachments by the Aurora kinase Ipl1p. *Cell* **111,** 163–172 (2002).
13. Westermann, S. *et al.* Architecture of the budding yeast kinetochore reveals a conserved molecular core. *J. Cell Biol.* **163,** 215–222 (2003).
14. Liu, X., McLeod, I., Anderson, S., Yates, J. R. 3rd & He, X. Molecular analysis of kinetochore architecture in fission yeast. *EMBO J.* **24,** 2919–2930 (2005).
15. Meraldi, P., McAinsh, A. D., Rheinbay, E. & Sorger, P. K. Phylogenetic and structural analysis of centromeric DNA and kinetochore proteins. *Genome Biol.* **7,** R23 (2006).
16. Westermann, S., Drubin, D. G. & Barnes, G. Structures and functions of yeast kinetochore complexes. *Annu. Rev. Biochem.* **76,** 563–591 (2007).
17. Malik, H. S. & Henikoff, S. Major evolutionary transitions in centromere complexity. *Cell* **138,** 1067–1082 (2009).
18. Hori, T., Okada, M., Maenaka, K. & Fukagawa, T. CENP-O class proteins form a stable complex and are required for proper kinetochore function. *Mol. Biol. Cell* **19,** 843–854 (2008).
19. De Wulf, P., McAinsh, A. D. & Sorger, P. K. Hierarchical assembly of the budding yeast kinetochore from multiple subcomplexes. *Genes Dev.* **17,** 2902–2921 (2003).
20. Hori, T. *et al.* CCAN makes multiple contacts with centromeric DNA to provide distinct pathways to the outer kinetochore. *Cell* **135,** 1039–1052 (2008).
21. Gascoigne, K. E. *et al.* Induced ectopic kinetochore assembly bypasses the requirement for CENP-A nucleosomes. *Cell* **145,** 410–422 (2011).
22. Nishino, T. *et al.* CENP-T-W-S-X forms a unique centromeric chromatin structure with a histone-like fold. *Cell* **148,** 487–501 (2012).
23. Burley, S. K., Xie, X., Clark, K. L. & Shu, F. Histone-like transcription factors in eukaryotes. *Curr. Opin. Struct. Biol.* **7,** 94–102 (1997).
24. Luger, K., Mader, A. W., Richmond, R. K., Sargent, D. F. & Richmond, T. J. Crystal structure of the nucleosome core particle at 2.8 A resolution. *Nature* **389,** 251–260 (1997).
25. Sandman, K. & Reeve, J. N. Archaeal histones and the origin of the histone fold. *Curr. Opin. Microbiol.* **9,** 520–525 (2006).
26. Talbert, P. B. & Henikoff, S. Histone variants–ancient wrap artists of the epigenome. *Nat. Rev. Mol. Cell Biol.* **11,** 264–275 (2010).
27. Tanaka, K., Chang, H. L., Kagami, A. & Watanabe, Y. CENP-C functions as a scaffold for effectors with essential kinetochore functions in mitosis and meiosis. *Dev. Cell* **17,** 334–343 (2009).
28. Amano, M. *et al.* The CENP-S complex is essential for the stable assembly of outer kinetochore structure. *J. Cell Biol.* **186,** 173–182 (2009).
29. Yan, Z. *et al.* A histone-fold complex and FANCM form a conserved DNA-remodeling complex to maintain genome stability. *Mol. Cell* **37,** 865–878 (2010).
30. McAinsh, A. D. & Meraldi, P. The CCAN complex: linking centromere specification to control of kinetochore-microtubule dynamics. *Semin. Cell Dev. Biol.* **22,** 946–952 (2011).
31. Petrovic, A. *et al.* The MIS12 complex is a protein interaction hub for outer kinetochore assembly. *J. Cell Biol.* **190,** 835–852 (2010).
32. Maskell, D. P., Hu, X. W. & Singleton, M. R. Molecular architecture and assembly of the yeast kinetochore MIND complex. *J. Cell Biol.* **190,** 823–834 (2010).
33. Hornung, P. *et al.* Molecular architecture and connectivity of the budding yeast Mtw1 kinetochore complex. *J. Mol. Biol.* **405,** 548–559 (2011).
34. Ciferri, C. *et al.* Implications for kinetochore-microtubule attachment from the structure of an engineered Ndc80 complex. *Cell* **133,** 427–439 (2008).
35. Kiermaier, E., Woehrer, S., Peng, Y., Mechtler, K. & Westermann, S. A Dam1-based artificial kinetochore is sufficient to promote chromosome segregation in budding yeast. *Nat. Cell Biol.* **11,** 1109–1115 (2009).
36. Lacefield, S., Lau, D. T. & Murray, A. W. Recruiting a microtubule-binding complex to DNA directs chromosome segregation in budding yeast. *Nat. Cell Biol.* **11,** 1116–1120 (2009).
37. Westermann, S. *et al.* The Dam1 kinetochore ring complex moves processively on depolymerizing microtubule ends. *Nature* **440,** 565–569 (2006).
38. Wigge, P. A. *et al.* Analysis of the *Saccharomyces* spindle pole by matrix-assisted laser desorption/ionization (MALDI) mass spectrometry. *J. Cell Biol.* **141,** 967–977 (1998).
39. Screpanti, E. *et al.* Direct binding of Cenp-C to the Mis12 complex joins the inner and outer kinetochore. *Curr. Biol.* **21,** 391–398 (2011).
40. Suzuki, A. *et al.* Spindle microtubules generate tension-dependent changes in the distribution of inner kinetochore proteins. *J. Cell Biol.* **193,** 125–140 (2011).
41. Akiyoshi, B. *et al.* Tension directly stabilizes reconstituted kinetochore-microtubule attachments. *Nature* **468,** 576–579 (2010).
42. Bock, L. J. *et al.* Cnn1 inhibits the interactions between the KMN complexes of the yeast kinetochore. *Nat. Cell Biol.* http://dx.doi.org/10.1038/ncb2495 (2012).
43. Powers, A. F. *et al.* The Ndc80 kinetochore complex forms load-bearing attachments to dynamic microtubule tips via biased diffusion. *Cell* **136,** 865–875 (2009).
44. Kiyomitsu, T., Obuse, C. & Yanagida, M. Human Blinkin/AF15q14 is required for chromosome alignment and the mitotic checkpoint through direct interaction with Bub1 and BubR1. *Dev. Cell* **13,** 663–676 (2007).
45. Cheeseman, I. M. *et al.* A conserved protein network controls assembly of the outer kinetochore and its ability to sustain tension. *Genes Dev.* **18,** 2255–2268 (2004).
46. Cole, C., Barber, J. D. & Barton, G. J. The Jpred 3 secondary structure prediction server. *Nucleic Acids Res.* **36,** W197–W201 (2008).

© 2012 Macmillan Publishers Limited. All rights reserved.

METHODS

Homology searches and protein annotation. All searches were performed in the NCBI non-redundant protein database[47], or within specified proteomes, listed in Supplementary Table S4. Species and accession numbers are listed in Supplementary Table S2. We used NCBI BLASTP and PSI-BLAST version 2.2.24 (ref. 48), and HMMer v.3.0 (ref. 49) with significant E values below 0.01. Fold predictions were executed with HHpred in the PDB protein structure database[50,51]. Domains were annotated with Pfam and Smart databases[52,53], coiled coils were predicted using COILS (window 21; ref. 54), low-complexity regions with SEG (window 12; ref. 55) and secondary structure with Jpred3[46]. Sequences were aligned with MAFFT version 6 (L-INS-I method; ref. 56), and visualized and processed with Jalview (ref. 57) (Clustalx colouring scheme). To search for short motifs outside conserved domains, we used MEME (one occurrence per sequence, motif width 10–25; ref. 58).

Ame1 homology search. The budding yeast protein Ame1 is 324 residues in length and has a predicted coiled-coil region between amino acids 199 to 263. In homology searches, it is a common practice to disregard compositionally biased regions such as low-complexity, transmembrane or coiled-coil regions. When masking the coiled-coil region, an iterative PSI-BLAST search within the NCBI non-redundant protein database identified only Saccharomycetes strains closely related to *S. cerevisiae*, such as *Vanderwaltozyma polyspora*, *Zygosaccharomyces rouxii*, *Kluyveromyces lactis* or *Ashbya gossypii*, with significant E values $<5\times10^{-4}$ (round 1). The search converged in round 2 without incorporation of further hits. A multiple alignment of these orthologues revealed a conserved short region at the N terminus (rich in positively charged residues—corresponding to positions 2–22 in *S. cerevisiae* Ame1) and a conserved, α-helical domain (residues 115–314), where the coiled-coil region is a central part of it. We included the coiled-coil region in further searches, allowing for the incorporation of unrelated coiled-coil proteins as false positive hits. A search with a more sensitive HMM profile using sequences comprising the conserved domain detected significant hits in the more distantly related *Penicillium marneffei* (E value 1.3×10^{-5}) and to other Pezizomycotina fungi, such as *Uncinocarpus reesii* and *Arthroderma gypseum* (E values 0.0029 and 0.0046, respectively). We used BLASTP searches to enlarge the sequence family within the Pezizomycotina fungi (E values $<1\times10^{-5}$). They all belong to a group of conserved hypothetical proteins, without known function. In the subsequent HMM search within the *S. pombe* proteome, only one significant hit was identified, namely Mis17 (E value 5.1×10^{-5}; Supplementary Fig. S1).

Intriguingly, Mis17 has been identified as a centromere protein in genetic screens and is involved in the stable deposition of CENP-A to centromeres; thus, functionally it acts like a CCAN subunit[59]. In addition to other Ascomycota, we enlarged our search to the proteome of the Basidiomycota *Ustilago maydis*. Using a HMM profile covering the α-helical Ame1/Mis17 domain, we identified one significant protein (UM03572, E value 0.00035). Applying the expanded model to the NCBI non-redundant protein database resulted in 11 newly identified proteins below the inclusion threshold (E value 0.01, apparent isoforms were not counted). Out of these, 5 proteins belong to the mammalian CENP-U gene family, with the CENP-U protein from *Bos taurus* as the best hit (E value 4.3×10^{-7}). CENP-U (also called CENP-50) is a CENP-A co-purifying protein[10] that forms a biochemically stable complex with CENP-O, -P and -Q (ref. 18). The six remaining proteins were unrelated coiled-coil proteins from Trypanosoma, Nematoda, Ascomycetes, Bacteria (2 proteins) and Archaea. Searching with the Ame1/Mis17 domain within the *Mus musculus* or *Homo sapiens* proteome results in CENP-U proteins as the only significant hits (E value 1.2×10^{-8} and 0.0051, respectively). In an alternative approach, a HMM–HMM comparison with the Ame1/Mis17 alignment identified a model built from mammalian CENP-U proteins as the next best hit (besides the known fungi ones) with a sub-significant E value (0.016, UniProt20 database; ref. 60). CENP-U orthologues can be easily collected from mammals to fish with BLASTP searches applying highly significant E values ($<1\times10^{-15}$). As is the case for Ame1 and Mis17, they all share a coiled-coil region at the C terminus that is part of a highly conserved domain and predicted to be α-helical.

Okp1 homology search. Okp1 is similar in architecture to Ame1, with a length of 406 residues and a coiled-coil region from 239 to 285. A BLASTP search with a coiled-coil masked sequence identified proteins in the closest Saccharomycetes organisms, such as *Lachancea thermotolerans*, *K. lactis* or *A. gossypii*, with significant E values ($<9\times10^{-9}$). As in Ame1, the conserved domain is located at the C-terminal region that is predicted to be α-helical and includes the coiled-coil region. The sequence conservation score is slightly higher than for Ame1 and so we could establish a linkage between Okp1 and the fission yeast Fta7 using a series of PSI-BLAST searches: the conserved region of the *Lachancea* Okp1 orthologue (including the coiled-coil region) hit one protein in *Sclerotinia sclerotiorum* with a significant E value (4×10^{-5}) in round 2, and the *Sclerotinia* Okp1 domain in turn found one protein in *Tuber melanosporum* (E value 5×10^{-21}, round 2), which finally led to the identification of *S. pombe* Fta7 (E value 8×10^{-4}, round 1). A HMM profile search with the fungi Okp1/Fta7 domain included 5 non-fungal proteins, all CENP-Q orthologues (inclusion value 0.01), such as the acorn worm *Saccoglossus kowalevskii* (E value 4×10^{-4}) or the house mouse *Mus musculus* (E value 8×10^{-3}; Supplementary Fig. S2).

Mcm22 and CENP-K are orthologous. *S. cerevisiae* Mcm22 is 239 residues long and has a predicted coiled coil from 113–134. A BLASTP search using the full-length Mcm22 (masking the coiled-coil region) identifies orthologues in the closest Saccharomycetes organisms, such as *Candida glabrata* (E value: 3×10^{-8}) or *A. gossypii* (E value: 5×10^{-11}). The conserved domain is spanning nearly the whole protein length (*S. cerevisiae* Mcm22: 7–233) and the coiled-coil predictions of the orthologues overlap with the one of *S. cerevisiae*. We constructed a HMM out of the conserved domain (the regions corresponding to the *S. cerevisiae* coiled coil were masked) and searched in the proteomes of *Candida dubliniensis*, *Pichia guilliermondii*, *Candida albicans* and *Aspergillus niger*, where in each case one protein was found below the inclusion value (E value <0.01; Cd36_87730, PGUT_03964, CAWT_03094, jgi|Aspni1|178612|). In the following iterative PSI-BLAST search within the NCBI non-redundant protein database, more Pezizomycotina proteins were collected in round 1 with significant E values ($<2\times10^{-6}$), among those *Gibberella zeae* and *Tuber melanosporum*. The subsequent HMM search identified proteins from *Strongylocentrotus purpuratus* (E value: 2.1×10^{-6}), *Gallus gallus* (0.0019), *Pan troglodytes* (0.0031), *Xenopus laevis* (0.0055) and six more animal proteins below the significant inclusion value (0.01). They all belong to the CENP-K family, where *S. pombe* Sim4 is included as well[52] (Supplementary Fig. S3). In a reciprocal approach, the Pfam CENP-K HMM identified the *Giberella zeae* and other Pezizomycotina orthologues, and a subsequent search with a HMM including the Pezizomycotina proteins hit *C. glabrata* Mcm22 (E values <0.01).

CENP-W homology search. In mammals, besides CENP-T, three further histone-fold proteins are known to interact with the core CCAN complex: CENP-S, CENP-W and CENP-X (refs 20,28), forming CENP-S/CENP-X (ref. 29) and CENP-T/CENP-W heterodimeric complexes. Unlike CENP-T, these three proteins are much shorter (81–138 residues), hardly extending the histone domain (CENP-S has an extension of around 30 amino acids at the C terminus rich in positively charged residues). CENP-X and CENP-S are well conserved and homologues in *S. pombe* and *S. cerevisiae* were identified with BLASTP. CENP-W family members can be detected in Pezizomycotina fungi, such as *A. niger*, and in *Schizosaccharomyces japonicus* with iterative PSI-BLAST searches, but the model iterated into histone-fold proteins, such as the transcription factors NC2β or Hap3. To find Saccharomycetes homologues, a HMM model containing the CENP-W histone domain identified the orphan protein DEHA2G10538g in *Debaryomyces hansenii* with a highly significant E value (1.2×10^{-11}), followed by the NC2β-like protein DEHA2E16126g (E value 7×10^{-07}), whereas we failed to detect any significant *S. cerevisiae* proteins.

In a biochemical isolation of CCAN-complex-binding proteins from budding yeast cell extracts, several hypothetical proteins were characterized by mass spectrometry, using Mcm16 and Cnn1 as bait (Supplementary Table S3). Among those, the protein YDR374W-A was of particular interest, owing to its short length (89 amino acids) and a high α-helical content. YDR374W-A is very weakly conserved and when applying sensitive HMM searches we found orthologues in *Z. rouxii*, *K. lactis* and *A. gossypii*. In the proteome of *Debaryomyces hansenii*, we identified one protein DEHA2G10538g with a significant E value (3.4×10^{-5}). Interestingly, *D. hansenii* DEHA2G10538g had been previously identified in the search for CENP-W candidates. Thus, it is very likely that budding yeast YDR374W-A is the orthologue of mammalian CENP-W (Supplementary Fig. S4).

Yeast strains and plasmids. Yeast strains are based on S288C and were generated by standard procedures. A list of used yeast strains and plasmids can be found in Supplementary Table S5.

Protein biochemistry. Ndc80 and Mtw1 complexes were expressed and purified as described previously[33,61] with the following modifications: for the Mtw1 complex an N-terminal 6×His-tagged Dsn1 subunit was cloned into a pST39 expression plasmid harbouring the Nnn1, Nsl1 and Mtw1 subunits.

Overexpression and purification of proteins from yeast extracts were performed as described previously[62] with the following modifications. Yeast pellets (60 g) were lysed with a freezer mill (Spex Centriprep) and the resulting yeast powder was stored at −80 °C. For purification of Flag-tagged proteins, 10 g yeast powder was combined with 50 ml lysis buffer (25 mM HEPES at pH 8.0, 2 mM MgCl$_2$, 0.1% NP-40, 150 mM KCl, 15 (v/v) % glycerol, 1 mM dithiothreitol and protease inhibitors), left on ice for 30 min and centrifuged at 60,000g for 30 min at 4 °C. The supernatant was further ultracentrifuged (100,000g, 45 min, 4 °C), cleared by filtration through a 0.2 μm filter and collected. A 300 μl solution of anti-Flag M2 agarose beads was added and rotated for 3 h at 4 °C. Beads were washed five times with wash buffer (lysis buffer with 0.5 M KCl, 1 mM ATP and 2 mM MgCl$_2$) and eluted three times with 1 mg ml^{-1} 3×Flag peptide in buffer H. Proteins were snap-frozen in liquid N$_2$ and stored at −80 °C.

Interaction studies. Interaction studies were performed by size-exclusion chromatography on Superose 6 PC3.2/30 columns. The indicated proteins or complexes

© 2012 Macmillan Publishers Limited. All rights reserved.

were used at 1 μM concentration, mixed and left on ice for 30 min before injecting 50 μl onto the column. Fractions of 100 μl were collected, and proteins were precipitated using chloroform/methanol and subjected to SDS–PAGE.

Isothermal titration calorimetry. Thermodynamic values of the interaction between Cnn1-derived peptides and Spc24–25 were determined by ITC (MCS-ITC, Microcal). All experiments were conducted at 25 °C. A 1.8 ml solution of Spc24–25 (30 μM) was placed in the temperature-controlled cell and titrated with Cnn1 peptide at 500 μM in the syringe. The buffer used was 25 mM HEPES at pH 8 with 150 mM KCl. Data were analysed using ORIGIN following the instructions of the manufacturer.

Mass spectrometry. The nano-HPLC system used in all experiments was an UltiMate 3000 Dual Gradient HPLC system (Dionex), equipped with a Proxeon nanospray source (Proxeon), coupled to an LTQ Velos Orbitrap mass spectrometer (Thermo Fisher Scientific), operated in data-dependent mode using a full scan in the ion cyclotron resonance cell followed by tandem mass spectrometry (MS/MS) scans of the 12 most abundant ions in the linear ion trap. MS/MS spectra were acquired in the multistage activation mode, where subsequent activation was performed on fragment ions resulting from the neutral loss of −98, −49 or −32.6 m/z for potential follow-up phosphorylation site analysis. Precursor ions selected for fragmentation were put on a dynamic exclusion list for 180 s. Monoisotopic precursor selection was enabled.

Analysis of MS data. For peptide identification, all MS/MS spectra were searched using Mascot 2.2.04 (Matrix Science) and Sequest (Thermo Scientific) against the yeast SGD protein sequence database (6,717 sequences; 3,020,761 residues). The following search parameters were used: carbamidomethylation or methyl methylthiomethyl sulphoxide respectively on cysteine was set as a fixed modification; oxidation on methionine was set as variable modification. Monoisotopic masses were searched within unrestricted protein masses for tryptic, chymotryptic and unspecific (subtilisin digest) peptides. The peptide mass tolerance was set to ±5 ppm and the fragment mass tolerance to ±0.5 Da. The maximal number of missed cleavages was set to 2. Using a Thermo Proteome Discoverer 1.3.0.339 (Thermo Scientific), the results of both search engines were combined and filtered to 1% false discovery rate using an integrated Percolator algorithm. Furthermore, high-quality criteria filters such as peptide rank 1 and minimum 2 peptides per protein were applied.

Artificial kinetochore experiments. Experiments to examine artificial kinetochore function were performed as described previously[35] with the following modifications. TetR-fusion proteins were integrated at the LEU2 locus and expressed as extra copies. Expression was verified by western blotting of whole-cell extracts with an anti-TetR antibody. Strains were transformed with mini-chromosomes, selected on drop-out uracil (doURA) and grown non-selectively for 24 h in YPD medium. An attenuance of 0.6 at 600 nm was adjusted and 70 μl of a 1:1,000 dilution was plated on YPD or doURA plates, leading to the formation of approximately 600 colonies on YPD. Experiments were performed in triplicates.

ChIP. Cultures were grown in YPD to mid-log phase. Cells were crosslinked for 30 min with formaldehyde (1%). Chromatin extract preparation and ChIP were performed as previously described[63]. Samples were analysed by quantitative PCR using the Biorad iQ5 real-time PCR system and software.

47. Sayers, E. W. *et al.* Database resources of the National Center for Biotechnology Information. *Nucleic Acids Res.* **39,** D38–D51 (2011).
48. Altschul, S. F. *et al.* Gapped BLAST and PSI-BLAST: a new generation of protein database search programs. *Nucleic Acids Res.* **25,** 3389–3402 (1997).
49. Johnson, L. S., Eddy, S. R. & Portugaly, E. Hidden Markov model speed heuristic and iterative HMM search procedure. *BMC Bioinformatics* **11,** 431 (2010).
50. Berman, H. M. *et al.* The Protein Data Bank. *Nucleic Acids Res.* **28,** 235–242 (2000).
51. Soding, J., Biegert, A. & Lupas, A. N. The HHpred interactive server for protein homology detection and structure prediction. *Nucleic Acids Res.* **33,** W244–W248 (2005).
52. Finn, R. D. *et al.* The Pfam protein families database. *Nucleic Acids Res.* **38,** D211–D222 (2010).
53. Letunic, I., Doerks, T. & Bork, P. SMART 6: recent updates and new developments. *Nucleic Acids Res.* **37,** D229–D232 (2009).
54. Lupas, A., Van Dyke, M. & Stock, J. Predicting coiled coils from protein sequences. *Science* **252,** 1162–1164 (1991).
55. Wootton, J. C. & Federhen, S. Analysis of compositionally biased regions in sequence databases. *Methods Enzymol.* **266,** 554–571 (1996).
56. Katoh, K. & Toh, H. Recent developments in the MAFFT multiple sequence alignment program. *Brief Bioinform.* **9,** 286–298 (2008).
57. Waterhouse, A. M., Procter, J. B., Martin, D. M., Clamp, M. & Barton, G. J. Jalview Version 2–a multiple sequence alignment editor and analysis workbench. *Bioinformatics* **25,** 1189–1191 (2009).
58. Bailey, T. L. *et al.* MEME SUITE: tools for motif discovery and searching. *Nucleic Acids Res.* **37,** W202–W208 (2009).
59. Hayashi, T. *et al.* Mis16 and Mis18 are required for CENP-A loading and histone deacetylation at centromeres. *Cell* **118,** 715–729 (2004).
60. Remmert, M., Biegert, A., Hauser, A. & Soding, J. HHblits: lightning-fast iterative protein sequence searching by HMM–HMM alignment. *Nat. Methods* **9,** 173–175 (2012).
61. Lampert, F., Hornung, P. & Westermann, S. The Dam1 complex confers microtubule plus end-tracking activity to the Ndc80 kinetochore complex. *J. Cell Biol.* **189,** 641–649 (2010).
62. Rodal, A. A., Manning, A. L., Goode, B. L. & Drubin, D. G. Negative regulation of yeast WASp by two SH3 domain-containing proteins. *Curr. Biol.* **13,** 1000–1008 (2003).
63. Mendoza, M. A., Panizza, S. & Klein, F. Analysis of protein-DNA interactions during meiosis by quantitative chromatin immunoprecipitation (qChIP). *Methods Mol. Biol.* **557,** 267–283 (2009).

© 2012 Macmillan Publishers Limited. All rights reserved.

9. Curriculum vitae

Personal information

Name: Michael Josef Maier

Natianality: german

Date of Birth: 06.09.1983 in Cape Town, South Africa

Email: a0508282@unet.univie.ac.at

Education

2005-present: Studies of Molecular Biology
University of Vienna, Austria

2004-2005: Studies of Chemical Engineering,
Friedrich-Alexander University Erlangen

1993-2003: Staffelsee Gymnasium Murnau

10.Acknowledgements

In the last chapter of my thesis I want to thank everybody that has made this work possible. First and foremost I want to than my parents who have given me the opportunity to study and who have supported me throughout this time.

Thank you Stefan, not only for giving me the opportunity to work on this exciting project but also for involving me after my work was complete. You have an exceptional lab and it was a pleasure to work with you and everybody else there.

Thank you, Peter. Just like I could not have wished for a better lab for my thesis, I could not have wished for a better supervisor. You gave me the freedom to be creative but kept me on track.

Thank you Chrissi, Evi, Fabi, Francesca, Gabi, Kati, Paulina, Tom, Vero. You gave me advice but probably more important, your amiable character buffered the frustrating days in the lab. One rarely meets a group of people like you.

I am very grateful for my friends. Although I tend to focus on work and neglect them more often than not, they were always there when I called and never stopped calling me.

And finally, thank you Marion, you gave me the strength to see this through.